REFERENCE ONLY

UNIVERSITY OF LONDON THESIS

Degree ~~PhD~~ MD Year 2006 Name of Author SIBTAIN, A

COPYRIGHT

This is a thesis accepted for a Higher Degree of the University of London. It is an unpublished typescript and the copyright is held by the author. All persons consulting the thesis must read and abide by the Copyright Declaration below.

COPYRIGHT DECLARATION

I recognise that the copyright of the above-described thesis rests with the author and that no quotation from it or information derived from it may be published without the prior written consent of the author.

LOANS

Theses may not be lent to individuals, but the Senate House Library may lend a copy to approved libraries within the United Kingdom, for consultation solely on the premises of those libraries. Application should be made to: Inter-Library Loans, Senate House Library, Senate House, Malet Street, London WC1E 7HU.

REPRODUCTION

University of London theses may not be reproduced without explicit written permission from the Senate House Library. Enquiries should be addressed to the Theses Section of the Library. Regulations concerning reproduction vary according to the date of acceptance of the thesis and are listed below as guidelines.

A. Before 1962. Permission granted only upon the prior written consent of the author. (The Senate House Library will provide addresses where possible).

B. 1962 - 1974. In many cases the author has agreed to permit copying upon completion of a Copyright Declaration.

C. 1975 - 1988. Most theses may be copied upon completion of a Copyright Declaration.

D. 1989 onwards. Most theses may be copied.

This thesis comes within category D.

☑ This copy has been deposited in the Library of UCL

☐ This copy has been deposited in the Senate House Library, Senate House, Malet Street, London WC1E 7HU.

THE EVALUATION OF HYPOXIA IN HUMAN BLADDER CARCINOMA USING INTRINSIC AND EXTRINSIC MARKERS

A thesis to be submitted to the University of London

for the degree of Doctor of Medicine

Amen Sibtain

Marie Curie Research Wing
Mount Vernon Hospital
Rickmansworth Road
Middlesex
HA6 2RN
UK

ProQuest LLC
789 East Eisenhower Parkway
P.O. Box 1346
Ann Arbor, MI 48106-1346

Dedication

Like everything else...

for Theo, Isabella and Anna.

Acknowledgements

Professor Michele Saunders for her ongoing support and guidance.

Frances Daley and Sonia Noble for their work on the immunohistochemistry.

Professor George Wilson for his advice and supervision though the project.

The patients for agreeing to take part in these studies.

Urology teams at Watford and Luton Hospitals for help in recruiting patients.

Dr Peter Hoskin for his endless time, help, advice, support and encouragement.

Abstract

Hypoxia has been evaluated in a series of human bladder carcinomas using pimonidazole. The relationships of hypoxia with vascularity and with proliferation have been explored. Two intrinsic markers of hypoxia have been validated against pimonidazole and then used to assess the impact of hypoxia on a cohort of bladder tumours treated with a hypoxia modifying treatment stratagem.

Thirty-one patients with confirmed transitional cell carcinoma of the bladder received pimonidazole before transurethral resection of the tumour. Sections from 26 tumours were stained for pimonidazole. The median hypoxic fraction was 9% (range 0 to 38%).

Twenty-one tumours were double stained for pimonidazole with Ki67 (proliferation), and pimonidazole with CD31/34 (vascularity). Most staining was distant from vessels (median 100μm). Some hypoxia was close to vessels (<40μm), suggesting a perfusion limiting mechanism in these areas. Dual staining for pimonidazole and proliferation showed a predominantly inverse relationship between these factors. However, some hypoxic regions of less than 40μm from a vessel had a higher proliferative index than those further away from vessels

Having confirmed GLUT1 and CA9 as appropriate intrinsic markers for hypoxia, archived samples of bladder carcinoma from 64 patients treated with ARCON were obtained. Sections were stained for GLUT1, CA9, Ki67 and CD31/34 and analysed as above. The median follow up time was 24 months The median stained fraction for GLUT1 was 6.5% (range 0 to 62%) and for CA9 was 3.5% (range 0 to 67%). Those

patients above the median (more hypoxic tumours) for each marker had a statistically significantly poorer cause specific survival (GLUT1 $p<0.005$, CA9 $p<0.003$) but not local recurrence or metastasis free survival, analysed with a log rank test. A multivariate analysis, accounting for stage, age, grade, Ki67 index and vascularity confirmed hypoxic fraction as an independent factor in cause specific survival (GLUT1 $p<0.02$, CA9 $p<0.03$).

In conclusion, hypoxia is a significant factor in bladder cancer, and is quantifiable with both extrinsic and intrinsic markers. Staining patterns are consistent with diffusion limited and perfusion limited mechanisms of hypoxia. Proliferation is reduced in hypoxic areas but less so in those that are acutely hypoxic. In a cohort of patients with bladder cancer treated with ARCON, patients with more hypoxic tumours, assessed with intrinsic markers, tend to a poorer cause specific survival.

CONTENTS

TITLE ---------- 1

DEDICATION ---------- 2

ACKNOWLEDGEMENTS ---------- 3

ABSTRACT ---------- 4

CONTENTS ---------- 6

LIST OF FIGURES ---------- 15

LIST OF TABLES ---------- 20

CHAPTER ONE ---------- 23

INTRODUCTION

TUMOUR HYPOXIA ---------- 23

DEFINITION AND DISCOVERY OF TUMOUR HYPOXIA ---------- 23

REDUCING HYPOXIA FOR CLINICAL BENEFIT ---------- 31

Hyperbaric oxygen ---------- *31*

Hypoxic cell radiosensitisers ---------- *33*

Normobaric oxygen – carbogen gas breathing ---------- *37*

'ACUTE' HYPOXIA ---------- 40

Reducing perfusion related hypoxia ---------- *46*

The return of carbogen: combination with nicotinamide ---------- *51*

EXPLOITING TUMOUR HYPOXIA WITH BIOREDUCTIVE DRUGS ---------- 53

Nitroaromatics ---------- *53*

Quinones ---------- *54*

Aromatic N-oxides ---- *54*

Aliphatic N-oxides ---- *55*

Transition metal complexes ---- *55*

THE CELLULAR RESPONSE TO HYPOXIA. ---- 57

Hypoxia and tumour cell protein expression ---- *57*

Oxygen mediated genomic regulation in normal cells ---- *58*

Vascular endothelial growth factor ---- *66*

Platelet derived endothelial growth factor ---- *67*

Nitric Oxide ---- *68*

Carbonic anhydrase ---- *68*

P53 ---- *69*

Nuclear factor kB ---- *70*

THE MEASUREMENT OF TUMOUR HYPOXIA ---- 73

MICROSENSOR TECHNIQUES ---- 73

Polarographic Methods ---- *73*

Luminescence sensor ---- *79*

HYPOXIC MARKERS ---- 81

Invasive hypoxia marker techniques ---- *81*

Nitroimidazoles ---- 81

The metabolism of 2-nitroimidazoles ---- 82

Radiolabelled 2-nitroimidazoles ---- 85

Immunohistochemical nitroimidazole labelling ---- 86

Intrinsic markers of hypoxia ---- 89

Carbonic Anhydrase 9 ---- 90

Glucose transporter 1 ---- 91

Non invasive hypoxia marker techniques ---- *93*

Detection of sensitiser adducts ---- 93

Magnetic resonance spectroscopy of fluorinated nitroimidazoles ---- 95

BLADDER CARCINOMA: AN OVERVIEW ---------- 95

INCIDENCE ---------- 97

AETIOLOGY ---------- 97

Cigarette Smoking ---------- *97*

Occupational Exposure ---------- *97*

Drugs ---------- *98*

Chronic infection ---------- *98*

PATHOLOGY ---------- 98

Transitional cell carcinoma ---------- *98*

Squamous cell carcinoma ---------- *98*

Adenocarcinoma ---------- *99*

Undifferentiated ---------- *99*

STAGING AND GRADING ---------- 99

CLINICAL PRESENTATION ---------- 102

DIAGNOSIS ---------- 102

TREATMENT OUTLINE ---------- 103

PROGNOSIS ---------- 104

CHAPTER TWO ---------- 107

THE ASSESSMENT OF HYPOXIA IN BLADDER CARCINOMA USING PIMONIDAZOLE

AIM ---------- 107

METHODS AND MATERIALS ---------- 107

ETHICAL APPROVAL ---------- 107

PATIENT SELECTION ---- 107
PIMONIDAZOLE STORAGE AND PRESENTATION. ---- 108
PIMONIDAZOLE DELIVERY ---- 108
SAMPLE COLLECTION AND PREPARATION ---- 108
IMMUNOHISTOCHEMISTRY: PIMONIDAZOLE STAINING ---- 109
Principle of the Avidin-Biotin Complex method ---- *109*
Procedure ---- *110*
IMAGE ANALYSIS ---- 112
Set up ---- *112*
Measuring the pimonidazole stained fraction and the necrotic fraction ---- *112*
Definition of 'Light' and 'Dark' pimonidazole staining ---- *114*
INTER-OBSERVER AND INTRA-OBSERVER VARIATION ---- 114
DATA OBTAINED ---- 114
STATISTICS ---- 115

RESULTS ---- 115

PATIENT DETAILS ---- 115
PIMONIDAZOLE TOLERANCE ---- 115
INTRA-OBSERVER VARIATION IN ASSESSMENT OF PIMONIDAZOLE BINDING ---- 115
INTER-OBSERVER VARIATION IN ASSESSMENT OF PIMONIDAZOLE BINDING ---- 118
QUANTITY OF STAIN ---- 120
PATTERN AND INTENSITY OF STAIN ---- 123
NECROTIC FRACTION ---- 124
PIMONIDAZOLE STAINED FRACTION AND TUMOUR GRADE ---- 126

DISCUSSION ---- 127

CONCLUSION ---- 132

CHAPTER THREE ---- 134

PROLIFERATION IN BLADDER CARCINOMA AND ITS RELATIONSHIP TO HYPOXIA

AIMS ---- 134

METHODS AND MATERIALS ---- 134

PROCEDURE ---- 134

IMMUNOHISTOCHEMISTRY: DOUBLE STAINING FOR PIMONIDAZOLE AND KI67 ---- 135

IMAGE ANALYSIS ---- 136

DATA OBTAINED ---- 140

STATISTICAL ANALYSIS ---- 140

RESULTS ---- 140

PROLIFERATION INDICES ---- 140

Ki67 indices ---- *140*

Pattern of Ki67 staining ---- *141*

CyclinA indices ---- *143*

Pattern of CyclinA staining ---- *143*

Relationship between proliferative index and hypoxic fraction ---- *144*

Relationship between Ki67 and CyclinA ---- *144*

DISCUSSION ---- 161

CONCLUSION ---- 166

CHAPTER FOUR ---- 167

VASCULARITY IN BLADDER CARCINOMA AND ITS RELATIONSHIP TO HYPOXIA

AIMS ---- 167

METHODS AND MATERIALS ---- 167

PROCEDURE ---- 167

IMMUNOHISTOCHEMISTRY: DOUBLE STAINING FOR PIMONIDAZOLE AND CD31/34 ---- 168

IMAGE ANALYSIS ---- 169

Set up ---- *169*

Assessment of Vascularity ---- *169*

'Hot spot' Method ---- 169

Vascular Density ---- 173

ASSESSMENT OF VESSEL TO HYPOXIA DISTANCE ---- 173

EXCLUSIONS ---- 173

DATA OBTAINED ---- 173

RESULTS ---- 176

THE VASCULARITY ---- 176

Overall vascular density ---- *176*

Vascular density in oxic and hypoxic regions ---- *178*

Combined vascular density in oxic and hypoxic regions for all tumours ---- 178

Vascular density in each tumour ---- 180

Correlation between oxic and hypoxic vascularity within indivicual tumours ---- 180

Hot spot count ---- *183*

Overall hot spot count ---- 183

Hot spot count in oxic and hypoxic regions ---- 183

COMPARISON BETWEEN HOTSPOT COUNT AND VASCULAR DENSITY ---- 188

RELATIONSHIP BETWEEN PIMONIDAZOLE STAINED FRACTION AND VASCULARITY ---- 190

VESSEL TO HYPOXIA DISTANCE ---- 193

DISCUSSION ---------- **196**

METHODS OF MEASURING VASCULARITY ---------- 196

THE VESSEL TO HYPOXIA DISTANCES ---------- 197

VASCULAR DENSITY RELATED TO HYPOXIA ---------- 203

CHAPTER FIVE ---------- 208

INTRINSIC MARKERS OF HYPOXIA IN BLADDER CANCER

AIMS ---------- **208**

METHODS AND MATERIALS ---------- **208**

PATIENTS ---------- 208

PROCEDURE ---------- 209

IMMUNOHISTOCHEMICAL PROCEDURES ---------- 209

Staining for GLUT1 ---------- *209*

Double staining for CA9 and CD31/34 ---------- *210*

IMAGE ANALYSIS ---------- 213

STATISTICS ---------- 213

DATA OBTAINED ---------- 213

RESULTS ---------- **214**

COMPARISON OF STAINED FRACTIONS OF GLUT1 AND CA9 ---------- 214

VESSEL TO STAIN DISTANCE ---------- 220

STAINING PATTERNS AND CO-LOCALISATION. ---------- 229

DISCUSSION ---------- **236**

CONCLUSION ---------- **239**

CHAPTER SIX ---------- 240

THE INFLUENCE OF HYPOXIA, PROLIFERATION AND VASCULARITY ON OUTCOME IN A COHORT OF PATIENTS WITH MUSCLE INVASIVE BLADDER CANCER TREATED BY ACCELERATED RADIOTHERAPY, CARBOGEN AND NICOTINAMIDE: INTRINSIC MARKERS OF HYPOXIA IN PRACTICE

AIMS ---------- 240

METHODS AND MATERIALS ---------- 240

ETHICAL APPROVAL ---------- 240

PATIENTS ---------- 240

TREATMENT DETAILS ---------- 241

Nicotinamide ---------- *242*

Carbogen breathing ---------- *242*

Radiotherapy details ---------- *242*

Follow up ---------- *242*

PROCEDURE ---------- 243

IMAGE ANALYSIS ---------- 243

DATA OBTAINED ---------- 243

STATISTICS ---------- 244

RESULTS ---------- 246

BIOLOGICAL PARAMETERS ---------- 246

RELATIONSHIPS BETWEEN BIOLOGICAL PARAMETERS ---------- 246

RELATIONSHIP OF BIOLOGICAL PARAMETERS WITH OUTCOME ---------- 248

UNIVARIATE ANALYSES ---------- 248

Hypoxic fraction and the pattern of treatment failure ---------- *252*

MULTIVARIATE ANALYSES ---------- 255

DISCUSSION ---------- **258**

CONCLUSION ---------- **265**

OVERALL CONCLUSIONS ---------- **265**

REFERENCES ---------- **267**

List of Figures

Figure 1 Critical O_2 levels that characterise the upper limit of the hypoxic range----------24

Figure 2 Comparison between the effect of oxygen tension on cytological damage induced in mouse ascites cells by x-rays and neutrons ----------29

Figure 3 The differing response to radiotherapy of a tumour implanted in the mouse hind leg whilst breathing air or oxygen right leg ----------29

Figure 4 The infuence of a subpopulation of cells on the survival curve obtained for an irradiated tumour. ----------30

Figure 5 The chemical structures of a range of 2-nitroimidazoles----------35

Figure 6 Cure rates of treated tumours in mice ----------39

Figure 7 Radiation cell survival curves of the RIF 1 tumour ----------42

Figure 8 Surviving fraction following 10Gy of irradiation----------43

Figure 9 The effect of timing between drug administration and radiation on tumor cell survival in three tumor models. ----------48

Figure 10 Relative changes in mean tumour cell fluorescence as a function of time after nicotinamide injection. ----------49

Figure 11 The effect of nicotinamide on the radiation dose response curve as measured by a regrowth delay assay. ----------50

Figure 12 The structure of CB-1954 ----------53

Figure 13 The reductive activation of tirapazamine ----------55

Figure 14 The fate of HIF under hypoxic and oxic conditions ----------71

Figure 15 A comparison of pretreatment tumour oxygenation in patients undergoing planned post radiotherapy neck dissection ----------77

Figure 16 The bioreductive metabolism of nitroimidazoles----------84

Figure 17 T-staging system for bladder carcinoma ---------- 100

Figure 18 Histological sections through normal urothelium transitional cell carcinoma------ 101

Figure 19 An intravenous urogram showing a large filling defect in the bladder ---------- 102

Figure 20 Recurrence-free survival and overall survival in 1,054 patients undergoing radical cystectomy with intent to cure for invasive bladder cancer. ---------- 105

Figure 21 Screenshot of image analysis program ---------- 113

Figure 22 Plot of comparison of two measurements of total stained fraction ---------- 116

Figure 23 Plot of comparison of two measurements of dark stained ---------- 117

Figure 24 Plot of comparison of obsever variation of pimonidazole stained fraction --------- 119

Figure 25 Plot of comparison of obsever variation of pimonidazole stained fraction --------- 119

Figure 26 A histogram of pimonidazole stained fractions---------- 120

Figure 27 Plot of the fraction of dark staining versus total stain ---------- 121

Figure 28 Sections of bladder carcinoma from four different patients illustrating heterogeneity of pimonidazole staining. ---------- 122

Figure 29 Section of bladder carcinoma stained for pimonidazole illustrating variable staining intensity and necrosis ---------- 123

Figure 30 Histogram of necrotic fractions ---------- 124

Figure 31 Plot of the necrotic fraction against the pimonidazole stained fraction---------- 125

Figure 32 Histogram of distance from stain edge to necrosis ---------- 125

Figure 33 Scatter plot of Pimonidazole stained fraction by grade. ---------- 126

Figure 34 Oxygen dependent binding curve (K-curve) for NitroImidazoleTheoPhylline ----- 131

Figure 35 Section (X20) stained for pimonidazole (red) and CD31/34 (brown) showing regions of hypoxia close to vessels (arrowed). ---------- 138

Figure 36 Section (X10) stained for pimonidazole (red) and KI67 (brown) . ---------- 138

Figure 37 Section (X40) stained for hypoxia (red) and Ki67 (brown) ---------- 139

Figure 38 Section (x10) stained for pimonidazole (red) and CyclinA (brown ---------- 139

Figure 39 Section (x20) showing Ki67 stain across a largely oxic region---------- 142

Figure 40 Quartile box plots of overall Ki67 (left) and CyclinA (right) proliferation index ---- 142

Figure 41 Section (x20) showing CyclinA stain across a largely oxic region, demonstrating regions with no proliferation and no hypoxia ---------- 144

Figure 42 Plots of the median and range of proliferation indices for the oxic regions, hypoxic regions distant from vessels and hypoxic regions close to vessels for each tumour. ------- 156

Figure 43 Plots of CyclinA proliferative index against hypoxic fraction for whole sample, oxic and hypoxic compartments ---------- 157

Figure 44 Plots of Ki67 proliferative index against hypoxic fraction for whole sample, oxic and hypoxic compartments ---------- 158

Figure 45 CyclinA index vs Ki67 index for whole tumour section, hypoxic and oxic compartments for each tumour ---------- 159

Figure 46 An example of a 'hypoxic field': . ---------- 171

Figure 47 An example of a 'hot spot' of vessels ---------- 171

Figure 48 An example of an oxic field: the vessels ---------- 172

Figure 49 Image (x10) showing the assessment of vessel-hypoxia distance, ---------- 175

Figure 50 A histogram of the coefficient of variations of vascularity ---------- 178

Figure 51 Comparison of vascular density in oxic and hypoxic regions ---------- 179

Figure 52 Scatter plot of the vascularity in oxic and hypoxic regions of each individual tumour, showing strong correlation in the two compartments. ---------- 182

Figure 53 Histogram of the hotspot count for each tumour, The highest count found in each tumour was assigned. ---------- 183

Figure 54 Comparison of hot spot counts in oxic and hypoxic regions of tumour. Black points represent the highest hot spot count in each field assessed; green lines show the mean with the 95% confidence intervals ---------- 185

Figure 55 Scatterplot comparing hotspot counts in oxic regions with hypoxic regions for each tumour ---------- 186

Figure 56 Plot of overall hot spot count vs overall vascular density for each tumour --------- 188

Figure 57 Plot of hot spot count vs vascular density for each tumour – hypoxic regions ---- 189

Figure 58 Plot of hot spot count vs vascular density for each tumour –oxic regions ---------- 189

Figure 59 Scatter plot of vascular density vs hypoxic fraction assessed by pimonidazole -- 190

Figure 60 Hot spot count vs hypoxic fraction assessed by pimonidazole ---------- 191

Figure 61 Scatter plot of the coefficiant of variation of vascular density vs hypoxic fraction assessed by pimonidazole ---- 192
Figure 62 Histogram of distances from vessels to hypoxia, pooled from all tumours ---- 193
Figure 63 Scatterplot of median vessel to hypoxia distance vs the pimonidazole stained fraction ---- 195
Figure 64 Scatterplot of median vessel to hypoxia distance coefficient of variation vs the pimonidazole stained fraction ---- 195
Figure 65 Schematic diagram explaining the finding of long vessel to hypoxia ---- 198
Figure 66 Image (x10) showing a vessel-hypoxia ---- 199
Figure 67 Figure illustrating variability in vessel to hypoxia distances due to the geometrical section through a vessel ---- 201
Figure 68 Variations in section angle relative to vessel orientation ---- 202
Figure 69 Schema of how fields were classified as hypoxic ---- 206
Figure 70 Schematic diagram of the various stages of evolution of angiogenesis ---- 207
Figure 71 Three images showing images of the same region of bladder tumour stained for GLUT1, CA9 with CD31/34 and pimonidazole with CD31/34 ---- 212
Figure 72 Histogram of CA9 stained fractions ---- 215
Figure 73 Histogram of GLUT1 stained fractions ---- 215
Figure 74 Plot of Carbonic Anhydrase 9 stained area against pimonidazole stained area - 216
Figure 75 Plot of GLUT1 stained area against pimonidazole stained area ---- 216
Figure 76 The absolute percentage difference between the area of pimonidazole and CA9 staining for each tumour ---- 218
Figure 77 The absolute percentage difference between the area of pimonidazole and GLUT1 staining for each tumour ---- 218
Figure 78 The absolute percentage difference between the area of CA9 and GLUT1 staining for each tumour ---- 219
Figure 79 Plot of the median vessel to stain ---- 222
Figure 80 Plot of the mean vessel to stain distances ---- 225
Figure 81 Histogram of vessel to CA9 stain distances ---- 226

Figure 82 Histogram of vessel to GLUT1 stain distances ---------- 226

Figure 83 Comparison of vessel to pimonidazole and vessel to CA9 distances ---------- 227

Figure 84 Comparison of vessel to pimonidazole and vessel to GLUT1 distances ---------- 228

Figure 85 Example of a field at low magnification with good overall co-localisation --------- 230

Figure 86 Example of more extensive staining for pimonidazole and relatively little staining for GLUT1 and CA9---------- 231

Figure 87 Example of a field at low magnification with good overall co-localisation of each stain for hypoxia ---------- 232

Figure 88 Example of a field at low magnification with moderate overall co-localisation of each stain for hypoxia, but with similar stained fraction for each marker---------- 233

Figure 89 An example of a field at high magnification (x20) with good co-localisation of each stain for hypoxia ---------- 234

Figure 90 An example of a field at high magnification (x20) with good co-localisation of each stain for hypoxia ---------- 235

Figure 91 Low power (x5) images of CA9 + Ki67(upper panel) and GLUT1 + CD31/34 (lower panel) stains of archived sections of bladder carcinoma ---------- 245

Figure 92 Plot of CA9 stained fraction against GLUT1 stained fraction---------- 246

Figure 93 Plot of vessel density against hot spot count for each patient ---------- 247

Figure 94 Overall survival plot comparing CA9 fraction---------- 250

Figure 95 Overall survival plot comparing GLUT1 fraction ---------- 250

Figure 96 Cause specific survival plot comparing CA9 fraction---------- 251

Figure 97 Cause specific survival plot comparing GLUT1 fraction ---------- 251

Figure 98 The pattern of recurrence and death in the cohort of 64 patients ---------- 252

Figure 99 Cause specific survival plot comparing CA9 fraction in recurrent disease -------- 253

Figure 100 Cause specific survival plot comparing GLUT1 fraction in recurrent disease -- 254

List of Tables

Table 1 Characteristics of the members of the bHLH/PAS family of proteins 59

Table 2 Gene products upregulated by hypoxia 65

Table 3 Enzymes involved in the 2-nitroimidazole metabolism 82

Table 4 The characteristics of pimonidazole 88

Table 5 The TNM staging system for bladder carcinoma 99

Table 6 Inter-observer comparisons of total staining 118

Table 7 Inter-observer comparisons of dark staining 118

Table 8 Ki67 index in oxic, hypoxic close to vessels and hypoxic far from vessels 141

Table 9 CyclinA index in oxic, hypoxic close to vessels and hypoxic far from vessels 143

Table 10 CyclinA to Ki67 ratio in oxic and hypoxic compartments 160

Table 11 Mean vascular density and the coefficient of variation 177

Table 12 Mean vascular density in oxic and hypoxic regions 181

Table 13 Hot spot count by oxic region 187

Table 14 Median and range of vessel to hypoxia distance for each tumour 194

Table 15 Stained fractions, number, median and rangeof vessel to stain distances 221

Table 16 Mean, SD, and coefficient of variation for the vessel to stain distances. 223

Table 17 Mean vessel to stain distances for each tumour 224

Table 18 Characteristics of study population and available patients 241

Table 19 Median values and ranges of biological parameters assessed 246

Table 20 Number of failures and censored observations in survival analyses 248

Table 21 Results of univariate analysis of overall survival (all cause) 248

Table 22 Results of univariate analysis of cause specific survival 248

Table 23 Results of univariate analysis of local recurrence free survival 249

Table 24 Results of univariate analysis of metastasis free survival 249

Table 25 Risk Ratios for each prognostic parameter for overall survival including CA9 255

Table 26 Risk Ratios for each prognostic parameter for overall survival including GLUT1 255

Table 27 Risk Ratios for cause specific survival including CA9 256

Table 28 Risk Ratios for cause specific survival including GLUT1 256

Table 29 Risk Ratios for local recurrence free survival including CA9 256

Table 30 Risk Ratios for local recurrence free survival including GLUT1 257

Table 31 Risk Ratios for metastasis free survival including CA9 257

Table 32 Risk Ratios for metastasis free survival including GLUT1 257

CHAPTER ONE

INTRODUCTION

Tumour Hypoxia

The influence of hypoxia on the treatment and biological behaviour of cancer is well established, nearly 100 years after the first published reference to the oxygen effect in radiotherapy. A clinically applicable method of determining tumour oxygenation, the polarographic oxygen electrode, became available in the late 1980's. It confirmed hypoxia as a common and influential feature of cancers and stimulated efforts to quantify hypoxia by other means. More recently, advances in molecular biology have revealed complex oxygen-regulated pathways in cellular gene expression. The following introduction to this thesis reviews the discovery, measurement and manipulation of tumour hypoxia from a historical perspective.

Definition and Discovery of Tumour Hypoxia

Hypoxia in normal cells, tissues or organs arises from an inadequate supply of oxygen that limits normal function (1). An inadequate oxygen supply can arise from a deficit at any point along the chain of supply, from a low pO_2 in arterial blood, inability of haemoglobin to carry O_2, poor tissue perfusion through inadequate vascular capacity or geometry, or a block in the intracellular O_2 pathway. Increased cellular O_2 consumption will lead to an increase in blood supply through homeostatic mechanisms, which, if defective, will also lead to cellular hypoxia (2).

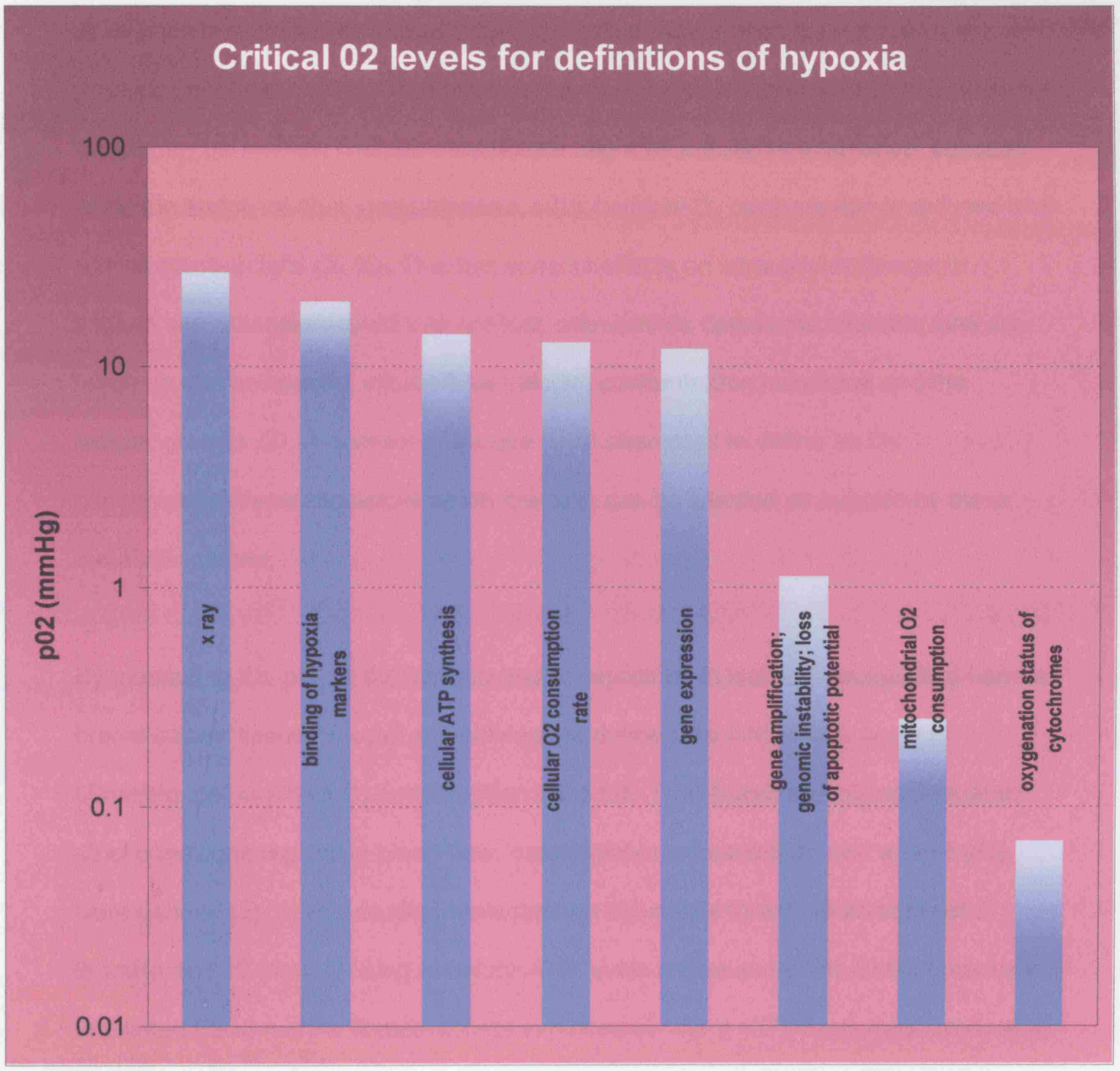

Figure 1 Critical O_2 levels that characterise the upper limit of the hypoxic range, below which activities or specific functions of tumour cells progressively change. The bars indicate the respective hypoxic ranges, with the lengths of the graded colour showing the variation in threshold values as found by various authors for different end points. pO_2 = O_2 partial pressure; mmHg = millimetres of mercury (adapted from (3))

Whilst hypoxia can be defined as a level of O_2 that leads to a loss of normal physiological function (4) it cannot be applied to tumours because normal physiological function has been impaired; tumour hypoxia therefore has to be defined by another parameter. Cellular metabolism might be a suitable alternative, because when the supply of O_2 is compromised, mitochondrial O_2 consumption is reduced and ATP production falls (5) (6). This has specific effects on intracellular transport: sodium and potassium gradients are lost, membranes depolarise, chloride ions are taken up, the cell swells, intracellular calcium concentration increases and the cellular pH falls (2). A number of groups have attempted to define an O_2 concentration threshold below which the cells can be labelled as hypoxic by these metabolic criteria.

By measuring the pO_2 at the venous end of capillaries in isolated xenografted human breast cancer tissue, Vaupel and colleagues defined the critical pO_2 as 45 to 50mmHg, below which O_2 consumption rates fall. This, however, only applies when strict conditions regarding blood flow, haemoglobin concentration and arterial pO_2 were defined (5). In vivo studies have defined the critical threshold as between 8mmHg and 10 mmHg, using absolute ATP levels as the end point. Subcutaneously implanted FSaII murine fibrosarcomas exhibited constant ATP levels measured using quantitative bioluminescence and photon imaging when pO_2 levels were maintained above 10mmHg. Median pO_2 levels less than 10mmHg led to cellular acidosis, ATP depletion and increases levels of inorganic phosphate (7). Mitochondrial O_2 consumption (oxidative phosphorylation) has been monitored in varying pO_2 environments in a number of in vitro studies. The thresholds vary between 0.5mmHg to 1mmHg, although one study using neuroblastoma cells defined a threshold of 8 -

10mmHg. The data vary according to the exact experimental conditions, the cell line used as the model and the characteristics of the culture medium (8-10). A pragmatic way of defining tumour hypoxia is to define a level of O_2 below which treatment is less effective. The basis for this originates from the first clinical observation of the influence of hypoxia on radiotherapy in 1909 by Gottwald Schwartz (11). He showed the radiation response of skin was reduced when compressed reducing blood flow, and thus oxygenation. Mottram in 1935 supported the hypothesis that "cells under anaerobiosis are relatively insensitive to radiation" with experiments on tar warts in mice. Eight of fourteen warts demonstrated less cell damage close to stroma in response to gamma radiation. He suggested that variation in tumour radiosensitivity depends on the size of tumour islands within a mass, which in turn governs the proportion of cells at a significant distance from vessels. This was the first time diffusion dependent hypoxia was suggested as a concept. Mottram observed that this phenomenon also exists in testicular irradiation, where spermatids distant from blood vessel continue to produce spermatozoa, even when the dose given is large enough to cause sterility (12). In 1942, two further papers described experiments showing that anoxic mice survived higher doses of whole body radiation (13) (14). Manipulating tissue oxygenation to overcome the hypoxia problem was shown to be feasible in a report by Hollcraft (15). The regression of lymphosarcoma xenografts produced by a fixed dose of radiation was greatest when breathing oxygen and 5% carbon dioxide, intermediate when breathing air and least when breathing 92% Nitrogen and 8% oxygen at the time of irradiation.

The relationship of radiosensitivity to varying oxygenation had been demonstrated in a number of plant and insect systems (16-19) but was first shown in mammals by Gray et al in 1953 in an Ehrlich mouse ascites model. A series of experiments

showed the dependence of radiosensitivity on oxygen, consistent with studies on non-mammalian cells. Cell viability was depressed by a factor of 2.5 to 3 when irradiated in oxic conditions (100% O_2 Vs 100% nitrogen). This enhancement did not occur when densely ionising radiation was used (figure 2). They also showed that the response to radiotherapy could be increased when oxygen was given to animals under 3 atmospheres compared to 1 atmosphere pressure. An increased incidence of bone necrosis was also noted (20) (figure 3).

Tomlinson and Gray reported the first histomorphometric analysis of the effects of hypoxia in a series of human lung cancers. These tumours were characterised by a particular appearance, in which cords of tumour cells of varying sizes were surrounded by stroma containing vascular supply. The larger tumour cords had a necrotic centre surrounded by a rim of intact cells. All tumour cords with radii greater than 200μm exhibited necrosis but no necrosis was seen in tumour cords with a radius less than 160μm. The surrounding sheath of intact tumour cells never exceeded 180μm, irrespective of the size of the necrotic centre. Tomlinson and Gray postulated the variability of measured values obtained around the mean was due to both tumour cords not running exactly perpendicular to the plane of the section, and to partial blood vessel compression reducing oxygen concentration at the periphery of the cords. These distances are equivalent to the calculated distance that oxygen would be expected to diffuse through the tumour and imply a rim of viable cells exist in a chronically hypoxic state around the edge of the necrotic regions (21).

Further evidence that a sub-population of viable hypoxic cells exists in tumours came from cell survival assays of solid lymphosarcoma xenografts in mice, published in 1964. Survival curves derived from endpoint dilution assays exhibited a steep slope

at low doses and a shallower slope at higher doses. When the experiment was repeated under anoxic conditions, cell survival was increased and the slope matched the steeper gradient across the whole dose. The proportion of hypoxic cells was estimated to be about 1% from the ratio of the cell survival in each experiment (22) (figure 4). Latterly the range of hypoxic cells in air breathing animals has been estimated to be in the range of 10 to 20% (23).

In this thesis, radiobiological hypoxia is used to define hypoxia, where the efficacy of cell kill by ionising radiation is reduced at lower levels of oxygen, generally taken as less than 10mmHg (3).

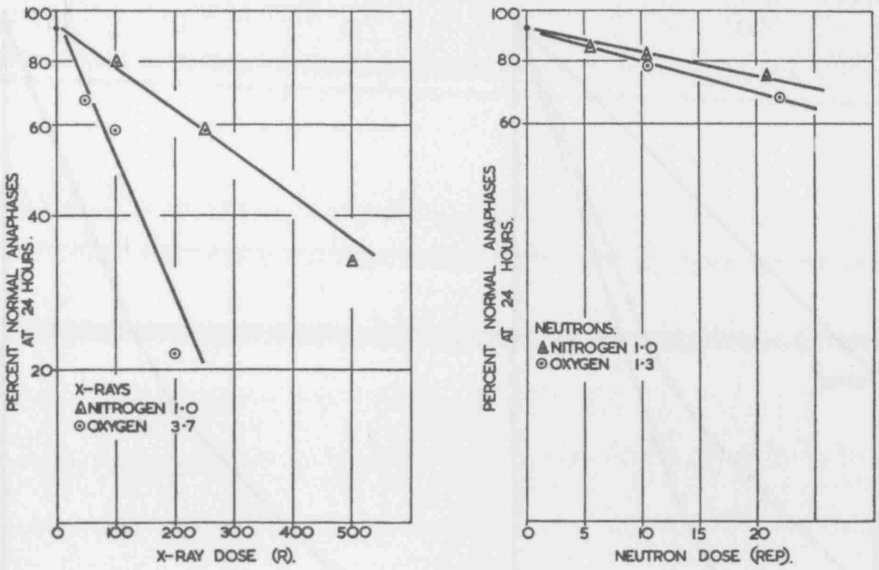

Figure 2 Comparison between the effect of oxygen tension on cytological damage induced in mouse ascites cells by x-rays and neutrons (20)

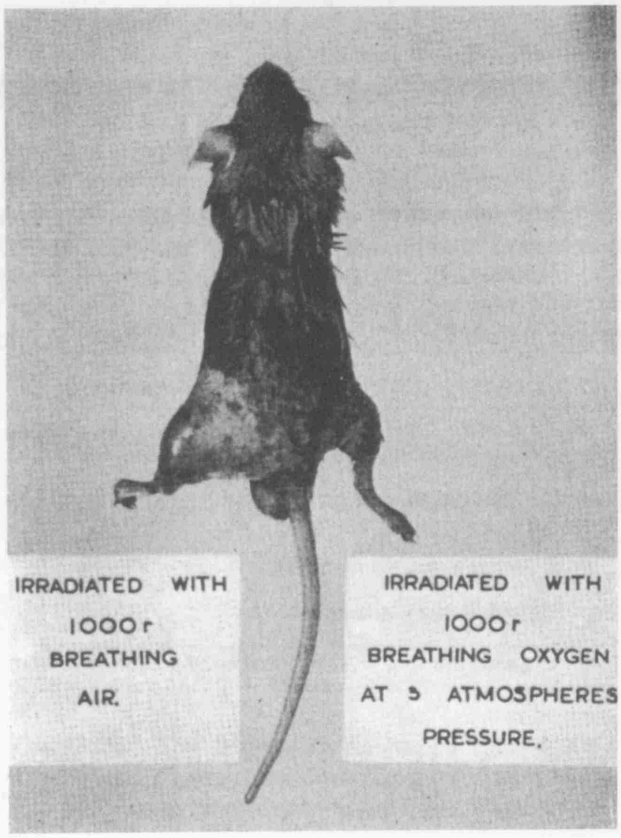

Figure 3 The differing response to radiotherapy of a tumour implanted in the mouse hind leg whilst breathing air (left leg) or oxygen right leg in an experiment performed by Gray (20)

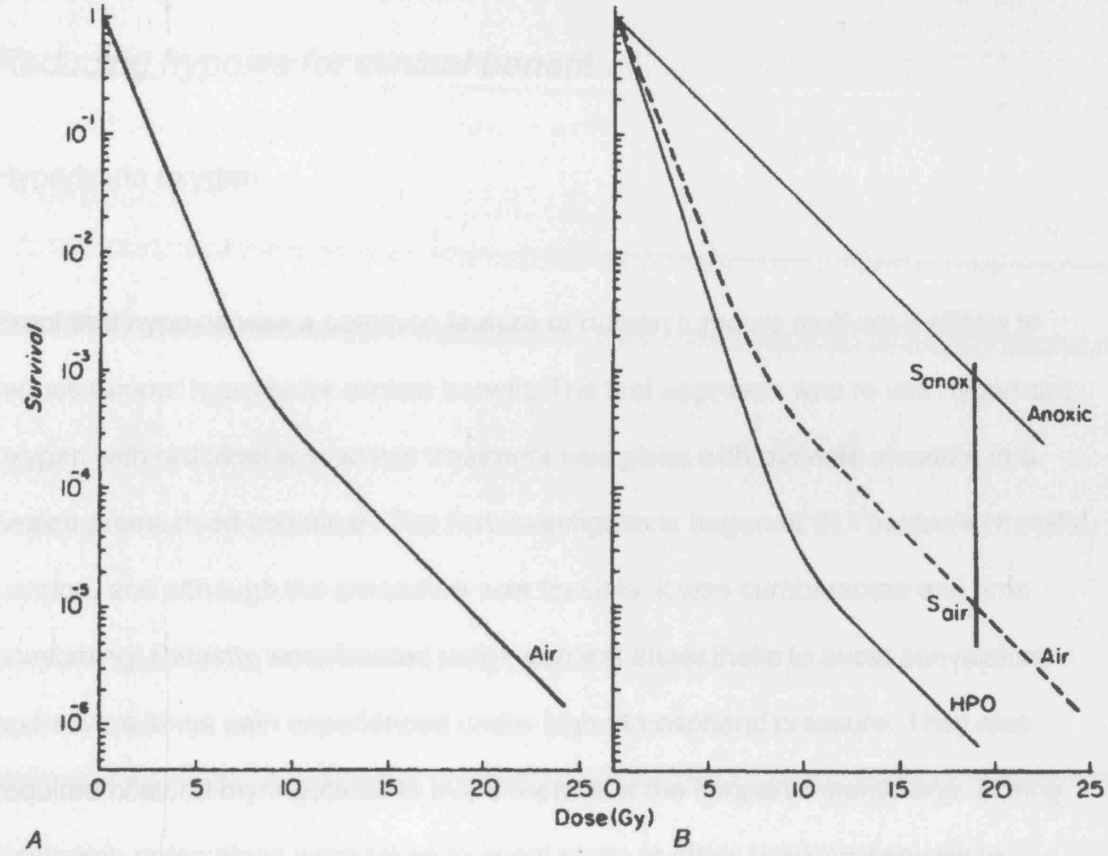

Figure 4 The influence of a subpopulation of cells on the survival curve obtained for an irradiated tumour. A. The curve was obtained when tumours were irradiated insitu in air breathing animals; the curve has two components with two different slopes. B- The curves marked Anoxic and HPO were obtained when the animals were killed or given high pressure oxygen to breathe before irradiation, respectively. The dotted line marked 'air' is from curve A (22).

Reducing hypoxia for clinical benefit

Hyperbaric oxygen

Proof that hypoxia was a common feature of human tumours motivated efforts to reduce tumour hypoxia for clinical benefit. The first approach was to use hyperbaric oxygen with radiotherapy, where treatment was given with patients encased in a sealed pressurised container. The first investigations began at St.Thomas's Hospital, London, and although the procedure was feasible, it was cumbersome and time consuming. Patients were treated under general anaesthetic to avoid convulsions and severe sinus pain experienced under high atmospheric pressure. They also required bilateral myringotomy to avoid rupture of the tympanic membrane. During treatment, precautions were taken to avoid static or other sparking dangers to prevent explosion. Each field took an average of 40 minutes to treat and after treatment between 7 and 15 minutes were spent slowly reducing the pressure from 3 atmospheres to normal. The first report by Churchill Davidson described how patients with large tumours were treated using two adjacent fields. One half of the tumour was treated at normal atmospheric pressure and the other half at three atmospheres to a dose of 1000 to 1500 rad in a single fraction. Either a biopsy from each field was taken or the whole tumour excised. In six of eight patients treated, the tumour irradiated in high-pressure oxygen conditions displayed more damage, as assessed by a histopathologist (24)

Over the next 30 years a series of clinical trials were reported focussing on the treatment of head and neck, bladder, lung and cervix cancers. Although the trials of

hyperbaric oxygen (HBO) in head and neck carcinoma were small and employed unconventional fractionation regimens, some realised significant improvement in local control. The largest of these trials, performed in Cardiff (25) used a ten-fraction schedule, randomising patients to receive the treatment in either air or HBO. A significantly improved local control in the HBO group was seen, but morbidity was greater and overall survival was equal. A second trial randomised patients to receive either the ten fraction HBO regimen or a 30 fraction treatment over six weeks. Doses were reduced in larger volume treatments to equalise normal tissue effects in the test and standard arms of the trial. Again, an improved local control was seen in the HBO arm, but with a reduction in morbidity and an improved overall survival rate. The trial was criticised for the policy of reducing doses for larger volumes, and the number of patients who were deemed unfit to be treated in the hyperbaric chamber.

Trials in cervix carcinoma performed in the UK, South Africa and the USA have shown no clear benefit for HBO (26-28). A statistically significant benefit was seen in the UK trial run by the Medical Research Council; an increase in tumour control of 20% to 24% at 5 years occurred, the benefit being greatest in those younger than 55 years with stage III disease. However, the studies performed in Cape Town, Houston and Leeds (UK) showed no significant benefit.

The MRC also ran a trial in bladder cancer (29) randomising 241 patients with no benefit to HBO after 13 years of follow up. Trials by Plenk (30) and Brenk (31) did show benefit to HBO but the interpretation was difficult as the trials were small (40 and 16 patients respectively), different fractionation regimens were used in each arm of each trial, and morbidity was not reported.

The bronchial carcinoma trials were largely negative for any benefit to HBO but a trial performed at Portsmouth that used six 600 rad fractions in 18 days led to improved survival (32). The two and four year survival for the HBO arm was 24.6% and 15.9% versus 12.4% and 2.5% in the air-breathing arm. Earlier trials at the same centre used smaller fraction sizes (6000 rad in 40 fractions and 4500 rad in 30 fractions) did not show any benefit to HBO.

Hyperbaric oxygen fell out of favour despite reasonably encouraging results in some sites and where larger fraction sizes were used. A recent meta-analysis of 17 trials of HBO defined an odds ratio of 1.3 (95% CI 1.13 to 1.48) in its favour (33). The absolute improvement in local control was 6.6%. The negative trials may have failed because hypoxia was not a limiting factor in the treatment, from either reoxygenation or a lack of stratification. Another possibility is that hyperbaric oxygen reversed hypoxia in only a proportion of cells. Practically, a combination of poor patient compliance, the time it took to perform, and the emotional reaction to "having one of these monsters" (34) in the radiotherapy department led to the demise of HBO. The presence of hypoxia and its modification was proven however, and attention turned to the hypoxic cell radiosensitisers. Giving patients a tablet to counteract hypoxia in tumours was much more attractive than the cumbersome hyperbaric chamber.

Hypoxic cell radiosensitisers

Hypoxic cell sensitisers were developed on the basis that oxygen enhanced radiosensitivity due to its electron affinity. A group of compounds was found to act in a similar way to oxygen in combination with radiation, reacting with radiation induced

free radicals and preventing repair. After early work on nitrobenzene and nitrofuran compounds, the nitroimidazoles were found to be potent (figure 5)(35). Metronidazole was the first to undergo clinical trials as a radiosensitiser in patients with glioblastoma multiforme in 1973. The dose of 6g per m^2 was ten times higher than when the drug was used as an antibiotic and gastrointestinal toxicity was dose limiting. Two studies were performed, the first compared nine-fraction radiotherapy with or without metronidazole, showing a benefit in mean survival for patients receiving the drug (26 vs 15 weeks). However, the control arm appeared to have a significantly lower survival rate than would be expected. The second study showed no difference between nine fractions of radiotherapy with metronidazole when compared with conventionally fractionated radiotherapy alone (36, 37). No further trials of metronidazole have been performed.

Misonidazole was first given in the clinic in 1974, supported by animal work demonstrating its potency as a radiosensitiser. A number of clinical trials testing its role were undertaken over the following 10 years, but it was generally ineffective in improving patient outcome from radiotherapy as well as producing a troublesome dose dependent peripheral neuropathy. The only positive findings emerged in a sub group of patients with pharyngeal tumours in the DAHANCA2 trial (38) and in a trial by Sealy (39) who combined misonidazole with HBO in head and neck carcinoma.

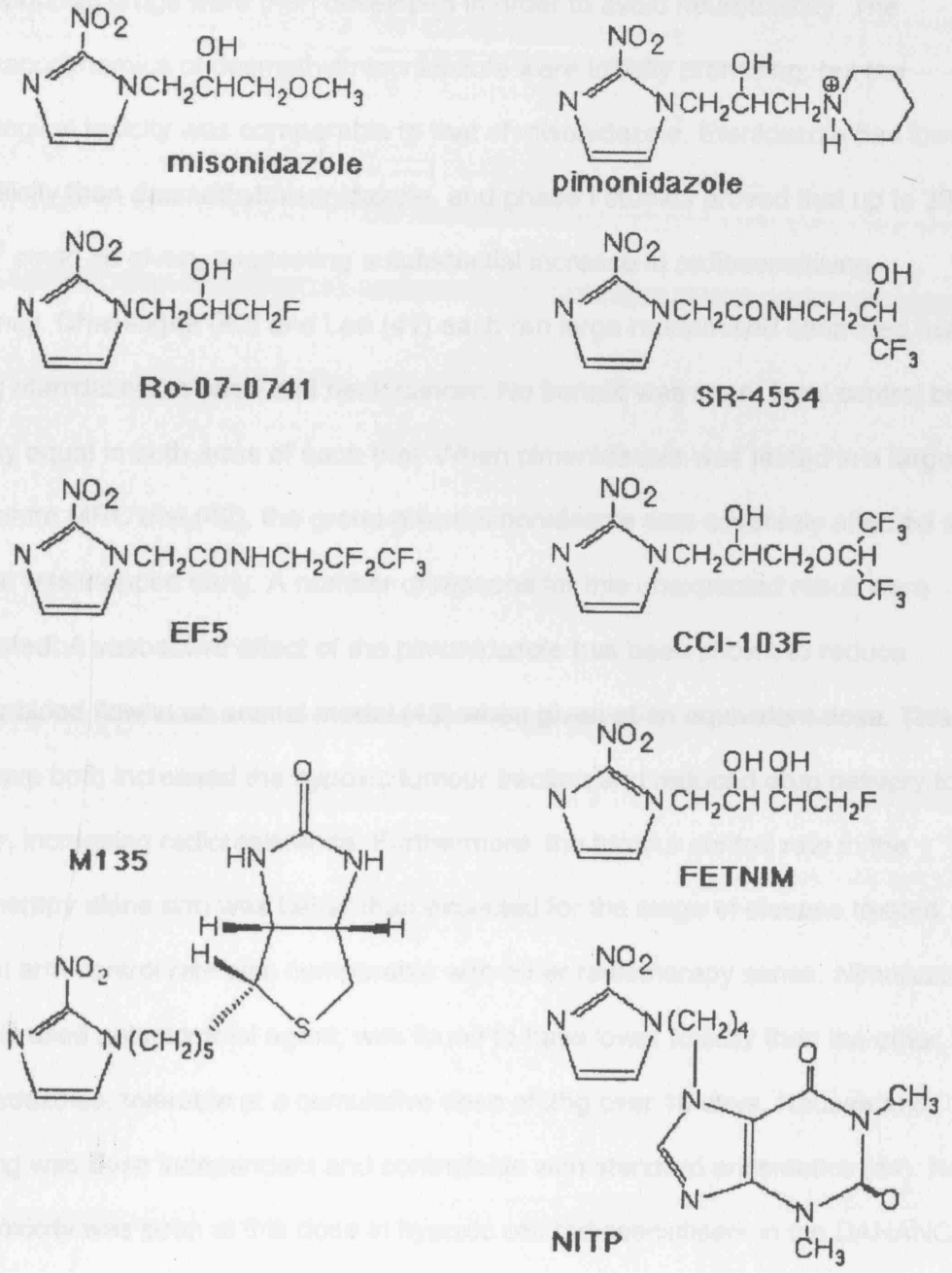

Figure 5 The chemical structures of a range of 2-nitroimidazoles

Less lipophilic drugs were then developed in order to avoid neurotoxicity. The pharmacodynamics of desmethylmisonidazole were initially promising, but the neurological toxicity was comparable to that of misonidazole. Etanidazole has lower lipophilicity than desmethylmisonidazole, and phase I studies proved that up to 30g per m^2 could be given, suggesting a substantial increase in radiosensitising efficiency. Chassagne (40) and Lee (41) each ran large randomised controlled trials testing etanidazole in head and neck cancer. No benefit was seen, local control being virtually equal in both arms of each trial. When pimonidazole was tested in a large multicentre MRC trial (42), the group given pimonidazole was adversely affected and the trial was stopped early. A number of reasons for this unexpected result were suggested. A vasoactive effect of the pimonidazole has been shown to reduce tumour blood flow in an animal model (43) when given at an equivalent dose. This may have both increased the hypoxic tumour fraction and reduced drug delivery to tumour, increasing radioresistance. Furthermore, the tumour control rate in the radiotherapy alone arm was better than expected for the stage of disease treated, but the test arm control rate was comparable with other radiotherapy series. Nimorazole, a widely used antimicrobial agent, was found to have lower toxicity than the other nitroimidazoles, tolerable at a cumulative dose of 25g over 10 days. Nausea and vomiting was dose independent and controllable with standard antiemetics (44). No neurotoxicity was seen at this dose in hypoxic cell radiosensitisers in the DAHANCA studies (45) but a phase I study of Continuous Hyperfractionated Accelerated Radiotherapy (CHART) with nimorazole in head and neck carcinoma, two patients suffered mild parasthesia at a cumulative dose of 28.8g per m^2 over 12 days (46). The Phase III DAHANCA trial randomised 422 patients to receive nimorazole or placebo in combination with radiotherapy to a dose of 62-68 Gy. Better loco-regional

control was seen in the nimorazole group (49 vs 33%, p=0.002). The 10-year actuarial overall survival reflected this benefit (26% vs 16%), but was not statistically significant (p=0.32). As a result of this trial, the use of nimorazole has become standard in the treatment of most head and neck cancers in Denmark, 28 years after the first clinical trial in hypoxic cell radiosensitisers.

Normobaric oxygen – carbogen gas breathing

Parallel to the hyperbaric trials, a number of animal experiments demonstrated the feasibility of high concentration oxygen gas breathing. Normobaric oxygen is attractive as a radiosensitising stratagem due to its low toxicity, ease of administration and low cost. Hollcraft's paper (15) showed the regression of lymphosarcoma xenografts produced by a fixed dose of radiation was greatest when breathing oxygen and 5% carbon dioxide. It was intermediate when breathing air and least when breathing 92% Nitrogen and 8% oxygen at the time of irradiation. In order to reproduce clinical conditions more closely, du Sault performed a similar experiment using *spontaneous* mammary adenocarcinomas in mice. An increased response was seen in those irradiated whilst breathing normobaric 95% oxygen/5% carbon dioxide (carbogen) compared with air. In a further study (47) the treatment was repeated, treating mice in either normobaric air, normobaric pure oxygen or hyperbaric oxygen (3 atmospheres). There was little difference in the cure rates between the pure oxygen and the normobaric air group, but the hyperbaric group had markedly improved cure rates. These two experiments taken together seemed to show that a low concentration of carbon dioxide had a beneficial effect. Carbon dioxide was known to vasodilate and increase the respiratory and heart rate, thus

increasing tissue oxygen delivery. To verify this observation, the experiment was repeated again, comparing cure rates between mice breathing air, normobaric carbogen or hyperbaric carbogen. Here the normobaric carbogen showed a marked improvement over air and normobaric oxygen. The hyperbaric oxygen/carbon dioxide mixture was equivalent in effect to hyperbaric pure oxygen. Furthermore, the highest early death rate was in those treated with normobaric pure oxygen, and the lowest was in those treated with the normobaric carbogen. These results suggested that carbogen, given at normal atmospheric pressure had the best therapeutic ratio of these methods (figure 6). After confirmatory studies (48), the RTOG undertook a multicentre randomised study of carbogen breathing in patients with tumours of the head and neck and oesophagus. Those randomised to the treatment arm breathed 100% oxygen prior to radiotherapy followed by a 10 to 20 minute period of 5% carbogen gas during radiotherapy. Three hundred and thirty nine patients were randomised and 315 completed treatment as planned. No benefit was seen from carbogen gas breathing in local control or overall survival. Similar lack of benefit was seen in studies of carbogen breathing in cervix (49). The failure of carbogen in these studies may have been because of the short pre-irradiation breathing times employed, typically half a minute before the start of treatment. A number of animal studies indicated that at least 5 minutes of pre-treatment gas breathing significantly reduced the hypoxic fraction and improved radiation response of tumours compared to pre-irradiation breathing times of under a minute (50). It was not until the discovery of 'acute' hypoxia that the use of carbogen gas to reduce tumour hypoxia came back under investigation.

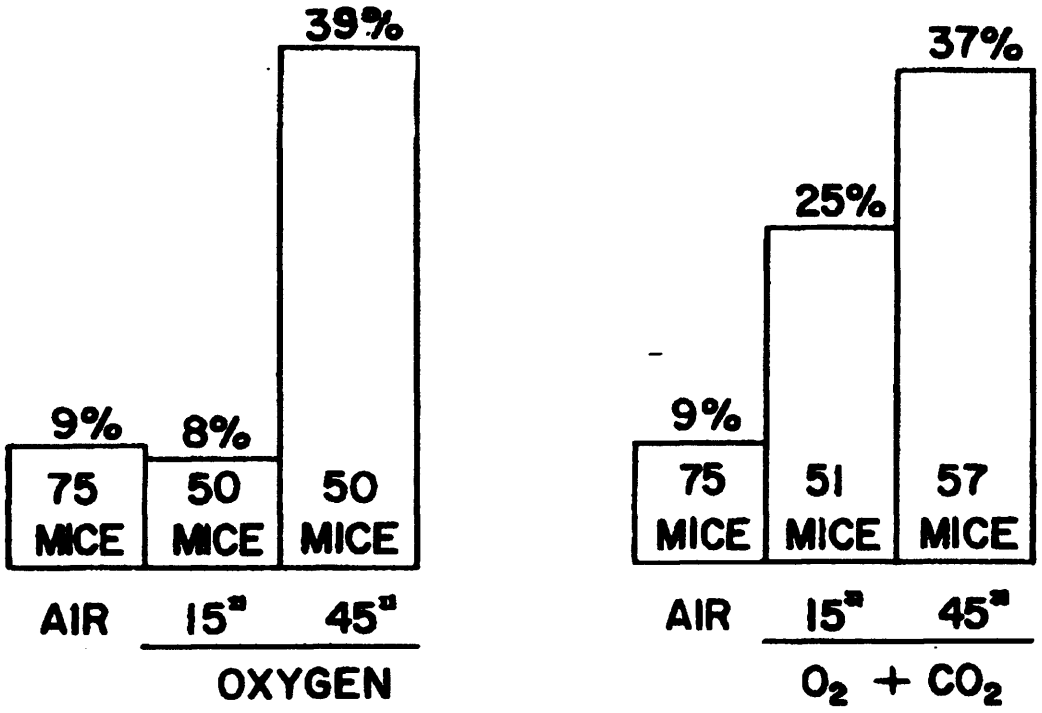

Figure 6 *Left panel*: Cure rates of treated tumours in mice completing the planned treatment of 1000R twice a week to 600R in 18 days whilst breathing air, pure oxygen at 1 atmosphere, or pure oxygen at 3 atmospheres respectively. *Right panel*: Cure rates of treated tumours in mice completing the planned treatment of 1000R twice a week to 6000R in 18 days whilst breathing air, 95% oxygen + 5% carbon dioxide at 1 atmosphere, or at 3 atmospheres respectively (From du Sault (47))

'Acute' Hypoxia

A second model of hypoxia in tumours was proposed whilst investigations of the radiosensitisers and gas breathing were ongoing. In animal studies of tumours implanted between closely applied parallel windows ('sandwich' tumours) blood flow was seen to slow down or stop in individual blood vessels (51). Other studies in similar experimental arrangements revealed that tumours regrew in well vascularised peripheral regions after high dose radiotherapy. Resistant cells were distant from necrosis and close to vasculature, suggesting these cells may have been temporarily hypoxic at the time of irradiation from a transient cessation in local blood flow and oxygen supply (52). Further work by Brown added weight to the concept of 'acute' hypoxia (53). EMT6 cells were implanted into mice that were infused with misonidazole, which is cytotoxic to hypoxic cells only. The hypoxic fraction of 7% found in the remaining tumour cells was calculated by determining the cell survival curve from the mice irradiated in air or immediately after sacrifice. This compared with a hypoxic fraction of 19% in controls. Histological examination of the tumours showed that the cells that had survived misonidazole treatment were close to the edge of the tumour mass, around a region of dead cells. This suggested they were not hypoxic at the time of misonidazole administration, but were at the time of irradiation. They were therefore fluctuating between normoxic and hypoxic states. A second study used the RIF 1 cell line, injected intradermally into the flanks and into the muscle of the right hind legs of a number of mice. The skin of the flank has a relatively poor blood supply whereas the muscle has a copious supply. Once the tumours had established, the mice were irradiated at various doses whilst either breathing air or soon after killing. Cell survival curves were constructed. Muscle

implanted tumours were assumed to contain only chronically hypoxic cells as the 'more vigorous' blood supply was thought to be less susceptible to temporary closure and thus not give rise to acute hypoxia. Chronically hypoxic cells were deemed to be of intermediate radioresistance, based on work done in spheroids (54). This was supported by the data obtained: cell survival curves showed that acutely hypoxic tumours (dead mice), whether in the flank or muscle were less radiosensitive and had a shallower cell survival curve than the tumours in the muscle in air breathing mice. In the flank tumours in the air-breathing mice, however, the slope of the terminal portion of the cell survival curve was parallel to the curve in the anoxic mice, and significantly shallower than the muscle implanted tumours. This led to the conclusion that acutely hypoxic cells were more radioresistant than chronically hypoxic cells in vivo (figure 7).

The first direct evidence of acutely hypoxic cells arising from short term changes in blood flow was shown in a murine squamous cell carcinoma line (SCCVII), using a fluorescence cell sorting technique and a bisbenzamide flourochrome, Hoechst 33342 (55). Hoechst diffuses quickly from blood but remains bound within cells with a half-life of 2 hours. This technique allows cells to be distinguished according to their proximity to vessels by the intensity of staining by Hoechst. The experiment involved separating cells of previously irradiated tumours into ten sub-populations according to the intensity of the Hoechst stain, and performing clonagenic assays on each of these. The Hoechst stain was injected twenty minutes before irradiation in either oxic or anoxic (clamped) conditions; a range of tumour sizes were used. The surviving fraction varied most across staining intensity categories among small tumours and least among the larger tumours. This may have been due to acute hypoxia occurring in the larger tumours. Cells categorised as being close to vessels implies those

vessels were patent at the time of injection, but not necessarily at the time of irradiation, when they might be acutely hypoxic and thus radioresistant leading to a greater surviving fraction. To assess this hypothesis further, a series of large tumours was irradiated whilst Hoechst was infused at a rate of 32μl/min. This was compared with results obtained from a group where the Hoechst was injected quickly over 20 minutes (figure 8).

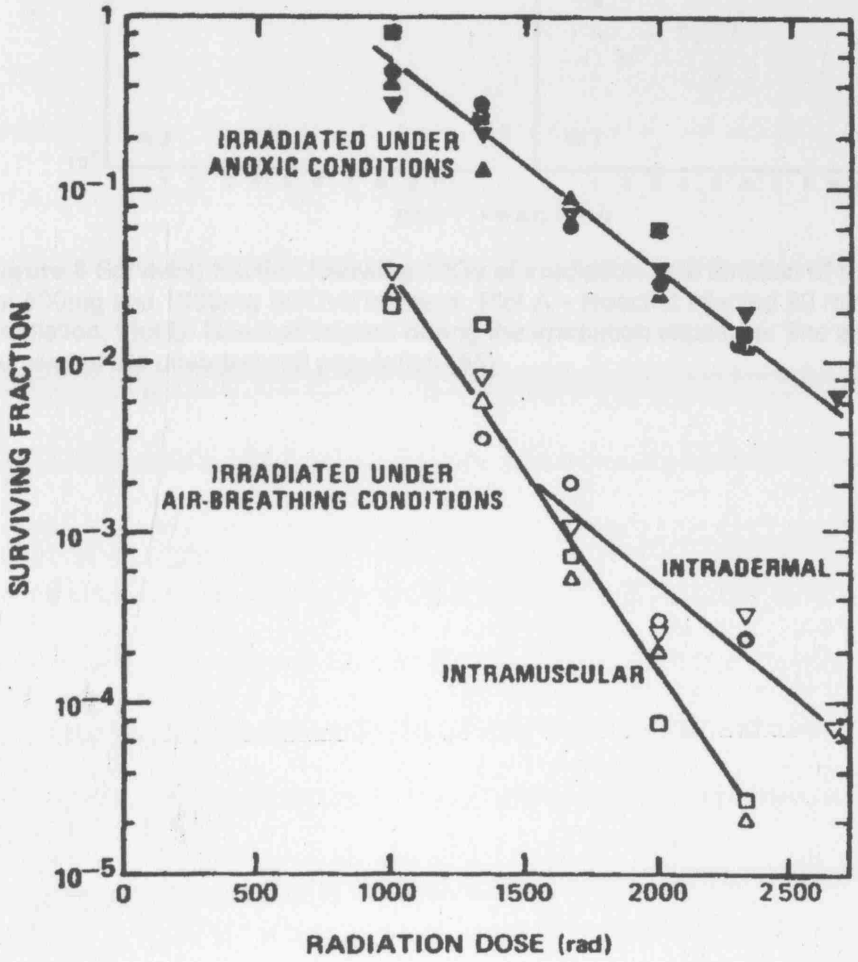

Figure 7 Radiation cell survival curves of the RIF 1 tumour implanted either intramuscularly (solid and open square, solid and open up pointing triangle) or intradermally (solid and open circle, solid and open down pointing triangle). The mice were not anaesthetised for irradiation under air breathing and anoxic conditions (54)

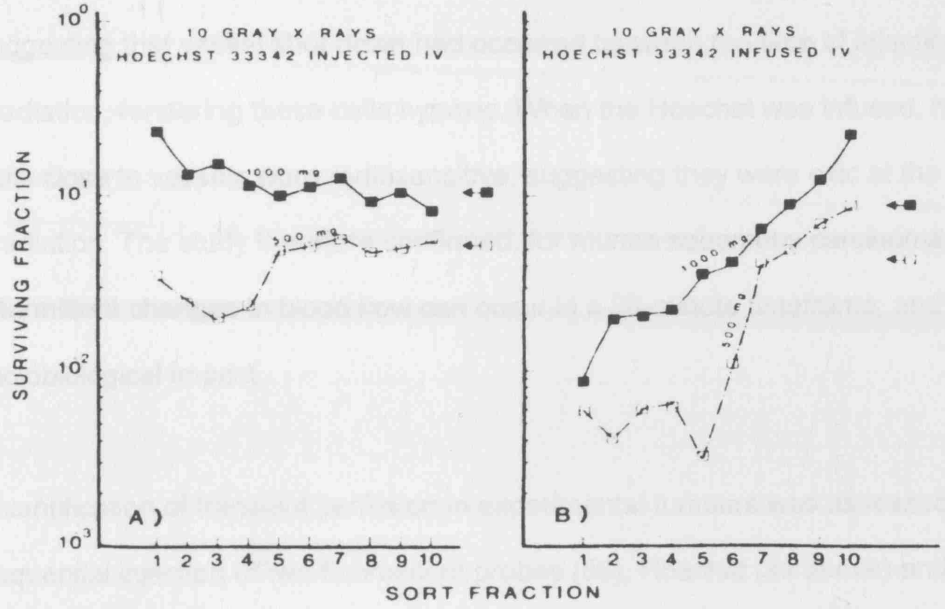

Figure 8 Surviving fraction following 10Gy of irradiation as a function of fluorescence intensity for 500mg and 1000mg SCCVII tumours. Plot A – Hoechst injected 20 minutes prior to irradiation. Plot B- Hoechst infused during the irradiation exposure. The arrows indicate the survival of the unsorted cell population (55)

When Hoechst was injected, the cells close to vessels were resistant to killing, suggesting that vessel shut down had occurred between the time of injection and irradiation, rendering these cells hypoxic. When the Hoechst was infused, however, cells close to vessels were radiosensitive, suggesting they were oxic at the time of irradiation. The study therefore confirmed, for murine squamous carcinoma SCCVII, intermittent changes in blood flow can occur in a 20-minute timeframe, and have a radiobiological impact.

Quantification of transient perfusion in experimental tumours was assessed using sequential injection of two fluorescent probes (56), Hoechst (as above) and $DiOC_7$, a stain that also diffuses from vessels but fluoresces green on blue light excitation. Sequential injection of these probes into tumour bearing mice results in two patterns of perfusion, such that regions staining with one probe but not the other demarcate where the blood flow has altered in the time between injections. In these studies, the probes were injected into mice bearing the SCCVII tumours using a schedule in which Hoechst was injected first followed by the $DiOC_7$ after 20 minutes. The mice were sacrificed 5 minutes later and the tumours sectioned. Vessels were counted, and the proportion of these surrounded by cells labelled with one stain (mismatched stain) were assessed. The perfusion mismatch was determined for both central and peripheral regions. Mismatched labelling was found in 8.9% +/- 2.4% (+/- 1SD), suggesting complete closure lasting at least 5 minutes (Hoechst labels cells close to vessels for 5 minutes post injection). The regions of transient blood flow were distributed through the sections, with no discernible pattern to the distribution. There were very few regions that exhibited neither stain, suggesting that long periods of intermittent vessel shut down were rare in this model, and that cycling times were approximately 5 minutes. Shorter cycling times would not have been detected with

this method. This dual marker technique was repeated in number of tumour models (57), and confirmed that temporal microregional fluctuations were a common feature. However, the kinetics of intermittent vascular patency were unresolved and the stains only demonstrated regions of plasma flow and not red cell flow.

The development of the multichannel laser Doppler system that allows real-time microregional blood flow recording has been used in several investigations, first in mouse tumours and eventually in human tumours. The first study in mouse tumours used a murine adenocarcinoma and an anaplastic sarcoma line (58). Red cell flux was measured in up to four sites in each tumour over a period of one hour. Overall, when traces from all tumour readings were averaged, no variation in flux was seen. However, temporal changes were visible in some individual tumours. The magnitude of change varied by a factor of 2 in 50% and by a factor of 5 in 20% of regions. The study demonstrated any change in red cell flux was reversible, as 20% of fluctuations returned to their baseline level. The cycles lasted between 6 and 45 minutes, and the time from minimum to maximum flow was typically 10 to 20 minutes. The model and technique confirmed that the acute hypoxia seen in radiobiological studies was most probably dependent on fluctuating perfusion. Laser Doppler probes have also been used to assess microregional red cell perfusion characteristics in human tumours (59). Six probes were inserted into a series of accessible human tumours and flow recorded over 60 minutes. Forty-six traces were analysable. A change in red cell flux by a factor of greater than 1.5 was seen in 54% of the traces, occurring in under 20 minutes in just over half of these. The flow returned to its original level in 37% of those exhibiting a change. This study demonstrated temporal variations of blood flow in human tumours exist, in turn suggesting acute hypoxia. Such variations in flow

may result in regions of acute hypoxia, that reverse when blood flow returns to normal.

Reducing perfusion related hypoxia

As the concept of perfusion related tumour hypoxia emerged, an agent that is now thought to work by reducing this type of hypoxia came under investigation. Nicotinamide is a derivative of Vitamin B_3 that belongs to a group of compounds called the benzamide analogues. In vitro studies on the benzamide analogues started in the mid-1980s, and were shown to radiosensitise a number of tumour and fibroblast cell lines (60-63). The mode of action appeared to involve inhibition of ADP ribosyl transferase, an enzyme that catalyses the synthesis of poly-(ADP-ribose) from NAD (64). ADP ribosyl transferase has a role in modifying the ligation step in the DNA repair process and is upregulated when single and double stranded DNA breaks occur. The radiosensitisation was maintained in vivo models, but results did not support DNA repair inhibition as the mechanism of action. In two tumour lines, EMT6 and C3H, nicotinamide was detectable in appropriate concentrations within minutes of injection, yet only radiosensitised the tumour if given before or during radiation. The optimal enhancement occurred when nicotinamide was given 1 hour pre-irradiation. Nicotinamide given after radiation, when repair inhibition would have maximum impact, had no effect (65) (figure 9). Nicotinamide produced no enhancement in radiation when EMT6 and CH3 tumours were made completely anoxic by clamping the feeding artery, despite being present in radiosensitising concentrations. This contrasted with misonidazole, suggesting nicotinamide did not act as a hypoxic cell sensitiser (66). A further study in SCCVII tumours showed

nicotinamide produced a near 75% reduction in the binding of misonidazole, indicating a reduction in hypoxic fraction. This was not the case when EMT6 was grown in vitro as a multicellular spheroid, reinforcing the fact that the mechanism of action was somehow dependent on the in vivo environment. Parallel experiments using Hoechst fluorescence staining and ^{86}RbCl extraction techniques showed blood flow increased by 30 to 40% after nicotinamide injection compared to controls, with a concomitant increase in radiosensitivity (figure 10). Therefore the data confirmed that nicotinamide enhanced tumour radiation response not by DNA repair inhibition, but by increasing blood flow, and consequently reducing hypoxia.

Confirmation that acute hypoxia was reduced as well as chronic hypoxia came from studies using the SCCVII tumour (67). Nicotinamide injected into tumour bearing mice 1 hour before irradiation produced enhancement ratios of 1.3 to 1.5 where response was assessed using growth delay assay (figure 11). This enhancement was not dependent on tumour size. The tumours were also disaggregated and cells sorted according to Hoechst staining, which had been injected after nicotinamide. The highest 20% and the lowest 20% of fluorescent cells were sorted and assayed for survival. When compared with tumours not exposed to nicotinamide, (using saline injection as a control), survival increased equally in both populations. Since a proportion of the bright cells (i.e. those close to vessels) would have been hypoxic at the time of irradiation due to vessel shut down, as in Chaplin's data (68), the increase in response must have arisen from a reduction in this acute hypoxic fraction. Regions of mismatched stain in tumour sections indicated where a change in perfusion had occurred during 20-minute interval between injections. The nicotinamide treated tumours had significantly fewer mismatches than the saline group, and was equivalent to the background mismatch seen in a control group.

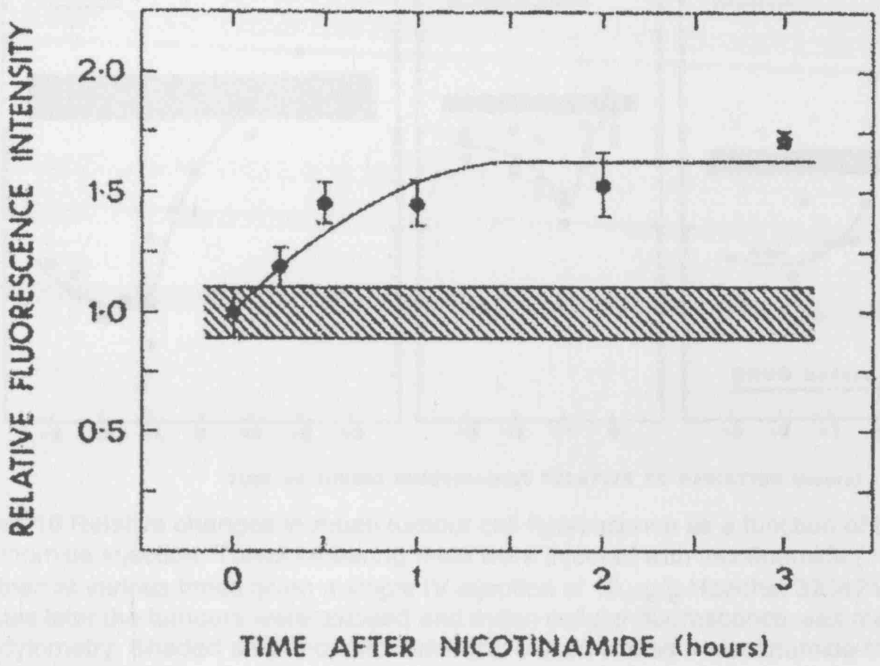

Figure 9 The effect of timing between drug administration and radiation on tumour cell survival in three tumour models. Mice were injected with saline or nicotinamide (1000 mglkg) at various times before or after irradiation with either 20 (EMT6), 12 (Lewis Lung), or 15 Gy (RIF- 1). Tumour survival was assayed 24 h after irradiation. Open circles, nicotinamide; closed circles, nicotinamide + X rays. The shaded area represents the mean response (±1 SE) for saline + X rays. Individual data points from three separate experiments are shown with the lines representing the best fit to the data by eye (65).

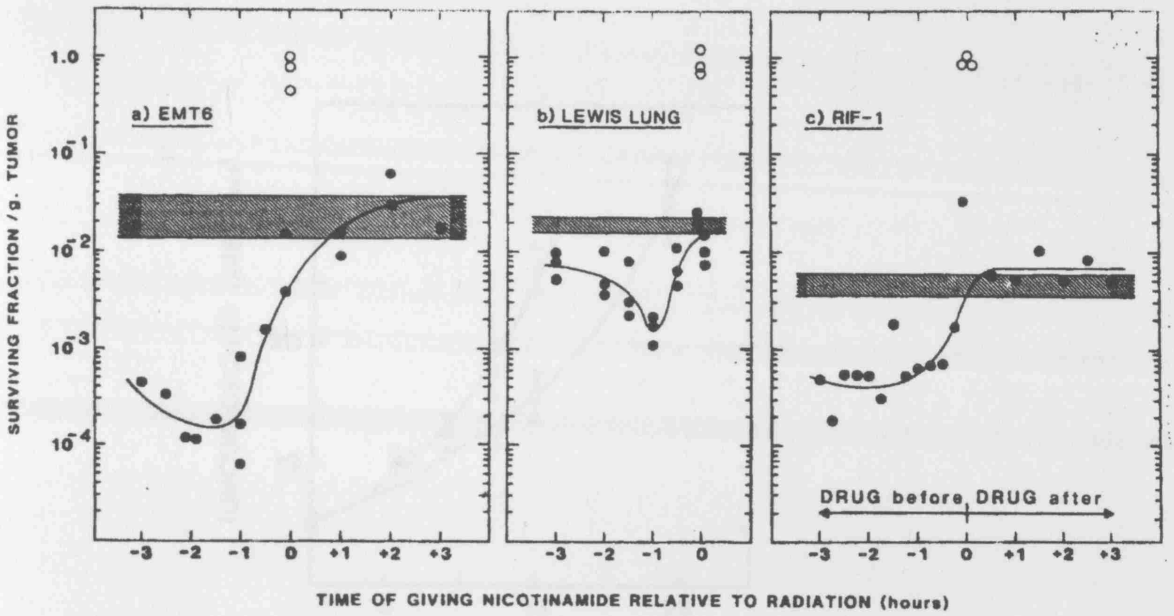

Figure 10 Relative changes in mean tumour cell fluorescence as a function of time after nicotinamide injection. Tumour-bearing mice were injected with nicotinamide (1000 mg/kg) and then at various times given a single IV injection of 10 μg/g Hoechst 333421. Twenty minutes later the tumours were excised and mean cellular fluorescence was measured by flow cytometry. Shaded area = control tumours; closed circles = nicotinamide-treated tumours, Values show the mean (66).

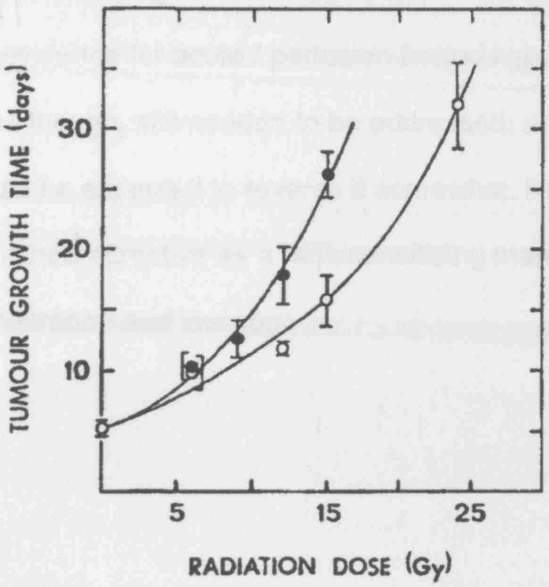

Figure 11 The effect of nicotinamide on the radiation dose response curve as measured by a regrowth delay assay. Mice with SCCVII back tumours were injected with nicotinamide (1000 mg/kg; i.p.) 1 h before irradiation with various X-ray doses. The tumour growth time represents the time in days for tumours to regrow to 3 times their treatment volume. (Open circles = X-rays alone; Closed circles=nicotinamide + X-rays.) Results show means (+/-1S.E.) for 4 to 5 mice/group (67)

The grounds for modifying tumour oxygenation in the clinic were rekindled by the experimental evidence for acute / perfusion limited hypoxia. Reversal of diffusion limited hypoxia though, still needed to be addressed, although an improvement in perfusion would be expected to reverse it somewhat. Normobaric high oxygen gas breathing remained attractive as a radiosensitising manoeuvre due to its low toxicity, ease of administration and low cost.

The return of carbogen: combination with nicotinamide

The combination of nicotinamide and carbogen gas breathing offered a method of simultaneously combating the two forms of hypoxia. The first animal study using this combination was by Chaplin et al (69). The effect of nicotinamide with Fluosol DA, a perfluorocarbon blood substitute, and carbogen breathing on the radiation response of SCCVII and KHT tumours was assessed. Fluosol DA and carbogen or nicotinamide each given alone before radiation resulted in modest improvements in cell kill by 10 to 30 %. The combination of nicotinamide and Fluosol DA/carbogen, however, resulted in an enhancement factor of 1.6; this was close to that expected for a fully oxygenated tumour. Using a fluorescence activated cell sorting technique, with the Hoechst stain, it was shown that nicotinamide significantly reduced the amount of 'acute hypoxia', but had a smaller effect on 'chronic' hypoxic cells. However, the combination of nicotinamide and Fluosol DA/carbogen significantly increased the response of both 'acutely' and 'chronically' hypoxic cells. The results provided evidence that the combination of Nicotinamide and Fluosol DA/Carbogen

could reoxygenate both types of hypoxic cells. The effectiveness of this approach was confirmed in other tumour lines with fractionated radiotherapy (70) and that, in this model at least, the normal tissue effect was enhanced to a lesser degree than the tumour effect.

Early clinical studies in head and neck cancer patients, undertaken in Nijmegen, showed carbogen breathing and nicotinamide was safe with manageable side effects. The main toxicity of intractable nausea occurred in 60% of patients caused 25% of patients to abandon taking nicotinamide (71). Patients were treated with an accelerated radiotherapy regime, taking the nicotinamide orally on a daily basis and breathing carbogen before and during radiotherapy. A larger phase I/II study in head and neck cancer conducted between 1993 and 1996 by the Co-operative Group of Radiotherapy of the EORTC was reported in 1999. Patients received either accelerated radiotherapy combined with carbogen, accelerated radiotherapy with daily nicotinamide, or accelerated radiotherapy with both carbogen and nicotinamide. No significant difference in radiation toxicity occurred between the three groups. There was also no significant difference in tumour response and local control in the three groups. These studies could provided the basis for a large randomised trial (72).

The ARCON regimen has also been piloted in the treatment of bladder carcinoma with similarly encouraging local control rates compared to a historical cohort (73).

Exploiting tumour hypoxia with bioreductive drugs

Bioreductive drugs that are delivered in a non-toxic, inactive form and are activated in a hypoxic environment exploit the specificity of hypoxia to solid tumours. The drugs have a common molecular design, consisting of a trigger unit and an effector unit. The trigger is rapidly reduced but can be reoxidised to the parent molecule in oxic conditions, making the drug specific to hypoxic conditions. The effector unit is cytotoxic to the target cells and adjacent cells (74). There are five classes of bioreductive drugs, distinguished by their effector units (75).

Nitroheteroaromatics

The nitroimidazoles, misonidazole and etanidazole, were early hypoxia-activated prodrugs originally developed as radiosensitisers, described above. They have low cytotoxicity and offer only 10-fold cell kill of hypoxic over oxic cells. CI-1010 is about 100 times more selective for hypoxic cells but is toxic to retinal cells (76). CB-1954 is a bioreductive drug investigated for gene therapy with an aerobic nitroreductase from Escherichia Coli (77).

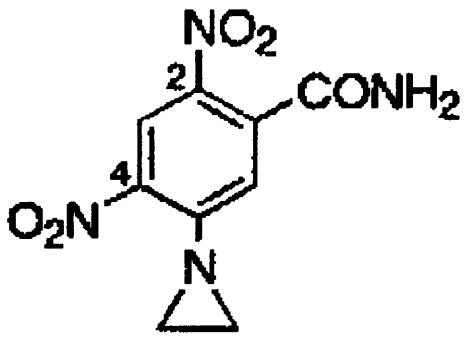

Figure 12 The structure of CB-1954

Quinones

Porfiromycin and Mitomycin C are both quinones. They reduce to a semiquinone radical anion (78) in hypoxic conditions, and can be re-oxidised by molecular oxygen. They then eventually reduce to crosslinking molecules that form guanine–guanine crosslinks in the major groove of DNA (79). EO9, a related molecule, is an indoloquinone and is activated under aerobic conditions, primarily by DT-diaphorase. EO9 has not shown single agent activity in phase II studies so far (80)

Aromatic N-oxides

Tirapazamine is an aromatic N-oxide. It is reduced by NAD(P)H:cytochrome P450 reductase to an oxidising radical that induces the formation of DNA radicals directly or through formation of superoxide. The resulting DNA breaks can be made permanent by tirapazamine itself, enhancing hypoxic cell cytotoxicity (81) (figure 13). Tirapazamine has shown clinical benefit in a randomised trial (82), where patients with previously untreated advanced non-small cell lung cancer were treated randomised to receive tirapazamine with cisplatin or cisplatin alone. The median survival and the response rate was significantly greater for patients who received tirapazamine plus cisplatin (median survival 34.6 v 27.7 weeks; $p = 0.0078$, response rate 27.5% v 13.7%; $p < 0.001$). The potentiation of cisplatin by tirapazamine is thought to be dependent on repair inhibition of cisplatin-mediated DNA crosslinks. Phase II trails in melanoma and in head and neck tumours have also shown encouraging results (83, 84)

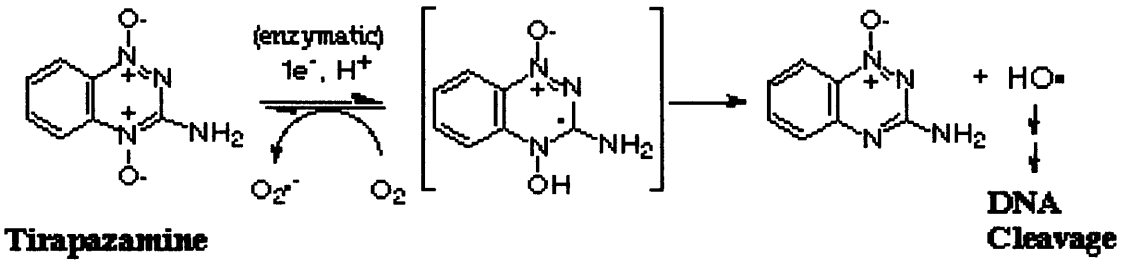

Figure 13 The reductive activation of tirapazamine by NAD(P)H:cytochrome P450 reductase to an oxidising radical

Aliphatic N-oxides

In this group of bioreductive drugs, exemplified by AQ4N, the trigger units are the tertiary amine N-oxides. The cytochrome P450 3A family of enzymes acts on these units. The action of these enzymes on the amine oxides is inhibited by molecular oxygen, thus these drugs are specific to hypoxic cells by a different mechanism to that of the other bioreductives (85). Reduction of the N-oxides AQ4, a cytotoxic diamine that binds tightly to DNA and topoisomerase II. AQ4N has shown activity in several in vivo tumours (86)

Transition metal complexes

These drugs consist of a mustard bound to a metal centre and are exemplified by the compound SN-24771. It contains a nitrogen complex of cobalt which is stable in the Co(III) oxidation state and unstable in the Co(II) state, which is formed in hypoxic

conditions. The cytotoxic mustard portion of the molecule is released in this unstable state. The drugs have shown little activity in vivo and have not been developed further (87).

The Cellular Response to Hypoxia.

Hypoxia and tumour cell protein expression

In vitro studies have revealed that hypoxic microenvironment has a number of effects on protein expression in tumour cells. These appear to be subsequent to gene expression or due to post-translational and transcriptional changes mediated by hypoxia. Such changes impair tumour growth by either triggering cell cycle arrest and subsequent apoptosis or terminal differentiation.

Under hypoxic conditions, cells have been shown to arrest at the G1/S boundary (88). Oxygen levels of 0.2 to 1 mmHg greatly lengthen or arrest the G1 phase and thus effect the rate of proliferation (89). Anoxia appears to cause immediate cell cycle arrest, irrespective of the position in the cell cycle.

The stimulation of terminal cellular differentiation by hypoxia is supported by observations made using cellular staining with pimonidazole. Pimonidazole staining is seen in the differentiating supra-basal cells of squamous epithelium. However, this may be purely a phenomenon of diffusion limited hypoxia, where cells are pushed away from their feeding blood vessels.

There is substantial evidence that hypoxia induces apoptosis in normal and neoplastic cells. Graeber (90) and colleagues completed a series of experiments that revealed the link between apoptotic mechanisms and hypoxia. Using Rat1 fibroblasts

that constitutively expressed a c-myc oestrogen receptor protein, cultured in either anaerobic or aerobic conditions in the presence of 4-hydroxytryptamine (which activates the oestrogen receptor and therefore c-myc mediated pathways), substantially more apoptosis was seen in the cells grown in the hypoxic environment. Further experiments using human cervical carcinoma cells expressing Human Papilloma Virus 16 oncoproteins (E6 and E7) showed that hypoxia stimulated both p53 induction and apoptosis. However, cervical fibroblasts infected with E6 and E7 did not undergo apoptosis when exposed to hypoxia, showing only growth arrest, suggesting hypoxia driven apoptosis is a feature of tumour cells and not fibroblasts. Other studies have demonstrated that the level of p53 in cells increases under hypoxic conditions, and this in turn induces apoptosis by pathways involving apaf-1 and caspase-9 as downstream effectors (91).

Oxygen mediated genomic regulation in normal cells

Cells respond to low O_2 levels by initiating mechanisms to compensate for the potentially injurious effects of hypoxia. Oxygen levels regulate a series of genes that code for transcription factors, growth factors, oncoproteins, glycolytic enzymes, pH regulating enzymes, and membrane transport proteins. Central to this cellular hypoxia response is the Hypoxia Inducible Factor-1 (HIF1), a transcription factor that singularly mediates this network of genes coding for hypoxia combating proteins.

HIF1 is a heterodimeric protein, consisting of an α and β subunit. Both subunits are basic-helix-loop-helix proteins (bHLH) containing a Per-aryl hydrocarbon receptor nuclear translocator-Sim (PAS) domain. The bHLH section binds to DNA and the

PAS domain is required for dimerisation between the subunits and target specificity. The PAS region of the protein is also found in the drosophila circadian rhythm regulator Per, the neurodevelopmental factor Sim, and the mammalian dioxin (aryl hydrocarbon) receptor (92). The HIF1 proteins belong to a family of bHLH/PAS proteins that are involved in a number of diverse biological roles (table 1).

Name	Function	Organism	Reference
Clock and Per	regulation of circadian rhythms	Drosophila and mammals	(93), (94), (95)
WC proteins	photoreceptors	Neurospora	(96)
Dioxin receptor	cellular detoxification responses	Mammals	(97)
Sim and Trachealess	critical development factors for neuronal and trachea development	Drosophila	(98), (99)

Table 1 Characteristics of the members of the bHLH/PAS family of proteins

HIF1 protein expression is greatly increased under hypoxic conditions. Jiang quantified HIF1 DNA-binding activity and protein levels of the HIF1 subunits in human HeLa cells exposed to a range of pO_2 levels, both with and without potassium cyanide to inhibit cellular O_2 consumption. HIF1 DNA-binding activity and HIF1α protein protein each increased exponentially as cells were subjected to decreasing O_2 concentrations. The half maximal response was between 1.5 and 2% O_2 (around 10mmHg) and the maximal response was at 0.5% O_2, both in the presence and absence of KCN (100).

HIF1α expression has been analysed by immunohistochemistry in tumour specimens (101). HIF1α was overexpressed in 13 of 19 tumour types compared with the respective normal tissues, including colon, breast, gastric, lung, skin, ovarian, pancreatic, prostate, and renal carcinomas. HIF1α expression showed correlation with aberrant p53 accumulation and cell proliferation in this study. Preneoplastic

lesions in breast, colon, and prostate overexpressed HIF1α, whereas benign tumours in breast and uterus did not. HIF1α overexpression was detected in only 29% of primary breast cancers but in 69% of breast cancer metastases. In brain tumours, HIF1α immunohistochemistry demarcated areas of angiogenesis (101). Work from the same group evaluated expression of HIF1α in rat and human prostate cancer cell lines. Increased expression of HIF1α mRNA in rat prostate cancer cell lines and hypoxia-induced expression of HIF1α protein in human prostate cancer cell lines were associated with increased cell growth rates and metastatic potential (102).

HIF1β is identical to the aryl hydrocarbon receptor nuclear translocator (ARNT) which is involved in the transcriptional response to xenobiotics. In this response, ARNT binds to the aryl hydrocarbon receptor (AHR). It has been shown that HIF1α has very high affinity for ARNT by in vitro co-immunoprecipitation assays, resulting in competition with the ligand-activated AHR receptor for recruitment of ARNT (103).

It appears that HIF1α is regulated by a post-transcriptional mechanism, since HIF1α mRNA levels are unaffected by hypoxia. Kallio et al demonstrated that HIF1β/ ARNT protein levels were not increased under conditions that induce a hypoxic response in HeLa and HepG2 cells. However, HIF1α protein levels were rapidly and dramatically up-regulated by more than 20 fold. HIF1α underwent a change in conformation when dimerised with ARNT, making HIF1α more resistant to proteolytic digestion in vitro. In cells exposed to oxygen, HIF1α is very unstable (104), with a half life of less than 5 minutes (105). Truncated forms of ARNT that could dimerise with HIF1α did not cause the conformational change in HIF1α and, by a process of elimination, the critical region was found to be in the C-terminal of the PAS domain. Also, the high

affinity DNA binding form of the HIF1α-ARNT complex was only generated by forms of ARNT that were able to alter conformation (106). These data suggested that hypoxia mediated HIF1α accumulation and stabilisation was essential to HIF1 activity and was regulated at the post-transcriptional level. Huang et al identified the actual domain on HIF 1α that prevented its degradation by oxygen. It is located in the central region of the protein and consists of about 200 amino acids. Deletion of this 'oxygen dependant domain' (ODD) stabilises the HIF1α protein and allows non-hypoxic mediation of HIF function. Fusion of ODD with a stable protein, Ga14, confers instability in hypoxic environments. Experiments also revealed that O_2 dependent HIF1α degradation occurred via the proteosome pathway and involved ubiquitination. Ubiquitination is a process in which ubiquitin molecules are added to proteins to tag them for degradation. It was noted that partial deletions within the ODD domain did not stabilise HIF1α in oxic conditions, suggesting some of the sequence is redundant. The activation process of HIF1 therefore has 3 steps:

1. HIF1α is stabilised by hypoxia through abrogation of ODD domain mediated ubiquitin proteosome degradation
2. the stabilised HIF1α heterodimerises with endogenous ARNT and
3. hypoxia enhances HIF1 transactivation of target genes.

The primary step is the stabilisation of HIF1. The actual mechanism by which HIF1α senses O_2 levels has not been fully elucidated. The fact that cobalt ions and iron chelators produced the same effects as hypoxia on HIF systems suggested their involvement in the O_2 sensor apparatus. Recent work has shown a role for a prolyl hydroxylase enzyme. Prolyl hydroxylase exists in a variety of mammalian cells. Ivan et al (107) demonstrated this enzyme hydroxylates proline 564 in the ODD of HIF1α

in the presence of oxygen and iron, and allows the von Hippel Lindau protein to bind. Other prolyl hydroxylase enzymes, such as collagen 4-prolyl hydroxylase, are also iron and oxygen dependent, and respond to similar cofactors and inhibitors, such as cobalt or nickel. In contrast, HIF1α prolyl hydroxylase, resides in the cytoplasm, whereas collagen 4-prolyl hydroxylase exists on the endoplasmic reticulum. Furthermore, the collagen based enzyme functions in a wide range of O_2 concentrations whereas HIF1α prolyl hydroxylase has a low affinity for oxygen, making it more responsive to small changes in intracellular O_2.

Other candidate proteins have been identified as possible oxygen sensors. The cytochrome b5/b5 reductase fusion protein is a flavohaem reductase (108), and an NADPH oxidase. It contains $gp91^{phox}$ that has been shown to act as an oxygen sensor in pulmonary neuroepithelial bodies (108).

A significant protein associated with HIF1α and O_2 control is the von Hippel Lindau protein and is essential in the degradation of HIF1a in oxic conditions. Von Hippel Lindau (VHL) syndrome is a hereditary cancer syndrome first reported around the turn of the 20^{th} century, where multiple haemangiomas affect the retina, cerebellum and spine. Renal and adrenal gland tumours may also develop. The gene was isolated in 1993 and functions as a tumour supressor gene. The protein product complexes with other proteins, namely elongin B, elongin C and Cul2. Elongin C and Cul2 bind to other proteins to enable ubiquitin binding, which in turn enables degradation by proteosomes, as described above. The structure of the VHL protein was described by Stebbins (109); it contains two subdomains, α, where the target protein binds, and β where elongin C binds. Ohh et al confirmed that pVHL binds

directly to HIF1 through its β-domain (110) and Maxwell et al demonstrated that cells lacking pVHL do not degrade HIF1α in well-oxygenated conditions (111).

HIF1α is therefore degraded rapidly in normoxic cellular environments, and stabilised when there is hypoxia. Under hypoxic conditions, it binds to the HIF1β subunit to form the stable heterodimer, which in turn stimulates transcription of a family of hypoxia responsive genes. On dimerisation, a conformational change in HIF1α creates a stable complex. This stability is essential for transcriptional activation within the nucleus because the individual subunits leak out of the nucleus in the absence of one another (112). It seems unclear whether the subunits come together in the cytoplasm or in the nucleus. Chilov showed that co-immunoprecipitation of HIF1α with HIF1β could be performed in nuclear extracts but not cytosolic fractions, implying the complex is formed in the nucleus (112).

The transit of the HIF1α complex into the nucleus may also be regulated by hypoxia, although these studies were carried out using a HIF1α-green florescent protein complex and not the whole heterodimeric HIF1 (113). It was shown that HIF1α transit into the nucleus is also hypoxia regulated, dependent on the activation of a nuclear localisation signal (NLS), situated within the C-terminal end of HIF1α. The PAS β domain of the protein may repress this, and this repression is maintained by the hsp90 protein. Destabilisation of the HIF1-hsp90 complex would allow activation of the NLS and thus nuclear entry. Once inside the nucleus, transcriptional activation requires binding between HIF1 and a protein called CBP/p300.

CBP/p300 participates in numerous biological processes, including cell cycle arrest, differentiation, and transcription activation (103). CBP has been shown to activate the transactivation domain of p53 as well as HIF1α.

The range of genes upregulated by HIF1 contain a hypoxia responsive element that consists of repeats of the codon sequence CGTG. This is common to a number of genes upregulated by hypoxia shown in table 2. The sequence contains a CpG island. CpG islands exist in high-density regions in limited parts of human genome and are usually associated with promoter regions. The fifth position of the cytosine ring is methylated in up to 90% of cases and this correlates inversely with the transcriptional activity of the promoter region. Methylation prevents the binding of sequence specific trans-acting proteins and in some cases promotes binding of blocking proteins. Yin et al have shown methylation of the hypoxia responsive element in the EPO gene represses transcriptional activation by HIF1, as a methyl CpG binding protein prevents it binding to this site (114).

Gene product	Transcription factor	Reference
Adenylate kinase 3	HIF1	(115)
α1B-Adrenergic receptor	HIF1	(116)
Adrenomedullin	HIF1	(117)
Aldolase A	HIF1	(104)
Aldolase C	HIF1	(104)
Carbonic anhydrase-9	HIF1	(118)
Ceruloplasmin	HIF1	
Cyclooxygenase-2	HMG I(Y), NF-κB	
Endothelin-1	HIF1	(119),(120)
Enolase-1	HIF1	(121)
Erythropoietin	HIF1	(122)
GADD153	Not determined	
Glucose transporter-1	HIF1	(123, 124)
Glucose transporter-3	HIF1	(123, 124)
Glyceraldehyde-3-phosphate dehydrogenase	HIF1	(121)
Heme oxygenase-1	AP-1, HIF1	(125)
Hexokinase-1	HIF1	(121)
Insulin-like growth factor-2 (IGF-2)	HIF1	(126)
IGF-binding protein-1	HIF1	(127)
IGF-binding protein-2	HIF1	(126)
IGF-binding protein-3	HIF1	(126)
Interleukin-6	NF-IL6	
Lactate dehydrogenase A	HIF1	(121)
Nitric oxide synthase-2	HIF1	(128)
NIP3	Not determined	
p21	HIF1	(129)
p27	Not determined	
p35srj	HIF1	
Phosphofructokinase L	HIF1	(121)
Phosphoglycerate kinase-1	HIF1	(121)
Plasminogen activator inhibitor-1	HIF1	
Prolyl-4-hydroxylase α(I)	HIF1	
Pyruvate kinase M	HIF1	(121)
Tissue factor	EGR-1	
Transferrin	HIF1	(130)
Transferrin receptor	HIF1	(131)
Transforming growth factor β3	HIF1	
Triosephosphate isomerase	HIF1	
Tyrosine hydroxylase	AP-1	
Vascular endothelial growth factor (VEGF)	HIF1	(121)
VEGF receptor FLT-1	HIF1	(132)
BNIP3	HIF1	(133)
NIX	HIF1	(133)

Table 2 Gene products upregulated by hypoxia

Key Hypoxia Regulated Genes

Vascular endothelial growth factor

Vascular endothelial growth factor (VEGF) is the central angiogenic growth factor in tumours. It exists in four isoforms each containing glycosylation sites that enable secretion, but are independent of biological activity. The molecule is homodimeric. There are two VEGF receptors so far described, flt1 and flk1/KDR, exclusively expressed on endothelial cells and function as tyrosine kinases. Their levels fall rapidly after the formation of vasculature in the embryo. On binding to these receptors, endothelial cell migration, invasion and formation and canalisation of tube structures is promoted. The receptor expression can be upregulated by VEGF itself (134). VEGF has been shown to increase vascular permeability (135, 136), and may promote metastases from primary tumours. Serum levels of VEGF are raised in metastatic disease when compared to non-metastatic disease (137). The prognostic value of VEGF expression in has been shown in a number of tumour types has been shown. These include cancer of the head and neck (138, 139), oesophagus (140), thyroid (141), lung (142), colon (143), brain (144) and breast (145-147).

Levels of VEGF increase in response to hypoxia, and mRNA levels have been shown to fall when reoxygenation occurs in vitro experiments. Charriotto and Hill determined that a pO_2 of approximately 1mmHg would increase levels of VEGF mRNA above baseline in a number of cervical cancer cell lines. In vivo, VEGF expression is increased adjacent to regions of necrosis in human gliomas. This was associated with upregulation of the VEGF receptors in adjacent endothelial cells (148). Hypoxia

independent factors also upregulate VEGF and thus angiogenesis, which might explain the non-correlation of VEGF staining with hypoxia in immunohistochemical studies. The oncogenes, raf and ras, and growth factors through protein kinase C both increase VEGF expression (149, 150). In human glioma spheroids and xenograft tumours, regions of severe hypoxia did not correspond to areas of up-regulated VEGF expression which was uniform through the tumour (151), providing further evidence of non-hypoxic regulation of VEGF. In an immunohistochemical analysis of human cervix carcinoma and head and neck carcinoma, VEGF protein expression did not correlate with pimonidazole staining, supporting non-hypoxic regulation of VEGF or diffusion of the protein through tissue (152). The HRE has been shown to govern translation of the VEGF gene (153). Hypoxia also confers stability to VEGF mRNA, providing a post translation influence on expression. An AU rich sequence at the 3' untranslated region of the mRNA is bound by an RNA binding protein called HuR (154). An untranslated region at the 5' end of the mRNA co-operates with that at the 3' end, conferring stability to the mRNA under hypoxia and instability under normoxia. The 5' site also has a complicated configuration that inhibits ribosomal binding, but under hypoxic conditions will alter to allow translation (155).

Platelet derived endothelial growth factor

Platelet derived endothelial growth factor (PD-ECGF), identical to thymidine phosphorylase, has also been shown to be hypoxia dependent. Levels of PD-ECGF protein increased 6-fold and an increase in enzyme activity in a breast cancer cell

line after growth in 0.3% oxygen. Immunohistochemical staining these cells grown in nu/nu mice showed increased expression of PD-ECGF regions of tumour proximal to necrosis. Increased staining for PD-ECGF protein was seen when the vascular supply was clamped and when the pH was lowered in vitro (156). The thymidine phosphorylase activity of this enzyme is responsible for activating 5-flourouracil, and the authors suggest a possible therapeutic role in the hypoxic modulation of PD-ECGF.

Nitric Oxide

The importance of nitric oxide as a modulator of vascular function in normal tissue and tumours is established. Nitric oxide synthetase (NOS) exists in three isoforms that are either calcium dependent or calcium independent (iNOS). An HRE region has been identified on the iNOS gene, and hypoxia driven transcription been identified in tumour endothelium and parenchyma. Endothelial cell NOS can be activated by the VEGF/kdr1 receptor complex. NO can in turn regulate production of VEGF. Deletion and mutation analysis showed that the NO-responsive elements are the HIF1 binding site and an adjacent sequence located immediately downstream HRE. NO and hypoxia induced a rise in HIF1 binding activity and HIF1α protein levels (157).

Carbonic anhydrase

A group of genes recently identified code for cellular carbonic anhydrases, two of which are hypoxia responsive. Carbonic anhydrases (CA) reside on the cell membrane and catalyse the reversible hydration of carbon dioxide to carbonic acid,

adjusting microenvironmental pH. Carbonic anhydrase 9 and 12 are downregulated by the VHL protein (158) and Wycoff et al have demonstrated the hypoxic upregulation of CA9, that it is dependent on HIF1 and that the HRE with the characteristic base sequence exists at the 3' end of the gene. Immunostaining human tumour samples revealed expression of CA9 exclusively in perinecrotic regions, localise to the membrane. VEGF mRNA expression was distributed widely, but more strongly in perinecrotic regions. Pimonidazole staining in tumour samples was more widespread than CA9 expression in 16 of 20 samples. No overall correlation between the percentage of tumour stained for CA9 and pimonidazole was found (118).

Another major study (159) examined the expression of CA9 alongside glucose transporter-1 (GLUT-1, discussed below) and pimonidazole binding in cervix carcinoma. Fourty-two patients were studied and a significant correlation was found between expression of CA9 and GLUT-1, and between GLUT-1 expression and pimonidazole binding.

P53

P53 is now known to be a tumour supressor gene, arresting the cell cycle if there is excessive DNA damage and initiating apoptosis, and a transcription factor for several genes. As mentioned, in vitro and in vivo experiments show hypoxic conditions stimulate apoptosis in p53 competent cells and thus select out p53 mutated cells. P 53 represses HIF1 transcription with obligate association with p300. P300 binds to HIF1 and p53 via distinct sites, suggesting they may be able to bind simultaneously, and that p53 inhibits HIF1 mediated transcription stoiciometrically (160). The degree of hypoxia required to stabilise HIF1α and upregulation of hypoxia dependent genes is insufficient to increase levels of p53 (161). Further insight into the p53-HIF1

interaction by Ravi et al (162) shows p53 null colorectal xenografts implanted in mice were unable to grow through lack of neovascularisation. P53 null cells cultured under hypoxic conditions expressed higher levels of VEGF mRNA compared to p53 competent cells. When a vector expressing p53 was transfected into the p53 null cells, however, VEGF expression (measured by β-galactosidase from the reporter VEGF-p11w) was completely repressed. P53 therefore inhibits HIF1 activity and VEGF expression in response to hypoxia. It was also shown that HIF1α protein half-life was less than 20 minutes in the p53-/- cells compared to over 40 minutes in p53+/+ cells. The p53 molecule facilitated the HIF1α ubiquitination by recruiting E3 ubiquitin ligase. Loss of p53 therefore will promote angiogenesis; thus, the hypoxic microenvironment not only selects for cells resistant to apoptosis, but also for those capable of forming vasculature.

Nuclear factor kB

Another transcription factor shown to be upregulated by hypoxia is Nuclear factor kB. It is upregulated at a pO_2 of 15mmHg in vitro (163), and releases the IkB inhibitory unit by phosphorylating tyrosine residues; increasing NF-kappa B DNA binding activity resulting in transactivation of a wide variety of early response genes (164).

Figure 14a Fate of HIF 1α in Hypoxic conditions

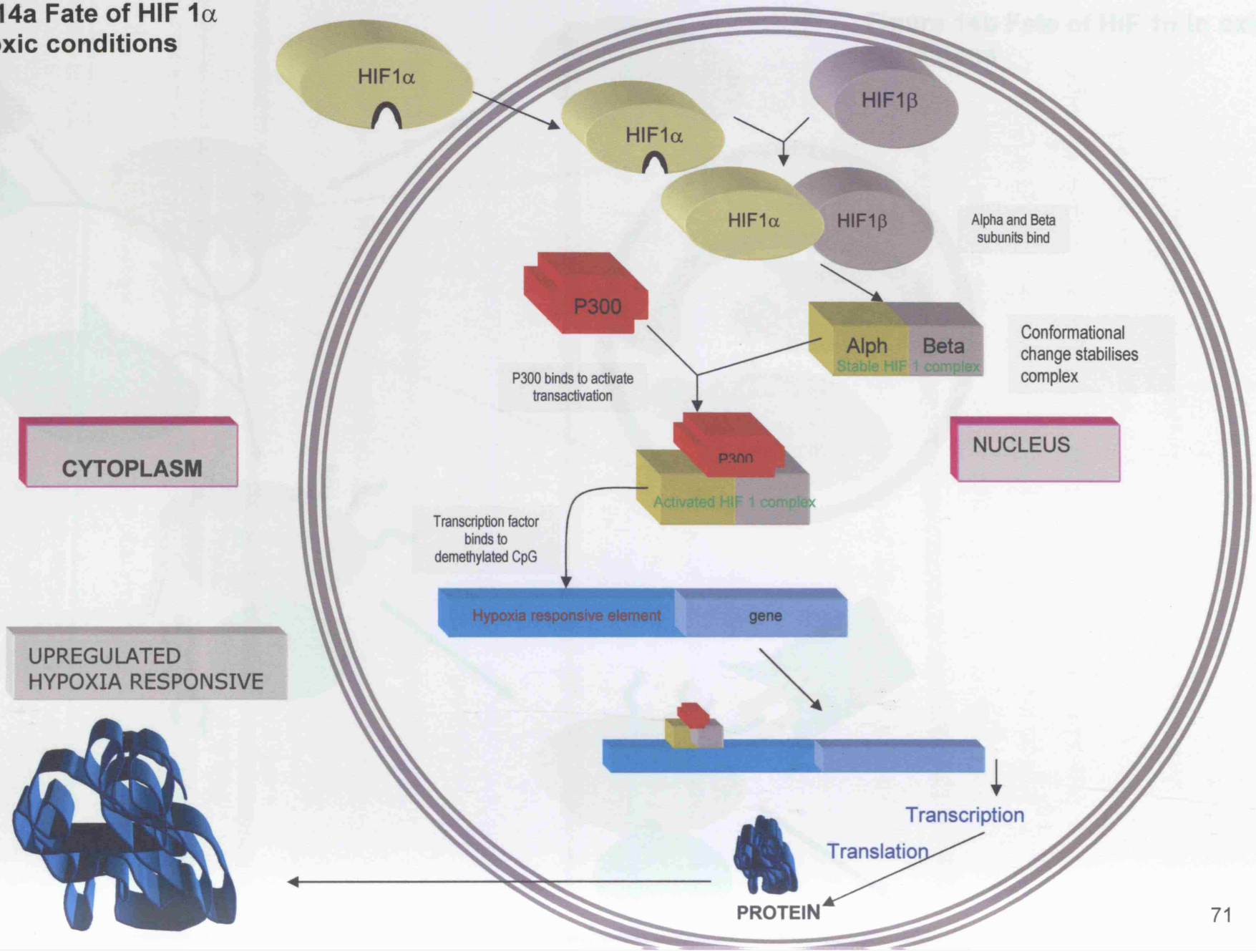

Figure 14b Fate of HIF 1α in oxic conditions

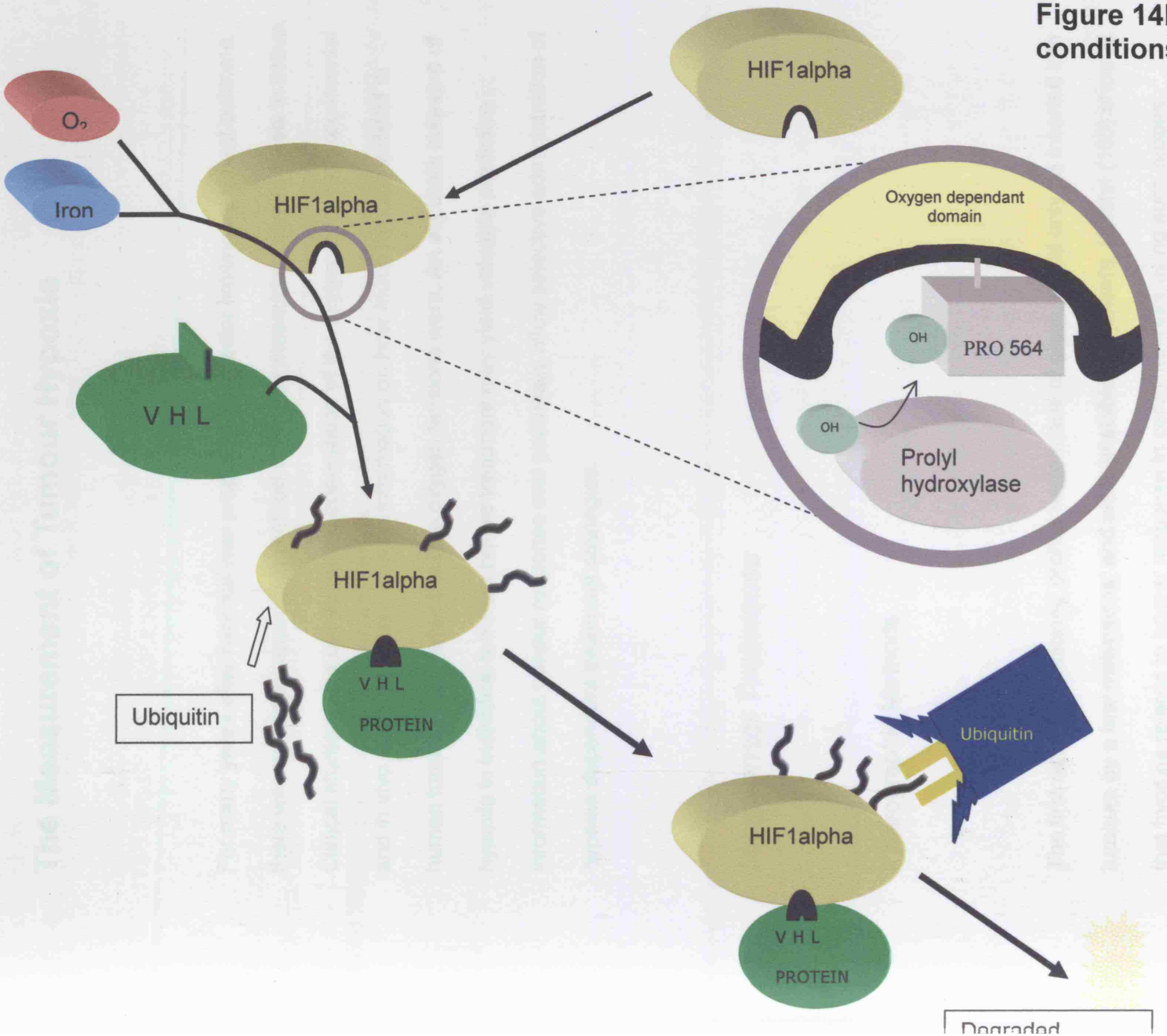

The Measurement of Tumour Hypoxia

For many years after hypoxia was proposed as a factor limiting treatment outcome, there was no widely applicable method of directly measuring oxygen levels in tissue. Clinical studies were based on the observation of the oxygen effect in experimental and in vivo systems. There was no information on how much hypoxia existed in human tumours or of what the true oxygen tensions were. An accurate measure of hypoxia in individual tumours before treatment may yield valuable predictive information about tumour response and potentially allow selective administration of hypoxia dependent treatment strategies.

Microsensor Techniques

Polarographic Methods

The first oxygen measuring probes were made of glass, could only be inserted into tumours by a few millimetres, and were unstable and unsafe. Kolstat (165) showed that hypoxia related to poorer response in cervix tumours using such probes. Gatenby and colleagues used a modified probe made of a platinum electrode 200μm in diameter, encased in a 22G needle and mounted on glass. A group from Mainz (166) in Germany introduced a polarographic oxygen electrode that was more reliable and clinically applicable. The first electrode measured 15μm and was

manufactured from gold. The data from the electrode were calibrated with cryospectrophotometric analysis of red cell oxygen saturation. By 1982 a 300μm steel probe became available, the Eppendorf Probe, and a modified version remains in use. The tip of the probe is sharply bevelled, where a membrane covers a recessed gold microcathode measuring 12 to 17 μm. When measurements are taken, the anode is placed on the skin of the subject close to where the measurements are taken. The probe attaches to a computer controlled stepping device that automatically advances it through the tumour 1 to 2 millimetres at a time. The gold cathode is polarised negatively to –0.7 volts. Oxygen is reduced at the reactive surface with water with concurrent oxidation of the reference electrode releasing electrons. The resulting current is directly proportional to the amount of oxygen in the tissue at the surface of the electrode.

Vaupel and colleagues compared the O_2 measurements by Eppendorf in normal breast tissue with those in stage T1 to T4 breast carcinomas. The median pO_2 in normal tissue was 65mmHg, whereas in tumour mean pO_2 was 28mmHg. Values of 0 to 2.5mmHg were present in 40% of tumours, whereas in normal breast tissue no values less than 12.5mmHg were found (167). The O_2 values had a bimodal distribution with the peaks indicating both hypoxic and normoxic regions, or that normoxic stroma contributed to the data significantly, which may skew the median values in tumours with more stroma. There was no correlation of median pO_2 with either tumour size, stage (167) or blood flow (168). Hormone receptor status, parity and smoking were also not related to median pO_2, but the data on histological grade are conflicting with one study finding a correlation between hypoxic fraction, differentiation and prognosis (169). The mean tumour O_2 varied from tumour to tumour to a greater extent than intratumoural O_2. However there was no consistent intratumoural distribution in hypoxic regions. Eppendorf studies of metastatic and

locally recurrent breast cancers have shown these to have lower median pO_2 levels than primary tumours (170).

The first report of the impact of hypoxia as measured by a polarographic electrode on radiation response was reported by Gatenby (171). Using the earlier version of the probe, his group demonstrated differences in pO_2 measurements in those patients who responded to therapy in comparison to those who responded poorly. Thirty-one patients with fixed lymph node metastases from head and neck carcinoma were assessed prior to radiotherapy. The mean pO_2 measurement in complete responding tumours was 20.6mmHg, in partially responding tumours 8.8mmHg and in non-responding tumours was 4.6mmHg.

In Aarhus, the Eppendorf probe was used in a series of studies to assess tumour oxygen levels in head and neck carcinoma, sarcoma and carcinoma of the uterine cervix. In the first study of 34 patients with head and neck carcinoma (172), involved neck nodes in 33 patients and a primary tumour in one patient were assessed for pO_2 prior to treatment. The proportion of readings below 2.5mmHg (Hypoxic fraction <2.5mmHg or HF2.5) was found to predict for local tumour control at 2 years; in 16 patients with recurrence the HF2.5 was 22%, whereas those free of disease had an HF2.5 of 6%. Using 15% HF2.5 as the cut off for designating a tumour as hypoxic or not, the 2 year local control rate was 33% in the hypoxic group compared to 77% in the well-oxygenated group. This result meant that hypoxia, measured by the Eppendorf electrode could predict outcome and potentially allow patient stratification. A confirmatory study repeated in 31 patients, using the same hypoxia classification criterion, produced a 45% 2-year local control rate in the hypoxic group compared with 90% in the well oxygenated group. A similar study was done at Duke University, USA, in 27 patients. Using Eppendorf probes under CT guidance, O_2 data were collected pre-treatment and again after 10 to15 Gy of radiotherapy

treatment. The average median pre-treatment pO_2 was 8mmHg compared with 10mmHg during radiotherapy treatment, supporting the occurrence of reoxygenation during radiotherapy. In a further 63 patients with head and neck carcinoma, the majority with primary disease in the oropharynx, pre-treatment pO_2 was measured. The primary tumour was assessed in 24 patients and nodal disease in 39. The median pO_2 level was not significantly different from site to site (median pO_2 5mmHg (range 0 to 25) for primary tumours and 4mmHg (range 0 to 60) for nodal disease), or from stage to stage. The patients were treated with radical intent, to a median dose of 69Gy using either a once or a twice-daily fractionation schedule. Chemotherapy was used concurrently in 25 patients. Planned neck dissections were undertaken in 35 patients, and residual tumour was found in 17 of these where the median pre-treatment pO_2 in those with residual disease was 4mmHg. This compared with 12 mmHg in those free of disease at neck dissection (figure 14). Hypoxic tumours, defined as those with a median pO_2 <10mmHg, had poorer local control at 2 years compared to non-hypoxic tumours (30% vs 73%). Disease-free survival (26% vs 73%) and overall survival (35% vs 83%) were also adversely affected by hypoxia. The negative effect also held for T1 tumours, where the overall prognosis is usually good (173). Stadler et al (174), defined a parameter, the hypoxic subvolume, that multiplied the HF5 by the total tumour volume. In a study of 59 head and neck carcinomas measuring tumour oxygenation using the Eppendorf, the HF5 and the hypoxic subvolume were predictive of overall survival, whereas tumour volume alone did not correlate with survival.

Cervix tumours have also been studied extensively in Eppendorf based hypoxia research. In 1989, a study to define the prognostic effect of pO_2 values in cervix carcinoma began, recruiting 103 patients by 1995. The interim analysis in 1993 (175) demonstrated the independent prognostic power of hypoxia in cervix carcinoma, where those with a median pO_2 of 10mmHg or less had a much poorer

prognosis after treatment with surgery, radiotherapy and/or chemotherapy. In the full analysis, there were 47 surgical specimens, where more lymphovascular spread and microscopic parametrial involvement was seen in hypoxic tumours. The 5-year overall and disease free survival was significantly lower in the hypoxic group, and Cox regression analysis suggested hypoxia was the strongest independent prognostic factor. The poorer prognosis occurred irrespective of the treatment, suggesting that hypoxia is a harbinger of a more aggressive tumour phenotype, as well as imparting radio and chemoresistance (176). Fyles (177) determined the

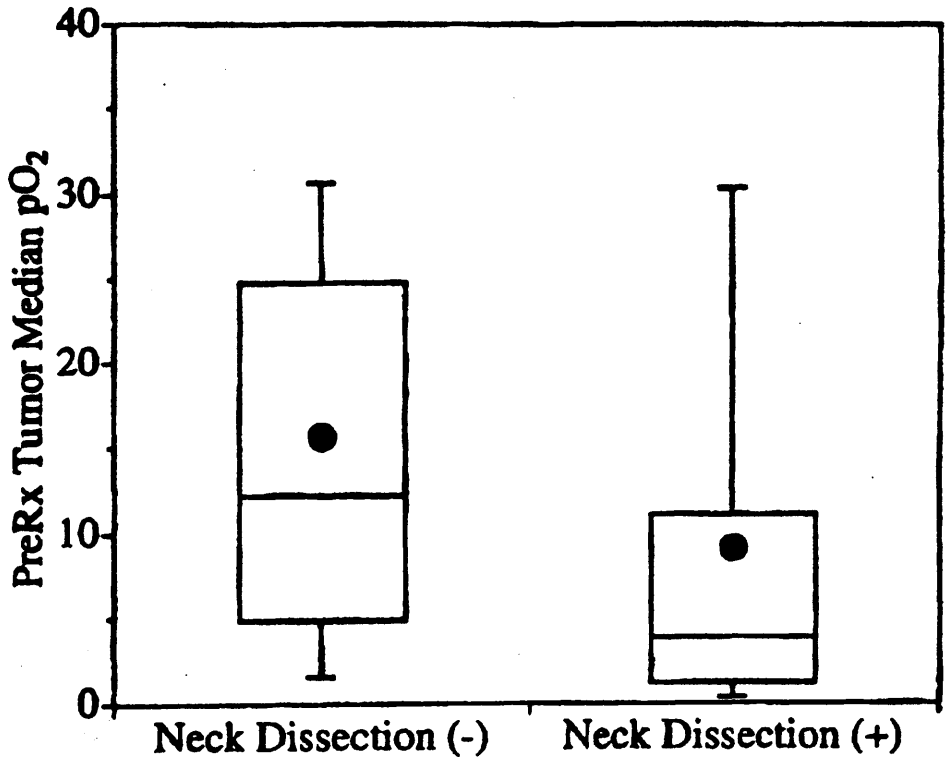

oxygenation in 74 patients with cervix carcinoma using the Eppendorf probe.

Figure 15 A comparison of pretreatment tumour oxygenation in patients undergoing planned post radiotherapy neck dissection stratified by residual diesase vs no residual disease. The box dedlineates the 25% and 75% interquartile range. The bars indicate the 10^{th} and 90^{th} centiles. Means are shown as closed circles ans medians by horizontal bars within the boxes (173).

Hypoxia was defined by the proportion of values less than 5mmHg (HF5), present in 50% of patients. At a median follow up of 1.2 years, the disease free survival was 69% for patients with HP5 less than 50%, compared with a disease free survival of 34% where the hypoxic fraction was greater than 50%. Tumour size was also a significant prognostic factor; hypoxic tumours above the median of 5cm had a 2-year disease-free survival of 12%, whereas the small tumours had a disease free survival of 65%. Knocke et al treated 51 cervix carcinoma patients with radiotherapy to a median dose of 49.6 Gy followed by brachytherapy boost treatments, and took pO_2 readings prior to treatment (178). Those tumours with a HF5 greater than the median of 22% had a three-year disease-free survival of 36% versus 66% in those with an HF5 less than the median. Cervix tumour oxygenation measurements using the Eppendorf became routine practice in the reporting institution.

Soft tissue sarcomas, due to their accessibility, have been good candidate tumours for oxygenation study. Brizel reported results in 45 patients' soft tissue sarcomas with median O_2 levels less than 10mmHg as the cut off, the 3-year disease-free survival was 30% compared with 60% in non-hypoxic tumours. Overall survival was 50% in hypoxic tumours versus in 80% non-hypoxic tumours. Most relapses were distant, suggesting more hypoxic primary tumours were phenotypically more aggressive and more likely to seed metastases, as shown in Hoekel's study on cervix carcinoma (179). Another study measured the O_2 profiles of 26 soft tissue sarcomas with the Eppendorf probe, and reported follow up results after a median time of 41 months. Median pO_2 levels were the only independent prognostic variable, with those having a median pO_2 lower than the overall median having a survival probability of 31% versus 71% for the better-oxygenated tumours (180).

The Eppendorf studies have therefore confirmed the presence of low oxygen tensions in human tumours, and quantified the degree of hypoxia. They also

confirmed the independent prognostic significance of hypoxia, demonstrating a worse treatment outcome where significant hypoxia was detected. Previously, this was thought to be due to radio- and chemoresistance of hypoxic cells. However, these studies suggested hypoxic tumours behaved more aggressively, reflected in their increased metastatic potential.

The question remained, however whether the malignant nature of the tumours predisposed to hypoxia or the hypoxic tumour microenvironment predisposed the tumour to greater malignant potential. The rapid increase in molecular biological techniques in the 1990's added to an understanding of how cells respond to the unique microenvironment found in tumours.

Luminescence sensor

There are inherent disadvantages to the Eppendorf pO_2 probe. The instrument consumes oxygen through electrochemical reduction therefore making it liable to underestimate the true pO_2 value in the environment. This is minimised by the tip being recessed, and using a stepping mechanism to move the probe through the tissue. However moving the probe through the tissue means that changes in pO_2 cannot be monitored at a single site in tissue. The other drawback is in the measurement of very low levels of oxygen and the resultant very low current. This is obviated by miniaturising the probe geometry, leading to lower currents becoming detectable through lower impedance. Luminescence based optical sensors offer advantages in not consuming oxygen or expressing the local oxygen tension as a

current, but as the lifetime of fluorescence from a group of compounds called flourophors. The lifetime of fluorescence emitted by the compound after a pulse of excitation laser light varies according to the oxygen tension the compound is in. By placing this at the tip of an optical fibre, and calibrating the luminescence lifetime, a usable oxygen probe has been constructed. The fluorophor of choice is a ruthenium based complex, chosen because of its large absorption coefficient and large Stokes shift (the difference in wavelength between absorbed and emitted quanta, in wavelength shifters or scintillators; the emitted wavelength is always longer if single photons are absorbed or equal to the incident wavelength, due to energy conservation; the difference is absorbed as heat in the atomic lattice of the material). The optimal pO_2 range for the sensor is between 0 to 15mmHg. The probe measures 230 μm and the current commercially available apparatus has multichannel capabilities. The accuracy is 0.8% between 1 and 10 mmHg falling to 8% between 10 and 100mmHg. The response time is 5 seconds and data acquisition time is 1 second, compared with the Eppendorf probe response of 0.5 seconds and acquisition time of 1.4 seconds.

In a study comparing pO_2 measurements obtained with the Eppendorf electrode in a murine sarcoma F mouse tumour against those of the optical sensor, Collingridge et al found the polarographic method detected more regions of pO_2 less than 2.5mmHg. The percentage of readings less than 5mmHg and less than 10mmHg were broadly comparable. The median pO_2, however, was significantly different (181). This may have been due to the excess of readings below 2.5mmHg recorded by the Eppendorf probe, through either pO2 consumption or sampling differences.

Nitroimidazoles

The nitroimidazoles are a group of nitro-aromatic molecules originally used as anti-protozoal agents. Their investigation grew out of the findings that nitroaromatic compounds were hypoxic cell radiosensitisers (see page 33), but compared to nitrofurans (182), nitropyrroles (183) and nitropyrazoles, they were found to be the most pharmacologically suitable. Although naturally occurring nitroimidazoles are rare, most organisms are capable of metabolising them with nitroreductase enzymes to reduce the nitro group. Varghese et al. (184) performed experiments using ^{14}C-labelled misonidazole on Chinese hamster ovary cells in vitro and KHT murine fibrosarcoma tumour cells in vivo. The radioactivity associated with the acid-insoluble precipitate from cells incubated in nitrogen in vivo was 400% higher than that of cells incubated in air. When aqueous extracts of a KHT tumour grown on a C3H mouse after intraperitoneal injection with misonidazole were analysed, the reduction product was found in higher concentration in the tumour compared with normal tissue. These experiments proved that misonidazole formed reduction products under hypoxic conditions and that they were retained within hypoxic cells. It was also the first identification of hypoxia using an 2 nitroimidazole within an in vivo tumour.

Hypoxic Markers

Invasive hypoxia marker techniques

The metabolism of 2-nitroimidazoles

The range of enzymes involved in the 2 nitroimidazole metabolism are the flavo enzymes, present in both the cytoplasmic and nuclear compartments of the cell. (table 3)

ENZYME	Site
Aldehyde oxidase	cytoplasm
DT-diaphorase	cytoplasm
Xanthine oxidase	cytoplasm
NADPH-cytochrome reductase	microsomes
Cytochrome p450	microsomes
Dihydrolipamide dehydrogenase	mitochondria
Cytochrome b5 reductase	mitochondria
NADH dehydrogenase	mitochondria
Succinate dehydrogenase	mitochondria

Table 3 Enzymes involved in the 2-nitroimidazole metabolism (185)

The metabolism of 2-nitroimidazoles occurs in a series of one-electron reductions (figure 16). However, the nitro-radical anion, produced by the first one-electron reduction step, avidly reacts with oxygen and is oxidised back to the parent molecule so that in well-oxygenated conditions there is effectively no substrate for the second step (186). This step in the metabolism produces numerous oxidising species, such as superoxides, which is the basis for the anti-parasitic activity of some 2-nitroimidazoles (187). In low oxygen concentrations, one-electron product is further reduced to the nitroso (2 e-), hydroxylamine (4 e-), and amine (6 e-) derivatives. Eventually, the imidazole ring fragments, the reactive portions of the molecule binding to a range of macromolecular components such as thiol groups. All atoms of the ring and side-chain of the 2-nitroimidazole are retained (188). The side-chain also binds to cellular macromolecules because of fragmentation of the amine

(189). Although variability in the rate of binding of nitroimidazoles by different cell lines was seen by Chapman in his work on TF MISO, an analogue of misonidasole (190), the local cellular oxygen concentration is the most important determinant of binding rate (191).

In totally anoxic conditions, binding is proportional to the square-root of the concentration of misonidazole (192). Small quantities of oxygen convert this to first-order kinetics (193) by reducing the concentration of a reactive free radical and so reducing its ability to react with itself by second order kinetics. The oxygen-dependence of 2-nitroimidazoles binding in cells is similar to their dependence of radiosensitivity. Hodgkiss et al (194) incubated Chinese Hamster cells in vitro with NITP, a theophylline bound 2-nitroimidazole, at a range of oxygen concentrations. Using a fluorescent antibody and flow cytometrical quantitation, the hypoxic:oxic differential was 1,400 ppm, similar to the value of 3800ppm for half the radiosensitising effect described by Begg (195).

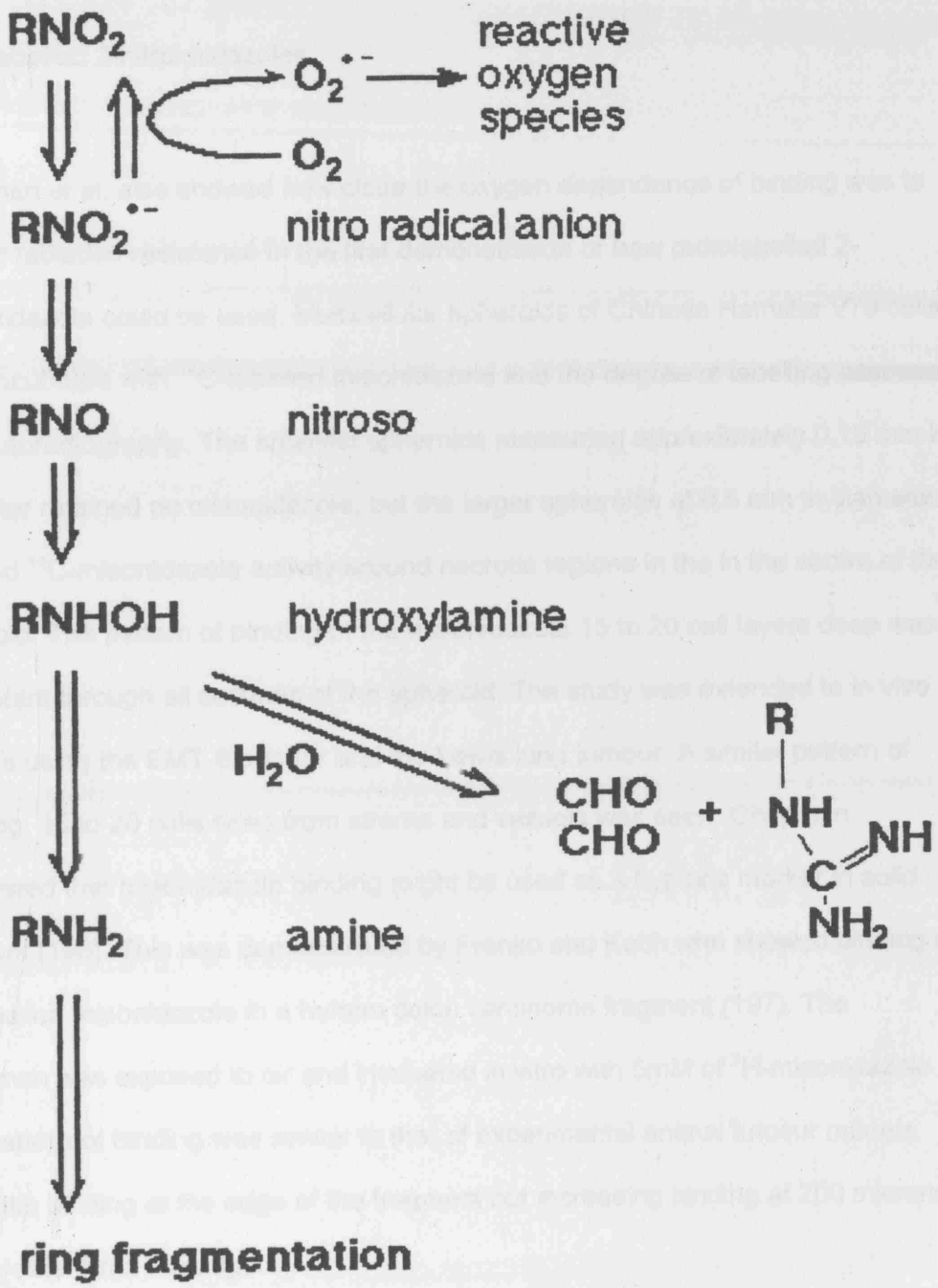

Figure 16 The bioreductive metabolism of nitroimidazoles

Radiolabelled 2-nitroimidazoles

Chapman et al. also showed how close the oxygen dependence of binding was to that for radiation resistance in the first demonstration of how radiolabelled 2-nitroimidazole could be used. Multicellular spheroids of Chinese Hamster V79 cells were incubated with ^{14}C-labelled misonidazole and the degree of labelling assessed with autoradiography. The smallest spheroids measuring approximately 0.15 mm in diameter retained no misonidazole, but the larger spheroids of 0.6 mm in diameter showed ^{14}C-misonidazole activity around necrotic regions in the in the centre of the spheroid. The pattern of binding of the misonidazole 15 to 20 cell layers deep was consistent through all sections of the spheroid. The study was extended to in vivo models using the EMT-6 tumour and the Lewis lung tumour. A similar pattern of staining, 15 to 20 cells deep from stroma and vessels was seen. Chapman suggested that misonidazole binding might be used as a hypoxia marker in solid tumours (196). This was demonstrated by Franko and Koch who showed binding of ^{3}H-labelled misonidazole in a human colon carcinoma fragment (197). The specimen was exposed to air and incubated in vitro with 5mM of ^{3}H-misonidazole. The pattern of binding was similar to that of experimental animal tumour models, with little binding at the edge of the fragment but increasing binding at 200 microns and greater from the edge.

The clinical feasibility of a hypoxia marker was shown in a patient with a melanoma, also using autoradiographic analyses of ^{3}H -misonidazole binding (198). The patient was given the misonidazole intravenously 22 hours prior to surgical excision of a subcutaneous deposit. Areas of dense and sparse labelling were seen, with little staining seen in stromal regions. The hypoxic fraction of the sample was estimated

to be about 6%. A further eleven patients' tumours were assessed by this method, with hypoxia detectable in 12 of 22 metastases. Binding was particularly sparse in sarcoma and squamous lung carcinoma patients. Despite these studies, the procedure had limited clinical use; the relatively large sample of tissue required, the large dose of radioactive label required, accumulation of the label in the liver and the wait of one to two months for autoradiography were prohibitive. This spurred the development of non-invasive assays using 2-nitroimidazoles, including single photon electron capture tomography, positron emission tomography, nuclear medicine analysis and magnetic resonance spectroscopy.

Immunohistochemical nitroimidazole labelling

A histological assessment of hypoxia in tumours would provide information on relationships between hypoxia and other microregional factors alongside a quantitative measure of hypoxia. It would also allow exploration of the association between hypoxia and factors such as necrosis, vascularity, proliferation, differentiation, apoptosis, and oxygen regulated protein expression. Raleigh et al raised polyclonal antibodies in rabbits to the haemocyanin adduct of a CCI-103F. Florescence studies showed that the marker bound within spheroids and tumour sections in patterns similar to those seen in the autoradiographic studies (199). Subsequent testing in spontaneous canine tumours clearly showed binding occurred 10-12 cell diameters away from tumour blood vessels, consistent with the where 'chronically' hypoxic cells would reside. The hypoxic fraction ranged from 4 to 13% according to a morphometric analysis of multiple tumour sections. Staining was seen adjacent to necrosis, although not exclusively and some binding occurred in cells close to blood vessels. Most staining was restricted to tumour cells although

some staining of smooth muscle cells surrounding arterioles in some sections of normal tissue and tumour tissue was observed (200). Further work from the same group confirmed immunohistochemistry was a feasible and straightforward method of assessing hypoxia in tumours (201) including the development of an enzyme linked immunosorbent assay for the binding of CCI-103F (202).

In addition, the first investigation of the spatial relationship between hypoxia and proliferation was demonstrated in canine tumours using this method (203). In this study, serial sections were stained for pre-administered CCI-103F (the hexafluorinated 2-nitroimidazole) to reveal hypoxic regions and proliferating cell nuclear antigen (PCNA) to localise proliferation. Characteristically, diffusion limited hypoxic staining away from vessels was evident, whereas proliferating cells were predominantly near blood vessels. The two cell populations showed some degree of geographical overlap to varying extents.

Whilst immunoglobulins could be raised to the fluorinated component of CCI-103F, it had not been clinically tested. Attention turned to pimonidazole, the 2-nitroimidazole with an immunologically-detectable piperidine side-chains (figure 5). There was a wealth of pharmacokinetic and pharmacodynamic data supporting its safe use in humans from the radiosensitiser trials of the 1980s. It also had good chemical stability, water solubility and wide tissue distribution. Details of the characteristics of pimonidazole are shown in table 4. Initial studies using pimonidazole showed the lifetime of hypoxic cells in canine tumours was of the order of days (204) and that the high binding of 2-nitroimidazoles in the liver did reflect normal tissue hypoxia and not native nitroreductases (205).

Characteristic	Value
Chemical name	1-[(2-hydroxy-3-piperdinyl)propyl]-2-nitroimidazole hydrochloride.
Molecular weight	290.7
Oxygen concentrations binding threshold.	Less than 14 micromolar O_2 Equivalent to pO_2 of 10 mm Hg at 37°C
Stability	Unchanged after 1.5 years at 4°C in subdued light as determined by high performance liquid chromatography and ultraviolet spectroscopy
Water solubility	High (400 millimolar; 116 grams per 1000 mL)
Plasma half life	5.1 ± 0.8 hours
Octanol-water partition coefficient	8.5
Biodistribution	Diffuses readily into tumours and normal tissues including brain concentrates approximately 3 fold above plasma levels in tumours and normal tissues
Volume of distribution	155 litres
Antibody detection	Both polyclonal and monoclonal antibodies can be used
Human dose	$0.5g.m^{-2}$
Toxicity	No CNS Toxicity at dose of $0.5g.m^{-2}$ Occasional Transient flushing with infusion
In vivo lifetime	At least 3 days

Table 4 The characteristics of pimonidazole

The first report using pimonidazole in humans as a hypoxic marker examined the distribution of hypoxia and proliferation in squamous carcinoma of the cervix. Five patients were given $0.5g/m^2$ of pimonidazole intravenously, followed 24 hours later by multiple punch biopsies of tumour. The tissue was processed into paraffin blocks and contiguous sections immunohistochemically stained for MIB-1, PCNA and pimonidazole. All five patients showed staining for pimonidazole, the mean stained fraction varying between 1.2% and 33.4%. There was little overlap between regions of proliferation and hypoxia (206).

Pimonidazole has gained widespread use as an investigational marker for hypoxia, and, as predicted by Raleigh, has allowed study of the interrelationships between hypoxia and other microenvironmental characteristics.

EF5 ([2-(-nitro-1H-imidazole-1-yl)-N-(2,2,3,3,3-pentaflouropropyl)acetamide]) is another 2-nitroimidazole, detectable by immunohistochemical means by virtue of its fluoro-substituents. It has been licensed for use in humans and the first use in humans was reported by Evans et al in 1999 (207). Six patients with squamous cell carcinoma received EF5 intravenously followed by biopsy. There were no acute or late adverse effects. Bound EF5 was demonstrated in frozen sections of biopsied tissue using monoclonal antibodies labelled with Cy3, a green-excited orange-emitting fluorescent dye. The pattern and quantity of binding was heterogeneous in intensity and distribution. EF5 provides an alternative to pimonidazole, although there have been no direct comparisons of the two markers in humans.

NitroImidazoleTheoPhylline (NITP, 7-(4'-(2-nitroimidazol-1-yl)-butyl)-theophylline) is another of the 2-nitroimidazole that is immunohistochemically detectable through a theophylline side-chain. It has not been used in humans, but has been a useful probe for hypoxia in animal studies. The first description of its use as a hypoxic marker demonstrated immunologically mediated detection using fluorescence cell sorting (208).

Intrinsic markers of hypoxia

Perhaps the ultimate marker of hypoxia would be an intrinsic factor upregulated by cells in response to a hypoxic microenvironment. The recent increase in understanding of cellular oxygen sensing, the identification of HIF and its transcriptional targets motivated the search for an intrinsic marker. Two possible candidate proteins have emerged- carbonic anhydrase 9 (CA9) and glucose transporter 1 (GLUT-1).

Carbonic Anhydrase 9

Carbonic anhydrase 9 is one of a group of zinc metalloenzymes that catalyse the reversible hydration of carbon dioxide to carbonic acid. They reside on the cell membrane and have an active extracellular site. They help maintain a range of physiological processes, particularly acid-base, ion and water balance. Zavada et al (209) originally identified CA9 as 'MN' protein in a HeLa cell line. It was found in clinical tumour specimens of ovarian, endometrium and cervical cancer but not in normal tissue of the corresponding organs. Pastorek identified the cDNA sequence and showed the amino acid sequence in the central region of the MN protein and carbonic anhydrase was identical. MN was thus reassigned as CA9.
CA9 is abundantly expressed in normal gut tissue throughout the GI tract (210) and particularly in cells with the highest proliferative capacity (211). More recently CA9, along with other CA types have been identified in epididymal ducts of the testes (212). CA9 has also been identified in renal cell (213), oesophageal (214), lung carcinoma (215) and colorectal cancer (211), pancreatic tumours (216) and head and neck carcinoma (217). CA9 has been suggested as a target for cancer therapy, shown in principle by the down-regulation of transmembrane carbonic anhydrases in renal cell carcinoma cell lines by wild-type von Hippel-Lindau transgenes (218). However, the existence of CA in normal gut as well as other organs may preclude this.

The dependence of CA9 upregulation on HIF1 was shown in a study by Wycoff et al. Renal cell carcinoma lines defective for the von Hippel Lindau protein lost hypoxic regulation of CA9 and CA12, supporting HIF 1 dependence. The upregulation of carbonic anhydrase by hypoxia was confirmed in a number of cell lines. Wycoff also

identified the hypoxia responsive element in the CA gene, to which the HIF transcriptional promoter binds. Furthermore the expression of CA9 was examined in human tumour specimens stained for pimonidazole and substantial overlap in the staining occurred supporting its role as an intrinsic marker of hypoxia within tumours (118).

Glucose transporter 1

Glucose transporter 1 (GLUT-1) is a widely expressed transmembrane glycoprotein and is one of a family of six facilitative glucose transporters (219). In the intestine and renal proximal tubule, glucose is transported against a concentration gradient by a secondary active transport mechanism in which glucose is cotransported with sodium ions. In all other cells, the GLUT family of glucose transporters mediates Na^+ independent transport of glucose into cells. The pattern of expression of the GLUT transporters in different tissues is related to the different roles of glucose metabolism in different tissues and their affinity for different monosaccharides varies accordingly. GLUT-1 has been located in many rodent tissues including erythrocytes, kidney, breast, placenta and amniotic membranes (219). It is also expressed in a wide variety of human tumours, including renal cell carcinoma (220), oesophageal cancer, colon cancer, head and neck cancers (221), brain haemangioblastoma (222), breast cancer (223), ovarian cancer (224, 225) and gastric cancer (226).

GLUT-1 is upregulated by a variety of mechanisms and can be expressed at different rates according to the stimulus. Acute stimulation can occur within minutes, probably from activation of pre-existing GLUT on the cell surface (227) or rapid

transport of GLUT stored intracellular vesicles (228). Reduction of oxidative phosphorylation appears to be the trigger, which occurs in hypoxic conditions (229). Chronic stimulation arises from transcriptional activation. (230). The identification of an HRE on the GLUT-1 gene by Ebert et al (231) and the proof that HIF 1 upregulates GLUT-1 mRNA (232), added GLUT-1 to the list of hypoxia regulated genes.

Non invasive hypoxia marker techniques

Detection of sensitiser adducts

As well as 3H and 14C labelled 2-nitroimidazoles, a range of other isotopes have been used to label nitroimidazoles as hypoxia markers, including ^{75}Br, ^{76}Br, ^{77}Br (233), ^{18}F (234, 235), ^{123}I (236) (237, 238), ^{131}I (239) and ^{99}mTc (240). ^{123}I, ^{131}I and ^{99}mTc labelled compounds are suitable for single photon emission tomography (SPECT) (241). Iodinated azomycin arabinoside (IAZA) (238) has been developed and clinically evaluated as a SPECT imaging agents (242). Clinical investigation of IAZA in 51 patients and F-MISO in 37 patients have been reported. No reported adverse effect from either the drug or the radiation effect from the isotope occurred.

In the study of 52 different tumours in 51 patients by Urtasun (243), IAZA was administered 18–24 hours prior to SPECT imaging. Activity within tumour regions of interest (ROI) was compared to that within equal ROIs in contralateral normal tissue. Significant hypoxia, defined as a tumour/normal tissue (T/N) ratio of marker activity of 1.1 or more, was seen in 21 tumours. For the other 31 tumours, T/N ratios were 1.0. These data suggested that the hypoxic fraction of solid human tumours is significantly lower than in rodent tumours, consistent with data obtained from Eppendorf pO_2 histograph (244). Twenty-seven tumours in this study also had their tumour perfusion measured with Tc-99m-hexamethylpropyleneamine oxime (HMPAO) by SPECT (245).

For the IAZA images, 13 tumours showed hypoxia. For the HMPAO images, 13 tumours that showed decreased perfusion by HMPAO, only eight showed increased

avidity for IAZA, indicative of hypoxia. When the glioblastomas (to which IAZA delivery was possibly inefficient) were excluded from this analysis, eight of nine tumours that showed decreased perfusion showed increased avidity for IAZA. In addition, 50% of the (3/6) head and neck tumours showed significantly increased perfusion measured by HMPAO with an increase in the hypoxic signal. These findings indicated the relationship between perfusion and oxygenation is not simple.

The clinical study of PET images of F-MISO detected significant hypoxia in 97% (36/37) of the investigated tumours (246). Marker radioactivity was analysed for each pixel through tumour cross-sections. The fractional hypoxic volume (FHV) was defined as the proportion of pixels within the imaged tissue with tumour to blood ratios of marker radioactivity greater than 1.4. Thirty-six of the 37 tumours investigated (21 non-small cell lung cancers, seven head and neck cancers, four prostate cancer and five other malignancies) showed this level of increased radioactivity in at least in one or more of their tumour pixels. The median FHV was 47.6% for the non-small cell lung cancers and 8.8% for the head and neck carcinomas. Marked intra- and inter-tumour heterogeneity of marker uptake was seen. Tumour size and the degree of tumour hypoxia did not correlate.

The importance of the 'cut off' parameters for investigating tumour hypoxia in this way is clear when these two studies are compared. In the IAZA/SPECT study contralateral normal tissue was used as the oxygenated reference. Even when the SPECT assay was done at two plasma clearance half-lives of IAZA to improve differentiation of hypoxia-linked radioactivity from the background of unbound marker, ratios were rarely exceeded 2.0. However, in the PET study with F-MISO where the blood activity level was the reference, ratios of marker of 1.4 and greater only 2–3 hours after administration were found in most tumours. F-MISO ratios of greater than 1.4 were found in 13.1 and 16.6% of the pixels analysed from normal

muscle and brain tissue respectively, suggesting a substantial hypoxic fraction in normal tissue by this definition. The timing of image acquisition, the choice of the reference tissue and the threshold ratio all need to be carefully validated. The timepoint for image acquisition with both IAZA and F-MISO were defined from physical half lives of ^{123}I and ^{18}F that probably led to sub-optimal estimates. Markers labelled with ^{131}I and ^{124}I may be required for optimal SPECT and PET procedures, respectively (247).

Aside from the technical difficulties, the isotopes with short half-lives (e.g. ^{123}I, ^{18}F) are produced in a particle accelerator and then require incorporation into the nitroimidazole for each patient, which may limit use to a small number centres. 99mTc ($t_{½}$ 6 hours) is produced by decay of the 99Mo ($t_{½}$ 66 hours) and its use does not require such elaborate procedures. Earlier technetium-labelled 2-nitroimidazoles suffered from high lipophilicity and thus high uptake in the liver. Less lipophilic 99mTc-labelled probes have been developed, which reduces liver binding. A lead compound currently under investigation as a bioreductive hypoxia marker, 99mTc-HL91, does not contain a 2-nitroimidazole moiety, but can be enzymatically reduced by xanthine oxidase (248-251).

Magnetic resonance spectroscopy of fluorinated nitroimidazoles

Magnetic resonance spectroscopy (MRS) provides details of various aspects of tissue chemistry from of variety of administered nuclei including ^{1}H, ^{31}P, ^{13}C, ^{23}Na. The para-magnetic molecule, ^{19}F can be relatively easily conjugated with other molecules to allow particular aspects of the tissue of interest to be evaluated. Fluorinated 2- nitroimidazoles have been produced to allow hypoxic cells to be

identified by this method. Raleigh et al (252) synthesised a hexafluorinated 2-nitroimidazole (CCI-103F). In Balb/C mice it was preferentially bound within tumour with a plasma-to-tumour ratio of 0.8. Li et al used this technique in SCCVII tumours finding that the signal obtained positively correlated with tumour size consistent with the fact that larger SCCVII tumours have larger hypoxic fractions (253). Further analysis of the fraction of surviving tumour cells after a single fraction of 10Gy irradiation revealed that tumours that retained larger amounts of CCI-103F had higher surviving fractions. Further studies established the proof of principle that fluorinated probes were suitable MRS directed markers of hypoxia (254, 255). The same analogue was evaluated with another fluorinated 2-nitroimidazole (Ro 07-0741) by Maxwell et al (256). Ro 07-0741 is a mono-fluorinated probe and was found to be less lipophilic than its hexafluorinated counterpart. Signal was readily detectable by MRS in EMT6 tumour, liver, and brain soon after i.v. injection in BALB/c mice. Tumour levels remained constant upto 10 hours after injection whilst there was a reduction in signal intensity from brain and liver. The work was repeated in KHT and RIF-1 tumours in C3H/He mice. RIF-1 tumours have a lower hypoxic fraction than KHT tumours and the comparative signal obtained reflected this difference. However, the problem of the lipophilic nature of these compounds remains to be solved: a hydrophilic compound would not only be less neurotoxic, but also be less susceptible to metabolism by non-nitroreductive pathways. This was the rational for the design of SR4554, that consists of a hydrophilic side chain, three fluorine atoms to enhance magnetic detection and the 2-nitroimidazole ring to bioreduce only within hypoxic cells (257). In vivo and clinical studies are in progress.

Bladder Carcinoma: an overview

Incidence

Bladder carcinoma has become more common over the last 20 years, with over 10000 cases diagnosed in the UK each year. It accounts for 5000 deaths per year. The disease is three times more common in males than females and the incidence increases with age. However, well-differentiated tumours occur more commonly in those younger than 30 years (258).

Aetiology

A number of aetiologic factors have been identified.

Cigarette Smoking

Cigarette smoking is the main aetiologic factor associated with bladder cancer with a 2 to 5 fold increase in risk (259).

Occupational Exposure

Those who work with aniline dyes, exposed to aromatic amines, have a relative risk of 1.7 to 8.8 of developing bladder cancer. Other chemical carcinogens have been identified, including 2-napthylamine, benzidine, 4-aminobiphenyl, dichlorobenzidine, orthodianisidine and orthotolidine. Rubber manufacturers, coal gas producers, sewage workers, firelighter manufactures, pest controllers and textile printers are all exposed to potential carcinogens (260).

Drugs

Certain drugs are associated with bladder carcinoma, including phenacetin and cyclophosphamide(260).

Chronic infection

Chronic infection with indwelling catheters has been associated with an increased risk of squamous cell bladder cancer. Schistosomia Haematobium infection is also associated with bladder carcinoma, and produces 70% rate of bladder cancer in endemic regions in Egypt.

Pathology

Transitional cell carcinoma

Transitional cell carcinoma accounts for 90% of cases of bladder carcinoma in industrialised nations. It may be of papillary type and non-invasive, or of solid type, which is invasive. Another subtype is carcinoma in situ, which is a flat, intraepithelial anaplastic form of the disease. Half of CIS occurs with either papillary or solid tumours.

Squamous cell carcinoma

This has a nodular and invasive growth pattern, and makes up to 10 % of cases in industrialised countries. It is much more common in developing countries.

Adenocarcinoma

This type is rare, accounting for only 2% of cases. One third of adenocarcinomas of the bladder arise from the urachus. These tumours are usually solitary and ulcerative, and are histologically identical to lower gastrointestinal tract tumours.

Undifferentiated

These are small cell carcinomas, similar to small cell carcinoma of the lung. Cells have high nuclear to cytoplasmic ratios and form in sheets or nests.

Staging and grading

The TNM (Tumour- Node- Metastasis) staging system is most commonly used (UICC 1997)(table 5, figure 17). Tumours are graded according to a three-grade system that takes into account the degree of anaplasia according to the nuclear to cytoplasmic ratio and nucleolar frequency (figure 18).

TNM Staging (UICC 5th Edition 1997)		
TIS	-	Carcinoma insitu
Ta	-	Papillary non-invasive
T1	-	Tumour invades subepithelial connective tissue
T2	-	Tumour invades muscle
	T2a-	Tumour invades muscle (inner half)
	T2b-	Tumour invades deep muscle (outer half)
T3	-	Tumour invades perivesical tissue
	T3a-	Microscopically
	T3b-	Macroscopically
T4	-	Tumour invades any of following: prostate, uterus, vagina, pelvic/abdominal wall
	T4a-	Tumour invades prostate or uterus or vagina
	T4b-	Tumour invades pelvic wall or abdominal wall

Table 5 The TNM staging system for bladder carcinoma

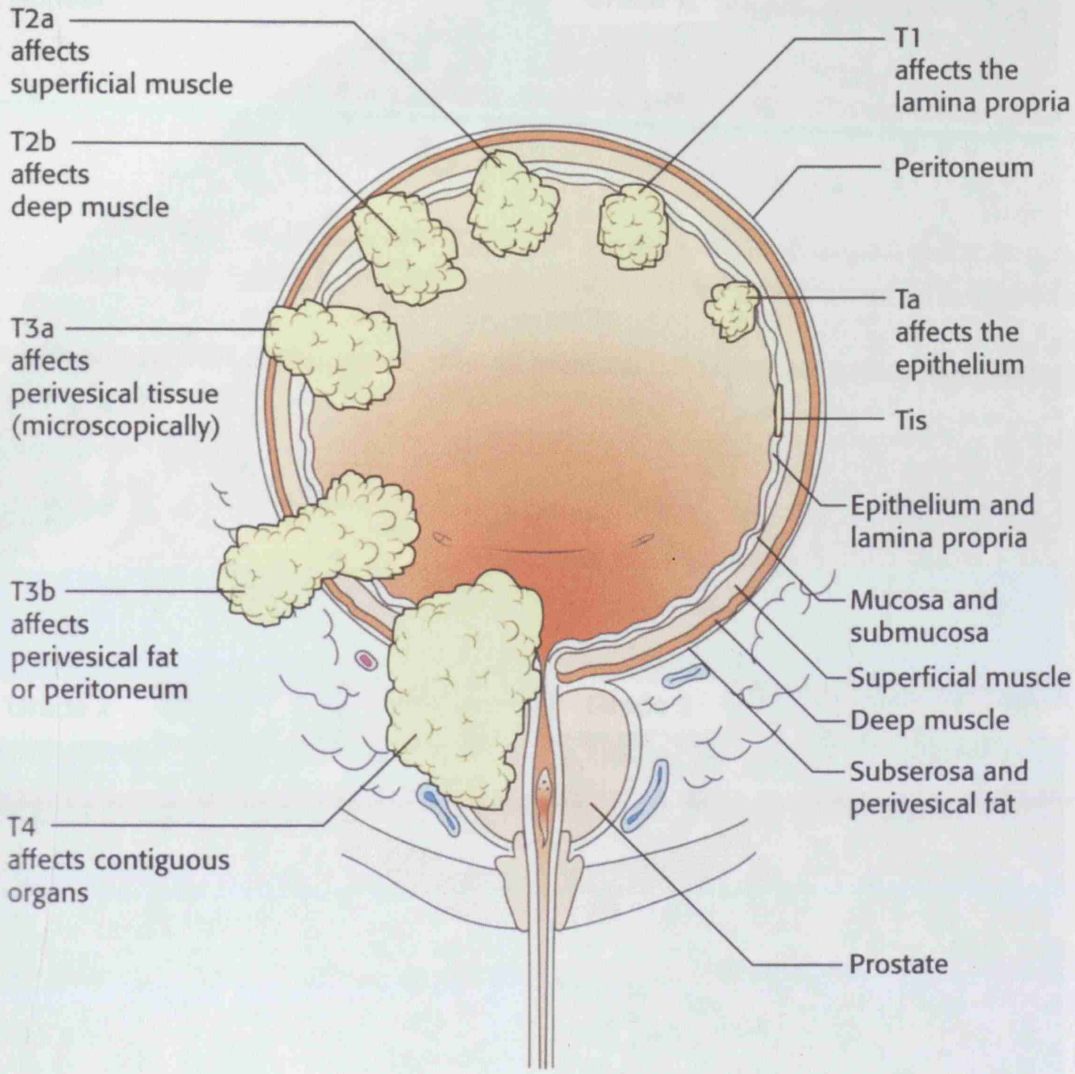

Figure 17 T-staging system for bladder carcinoma

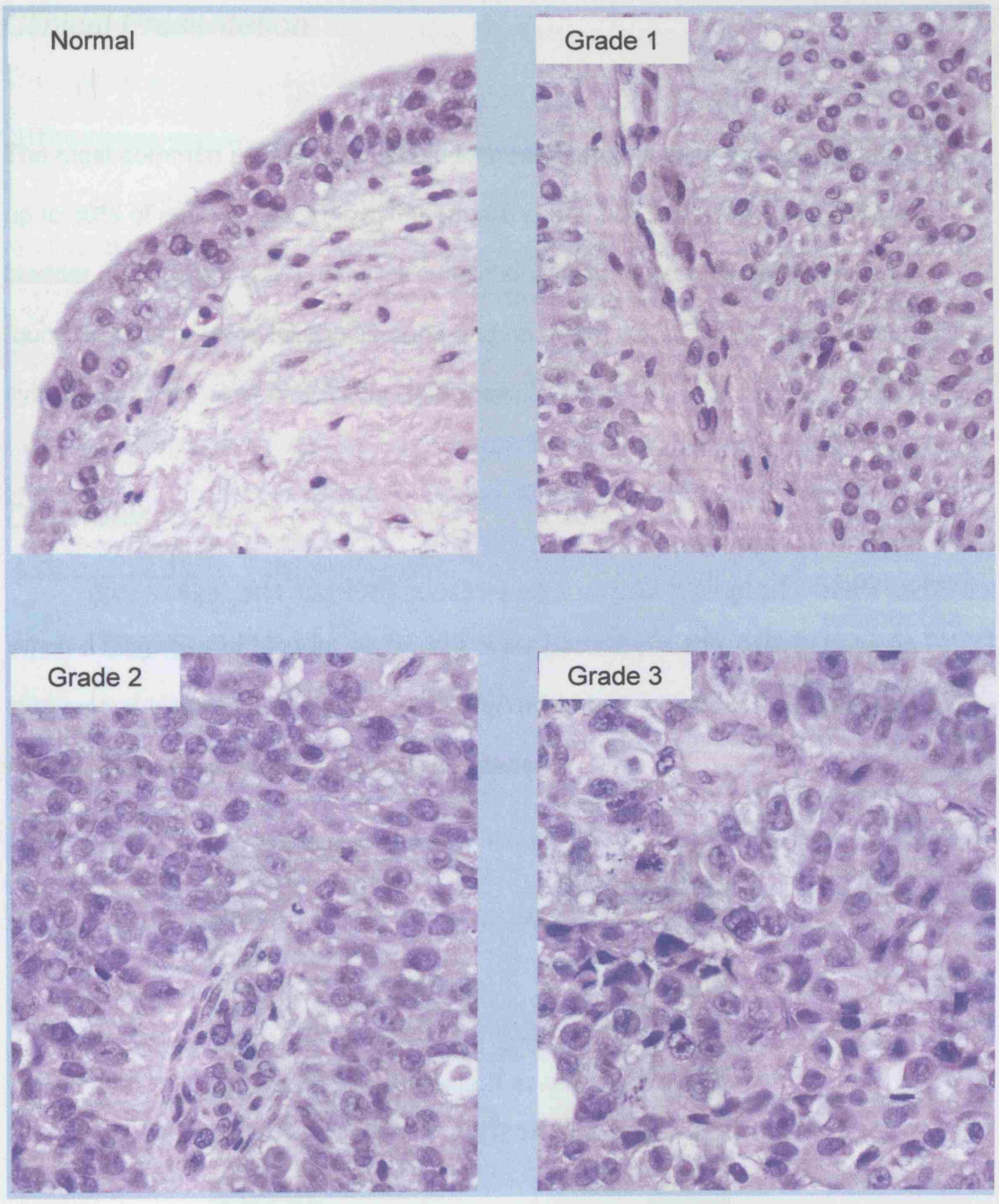

Figure 18 Images of histological sections through normal urothelium and grades 1,2 and 3 transitional cell carcinoma

Clinical Presentation

The most common presentation of bladder carcinoma is painless haematuria, with up to 30% of patients with this symptom are eventually diagnosed as having a bladder malignancy (261). Other presentations include microscopic haematuria, found on routine urine testing, dysuria and recurrent infections, or systemic symptoms in the case of advanced disease.

Diagnosis

When a diagnosis of bladder carcinoma is suspected, patients usually have an intravenous urogram that will show a filling defect in the bladder if a mass is present or irregularity in the case of superficial disease.

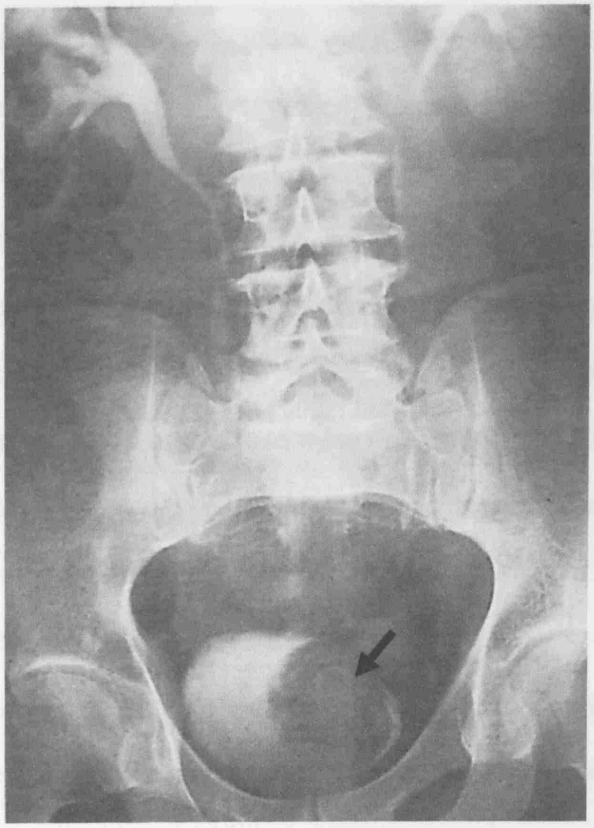

Figure 19 An intravenous urogram showing a large filling defect in the bladder (arrowed)

Cystoscopy is usually performed to confirm the diagnosis histologically. A flexible cystoscopy is performed if the IVU is not diagnostic and can be done under local anaesthetic as a day procedure. Otherwise, a rigid cystoscopy is done under general anaesthetic that allows diathermic resection of the tumour mass. The diagnosis and T-stage is confirmed from these samples. If muscle invasive disease is found, a pelvic and abdominal CT scan is done to assess for lymphadenopathy in these regions.

Treatment outline

The treatment offered depends on the stage of disease. For in situ disease, intravesical BCG is recommended, having shown complete remission rates of up to 80%. If there is no response, then cystectomy is offered. For stage Ta disease, a transurethral resection is often adequate, but if there are multiple sites of superficial disease or it is serially recurrent, intravesical therapy is used. This is usually with mitomycin c for lower risk disease and BCG for high-risk disease. A similar management plan is used in stage T1 bladder cancer, although for high-grade tumours, cystectomy is recommended because of its high propensity to progress despite intravesical treatment or radiotherapy. For muscle invasive disease, either radical radiotherapy is used or cystectomy is recommended. Radical radiotherapy has the advantage of being organ preserving and many centres prefer this as a first choice option, saving surgery for salvage of treatment failures. Chemotherapy does not have an established role in radical treatment.

In metastatic disease and sometimes in locally advanced disease a palliative approach may be taken, employing symptom control manoeuvres in which radiotherapy and /or chemotherapy may have a role.

Prognosis

Recent results of 10-year follow-up of 1054 patients with invasive bladder cancer treated with radical cystectomy and pelvic lymph node dissection with curative intent confirmed its efficacy as a standard approach. The perioperative death rate was 2.5%, with 28% early complications. The 5-year disease-free survival (DFS) for the whole group was 68%, with 66% at 10 years. For the organ-confined, lymph node-negative tumours, the 5-year and 10-year DFS figures were 92% and 86% for T0, 91% and 89% for Tis, and 83% and 78% for T1. For node negative, muscle-invasive tumours, T2 had 89% and 87% DFS, and T3a had 78% and 76% DFS. For node negative, non-organ-confined tumour, T3b had 62% and 61% 5-year and 10-year DFS, whereas T4 had 50% and 45%. Lymph node-positive tumours faired less well, with 35% and 34% 5-year and 10-year DFS, respectively. Overall, bladder cancer recurred in 30% of the patients, 22% distantly and 7% locally, supporting the concept that aggressive surgical management of invasive bladder cancer can achieve excellent long-term survival with a low incidence of pelvic recurrence (262).

Inter-trial comparison of the outcomes of radical radiotherapy and surgical treatments is difficult due to selection bias to fitter patients undergoing radical cystectomy. However, a review of 13 selected studies with a total of 3,824 patients treated with radiotherapy alone and using various treatment techniques, showed 5-year survival rates ranging from a low of 7% to a high of 32%. The 10-year survival based on five reported studies show survival rates of 7% to 19% (263).

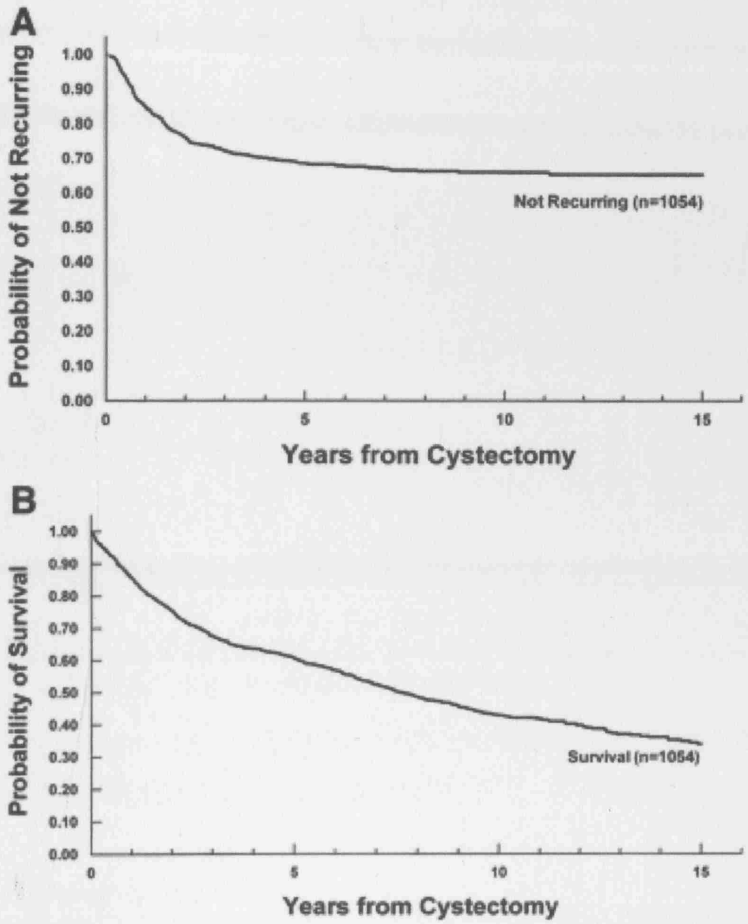

Figure 20 Recurrence-free survival (A) and overall survival (B) in 1,054 patients undergoing radical cystectomy with intent to cure for invasive bladder cancer.

CHAPTER TWO

The Assessment of Hypoxia in Bladder Carcinoma using Pimonidazole

Aim

The aim was to

- confirm and quantify the existence of hypoxia in bladder carcinoma
- assess the clinical applicability of pimonidazole as an extrinsic marker of hypoxia
- assess the reproducibility of the method of measurement of pimonidazole staining.

Methods and Materials

Ethical approval

The local ethics committee approved the study.

Patient Selection

All patients were able to give informed consent and over the age of 18. Patients were recruited from local urology units where a diagnosis of bladder cancer had been made by flexible cystoscopy. Those with larger tumours were selected to allow sufficient material for diagnostic and staging purposes as well as for the study.

Pimonidazole storage and presentation.

Pimonidazole (trade name: hypoxyprobe-1) was obtained from Chemicon International, Inc, (28820 Single Oak Drive, Temecula, CA 92590, USA). Initially pimonidazole was delivered as a solid formulation, requiring dissolution into 10 millilitres of normal saline, then diluted in a further 100 mls. Latterly, pimonidazole was supplied in liquid form that could be injected directly into a bag of 100 mls of normal saline. Twenty patients received the solid formulation and eleven received the liquid formulation. All vials were stored in a fridge at 4°C and protected from light. Liquid pimonidazole was allowed to reach room temperature before dilution to circumvent any problems of crystallisation at low temperature, which could potentially reduce the delivered dose.

Pimonidazole delivery

Patients were given 0.5 g/m^2 of pimonidazole in 110ml of normal saline intravenously via a 20-G cannula inserted into a superficial vein in the forearm. Infusions lasted between 15 and 20 minutes and the bag containing the drug was protected from light throughout. The drug was given between 8 and 18 hours prior to a formal rigid cystoscopy.

Sample collection and preparation

Patients underwent a transurethral resection of bladder tumour with a rigid cystoscope and diathermy under general anaesthetic. Fresh samples of tumour were placed into formalin (40% w/v formaldehyde in water) for fixation, protected from light and stored in a fridge. Tumour samples were paraffin embedded, cut into 4μm sections using a microtome and mounted on to glass slides for staining.

Immunohistochemistry: pimonidazole staining

Principle of the Avidin-Biotin Complex method

The reduced product of pimonidazole was stained using the avidin-biotin complex method. This method depends on the high affinity of avidin for biotin via four binding sites. A biotinylated immunoglobulin acts as a link antibody, possessing biotin molecules covalently bound to the constant regions of the heavy chain. Open sites on a separate avidin-biotin complex bind to the biotin on the link antibody. The avidin-biotin complex also consists of horseradish peroxidase, derived from the root of the horseradish plant, which acts on a chromogen. In this case, the chromogen is diaminobenzine tetrahydrochloride (DAB).

DAB is one of a number of electron donor molecules used as chromogens in peroxidase based immunohistochemistry. Endogenous cellular peroxidases need to be blocked to ensure the stain is specific to bound antibody. This is done by bathing samples in 0.1% hydrogen peroxide before adding the antibody. Peroxidases have an iron-containing group, haematin, which complexes with hydrogen peroxide to form water and atomic oxygen. If there is excess hydrogen peroxide, a catalytically inactive complex is formed. The staining procedure involves adding DAB and hydrogen peroxide to the avidin biotin complex; the peroxidase releases atomic oxygen from the hydrogen peroxide that oxidises DAB to produce a brown insoluble end product.

Procedure

- Slides were dewaxed in xylene for 5 minutes and rehydrated through graded alcohols (100,90, 70%) to water.
- Sections were then transferred to a 37°C water bath containing 0.01% pronase (Sigma) buffered to pH 7.8.
- After 10 minutes, sections were washed in running tap water for five minutes.
- Endogenous peroxidase was blocked in a 0.1% hydrogen peroxide dissolved in methanol for half an hour at room temperature, then washed well in water, then rinsed in tris buffered saline. The tris buffered saline was made up of 0.1M tris (12 g/L) and 0.1M HCL (10ml/L), and adjusted to a pH of 7.4 to 7.6. Tris buffer saline consisted of 250 ml of Tris buffer, 2250 ml of distilled water and 20.25g of sodium chloride, and the pH was adjusted to 7.6.
- The section was then encircled with resin using a resin pen to well in the solutions used in the rest of the staining process.
- Protein block (Dako X0909, 0.25% casein in PBS containing carrier protein and 15nM sodium azide) was added and left for five minutes to inhibit non specific staining. The excess was tipped off.
- Anti –Pimonidazole antibody mixture (Natural Pharmacia Cat 01800 Mab1) was added. This consisted of antibody diluted in 1/100 tris buffered saline and 50microlitres of Dako protein block for every millilitre of antibody. The antibody is a monoclonal antibody produced by clones of a single set of plasma cells. The first step in production involves exposing a mouse to pimonidazole. B-lymphocytes are harvested from the mouse spleen and fused with myeloma cells to form so called hybridoma cells. The hybridoma cells are propagated in culture medium and the antibody concentrates in the supernatant. Anti–

Pimonidazole antibody is supplied as an untreated exhausted supernatant from the hybridoma clone 4.3.11.3.

- Anti-pimonidazole antibody mixture was left in the slide for one hour at room temperature, and removed by three successive washes with tris buffered saline for a total of three minutes.
- The secondary antibody, a biotinylated rabbit anti-mouse antibody (Dako E0354) diluted in 1/400 in tris buffered saline, was then added for one hour.
- ABComplex Horseradish peroxidase was added (Dako K0355) for a further hour at room temperature.
- The section was then washed in tris buffered saline twice and once in Tris Buffer.
- Diaminobenzine substrate was then added (Vector SK4100). This was made up of 5 millilitres of distilled water, 2 drops of buffer and 4 drops of Diaminobenzine and 2 drops of 0.1% hydrogen peroxide.
- After five minutes the section was rinsed in tris buffer and washed in water.
- To stain nuclei blue, the sections were placed in Mayers Haematoxylin for between 10 to 60 seconds and then washed well in tap water.
- Finally the sections were dehydrated through graded alcohols, cleared by xylene and sections mounted in DPX (Merck 360294H) mounting media.

The resulting section shows nuclei as blue and pimonidazole bound cells as brown.

Image Analysis

Set up

A Zeiss Axioscope trans-illumination microscope with 5x, 10x, 20x, 40x objectives and a 10x eyepiece connected to a 3 CCD colour camera (JVC KY55F 1/3" (6.4 x 4.8mm) was used to capture tissue section images. Images were digitised with a Matrox Meteor™ frame grabber in a PCI bus 600MHz Pentium™ desktop PC monitor and a PC workstation. All measurements were taken with image analysis software (Visilog 1996).

Stained specimen slides were placed on the microscope stage and focussed at the required magnification. The image was captured and relevant stain measured.

Measuring the pimonidazole stained fraction and the necrotic fraction

Images were viewed through a 10x-objective and x10 eyepiece and the focussing and light level adjusted. The light level was set so as not to bleach any pimonidazole staining. Once the image was captured, the area measurement tool on Visilog was used to draw around the stained regions, overall tumour cell regions and necrosis. Stroma was excluded. Two sections from each tumour were assessed and between 3 and 45 fields were viewed (figure 21).

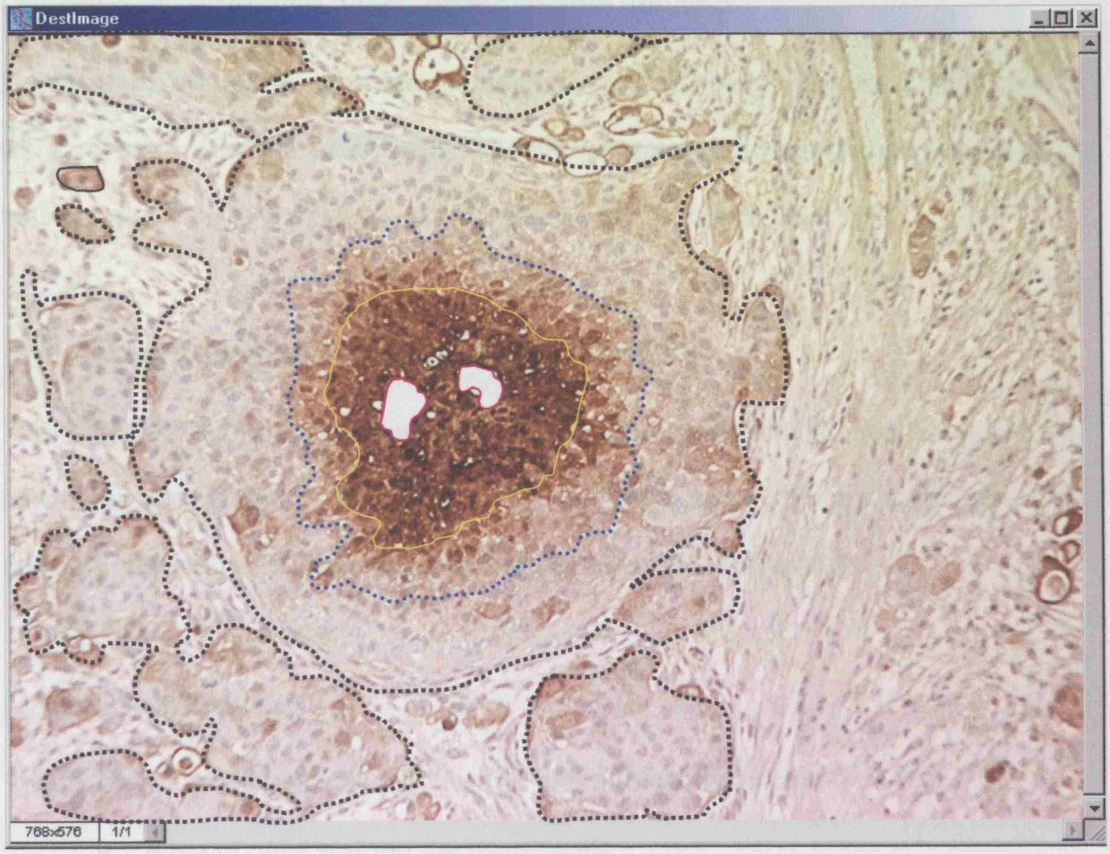

Figure 21 Screenshot of image analysis program showing a field of a section of bladder carcinoma immunohistochemically stained brown for bound pimonidazole. The variable stain intensity is seen with the tumour (·····), light stain (·····), dark staining (——) and necrosis (——) outlined. On this field, the total stained fraction is 23%, the dark stained fraction is 12.5% and the necrotic fraction is 1%.

Definition of 'Light' and 'Dark' pimonidazole staining

Lightly stained regions were demarcated by where staining and non-staining cells were adjacent. Darkly stained regions were demarcated by where the intensity of staining matched that adjacent to necrosis visibly reduced (figure 21).

Inter-observer and Intra-observer variation

Three independent observers assessing 25 fields of captured images assessed inter-observer variation. Intra-observer variation was assessed by a single observer (author) assessing 25 images in two sessions two months apart.

Data obtained

The following data were obtained for the entire tumour section:

- Area of cells stained darkly in pixels
- Area of cells stained lightly in pixels
- Total tumour area in pixels
- Area of necrosis in pixels
- Distance from edge of light pimonidazole staining to necrosis

The fraction of cells stained was expressed as a percentage of the total tumour area.

The fraction of necrosis was expressed as a percentage of the total tumour area.

The three shortest stain edge to necrosis distances were measured around each necrotic region

The areas of each region of staining assessed by the three observers were compared.

Statistics

The median and range of the stained fraction for the whole cohort was calculated. The inter- and intra-observer interpretations were compared between each observer using the Pearson correlation coefficient.

Results

Patient details

Thirty-one patients were recruited, all giving informed consent. Eight were female and twenty-three were male. The median age was 69.8 years. Five samples were inadequate; the tumour fragments were too small in 2 cases and no tumour was present in 3 cases. The histology of the remaining 26 patients' tumours was transitional cell carcinoma; 11 were grade III, 13 were grade II and 2 were grade I.

Pimonidazole Tolerance

All patients received the prescribed dose of pimonidazole. There were no serious adverse effects although two patients experienced a mild sensation of warmth similar to a hot flush. In both cases, this occurred towards the end of the infusion, and both patients were able to complete the administration.

Intra-observer variation in assessment of pimonidazole binding

There was strong intra-observer (author) agreement in the assessment of the overall pimonidazole bound fraction both for overall stained fraction ($r=0.98$, $r^2=0.96$, $p<0.0001$) (figure 22) and for dark staining ($r=0.98$, $r^2=0.95$, $p<0.0001$) (figure 23).

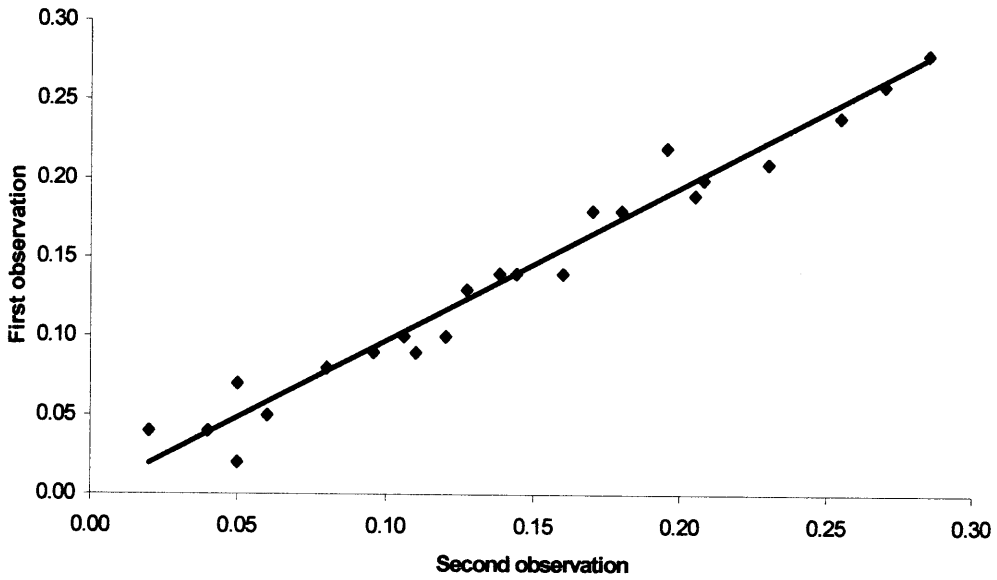

Figure 22 Plot of comparison of two measurements of total stained fraction taken by one observer separated by two months

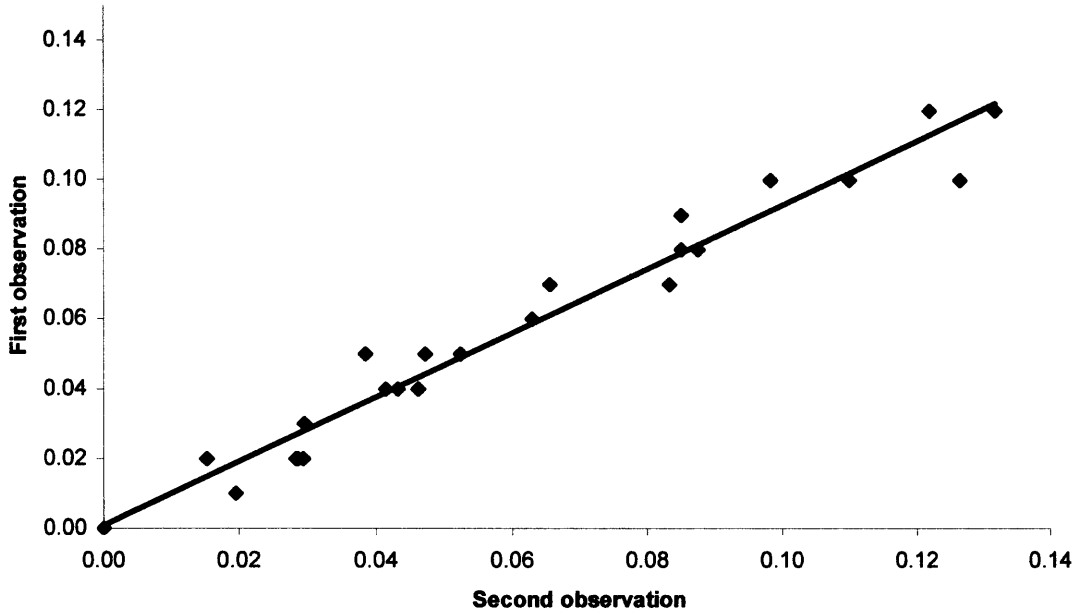

Figure 23 Plot of comparison of two measurements of dark stained fraction taken by one observer separated by two months

Inter-observer variation in assessment of pimonidazole binding

There was strong agreement between three independent observers in measuring the overall stained fraction (table 6, figure 24 and 25). The differentiation of the proportion of light and dark staining was less well correlated (table 7).

Observers compared	r	r^2	p-value
1 versus 2	0.90	0.81	<0.0001
1 versus 3	0.85	0.74	<0.0001
2 versus 3	0.90	0.82	<0.0001

Table 6 Correlation coefficients for inter-observer comparisons of total staining

Observers compared	r	r^2	p-value
1 versus 2	0.83	0.68	<0.0001
1 versus 3	0.90	0.81	<0.0001
2 versus 3	0.86	0.74	<0.0001

Table 7 Correlation coefficients for inter-observer comparisons of dark staining

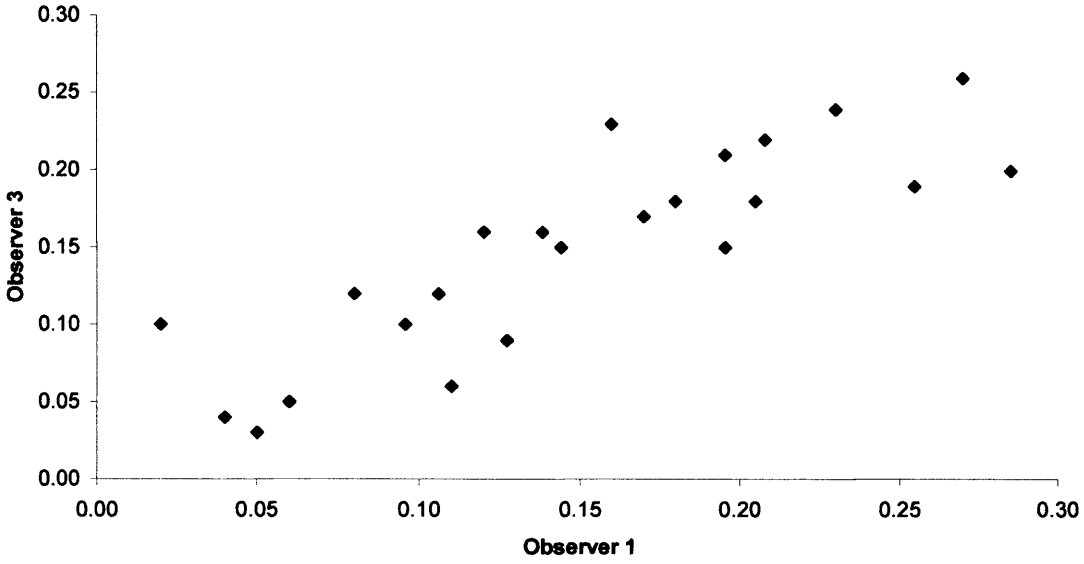

Figure 24 Plot of comparison of two measurements of total pimonidazole stained fraction taken by observers 1 and 3

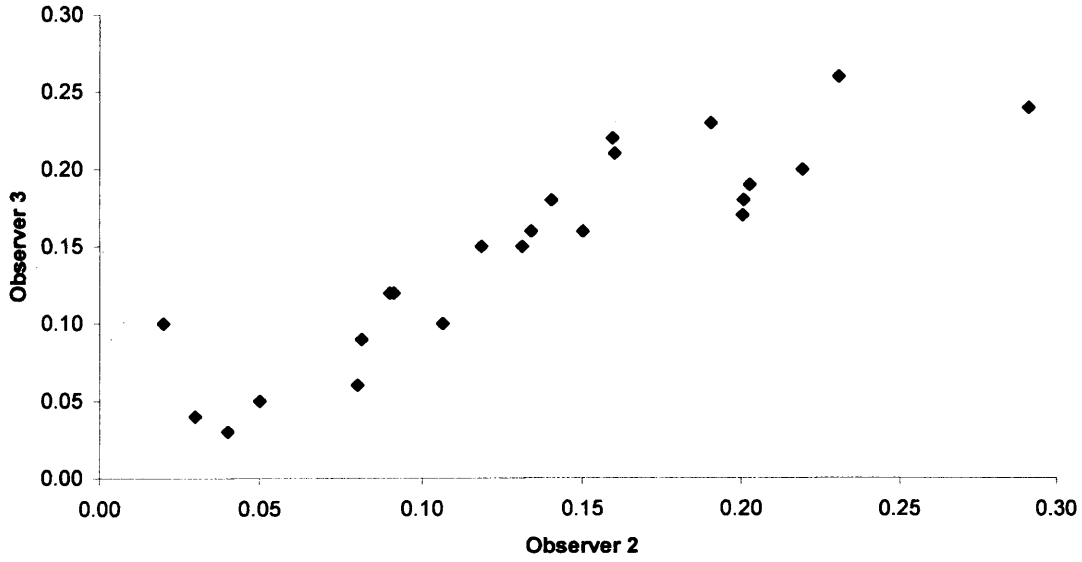

Figure 25 Plot of comparison of two measurements of total pimonidazole stained fraction taken by observers 2 and 3

Quantity of Stain

The stained fraction of tumour tissue ranged between 0 and 38%. The median stained fraction was 9%. The dark staining accounted for between 49% and 100% of the total stain, the greatest proportion in the lowest overall stained fractions (figures 26 and 27).

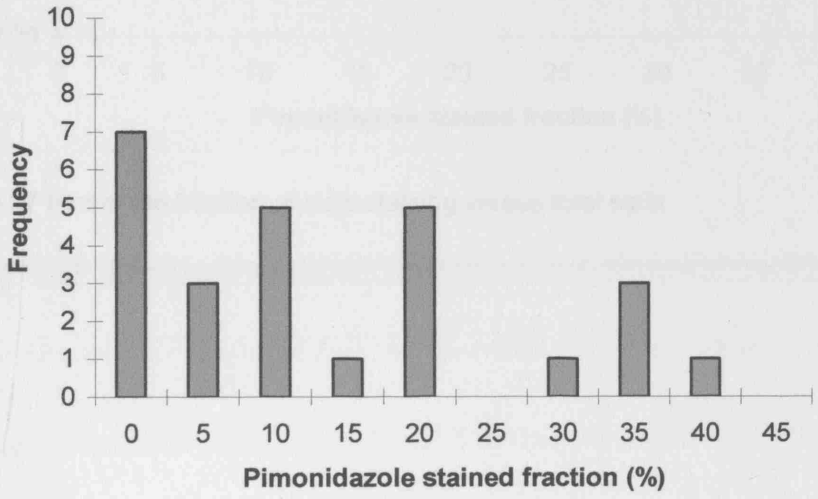

Figure 26 A histogram of pimonidazole stained fractions

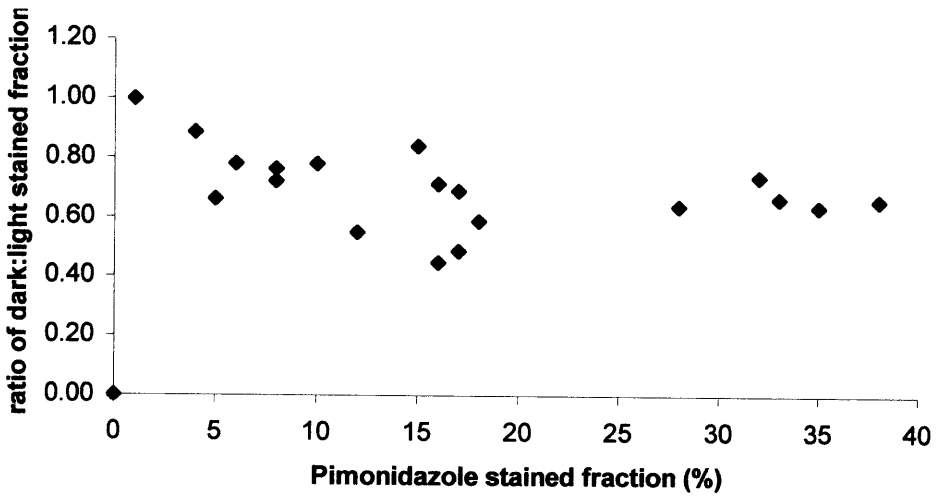

Figure 27 Plot of the fraction of dark staining versus total stain

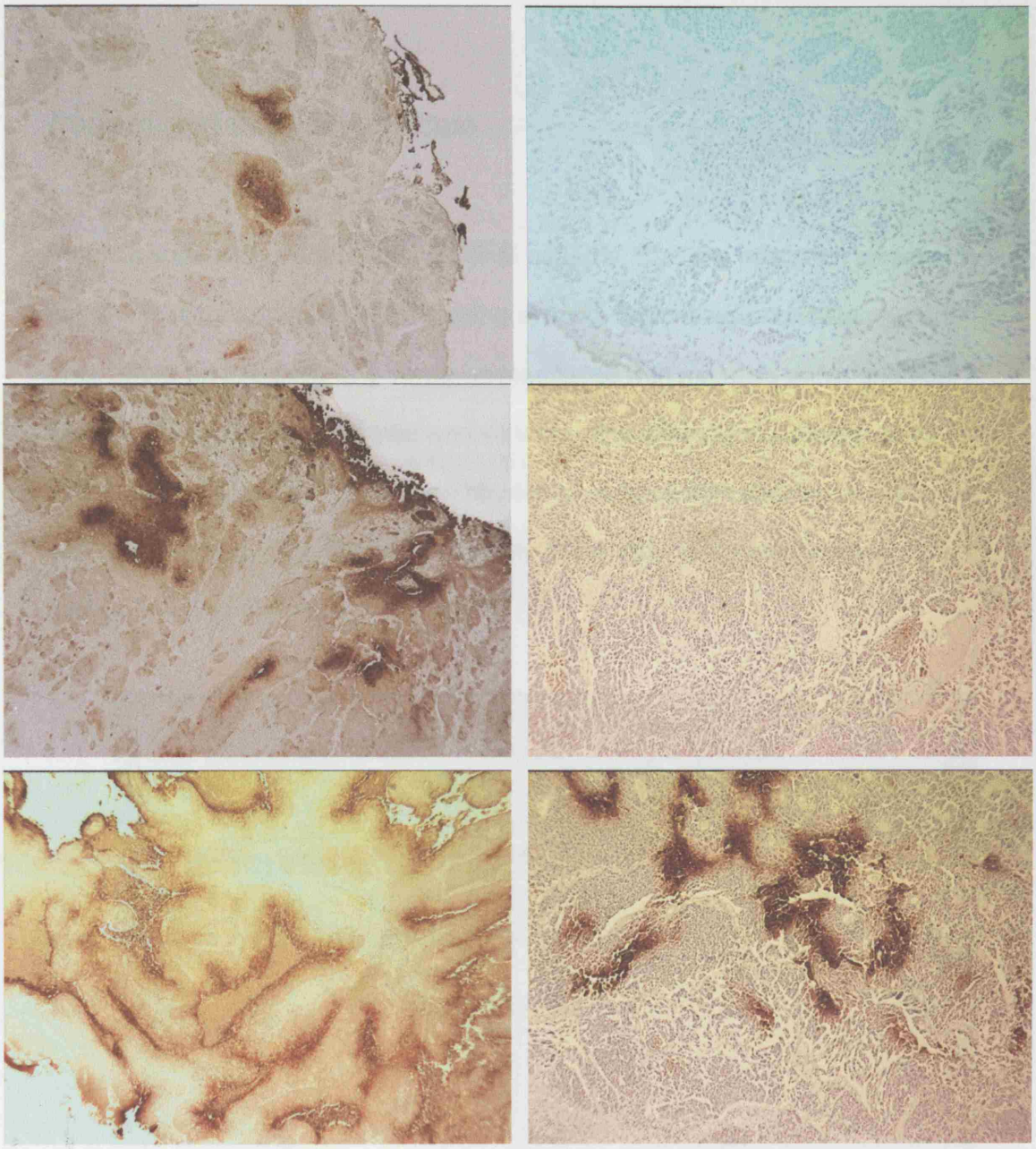

Figure 28 Sections of bladder carcinoma from six different patients illustrating heterogeneity of pimonidazole staining.

Pattern and Intensity of Stain

Staining appeared distributed in regional patterns. Staining was seen adjacent to but not within necrotic regions. The staining in these regions was consistently dark. There were also regions of staining unassociated with necrosis within a tumour section. The size of each region was variable. The intensity of staining varied from light to dark (figure 29). There were regions of isolated light staining unassociated with dark staining. The maximum intensity of the stain was comparable across all tumour samples (figure 28).

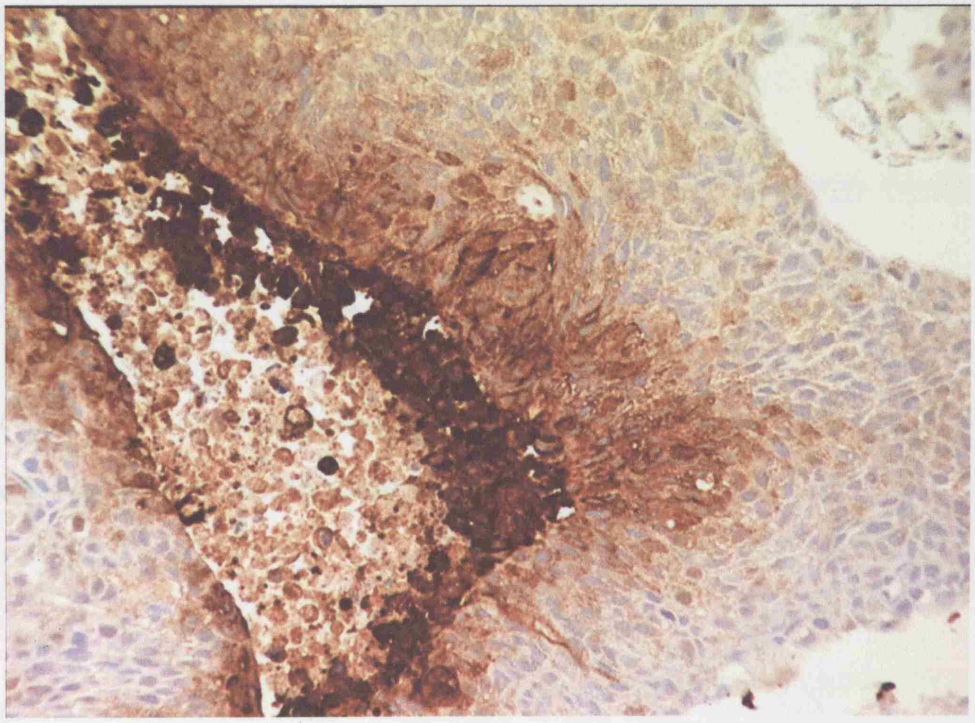

Figure 29 Section of bladder carcinoma stained for pimonidazole illustrating variable staining intensity and necrosis (mag x 20)

Necrotic fraction

The necrotic fraction ranged from 0 to 13%. Fifteen tumours showed no evidence of necrosis whilst in the other eleven it varied from 1 to 13% with a median of 5% (figure 30). There was no correlation between the fraction of pimonidazole staining and necrosis (r=0.57, p=0.0025) (figure 31). The median distance between the edge of light pimonidazole staining to the edge of necrosis was 58 μm, range 11 to 120 μm (figure 32).

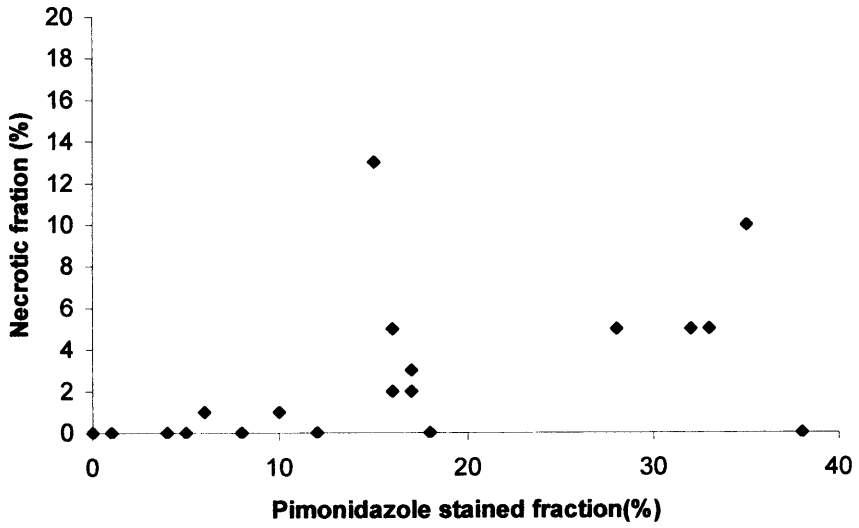

Figure 30 Histogram of necrotic fractions

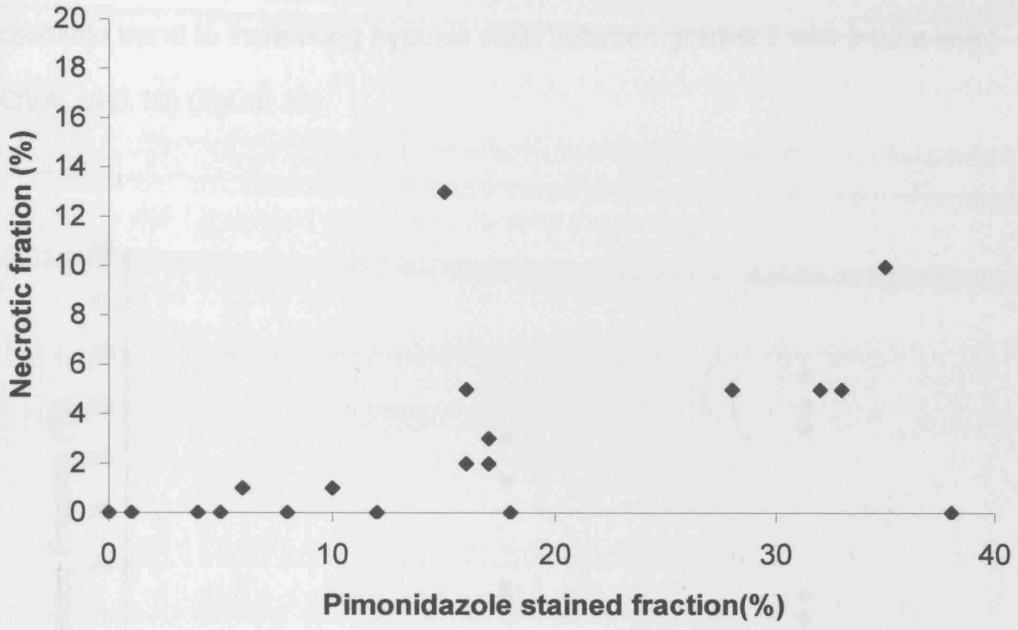

Figure 31 Plot of the necrotic fraction against the pimonidazole stained fraction

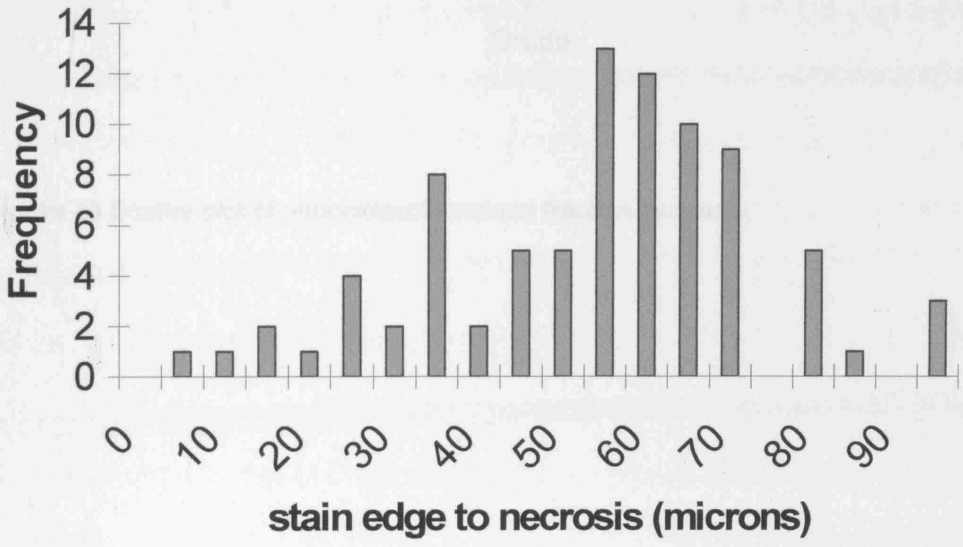

Figure 32 Histogram of distance from stain edge to necrosis (85 measurements across all tumours, measuring the three shortest distances around each region of necrosis)

Pimonidazole stained fraction and tumour grade

No pimonidazole staining was seen in the two grade 1 tumours. There was no discernable trend to increasing hypoxic stain between grades 2 and 3 (one way ANOVA, $p>0.19$) (figure 33).

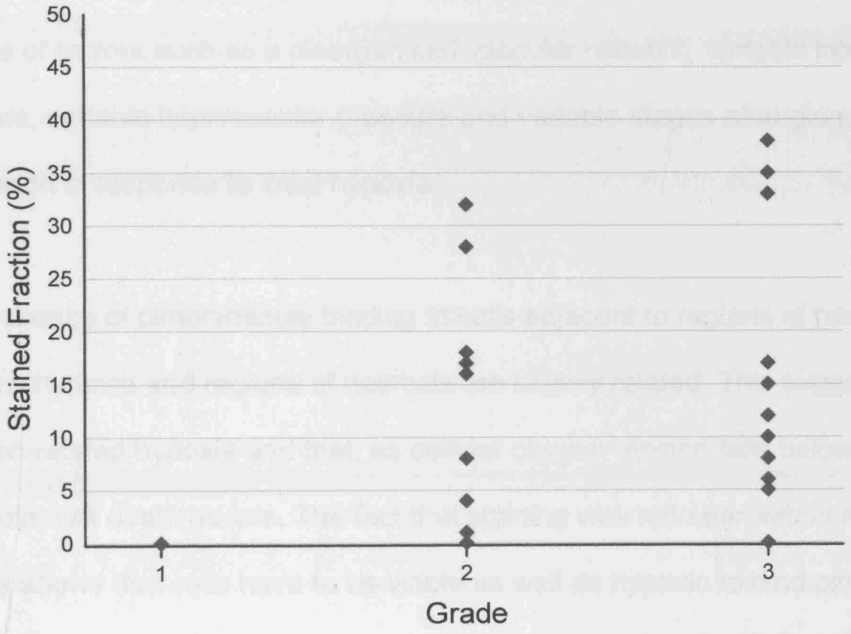

Figure 33 Scatter plot of pimonidazole stained fraction by grade.

Discussion

The presence of pimonidazole staining in this cohort of bladder carcinoma specimens confirms that tumour hypoxia exists in this disease. The staining pattern is heterogeneous indicating the known inconsistent pattern of tumour oxygenation assessed by the Eppendorf probe also applies to bladder tumours. This may reflect a range of factors such as a disorganised vascular network, variable interstitial pressure, variable intervascular pressure and variable stages of angiogenic stimulation in response to local hypoxia.

The presence of pimonidazole binding in cells adjacent to regions of necrosis confirms hypoxia and regions of necrosis are closely related. This suggests diffusion-related hypoxia and that, as cellular oxygen tension falls below a critical threshold, cell death occurs. The fact that staining was not seen within necrotic regions shows that cells have to be viable as well as hypoxic to bind pimonidazole. The histological approach also means that the hypoxic fraction defined by pimonidazole staining is a true fraction of the total tumour fraction. This contrasts with that of the Eppendorf probe, which does not distinguish between viable tumour, necrosis or stroma.

The range of values also demonstrates intertumour heterogeneity in hypoxia with a proportion of tumours showing no evidence of pimonidazole binding. The most likely explanation for a lack of staining is that these tumours have no regions of low oxygen tension and thus have an adequate vascular network, at least during the time of exposure of the tumour to effective levels of pimonidazole. Another possibility is that the section examined missed any region of hypoxia within the tumour. Although two non-consecutive sections were examined from each paraffin block of tumour, the measured regions actually sampled a wide distribution of the

tumour. Since tumour samples were obtained by wire diathermy, the tumour was collected as chippings. These were embedded within the paraffin block in a random fashion, so the sections taken and examined were likely to be representative of the whole tumour. The amount of material obtained would also be proportional to the tumour size, smaller amounts of material being obtained from smaller tumours. Another reason for a lack of pimonidazole binding may be that certain tumours may inherently lack the crucial enzymes to convert free pimonidazole to the bound product. These enzymes, the nitroreductases, however have been shown to be universally present in a number of tissues, including bladder cells (264).

The limitations of this method of measuring hypoxia include the invasive nature of the procedure. Although simple, it still requires the administration of a drug intravenously and thus subjects the patient to the small risks applicable to any intravenous procedure. The drug is safe, with only minor side effects reported. Worldwide, no serious adverse events attributable to pimonidazole have been reported [personal communication J Raleigh]. The inconvenience of a biopsy can be tempered by the need for tissue samples for either diagnostic or staging information, as in this study.

One well-documented side effect, seen in two patients in this group, is the development of a hot flush during infusion. This has raised questions of whether there may be a vasoactive component to pimonidazole that may increase blood flow and reduce the hypoxic fraction of cells in a tumour. This was investigated in experimental tumours where the blood flow was shown to decrease only at doses of the order of 100mg/kg to 1000mg/kg, making this effect unlikely in humans at the doses used (265). Furthermore, pimonidazole staining marks hypoxia over a period of hours rather than an instantaneous snapshot.

The method of measuring the stained fraction in this study was labour intensive, taking 3 to 4 hours for a large sample. This fully quantitative approach meant that comparison with the intrinsic markers, carbonic anhydrase 9 and glucose transporter 1, might have picked up smaller differences than with a semi-quantitative approach (chapter 6). However, for a rapid assessment of the extent of hypoxia in a tumour sample, the semi quantitative approach has been shown to be reproducible and reliable (266), and scoring systems are under development that would eliminate the need for digital image capture, speeding up assessment greatly. Alternatively, development of computer programs that automatically capture and analyse images could extract more precise and potentially important information rapidly, not possible with a manual semi-quantitative methods. For example, the double staining techniques described in chapters 3 and 4 that allow simultaneous visualisation of vascularity or proliferation with hypoxia could be automatically interpreted to quantify the different types of hypoxia and the relationships amongst these factors.

The inter- and intra-observer reproducibility of the method developed in this thesis is excellent and requires minimal training. However, the reproducibility declines when the observer is required to distinguish between light and dark staining. There is no consensus on what the difference between light and dark staining actually represents. It is unlikely to be due to the staining process as the positive controls used remained constant through all batches of staining. It has been suggested that the regions of light staining are either less hypoxic than dark regions or that they are only temporarily hypoxic during their exposure to pimonidazole. This means that lightly stained regions may demonstrate three types of cells:

1. Classical diffusion limited hypoxia where the cells nearest to the vessel show less pimonidazole binding than those further away.

2. Classical diffusion limited hypoxia that is developing where no dark stained cells are yet present.

3. Transient hypoxia which could be light or dark, depending on the duration of closure of the feeding vessel and on the duration of exposure to pimonidazole.

It may be possible to assign a pO_2 value to individual cells depending on their staining intensity, based on oxygen dependent binding curves for nitroimidazoles. Such a curve for NitroImidazoleTheoPhylline (NITP, 7-(4'-(2-nitroimidazol-1-yl)-butyl)-theophylline) is shown in figure 34 as an example. The distinction between dark and light staining may be made somewhere along the steep part of the curve to place cells to one of the above categories.

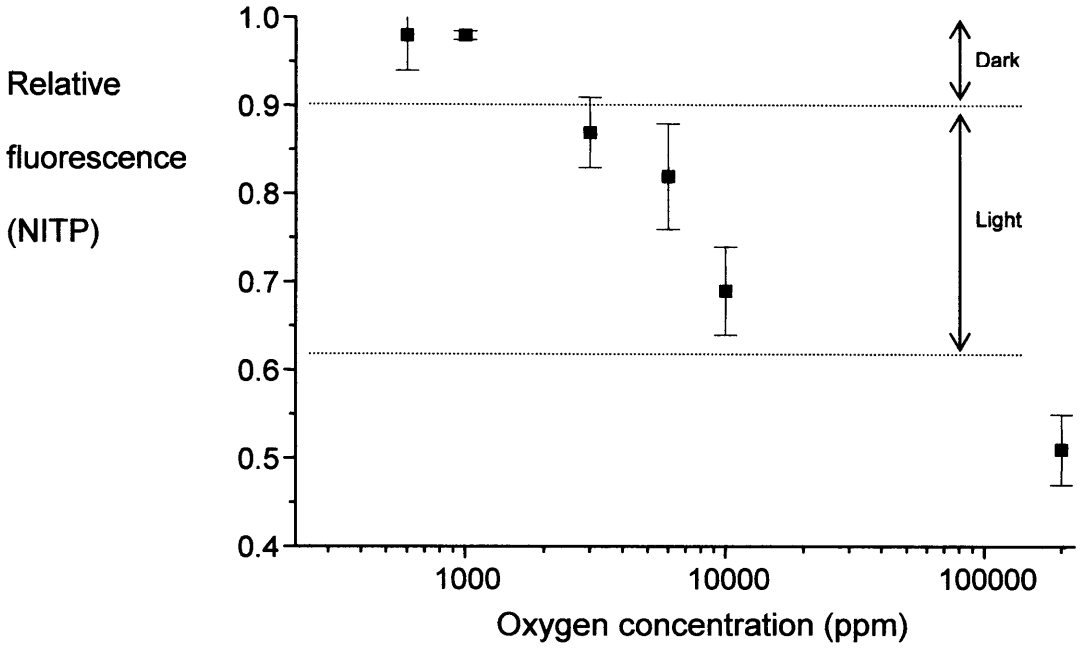

Figure 34 Oxygen dependent binding curve (K-curve) for NitroImidazoleTheoPhylline (NITP) (courtesy G.D. Wilson, unpublished data)

Those cells staining lightly may be less radioresistant than those staining darkly, or more likely to reoxygenate through frationated radiation therapy. The problem with this approach is that the binding intensity in hypoxic cells amongst different tissue depends on uncontrollable or difficult to measure factors. These including soluble thiol content, pimonidazole exposure, available redox enzymes and adduct catabolism rate [personal communication J Raleigh].

A practical assumption is that cells bind pimonidazole at a pO_2 of less than 10mmHg irrespective of staining intensity. This is based on a study by Raleigh (265), where a good correlation between cells binding pimonidazole and Eppendorf measurements for the percentage of readings <10mmHg in a C3H mouse mammary carcinoma was shown. Another study used flow cytometry to sort pimonidazole labelled cells from a range of experimental tumours (267). Binding per se, and not the intensity of

binding, correlated with the radiobiological hypoxic fraction. These facts, along with the data here showing that the dark stained fraction correlates well with the overall stained fraction in any case, mean that when scoring sections and ranking them in a semi-quantitative hypoxic scale, a distinction between staining intensity may not be necessary.

A quantitative association of pimonidazole staining with necrosis is expected, given the strong co-localisation element. However, the recognition of necrosis is unreliable, as it is difficult to distinguish between tissue artefact, diathermied edge of tumour sample and true necrosis, explaining the lack of correlation.

Some regions of staining were seen to be unassociated with necrosis. These regions may genuinely be isolated regions of viable hypoxic cells or associated with necrosis out of the plane of the section. This highlights another limitation in this approach of looking at the tumour in a 2 dimensional way, when tissue architecture is 3 dimensional. This also applies to regions of light staining- they may or may not be associated with darker stained regions that are out of plane. Such a detailed analysis could be achieved by sectioning through the entire tumour, and staining and scoring each section.

Conclusion

The clinical assessment of hypoxia by pimonidazole is feasible and its measurement is reproducible. The presence of hypoxia in bladder carcinoma has been demonstrated with this method. The varied extent of pimonidazole binding suggests an inter- and intratumour hypoxic heterogeneity. Light and dark staining areas are distinguishable, and may represent differing degrees of hypoxia, supported by the observation that necrotic regions are surrounded by darker stain only. The use of

image analysis software is time consuming but reproducible with little inter- and intra-observer variation. It provides a high resolution of measurement that may allow more accurate comparisons with other hypoxic stains.

CHAPTER THREE

Proliferation in Bladder Carcinoma and its Relationship to Hypoxia

Aims

The aim of this part of the study was to examine the relationship between proliferating cells and regions of hypoxia in transitional cell carcinoma, and to assess the influence of low oxygen tensions on proliferation. Two markers of proliferation were used; Ki67, which is expressed in all cycling cells, and CyclinA which is expressed when cells actively enter S phase.

Methods and Materials

Procedure

Twenty-one tumour samples staining for pimonidazole were selected, and sections were double stained for Ki67 and bound pimonidazole using a dichromic immunohistochemistry method, described below. Sections stained were in series with those double stained for CD31/34 and pimonidazole.

The procedure was repeated on a further serial section double stained for CyclinA and pimonidazole.

Immunohistochemistry: Double staining for pimonidazole and Ki67

- Slides were de waxed in xylene for 5 minutes and rehydrated through graded alcohols (100, 90, 70%) to water.
- Sections were then transferred to a 37°C water bath containing 0.01% pronase (Sigma) buffered to pH 7.8.
- Endogenous peroxidase was blocked with Dako peroxidase block (Envision kit) at room temperature for five minutes, then washed well in water, then rinsed in tris buffered saline.
- The section was then encircled with resin using a resin pen to well in the solutions used in the rest of the staining process.
- Protein block (Dako X0909) was added and left for five minutes. The excess was tipped off.
- Anti –Pimonidazole antibody diluted 1/100 (Natural Pharmacia Cat 01800 Mab1) was added left on the slide for one hour at room temperature, and washed off with tris buffered saline three times for a total of three minutes.
- Envision Alkaline Phosphatase mouse polymer (Dako K4017) was applied for 30 minutes and then washed off with tris buffered saline three times for a total of three minutes.
- Vector Alkaline Phosphatase red substrate (Vector SK5100) was applied for 5 to 10 minutes and monitored closely to prevent overstaining, then rinsed in tris buffer saline, and washed in water for a further 5 minutes.
- Sections were transferred to 10mM citric acid pH6 and microwaved on high power for 12 minutes. These were left to stand for ten minutes before washing well in running tap water.
- Ki67 antibody diluted 1/200 in tris buffered saline was added for one hour at room temperature.
- Sections were washed three times in tris buffer saline

- Envision Horseradish peroxidase mouse/rabbit polymer (Dako K5007) was applied for 30 minutes and then washed off with tris buffered saline three times for a total of three minutes.
- Diaminobenzine substrate was then added (Vector SK4100) for five minutes.
- The section was rinsed in tris buffer saline, then washed well in running tapwater.
- To stain nuclei blue, the sections were placed in Gills Haematoxylin for between 10 to 60 seconds and then washed well in tap water.
- Finally the sections were dehydrated through graded alcohols, cleared by xylene and sections mounted in DPX (Merck 360294H) mounting media.

The procedure for pimonidazole and cyclin A is identical, substituting cyclin A antibody diluted 1/50 in tris buffered saline for the Ki67 antibody.
Resulting sections show pimonidazole as red, Ki67/cyclinA positive cells as brown and nuclei as pale blue.

Image Analysis

The same set-up and equipment as in the analysis of the hypoxic fraction were used (chapter 2). The CD31/34 and pimonidazole stained section was scanned on low power and regions of pimonidazole staining located. The nearest vessel to the region of hypoxia was identified. Regions of hypoxia were separated into those less than 40μm away from the vessel and those more than 40μm away. The corresponding region was found on the Ki67/pimonidazole stained section. Under high power, cells staining positively for Ki67 (brown) and negatively in the hypoxic region of interest were counted. The process was repeated so that each region of hypoxia identified had the proliferative index assessed in this way. The proliferative

index in regions not staining for pimonidazole i.e. oxic regions, was assessed, stepping through the sample.

The procedure was repeated for the CyclinA/pimonidazole stained sections.

Exclusions

Two tumours had no pimonidazole staining and were thus not included in the comparison of proliferation marker expression in oxic and hypoxic regions

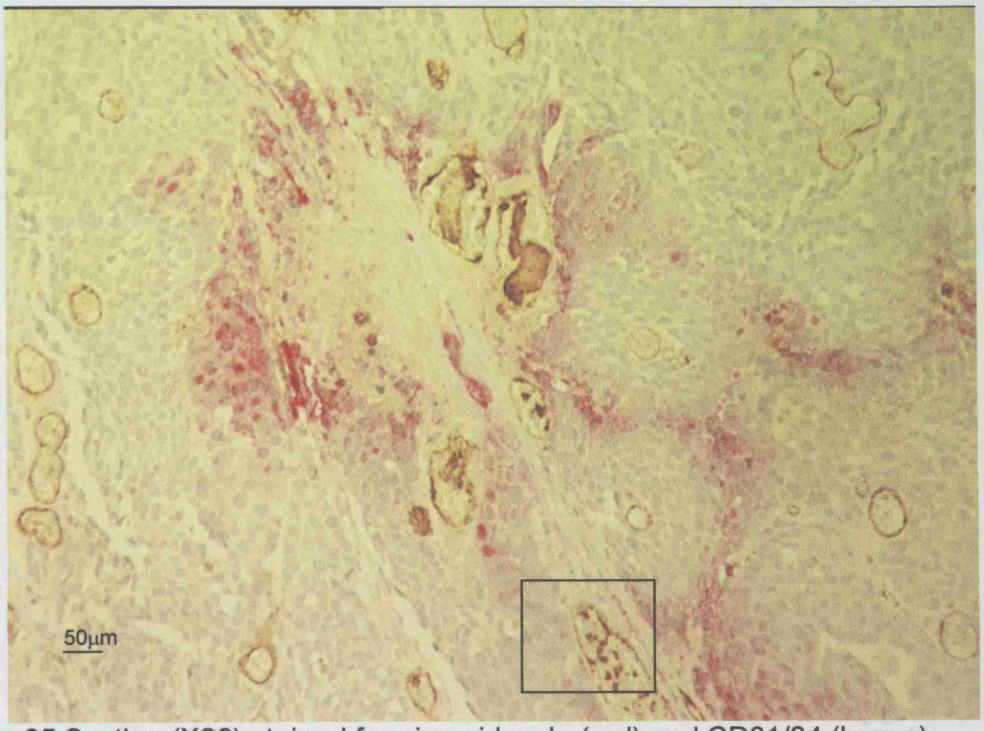

Figure 35 Section (X20) stained for pimonidazole (red) and CD31/34 (brown) showing regions of hypoxia close to vessels (arrowed). Rectangled area refers to figure 37.

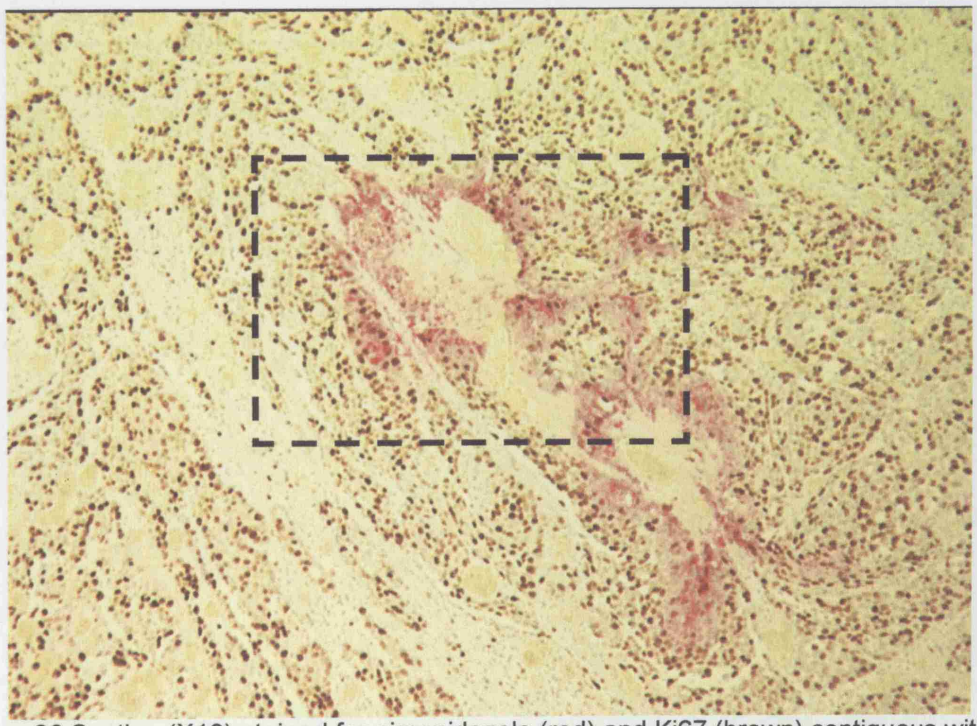

Figure 36 Section (X10) stained for pimonidazole (red) and Ki67 (brown) contiguous with that shown in figure 35, (in rectangle), showing regions of proliferation and hypoxia.

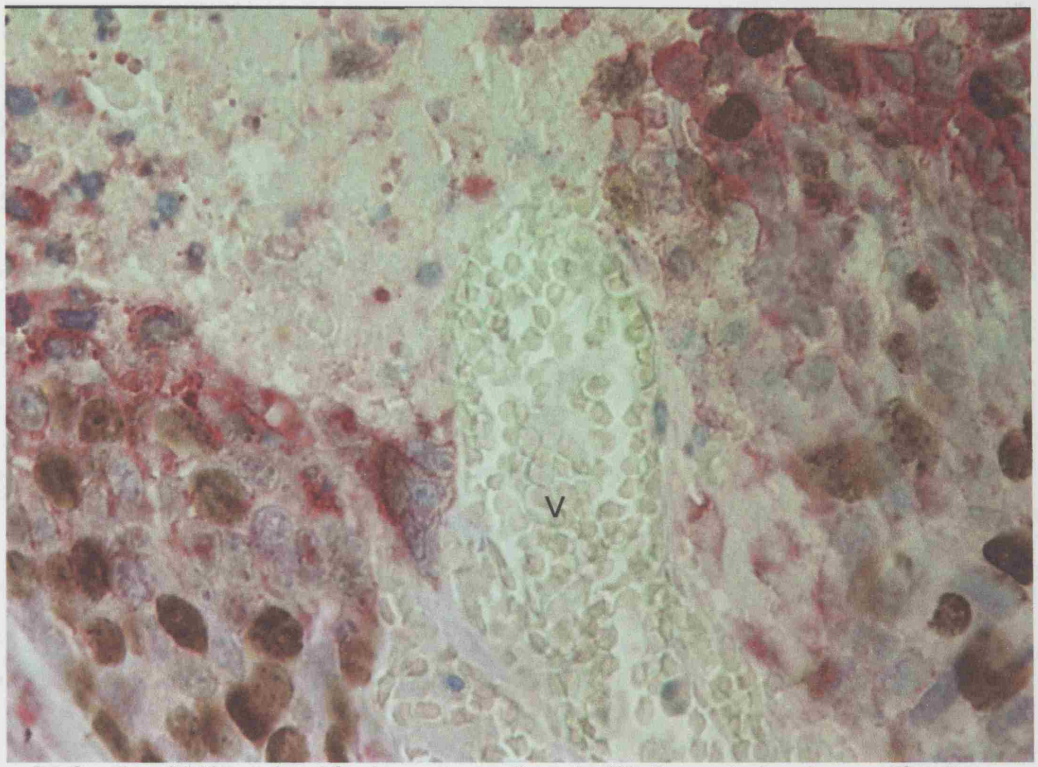

Figure 37 Section (X40) stained for hypoxia (red) and Ki67 (brown) showing proliferating cells within hypoxic regions adjacent to a blood vessel (V).

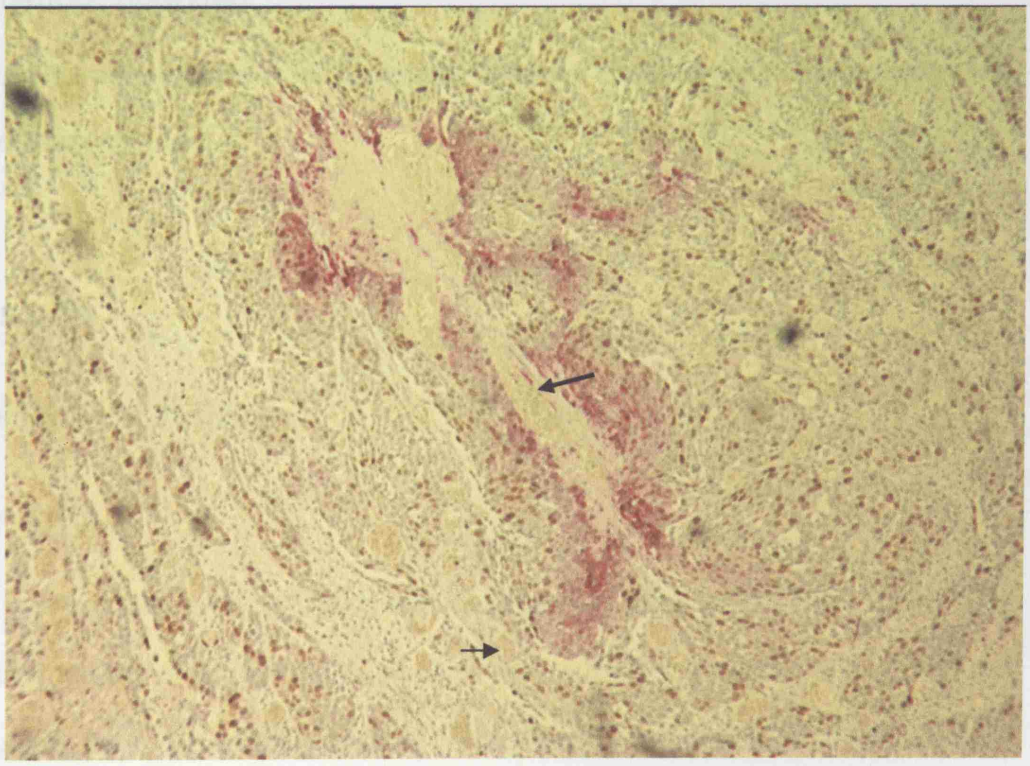

Figure 38 Section (x10) stained for pimonidazole (red) and CyclinA (brown), contiguous with that in figures 36 showing regions of hypoxia close to vessels (arrowed).

Data obtained

The following data was obtained:

- The overall percentage of cells binding Ki67 or CyclinA
- The percentage of cells that are positive for Ki67 or CyclinA in regions not binding pimonidazole
- The percentage of cells that are positive for Ki67 or CyclinA in regions that both bind pimonidazole and are further than 40μm away from the nearest vessel in the section
- The percentage of cells that are positive for Ki67 or CyclinA in regions that both bind pimonidazole and are closer than 40μm away from the nearest vessel in the section.

Statistical analysis

The proliferative indices were compared between compartments using a paired 2-sided Students t-test.

Results

Proliferation indices

Ki67 indices

The median number of oxic fields assessed per tumour was 16 (range 10-24). The median number of hypoxic fields close to vessels (<40μm) was 2 (range 1 to 7) and in hypoxic fields distant from vessels (>40 μm) was 12 (range 2-28). Hypoxia was not present in two tumours, and no hypoxic regions close to vessels were identified in a further 5 tumours. The median number of cells counted per section was 5032 (range 2090-13222). The median proliferation index overall was 35% (range 3 to

55%) (figure 40). The median in oxic regions was 40% (range 4 to 55%), in hypoxic regions close to vessels was 17% (range 0 to 53%) and in hypoxic regions far from vessels was 12% (range 0 to 30%). Comparing the three tumour compartments for all tumours, there was a statistically significant difference in the proliferative indices shown in table 8. The median and range of proliferation indices for each individual tumour are shown in figure 42.

Statistics	Oxic Vs Hypoxia-far	Oxic Vs Hypoxia – near	Hypoxia – near Vs Hypoxia - far
Number	19	14	14
Mean difference	24%	14%	8%
95% Confidence interval	18 to 29%	8 to 20%	3 to 14%
P value	<0.0001	<0.0001	<0.004

Table 8 Table comparing Ki67 proliferative index in oxic, hypoxic close to vessels and hypoxic far from vessels

Pattern of Ki67 staining

Ki67 positive cells were distributed throughout regions of tumour with uniform staining intensity within and between tumours. Regions of tumour with no proliferation and no hypoxia were present (Figure 39).

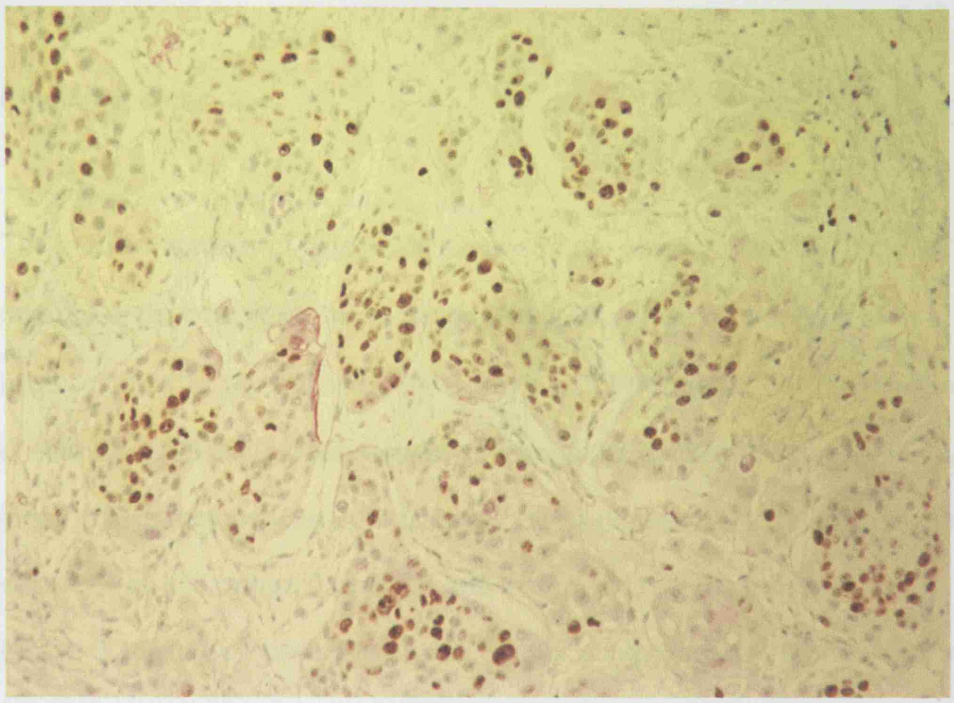

Figure 39 Section (x20) showing Ki67 stain across a largely oxic region, demonstrating regions with no proliferation and no hypoxia.

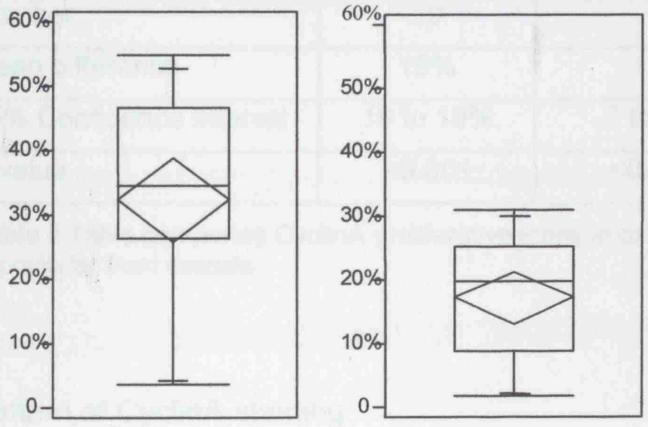

Figure 40 Quartile box plots of overall Ki67 (left) and CyclinA (right) proliferation index

CyclinA indices

The median number of oxic fields assessed per tumour was 15 (range 9-23), the number of hypoxic fields close to vessels (<40μm) was 2 (range 1 to 7) and in hypoxic fields far from vessels (>40 μm) was 11 (range 2-26). The median number of cells counted per section was 3742 (range 2370-13765). The median proliferation index in oxic regions was 20% (range 2-31%) (figure 40), in hypoxic regions close to vessels was 4% (range 0 to 22%) and in hypoxic regions far from vessels was 3% (range 0-15%). Comparing the three tumour compartments, there was a statistically significant difference in the proliferative indices (table 9). The median and range of proliferation indices for each individual tumour are shown in figure 42.

Statistics	Oxic Vs Hypoxia-far	Oxic Vs Hypoxia – near	Hypoxia – near Vs Hypoxia - far
Number	19	14	14
Mean difference	15%	12%	3%
95% Confidence interval	10 to 19%	7 to 17%	1 to 7%
P value	<0.001	<0.0001	<0.02

Table 9 Table comparing CyclinA proliferative index in oxic, hypoxic close to vessels and hypoxic far from vessels

Pattern of CyclinA staining

CyclinA positive cells were distributed throughout regions of tumour with uniform staining intensity within and between tumours. Regions of tumour with no proliferation and no hypoxia were present (figure 41).

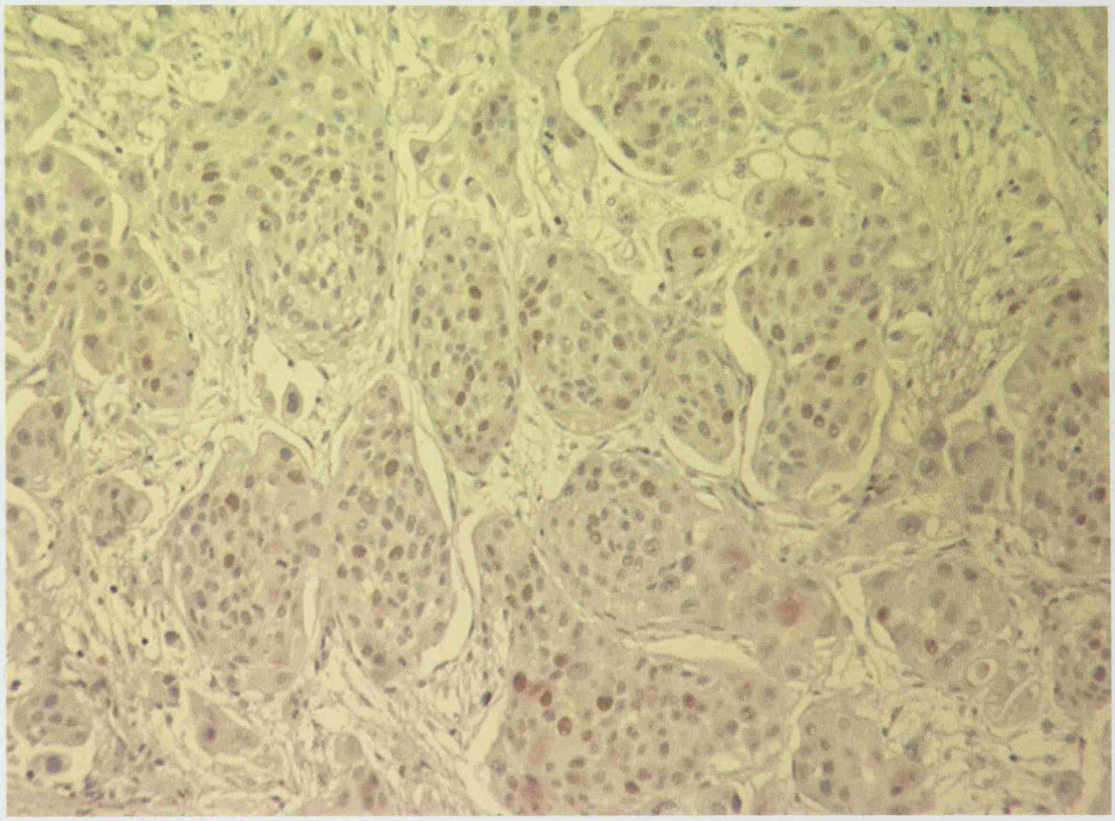

Figure 41 Section (x20) showing CyclinA stain across a largely oxic region, demonstrating regions with no proliferation and no hypoxia

Relationship between proliferative index and hypoxic fraction

There was no correlation between hypoxic fraction and proliferation in either hypoxic or oxic compartments (figure 43 and 44).

Relationship between Ki67 and CyclinA

The proliferation indices are compared for the whole section, oxic and hypoxic compartments for each tumour in figure 42. The gradient of the trend line in both the

whole tumour section and in oxic regions was 0.48, indicating the CyclinA index was about half that of Ki67. However for hypoxic regions the gradient was 0.19, indicating that in hypoxic regions the CyclinA index fell to about one fifth (figure 45).

1

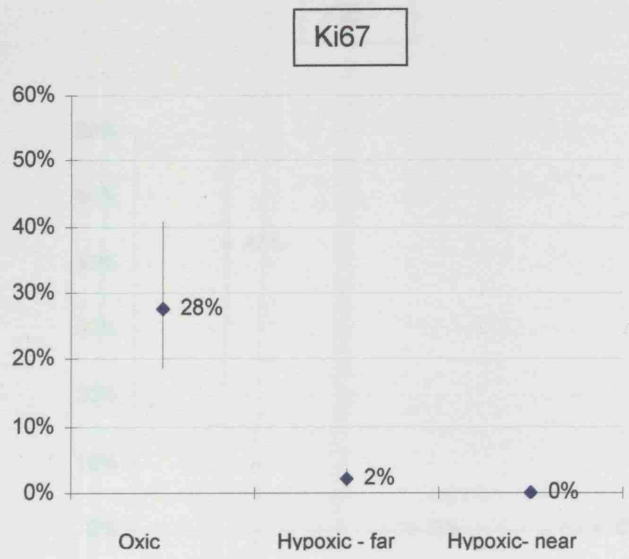
Ki67
60%
50%
40%
30%
20%
10%
0%
28%
2%
0%
Oxic
Hypoxic - far
Hypoxic- near

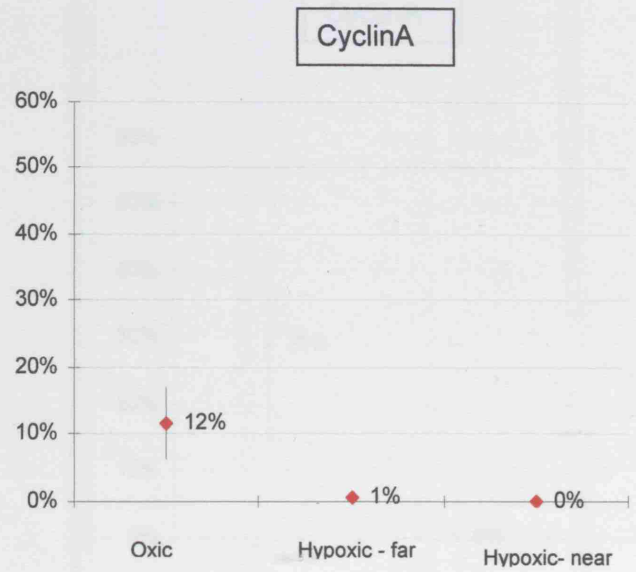
CyclinA
60%
50%
40%
30%
20%
10%
0%
12%
1%
0%
Oxic
Hypoxic - far
Hypoxic- near

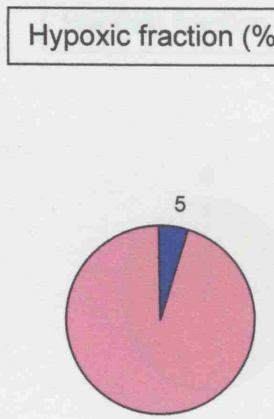
Hypoxic fraction (%)
5

2

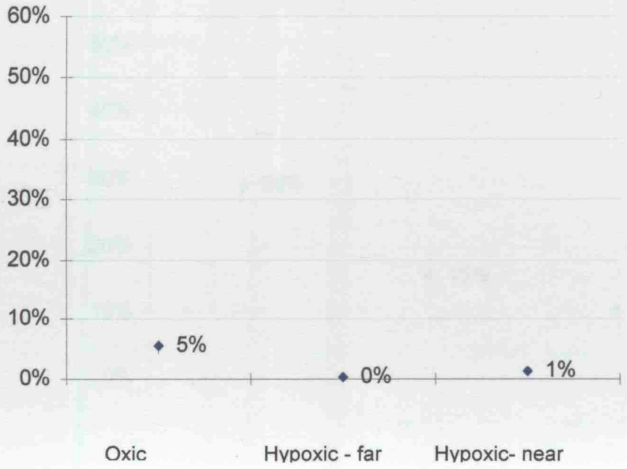
60%
50%
40%
30%
20%
10%
0%
5%
0%
1%
Oxic
Hypoxic - far
Hypoxic- near

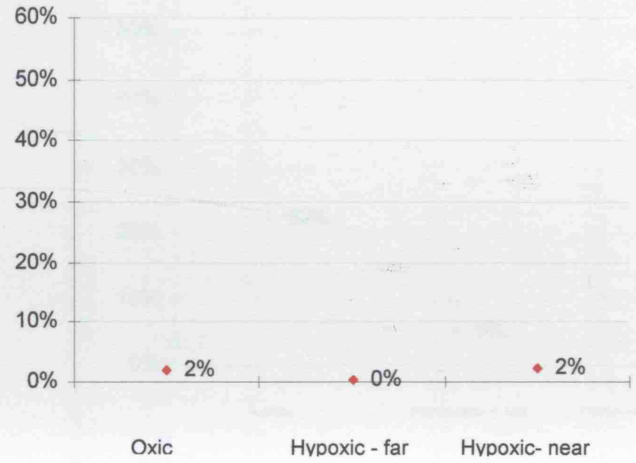
60%
50%
40%
30%
20%
10%
0%
2%
0%
2%
Oxic
Hypoxic - far
Hypoxic- near

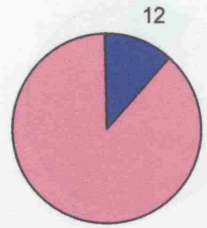
12

Ki67

CyclinA

Hypoxic fraction (%)

3

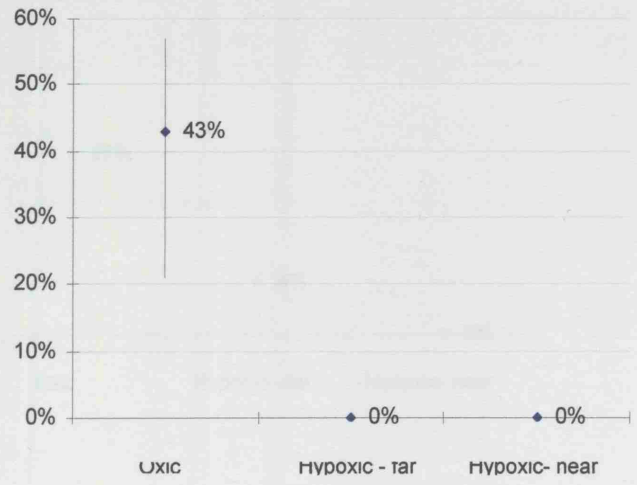

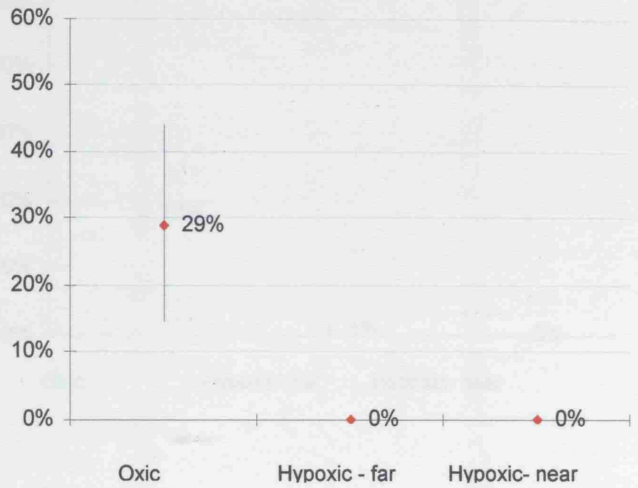

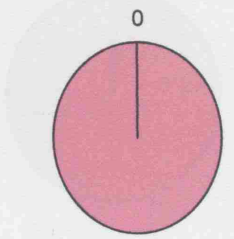

4

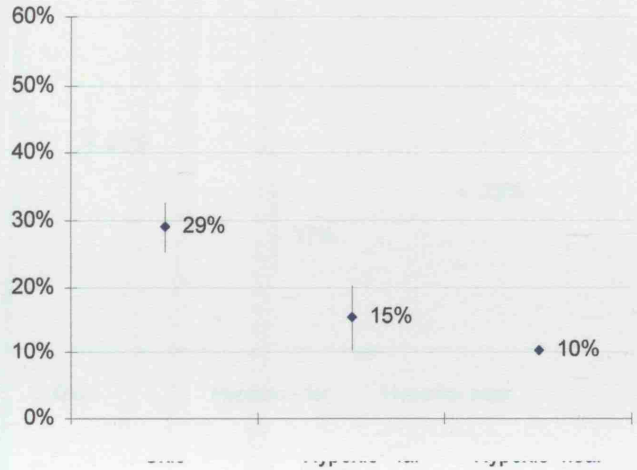

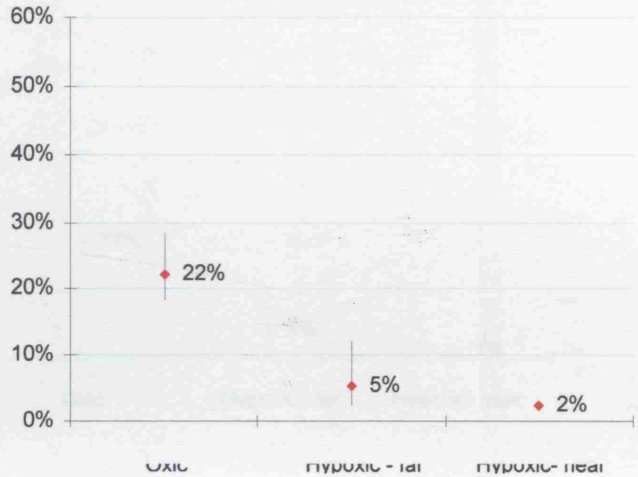

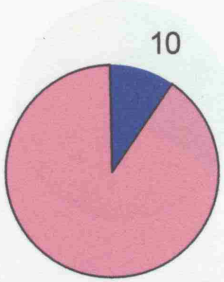

5

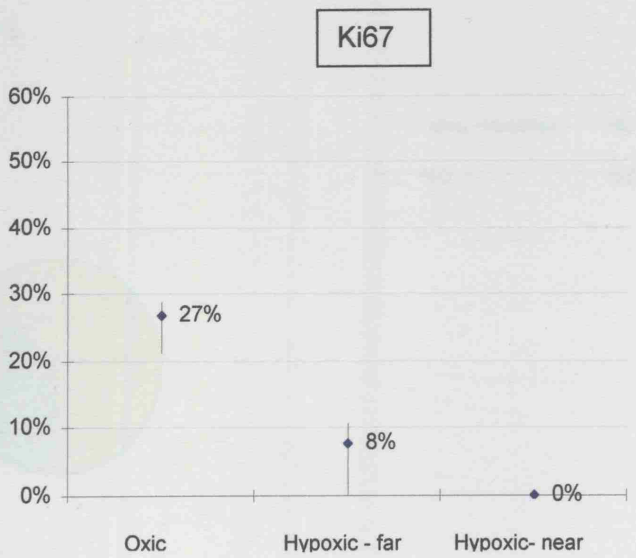
Ki67
60%
50%
40%
30%
20%
10%
0%
27%
8%
0%
Oxic
Hypoxic - far
Hypoxic- near

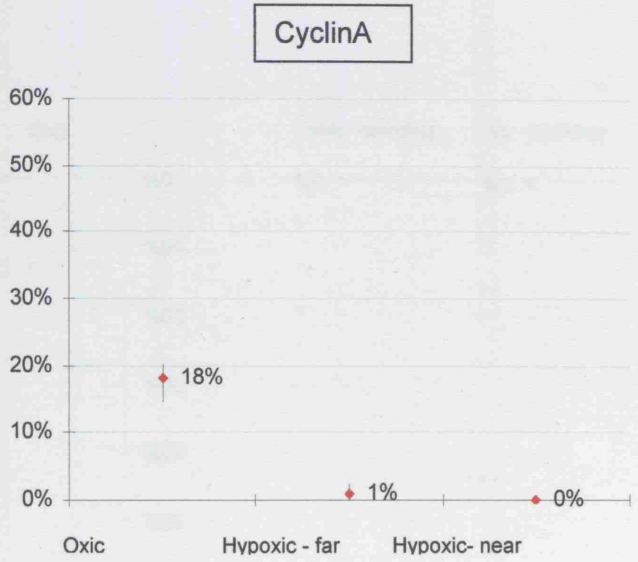
CyclinA
60%
50%
40%
30%
20%
10%
0%
18%
1%
0%
Oxic
Hypoxic - far
Hypoxic- near

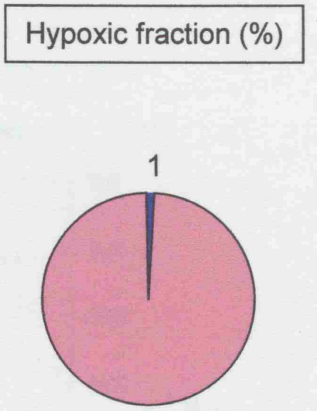
Hypoxic fraction (%)
1

6

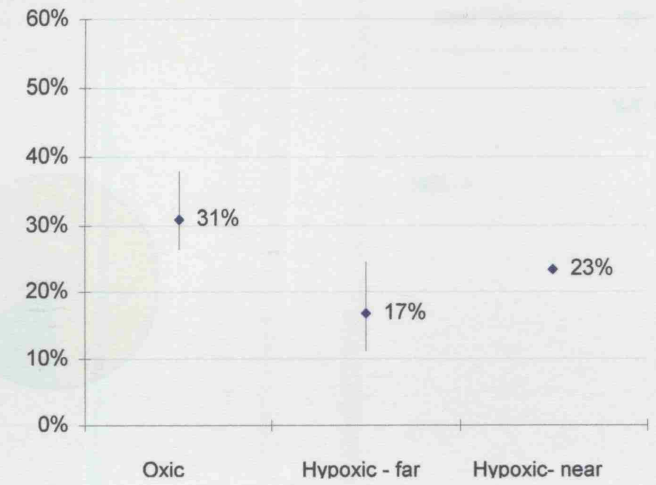
60%
50%
40%
30%
20%
10%
0%
31%
17%
23%
Oxic
Hypoxic - far
Hypoxic- near

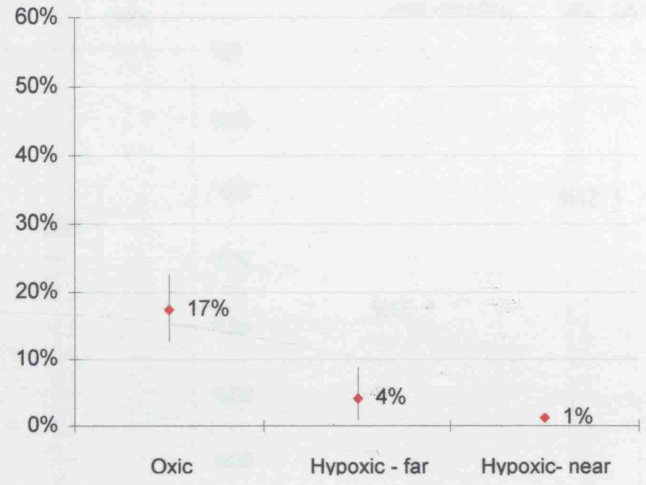
60%
50%
40%
30%
20%
10%
0%
17%
4%
1%
Oxic
Hypoxic - far
Hypoxic- near

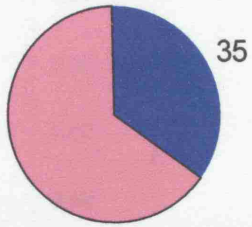
35

Ki67

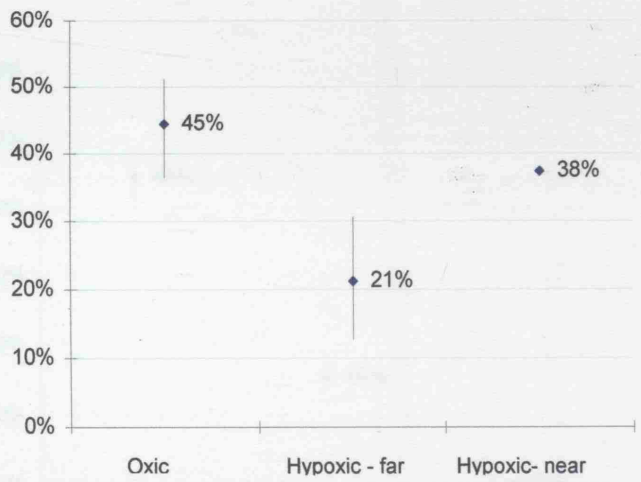

CyclinA

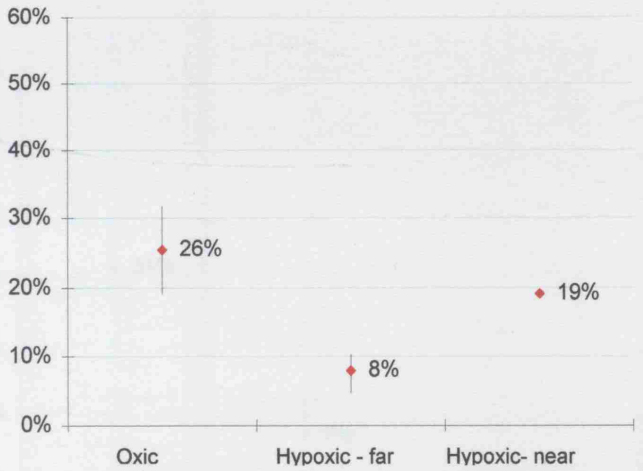

Hypoxic fraction (%)

7

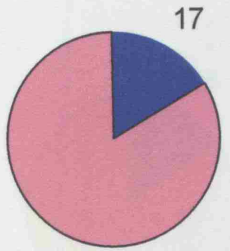

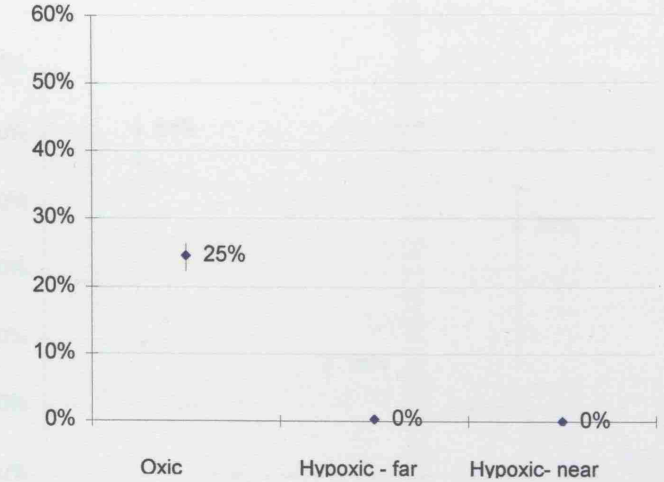

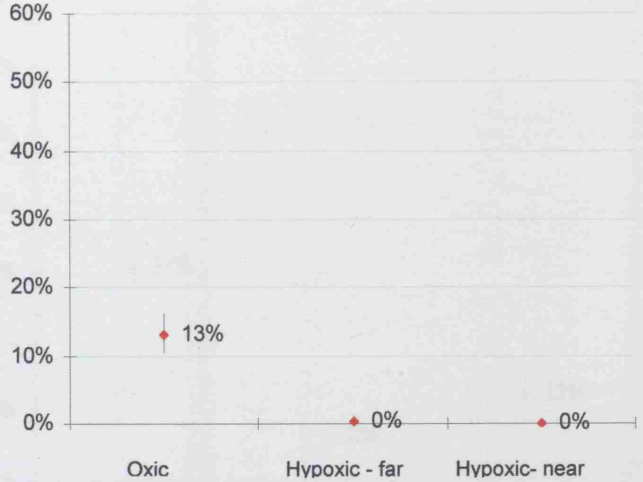

8

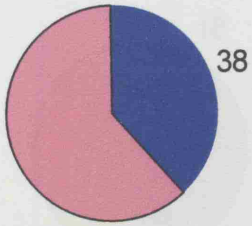

Ki67

CyclinA

Hypoxic fraction (%)

9

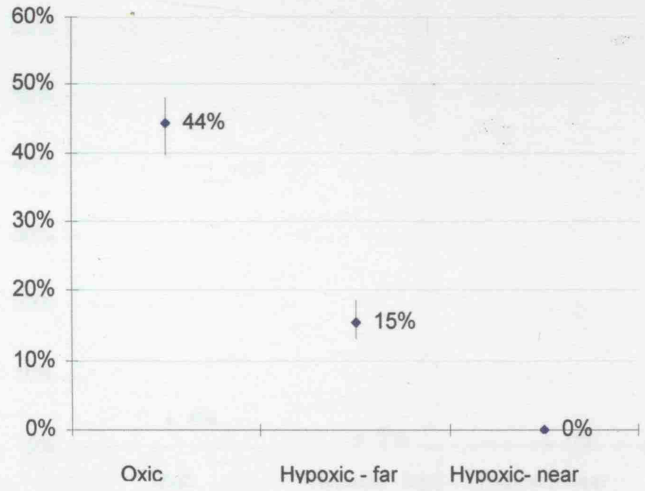

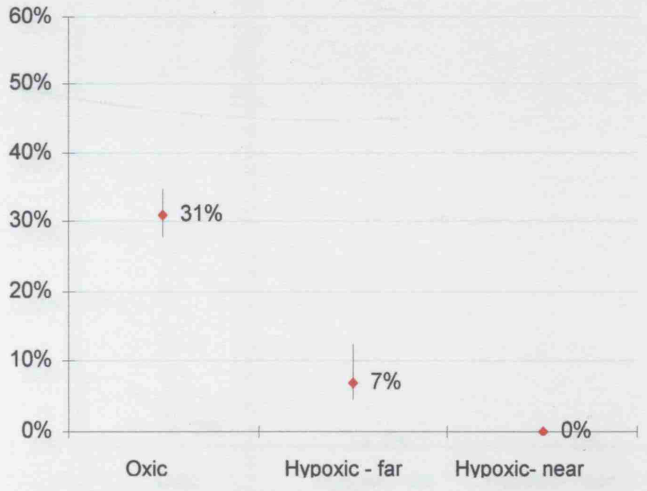

15

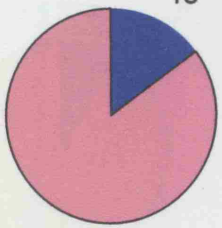

10

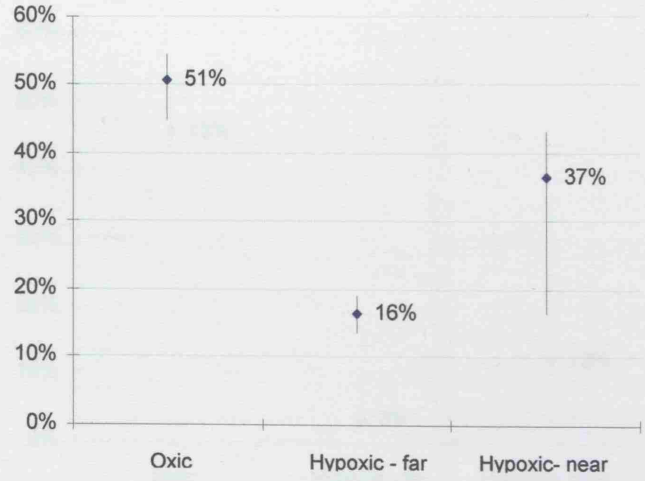

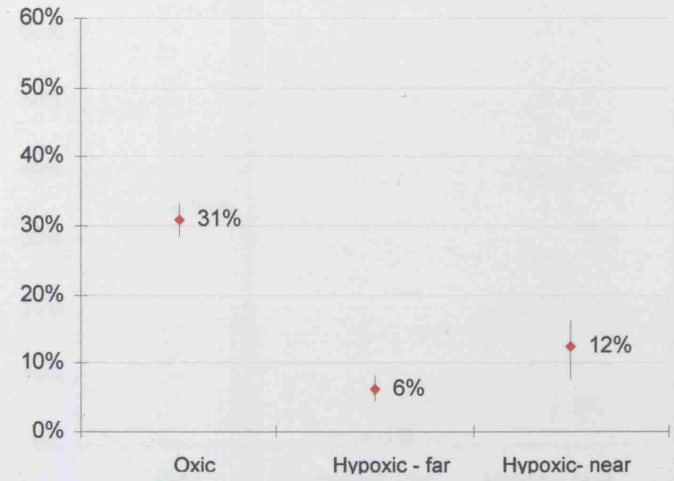

16

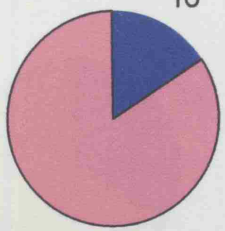

Ki67

CyclinA

Hypoxic fraction (%)

11

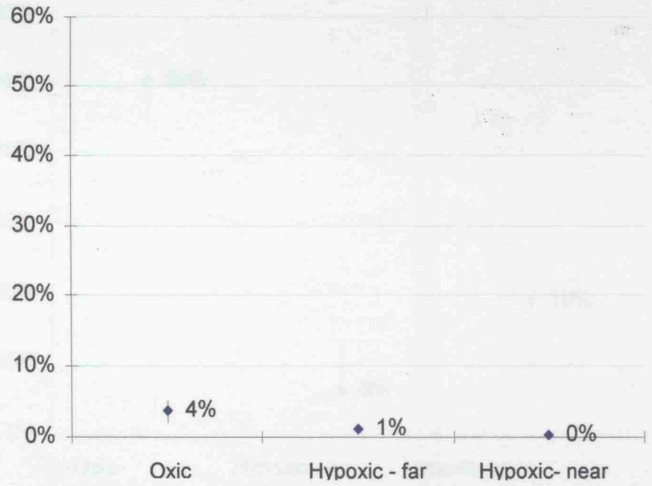

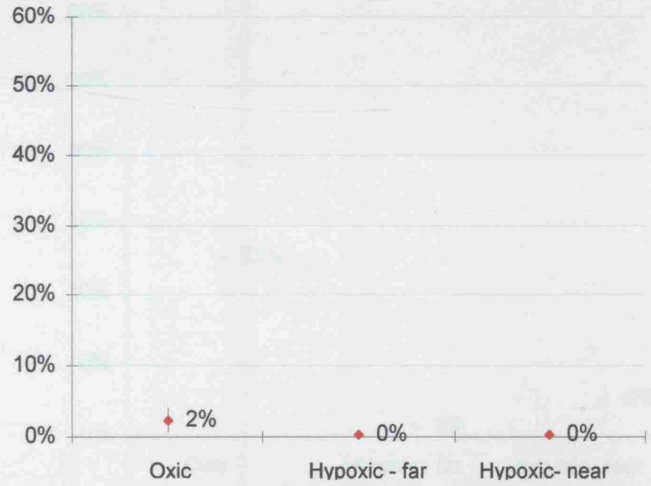

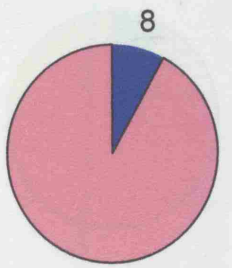

12

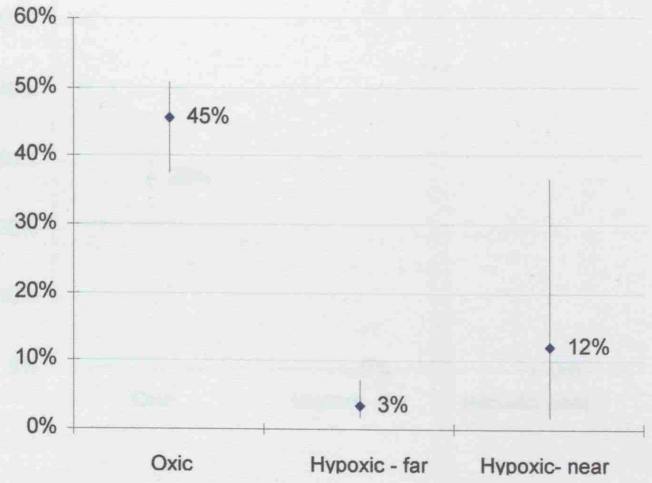

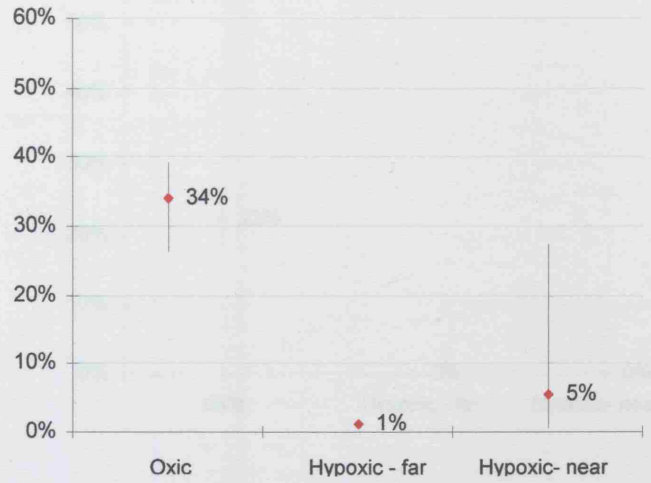

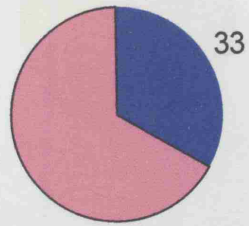

Ki67

CyclinA

Hypoxic fraction (%)

13

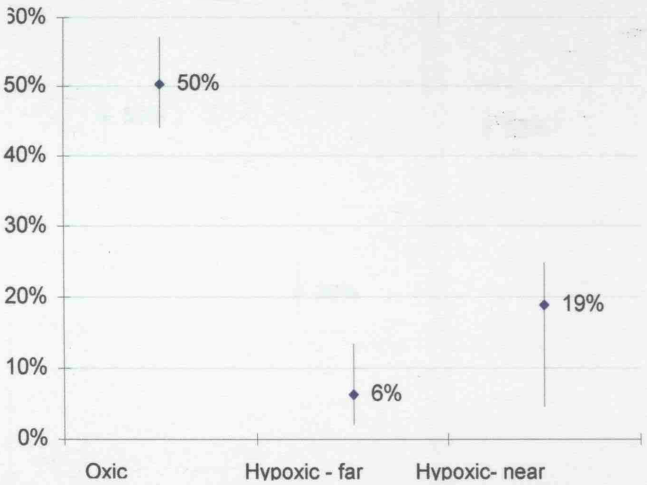

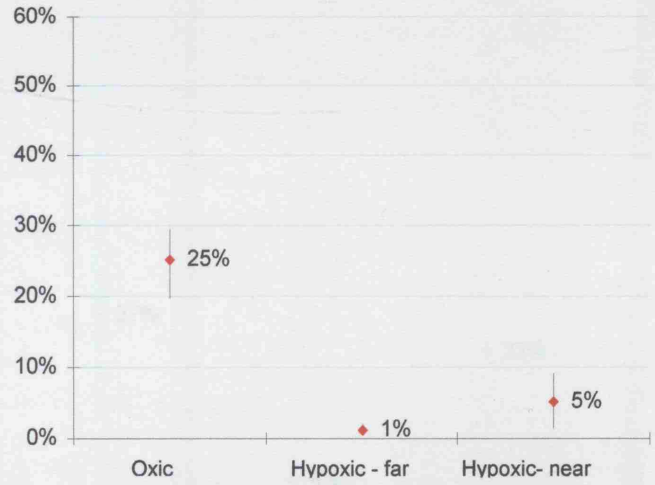

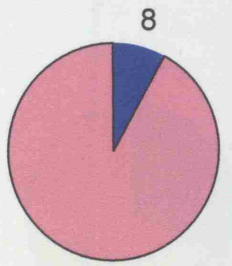

14

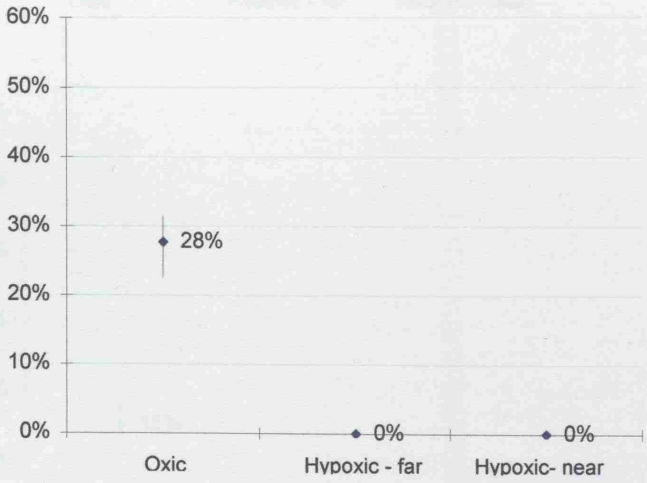

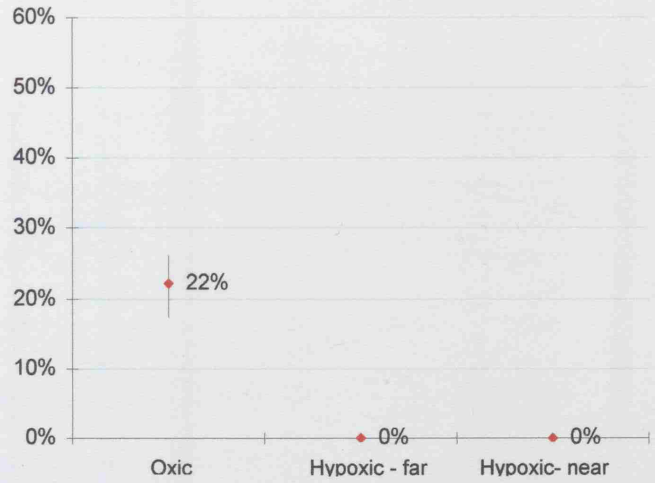

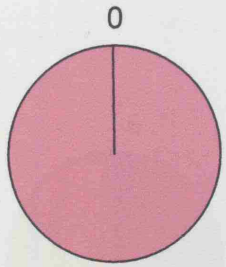

Ki67

CyclinA

Hypoxic fraction (%)

15

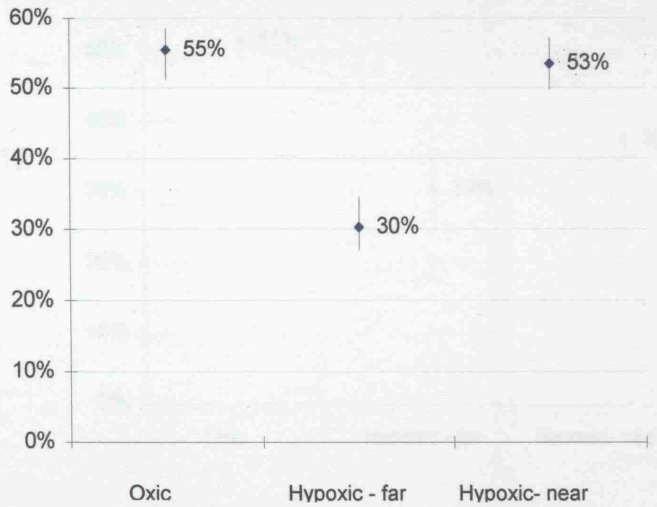

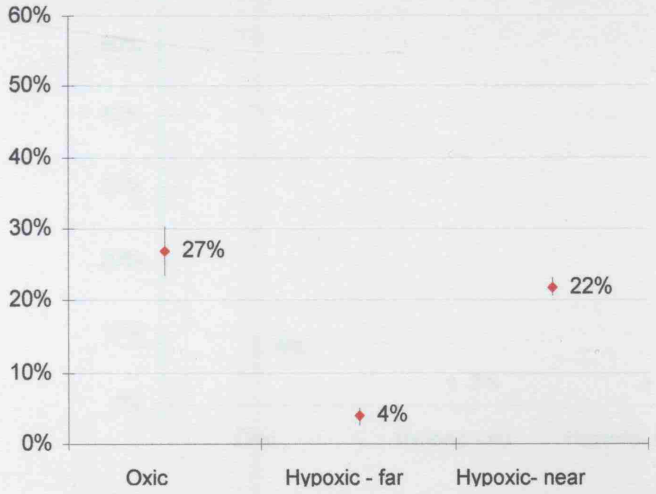

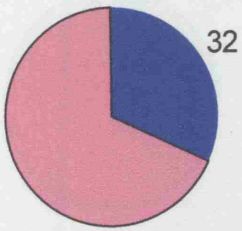

16

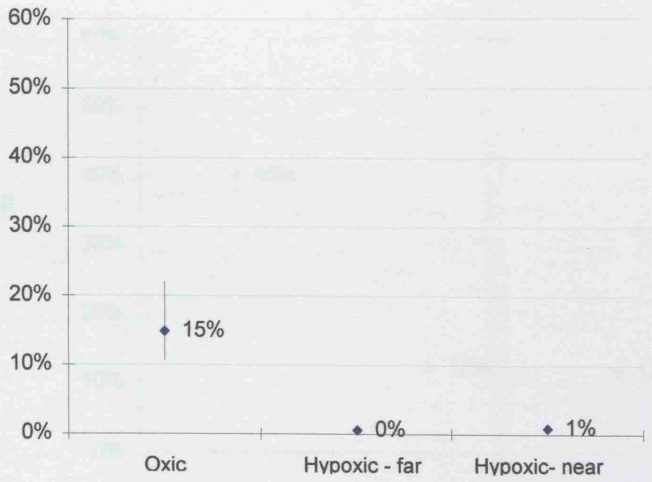

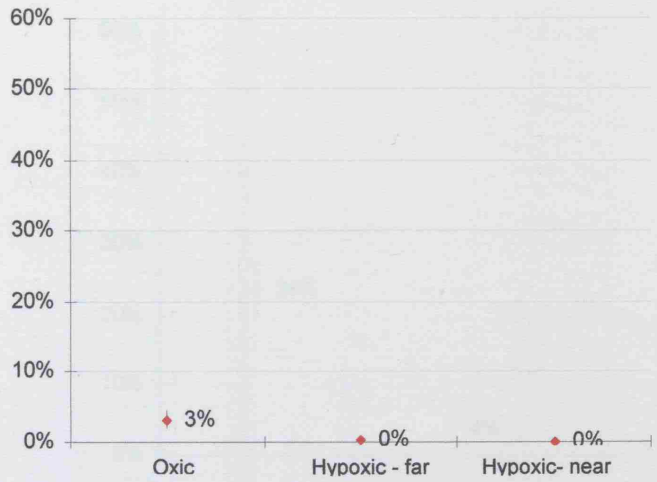

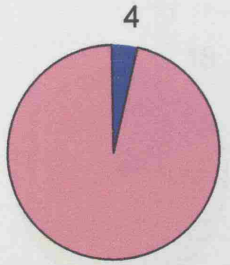

Ki67

CyclinA

Hypoxic fraction (%)

17

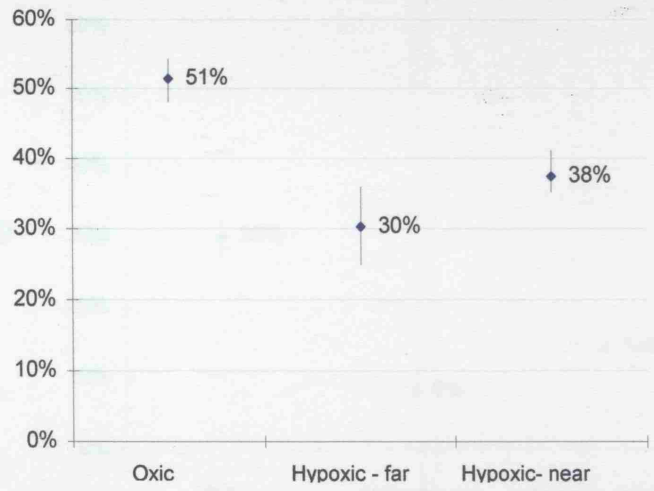

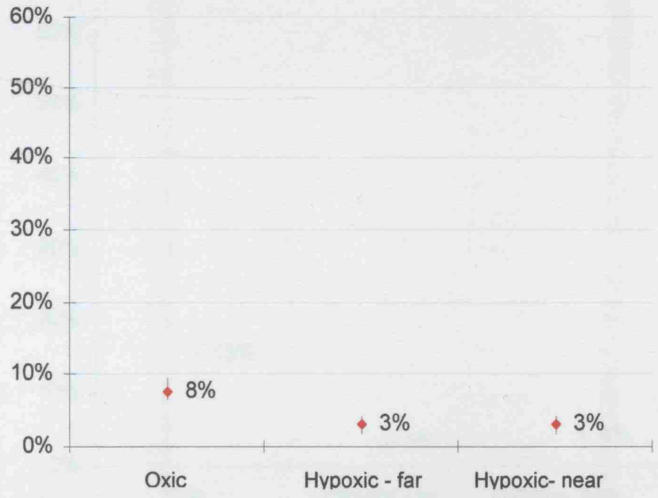

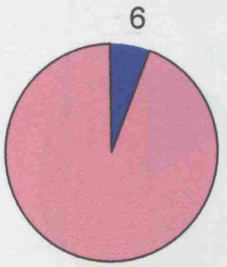

18

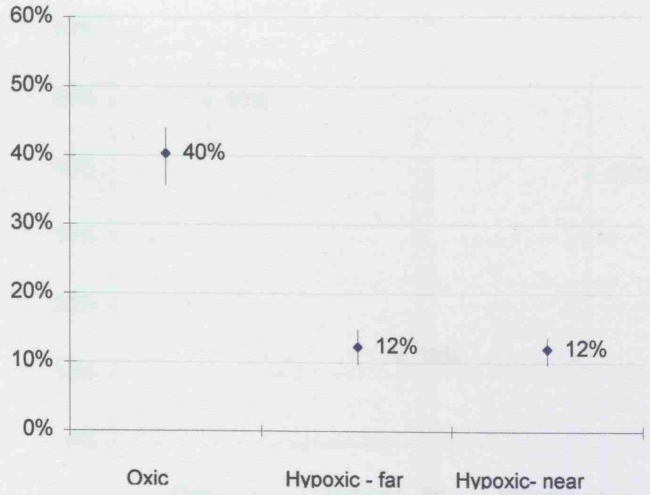

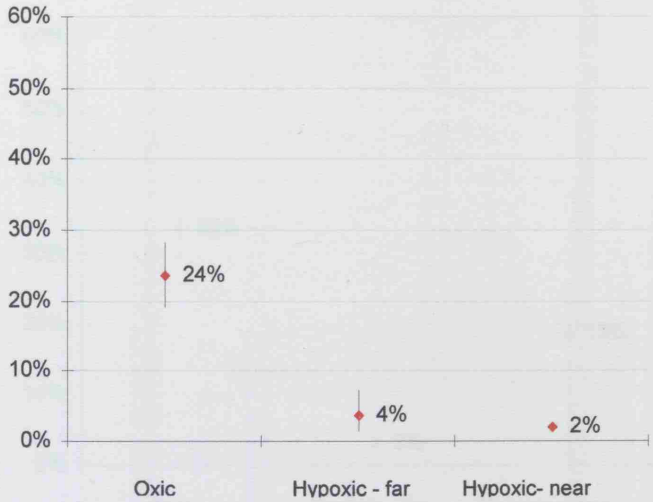

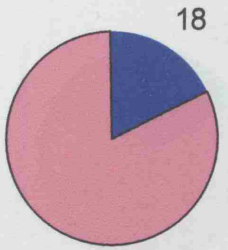

Ki67

CyclinA

Hypoxic fraction (%)

19

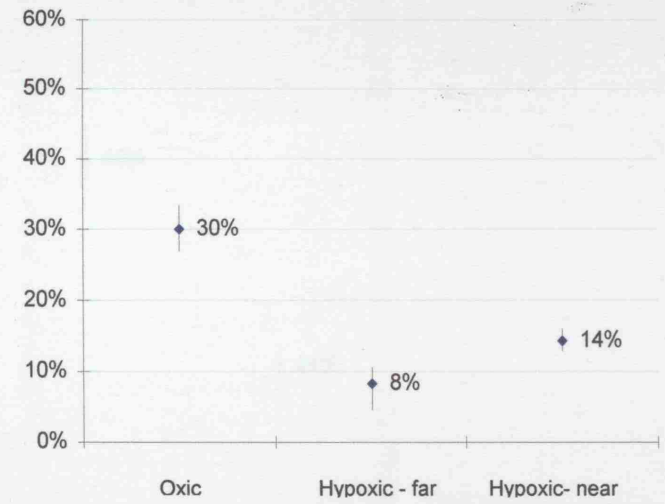

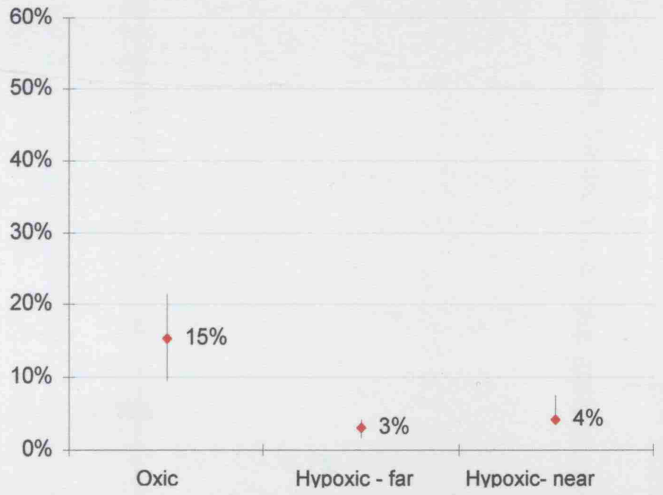

16

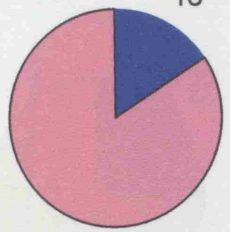

20

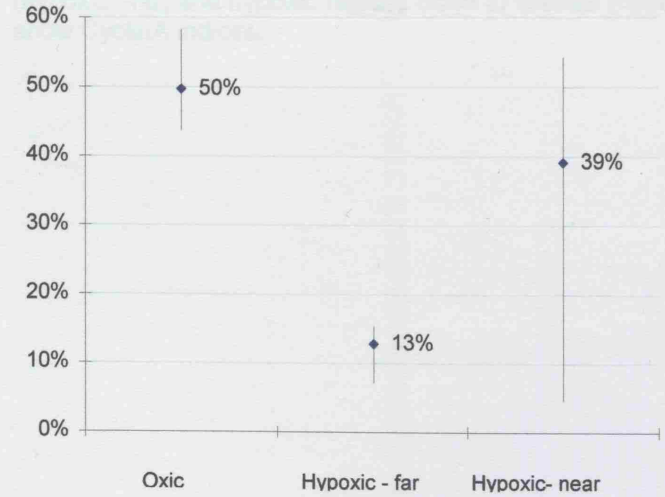

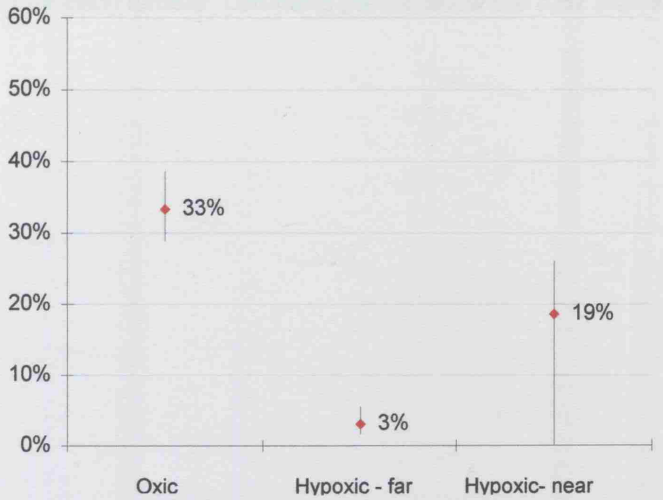

17

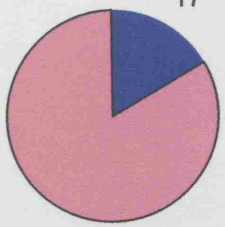

155

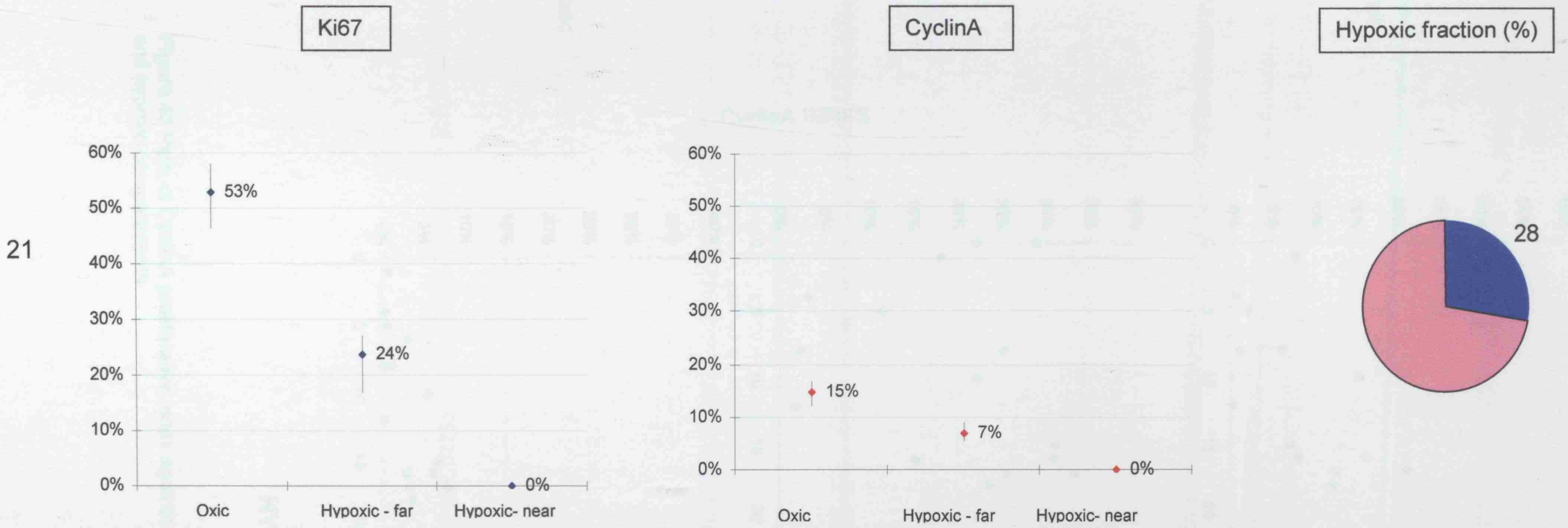

21

Figure 42 on previous 11 pages. Plots of the median and range of proliferation indices for the oxic regions, hypoxic regions distant from vessels (hypoxic –far) and hypoxic regions close to vessels (hypoxic-near) for each tumour. Left-hand panels show the Ki67 indices and right hand panels show CyclinA indices.

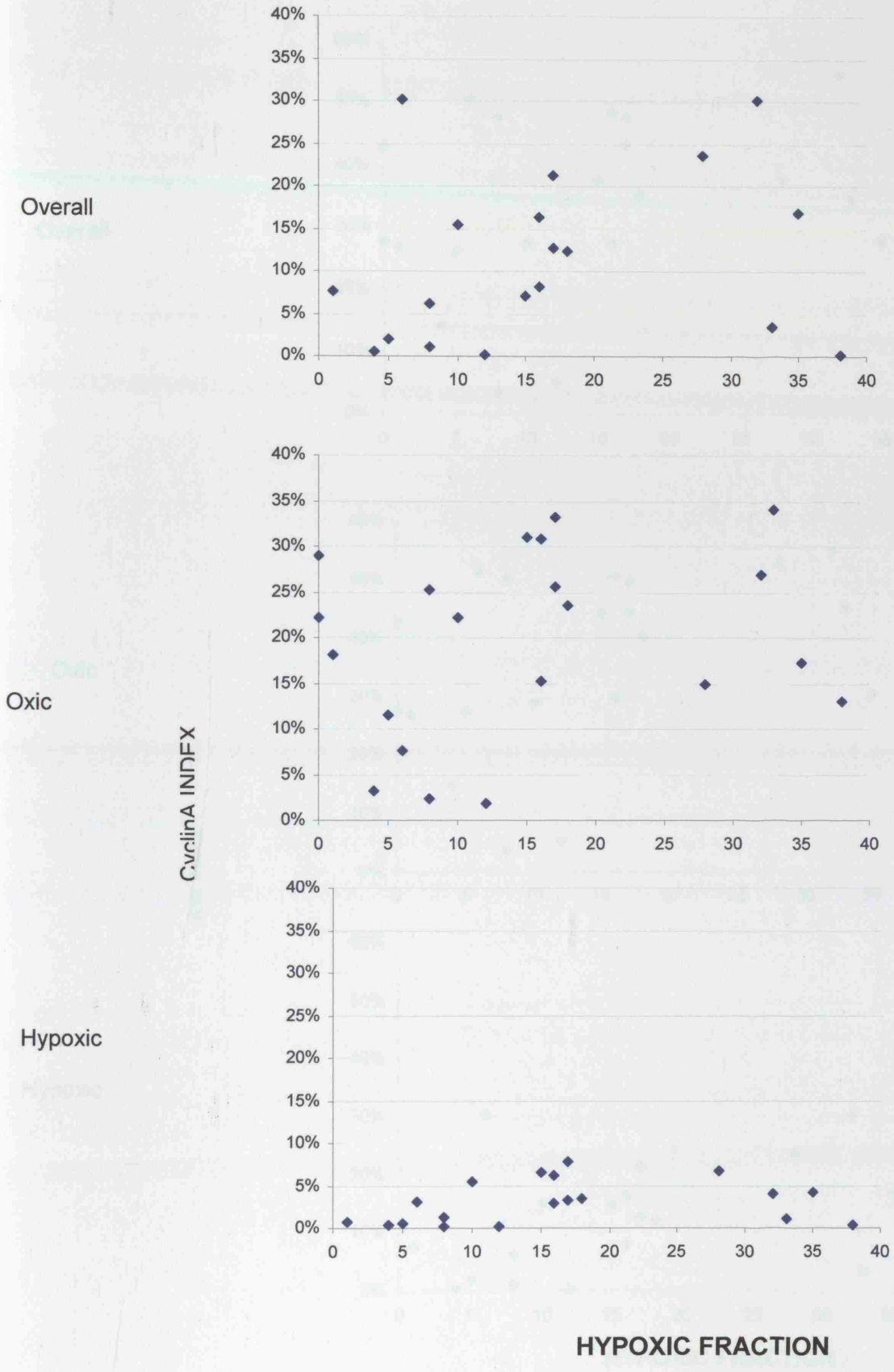

Figure 43 Plots of CyclinA proliferative index against hypoxic fraction for whole sample, oxic and hypoxic compartments

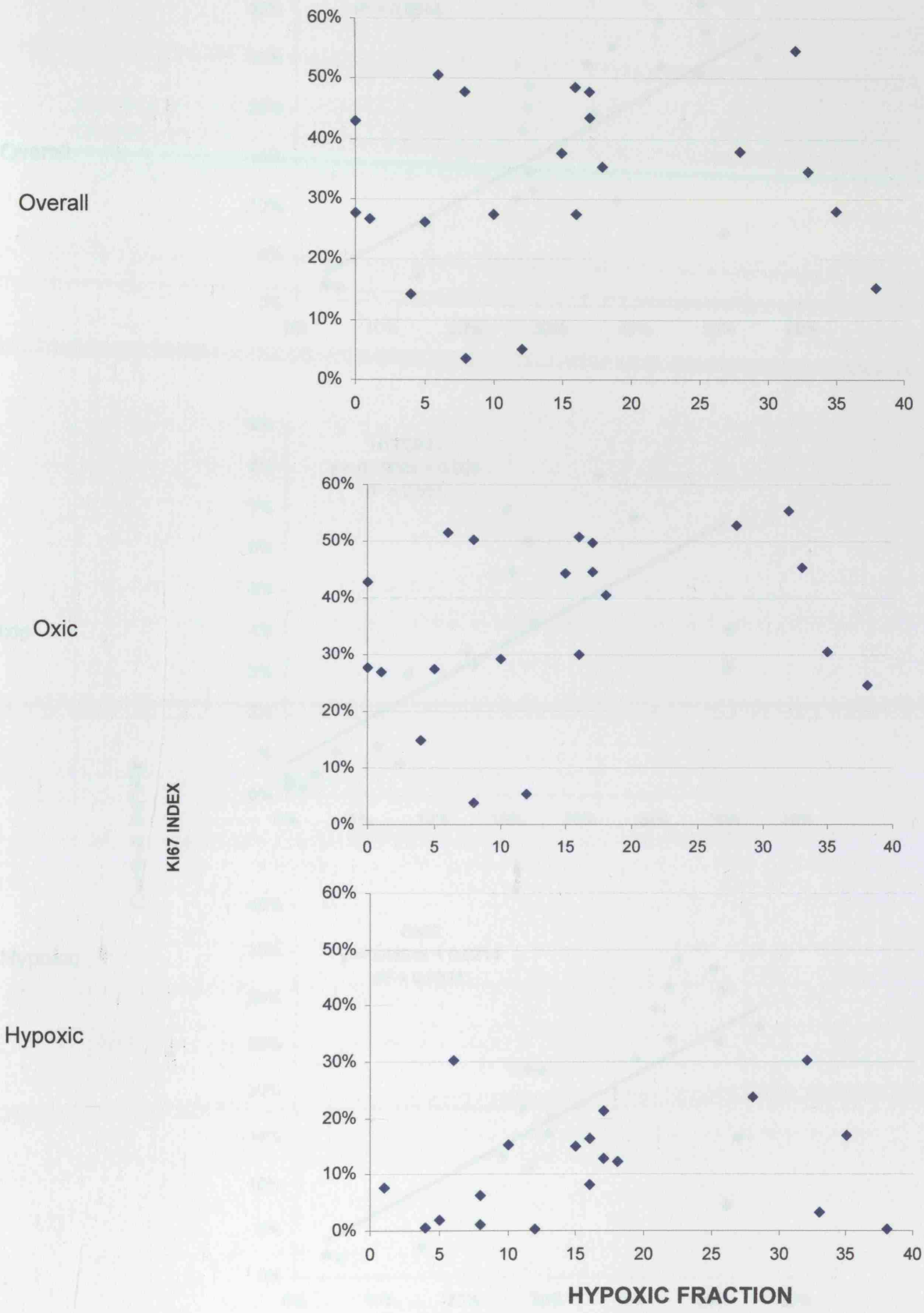

Figure 44 Plots of Ki67 proliferative index against hypoxic fraction for whole sample, oxic and hypoxic compartments

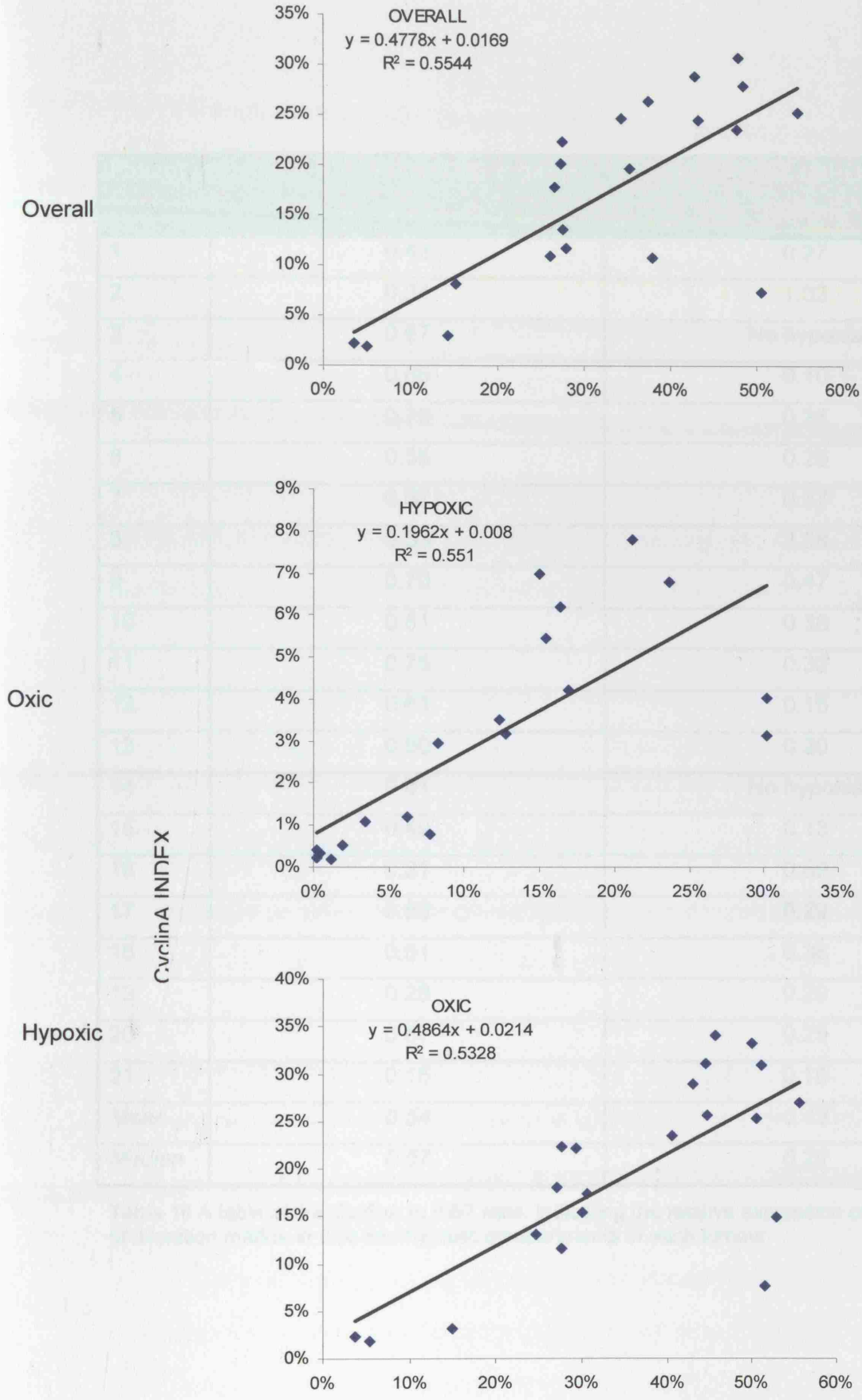

Figure 45 CyclinA index (y-axis) vs Ki67 index (x-axis) for whole tumour section, hypoxic and oxic compartments for each tumour

Patient	CyclinA:Ki67 ratio OXIC regions	CyclinA:Ki67 ratio HYPOXIC regions
1	0.42	0.27
2	0.34	1.03
3	0.67	No hypoxia
4	0.66	0.10
5	0.75	0.35
6	0.56	0.25
7	0.57	0.37
8	0.53	2.08
9	0.70	0.47
10	0.61	0.38
11	0.75	0.32
12	0.61	0.15
13	0.50	0.20
14	0.81	No hypoxia
15	0.49	0.13
16	0.21	0.69
17	0.58	0.29
18	0.51	0.36
19	0.28	0.29
20	0.67	0.25
21	0.15	0.10
Mean	*0.54*	*0.43*
Median	*0.57*	*0.29*

Table 10 A table of the CyclinA to Ki67 ratio, indicating the relative expression of each proliferation marker in oxic and hypoxic compartments of each tumour

Discussion

Cells within tissue exist in one of four states relating to their proliferation potential: proliferating, sterile, resting or dead. The proliferative compartment contributes to tumour growth and is the target of cancer treatment. The data in this chapter demonstrate that, overall, cellular proliferation is greatly reduced in hypoxic regions compared with oxic regions, and is consistent with other studies staining for hypoxia and proliferation simultaneously (206, 268, 269). This suggests that cells have moved from a proliferative to a quiescent or slowly proliferative state on becoming hypoxic. The data here show the relative reduction in proliferative index (Ki67) from oxic regions to those staining for hypoxia is 88%. A proportion of cells go on to die, reflected by the regional association of pimonidazole staining with necrosis, presumably through 'starvation' of cells being too distant from a feeding vessel to receive adequate nutrition. The switching from proliferating to non-proliferation may be an adaptive process. When a cell senses a poor oxygen supply it switches to producing 'hypoxia reducing proteins', mediated by the HIF transcriptional complex. HIF upregulation has been demonstrated in a variety of tumour types (270), including bladder carcinoma, and localises to perinecrotic regions when the epitope is detected immunohistochemically. There is no information on the relationship between HIF expression and proliferation markers. However, the perinecrotic location of HIF, where very little proliferation is observed in this study suggests it is unlikely that a cell will be dividing and produce HIF induced proteins simultaneously. Furthermore, the energy and oxygen requirements of the cell are much greater for cell division than for protein manufacture.

No overall relationship between proliferative index and overall hypoxic fraction emerged in this study, which may reflect low statistical power in this respect. This

agrees with clinical data from Tsang et al, who showed no association between hypoxia (measured by the Eppendorf) and proliferation assessed by bromodeoxyuridine labelling (271). However Raleigh showed an inverse relationship between hypoxia marker binding and proliferation (206, 272) yet Nordsmark showed the reverse in soft tissue sarcomas (273).

The impact of hypoxia on tumour cells in the in vitro setting has been studied by a number of groups. The data show that prolonged hypoxia leads to accumulation of cells in the G1 phase of the cell cycle (274-276). There is a restriction point in mid G1 mediated by the retinoblastoma protein and another in late G1. Hypoxia mediated inhibition of DNA replication has also been shown (277-279). Retinoblastoma protein competent cells therefore progress through all of the cell cycle from whatever stage they are in until they reach the pRB checkpoint in mid G1, and RB incompetent cells progress to the checkpoint at the late G1 stage (280). Cells in S phase are arrested immediately in hypoxic conditions (281), (277). In the light of these findings some interesting hypotheses can be made after consideration of the two proliferative markers used here.

Ki67 is a human nuclear protein named by the monoclonal antibody that identifies it (282) initially described in 1983 (283). It is tightly associated with cell proliferation upregulated in all proliferating cells that are in the active parts of the cell cycle, i.e. G1, S, G2, and mitosis, but absent in G0 cells. Its true function is still largely unknown, although a variety of new techniques such as confocal microscopy (284) and AgNOR double staining (285) show Ki67 changes cellular locality during the various phases of the cell cycle. It is nucleolar in interphase and S phase, but in prophase and anaphase associates with condensed chromosomes. During mitosis, Ki67 is seen in the cytoplasm. This redistribution is linked to post-translational

changes associated with phosphorylation, in common with other proteins controlling the cell cycle, hinting at a regulatory role as well as a structural component (286).

Cyclin A is also a marker of proliferation and is synthesised late in G1, throughout S phase, and into early G2 and associates with Cyclin Dependent Kinase 2 (cdk2) in early S phase and cdc2 in late S phase and early G2. Cyclin B becomes more important in G2. It binds to and activates cdk2, essential for initiation and progression through S phase, and is therefore short-lived in expression (287) compared to Ki67. The results here reflect this in that the proliferative index assessed by CyclinA was lower than that assessed by Ki67.

If the in vitro data described (284) (285) held true in the tumours examined here, then a higher degree of proliferation in hypoxic regions may be expected. Since Ki67 is expressed in all parts of the cell cycle, and if hypoxia induced cell cycle arrest occurs at the G1 and S phases, the proliferative index measured by Ki67 in hypoxic regions would supposedly be closer to that seen in oxic regions than when assessed by CyclinA. This supports a mechanism by which cells move from the cell cycle to G0 because of either hypoxia per se, or because of a local shortage of other vital nutrients due to inefficient tumour vasculature. The staining patterns show a relatively sharp fall in proliferation coincident with regions of hypoxia, suggesting a reasonably tight threshold for this regulatory mechanism. In addition, the ratio of CyclinA to Ki67 in hypoxic regions was about 1/5, compared to the oxic region ratio of about ½ (figure 45, table 10). This may indicate the proportion of cells actively involved in DNA synthesis is reduced in hypoxic regions. The relative proportions of 'G1' and 'G2' cells have increased and this is evidence for a slowing in the cell cycle as well. A slowing in G1 would have the effect of reducing the S and G2 components of the cycling population. The fact that the Ki67 index does not fall from

the oxic to hypoxic regions to the same degree as the CyclinA index may suggest a gradual slowing before quiescence.

Another example of where hypoxia is associated with cell cycle control can be seen in normal skin. Pimonidazole staining is seen in the squamous epithelium of normal skin, but not in the deeper, proliferating layers. This may just be a function of the diffusion distance of oxygen, but also raises the possibility that hypoxia promotes cellular differentiation. Raleigh showed the differentiation marker for squamous epithelium, involucrin co-localised with pimonidazole binding in 82% of a series of human squamous cell tumours, but no differentiation was seen morphologically (288). This could mean that one of the failures of cell cycle regulation that characterises cancer cells lies in a putative hypoxia-differentiation interaction.

The double staining method employed here has also shown some cells are actually *positive* for proliferation in hypoxic regions. Whether these cells are really proliferating in a low oxygen environment or have just arrested in a phase that upregulates the marker being stained for is unclear. Given the in vitro data above, these positive cells may have arrested at the G1 checkpoint or in S phase. CyclinA positive cells are present as well, indicating cells in G2 also exist. The exact fate of these cells is unknown- they may represent those in their last cycle before entering G0. However, the relatively low number of these cells suggests they are unique in some way, either retaining the ability to proliferate in hypoxia or being unable to cycle through to a stage where they are able to enter G0. These questions highlight the limitation of the immunohistochemical approach, which only provides a snapshot of cellular status.

Webster et al showed that hypoxic tumour cells from murine tumour models are able to progress through the cell cycle. Hypoxia, proliferation and cell cycle phase were

measured though time using the cell binding of NITP, bromodeoxyuridine and proprium iodide content respectively. Most hypoxic cells were in the G0/G1 phases, consistent with a G1 arrest, but some hypoxic cells were also found in the S phase and at the G2/M junction of the cell cycle (89).

In the present study, regions close to vessels, arbitrarily defined as those within 40μm, were assessed to examine the influence of so-called acute hypoxia on cellular proliferation. It has already been shown that the number of hypoxic microregions close to vessels is relatively low. There is a wide range of proliferative index in these regions. The proliferation was equivalent to oxic regions in some and to hypoxic regions distant from vessels in others. These regions must vary in some respect, most probably the length of time they are hypoxic. Those regions staining for pimonidazole and exhibiting a high proliferative index would perhaps be temporarily hypoxic. Should the oxygen supply to the region in question be interrupted for a significant period, proliferation would fall and not recover, and thus assume characteristics of chronically hypoxic cells in the same way as chronic diffusion related hypoxia, as seen in the regions distant from vessels. It can be hypothesised that hypoxic regions exhibiting proliferation similar to oxic regions are acutely hypoxic and those with a very low proliferative index are chronically hypoxic, the 'acute' and 'chronic' timeframes being defined by how long cells can withstand hypoxia and maintain their proliferative capacity.

The exact time period that defines 'acute' and 'chronic' hypoxia may vary from tumour to tumour and maybe even within tumours. An in vivo model used by Denekamp et al (289) to investigate hypoxic cell radiosensitisers suggested that 'acute' hypoxia could develop very quickly. The model involved making the skin of mice hypoxic by subjecting them to nitrogen breathing just before irradiation. Full resistance, by a factor of 2.8, could be achieved within 20 seconds of the start of

nitrogen breathing; the actual time the cells were hypoxic once irradiation had started was probably much shorter. An idea of the timing of chronic hypoxia can be gleaned from studies of energy depletion under hypoxic conditions. MRS studies have shown that levels of ATP fall in response to induced vessel shutdown (by clamping or administration of hydralazine) and this occurs within 15 to 30 minutes (290). In vitro studies indicate the energy potential of cells falls after 1 to 2 hours (291-292).

What is not known is how long cells have to remain hypoxic for before they are committed to non-clonagenicity even if they reoxygenate. However, the life time of chronically hypoxic cells was estimated by Azuma et al (204), who performed serial biopsies at three successive days on dog tumours undergoing treatment at the vetenary college of North Carolina State University. They demonstrated hypoxic cells that bind pimonidazole can remain viable for at least 72 hours implying the window of opportunity for reoxygenation may be substantial.

Conclusion

Within individual bladder tumours, there is an tendancy but no relationship between hypoxia and proliferation in this cohort of bladder tumours, although some cells positive for proliferation are present within hypoxic regions. These may be clonagenic, and since they are relatively radioresistant, are thus a source of treatment failure. In the few hypoxic regions identified close to vessels, the proliferative index varied. In some they were equivalent to that in oxic regions and these may represent 'truly' acute hypoxic regions; in others where proliferation was sparse, established 'chronic hypoxia' is postulated due to long term vessel shutdown.

CHAPTER FOUR

Vascularity in Bladder Carcinoma and its Relationship to Hypoxia

Aims

Tissue growth is dependent on an adequate supply of oxygen and other nutrients, delivered by adequately functioning vasculature. The relationship between a tumour and vessel is one of self-perpetuation, where tumour growth stimulates angiogenesis whilst vessel formation and function allow tumour growth. The aim of this part of the thesis was to examine the relationship between vascularity, measured by two different methods, and hypoxia in transitional cell bladder carcinoma.

Methods and Materials

Procedure

Twenty-one tumour samples staining for a range of pimonidazole (and thus hypoxic) fractions were selected. Four micron sections were double stained for CD31/34, to demonstrate vascular structures, and for bound pimonidazole using a dichromatic immunohistochemistry method, described below.

Immunohistochemistry: Double staining for pimonidazole and CD31/34

- Slides were de waxed in xylene for 5 minutes and rehydrated through graded alcohols (100,90, 70%) to water.
- Sections were then transferred to a 37°C water bath (300mls) containing 0.01% pronase (Sigma) buffered to pH 7.8.
- After 10 minutes, sections were washed in running tap water for five minutes. Endogenous peroxidase was blocked with Dako peroxidase block (Envision Kit) at room temperature for 5 minutes, then washed well in water.
- The section was then encircled with resin using a resin pen to well in the solutions used in the rest of the staining process.
- Protein block (Dako X0909) was added and left for five minutes. The excess was tipped off.
- Anti –Pimonidazole antibody mixture (Natural Pharmacia Cat 01800 Mab1) was added, left on the slide for one hour at room temperature, and washed off with tris buffered saline three times for a total of three minutes.
- Envision alkaline phosphatase mouse polymer (Dako K4006) was added for 30 minutes and washed off with tris buffered saline three times for a total of three minutes.
- Vector Alkaline Phosphatase red substrate (Vector SK5100) was added for 5 to 10 minutes, watching the colour develop.
- Anti-CD31/CD34 antibody cocktail (Dako M0823/M7080) was applied, diluted 1/50 and 1/60 respectively in tris buffer saline for 30 to 60 minutes, and then washed three times in tris buffer saline.
- Envision Horseradish peroxidase was then added (Dako K4017) for 30 minutes and then washed three times in tris buffer saline.
- Diaminobenzine substrate was then added (Vector SK4100) for 5 minutes.

- The slides were then rinsed in distilled water, and then washed in running tap water.
- The section was rinsed in tris buffer saline, then washed in water and again in tris buffer saline.
- To stain nuclei blue, the sections were placed in Gills Haematoxylin for between 10 to 60 seconds and then washed well in tap water.
- Finally the sections were dehydrated through graded alcohols, cleared by xylene and sections mounted in DPX (Merck 360294H) mounting media.

The resulting section shows nuclei as blue, pimonidazole bound cells as red and blood vessels as brown.

Image Analysis

Set up

The hardware and software setup was as described in chapters 2 and 3

Assessment of Vascularity

Two methods were used to assess vascularity.

'Hot spot' Method

'Hot spot' counts were performed in 'oxic' fields that contained tumour without any stain for hypoxia, and in 'hypoxic' fields that did stain for hypoxia. The section was systematically surveyed for a 'hot spot' of vessels at a magnification of five times. The vessels were classified as being in a hypoxic field if they were within the same field as a region of tumour staining for hypoxia when viewed at 10 times magnification (figure 46). Vessels were classified as oxic if no hypoxia was seen in the same x10 and adjacent x10 fields. The hot spot was then centralised in the microscope field, viewed under a magnification of 20 times (figure 47) and individual

vessels were counted. Individual vessels were defined as being any group of endothelial cells staining with the brown of the oxidised diaminobenzene product, separated from other vessels. Vessel lumina or red cells were not required to define a vessel. Between 3 and 10 hot spots were counted for each tumour, depending on the size of the section. The highest hot spot count was assigned to the tumour (293).

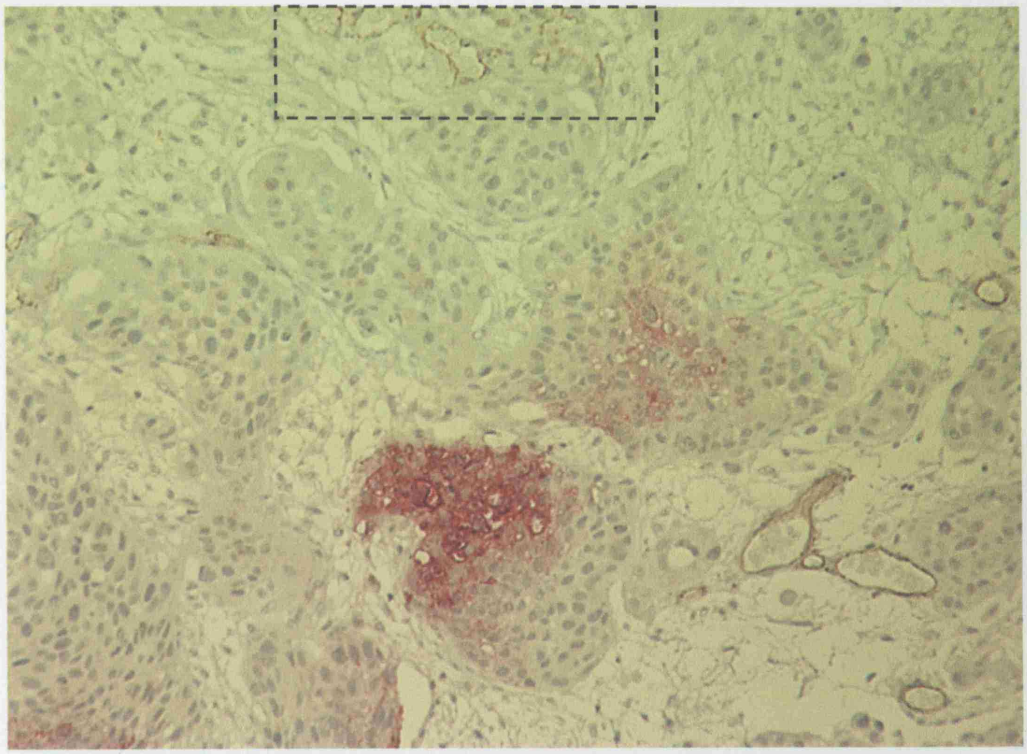

Figure 46 An example of a 'hypoxic field': the vessels in this image assessed by either the hot spot method or the simple vessel count were classified as those in a hypoxic field viewed at x10 magnification. The outlined region identifies the associated hot spot.

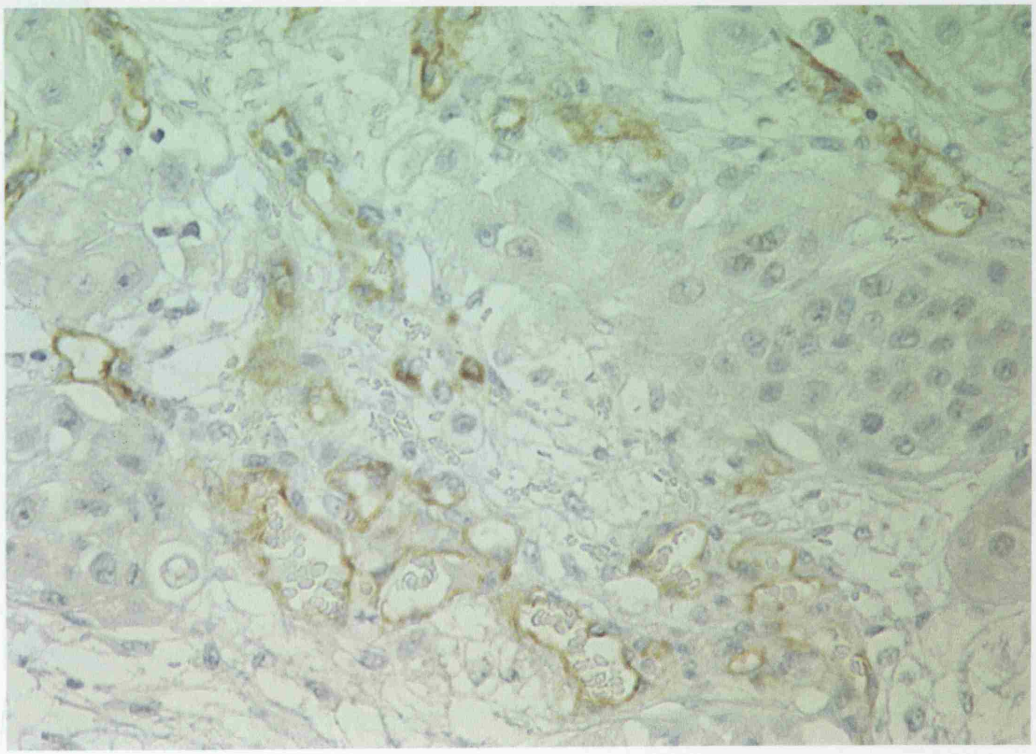

Figure 47 An example of a 'hot spot' of vessels, viewed at 20x magnification

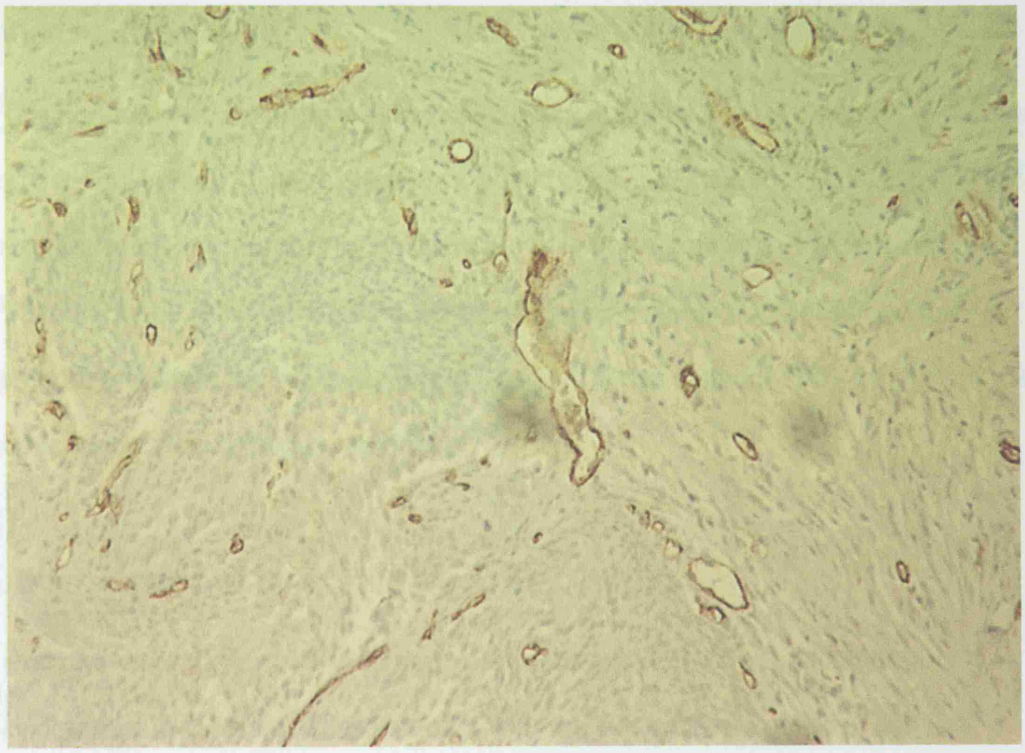

Figure 48 An example of an oxic field: the vessels viewed in this image, viewed at x10 magnification, were classed as being in an oxic field. Adjacent x10 fields were also free from hypoxia

Vascular Density

The second method of assessing vascularity involved simply counting all vessels at x10 magnification. This represented a field size of 0.710mm^2. The vascularity was expressed as the number of vessels per millimetre squared of tissue section. Vascularity by this method was assessed in 'oxic' fields that contained tumour without any stain for hypoxia, and in 'hypoxic' fields that did stain for hypoxia as described in the previous section.

Assessment of vessel to hypoxia distance

Regions of pimonidazole staining were identified at x10 magnification and centralised in the field. The distance from the edge of the region of light pimonidazole staining to the edge of the nearest 3 vessels was measured using image analysis software (figure 49).

Exclusions

Two tumours had no pimonidazole staining and were thus not included in the comparison of vascularity in oxic and hypoxic regions, or in hypoxia to vessel distance assessments.

Data Obtained

The following data were obtained:

- The 'hot spot' counts for the whole tumour section.
- The vascular density (vessels per mm^2) for the whole tumour section.
- The 'hot spot' counts in regions staining for hypoxia and in regions not staining for hypoxia.

- The vascular density (vessels per mm^2) in regions staining for hypoxia and in regions not staining for hypoxia.
- Distance from vessels to hypoxia for the whole tumour section.

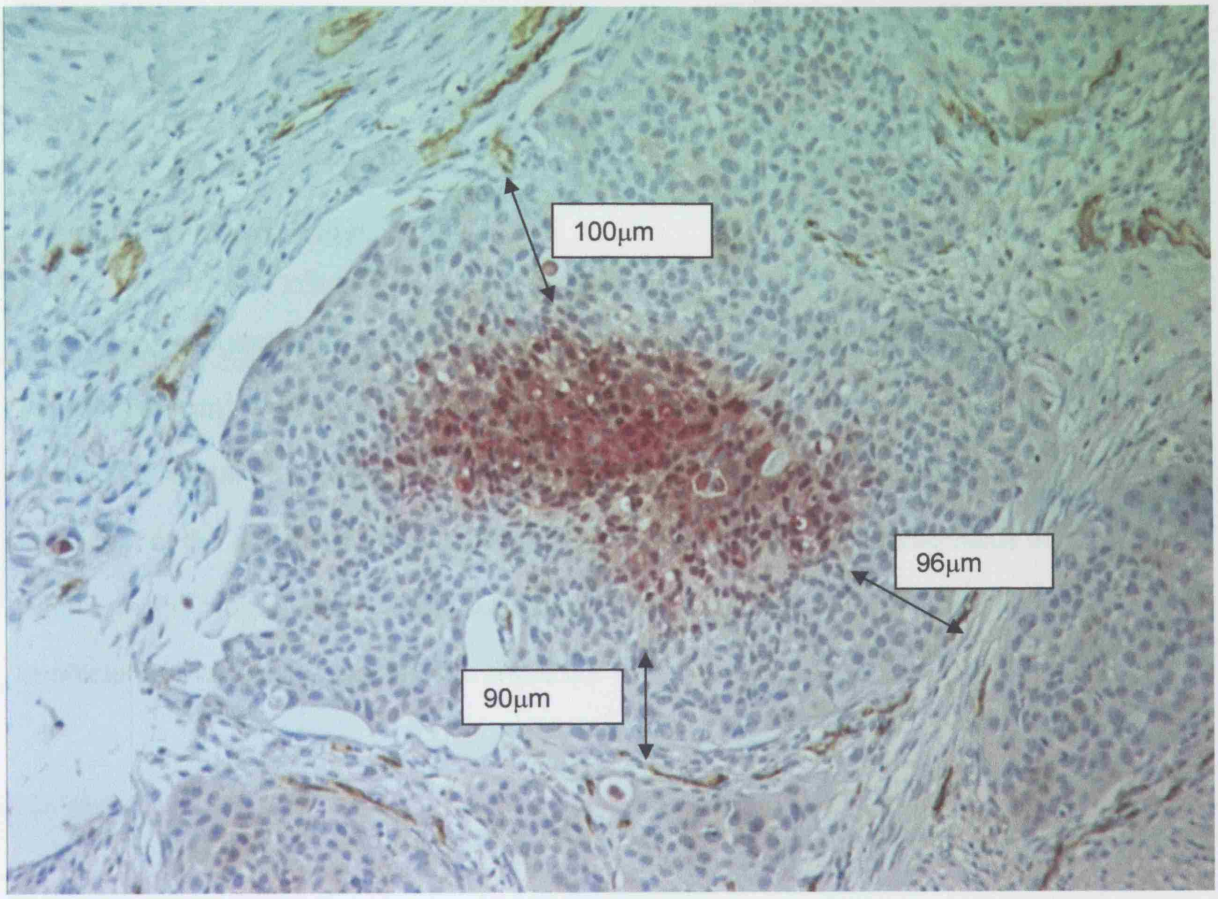

Figure 49 Image (x10) showing the assessment of vessel-hypoxia distance, with the region of pimonidazole staining centralised and the distance to the three nearest vessels being measured

Results

The vascularity

Overall vascular density

The mean vascular density within this group of tumours ranged from 16.7 to 160.6 vessels per mm^2. The overall mean for all 21 specimens was 60.8 vessels per mm^2 (table 11). A total of 514 fields were measured. The coefficient of variation, an indication of the degree of vascular heterogeneity across the measured fields in each tumour, ranged from 0.08 to 0.52 (figure 50). Eighteen of the specimens had a coefficient of variation between 0.2 and 0.5.

Patient	Mean vascular density (vessels/mm^2)	Standard Deviation	Coefficent of Variation
1	144.3	31.0	0.22
2	44.6	7.1	0.16
3	123.2	33.9	0.27
4	33.7	7.0	0.11
5	160.6	18.3	0.21
6	49.2	25.6	0.52
7	33.3	6.2	0.19
8	57.8	16.6	0.29
9	16.7	7.0	0.42
10	107.3	8.4	0.08
11	109.3	13.9	0.27
12	34.9	9.5	0.13
13	55.4	10.9	0.20
14	15.7	3.2	0.21
15	41.3	7.2	0.17
16	38.1	6.9	0.18
17	32.7	10.7	0.15
18	60.8	9.1	0.36
19	52.7	18.7	0.23
20	36.0	12.0	0.33
21	30.0	6.8	0.33

Table 11 Mean vascular density and the coefficient of variation for each tumour

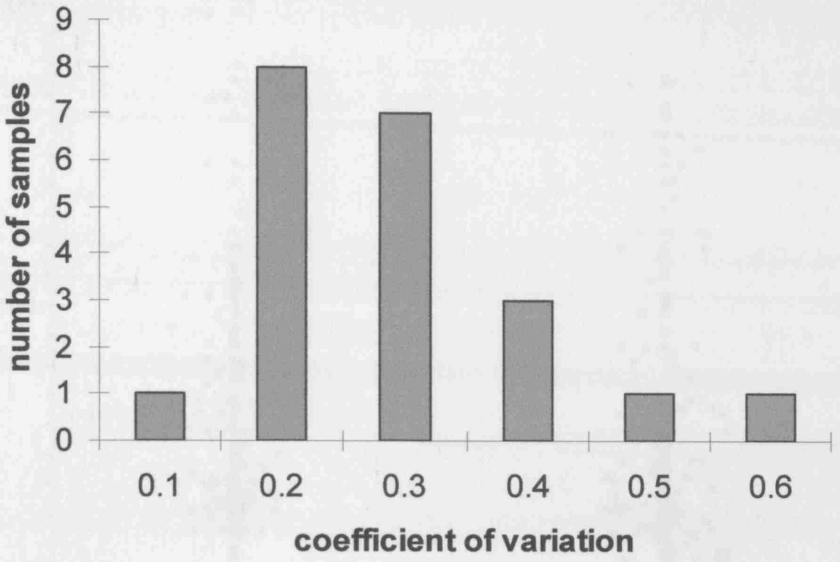

Figure 50 A histogram of the coefficient of variations of vascularity in the tumours analysed, illustrating the range of variability of vascularity across each individual sample. The lower coefficient implies less less variability.

Vascular density in oxic and hypoxic regions

Combined vascular density in oxic and hypoxic regions for all tumours

The mean vascular density for all patients was 54.8 vessels per mm^2 in oxic regions (95% confidence interval (CI) 50.0 to 58.2, n=297) and 63.6 vessels per mm^2 (95% CI 59.6 to 69.0, n=217) in hypoxic regions. This difference was statistically significant, (two sided t-test, p=0.02) (figure 51).

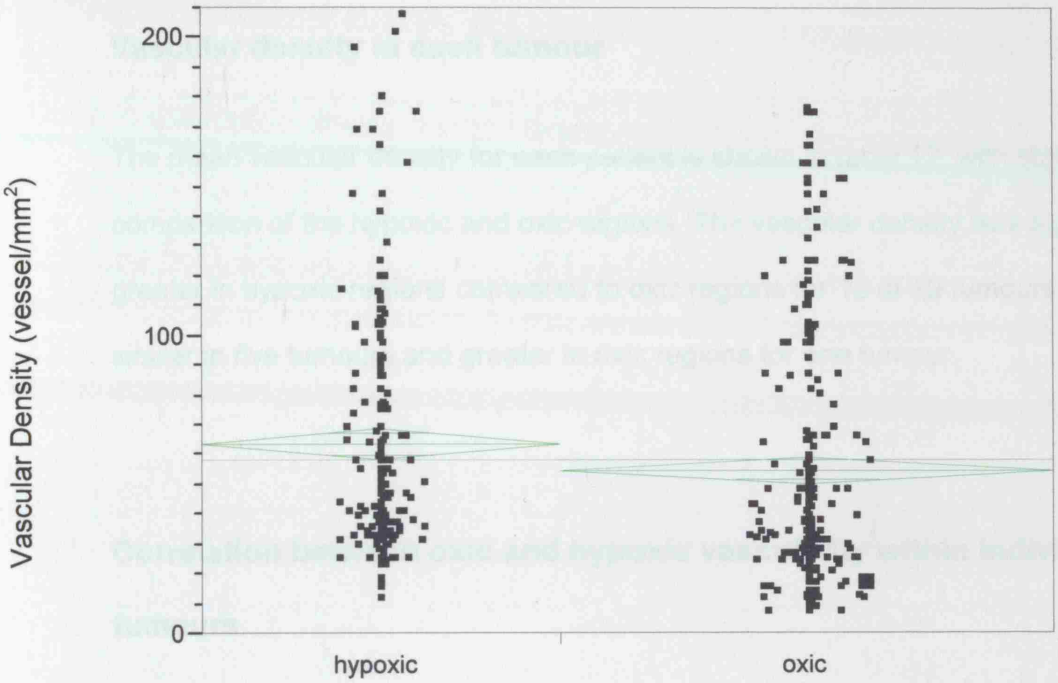

Figure 51 Comparison of vascular density in oxic and hypoxic regions of all fields analysed in all tumours. Black points represent vessel density in each field assessed (n=514); green lines show the mean with the 95% confidence intervals.

Vascular density in each tumour

The mean vascular density for each patient is shown in table 12, with statistical comparison of the hypoxic and oxic regions. The vascular density was significantly greater in hypoxic regions compared to oxic regions for 13 of 19 tumours. It was similar in five tumours and greater in oxic regions for one tumour.

Correlation between oxic and hypoxic vascularity within indivicual tumours

A scatter plot comparing the vascularity in oxic to hypoxic regions of each individual tumour is shown in figure 52. There is a strong correlation, ($r=0.92$, $p<0.0001$), showing the tendency to greater vascularity in these tumours affects both oxic and hypoxic compartments of the tumour.

Patient	Vascular density hypoxic regions (vessels/mm^2)	Vascular density oxic regions (vessels/mm^2)	Region with higher vascularity	p-value 2-sided t-test
1	178.6	136.4	hypoxic	0.04
2	49.1	42.0	hypoxic	0.03
4	39.4	30.7	hypoxic	<0.001
5	169.5	151.7	hypoxic	0.01
6	72.3	30.5	hypoxic	<0.001
7	38.9	28.3	hypoxic	<0.001
8	70.3	45.3	hypoxic	<0.001
9	22.8	12.5	hypoxic	<0.001
10	105.6	108.5	No difference	0.39
11	108.3	110.3	No difference	0.67
12	34.1	36.3	No difference	0.64
13	62.6	50.4	hypoxic	0.01
15	33.6	45.6	hypoxic	<0.001
16	42.3	34.8	hypoxic	0.03
17	41.6	25.2	hypoxic	<0.001
18	58.7	65.0	No difference	0.17
19	31.3	66.4	oxic	<0.001
20	42.1	30.3	hypoxic	0.01
21	29.2	30.5	No difference	0.71

Table 12 Comparison of mean vascular density in oxic and hypoxic regions, p-values

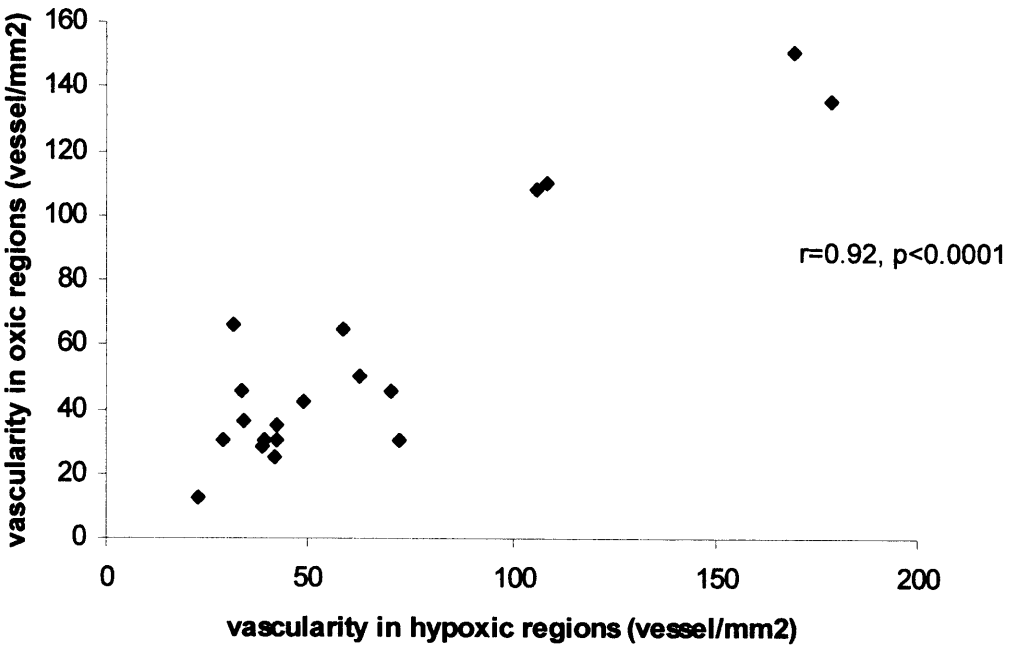

Figure 52 Scatter plot of the vascularity in oxic and hypoxic regions of each individual tumour, showing strong correlation in the two compartments.

Overall hot spot count

The median hotspot count was 30 (range 16 - 43), (figure 53).

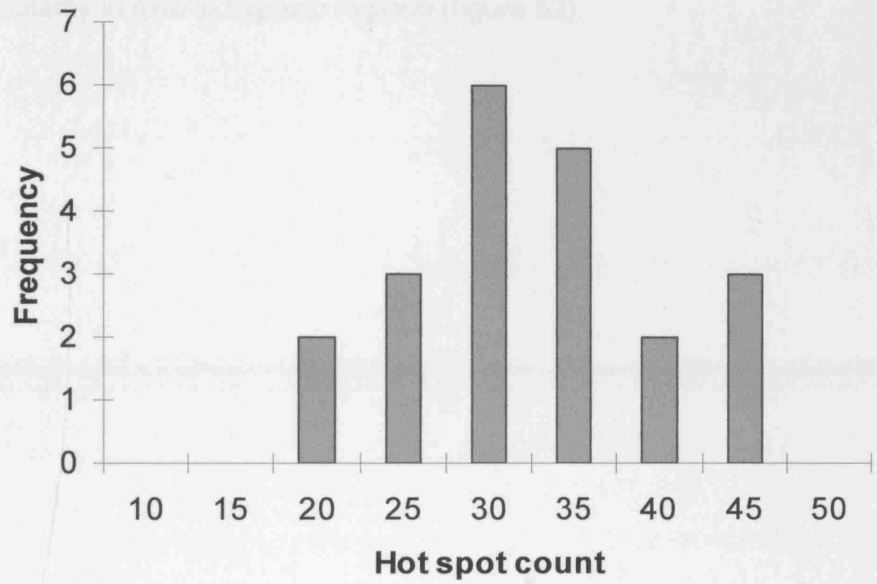

Figure 53 Histogram of the hotspot count for each tumour, The highest count found in each tumour was assigned.

Hot spot count in oxic and hypoxic regions

The median hotspot count was 28 (range 14 – 43, 63 fields) in hypoxic regions and 24 (range 10 – 42, 57 fields) in oxic regions. This difference is statistically significant, p=0.004 (figure 54).

The highest hot spot count for oxic and hypoxic regions in each tumour is shown in table 13. The hot spot count was greater in hypoxic regions compared to oxic regions for 12 tumours. It was similar (+/-2) in three patients and greater in the oxic regions in five patients.

A scatter plot comparing the hot spot counts in oxic with that in hypoxic regions of each individual tumour is shown in figure 55. The correlation coefficient is 0.65 ($p=0.002$), reflecting to some extent the relationship seen in the comparison of vascularity in oxic to hypoxic regions (figure 52).

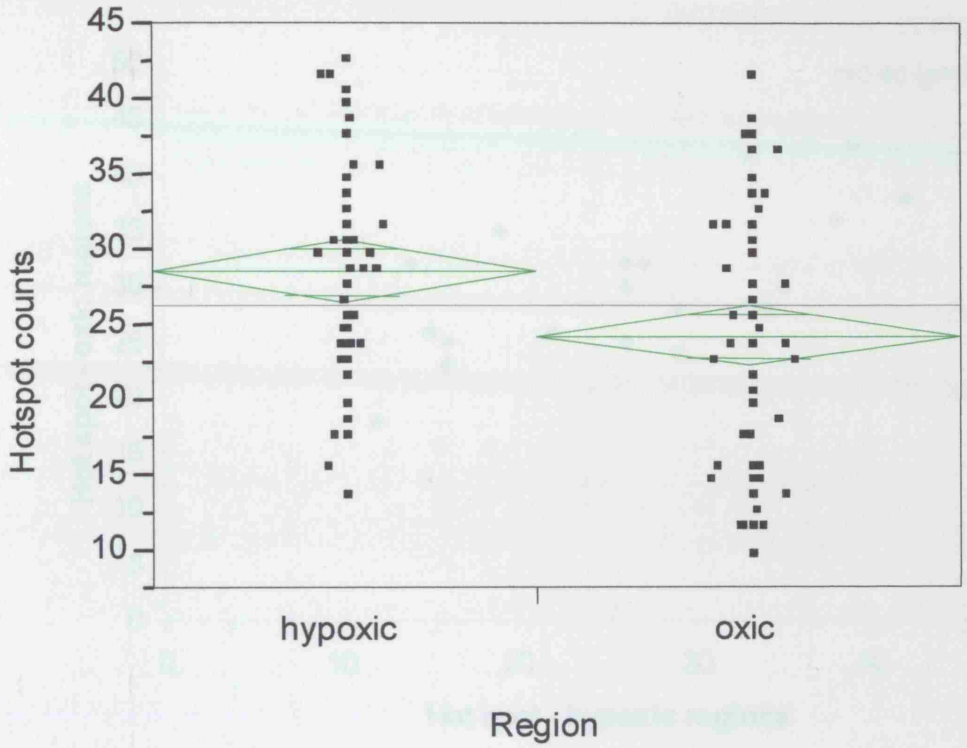

Figure 54 Comparison of hot spot counts in oxic and hypoxic regions of tumour. Black points represent the highest hot spot count in each field assessed; green lines show the mean with the 95% confidence intervals

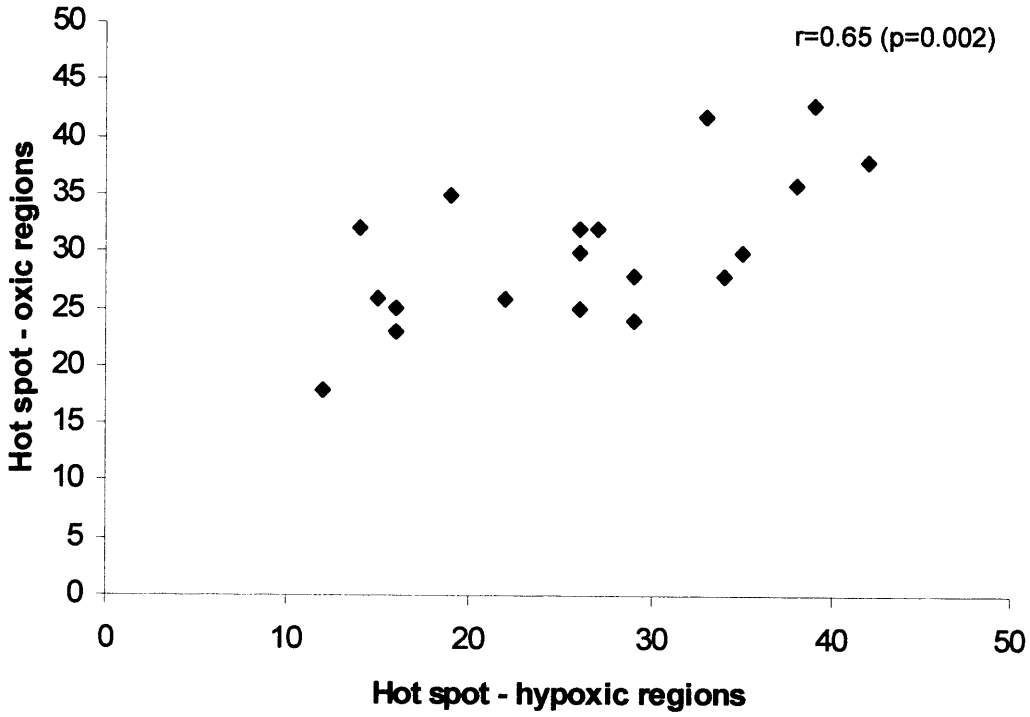

Figure 55 Scatterplot comparing hotspot counts in oxic regions with hypoxic regions for each tumour.

Patient	Hot spot- hypoxic	Hot spot - oxic	Higher
1	42	33	hypoxic
2	30	26	hypoxic
3	No hypoxia	30	-
4	35	19	hypoxic
5	36	38	oxic
6	26	22	hypoxic
7	25	16	hypoxic
8	32	14	hypoxic
9	18	12	hypoxic
10	43	39	hypoxic
11	30	35	oxic
12	28	29	oxic
13	38	42	oxic
14	No hypoxia	16	-
15	24	29	oxic
16	23	16	hypoxic
17	32	26	hypoxic
18	25	26	oxic
19	28	34	oxic
20	32	27	hypoxic
21	26	15	hypoxic
median	*26*	*26*	-
mean	*27*	*25*	*hypoxic*

Table 13 Table of the highest hot spot count for each tumour, by oxic region showing that in the majority of tumours, the hot spot count was higher in the hypoxic regions

Comparison between hotspot count and vascular density

Figues 56 to 58 show the correlation between the mean vascular density and the highest hot spot count for the specimens overall, within areas of oxia and hypoxia respectively.

A similar relationship was evident in all three analyses with correlation coefficients of 0.63 (p=0.002), 0.67 (p=0.002) and 0.63 (p=0.004) for overall, oxic and hypoxic areas. The data show that the vascular density has a greater range of intertumour variation than the hotspot count but there is a positive relationship between the two measures of vascularity.

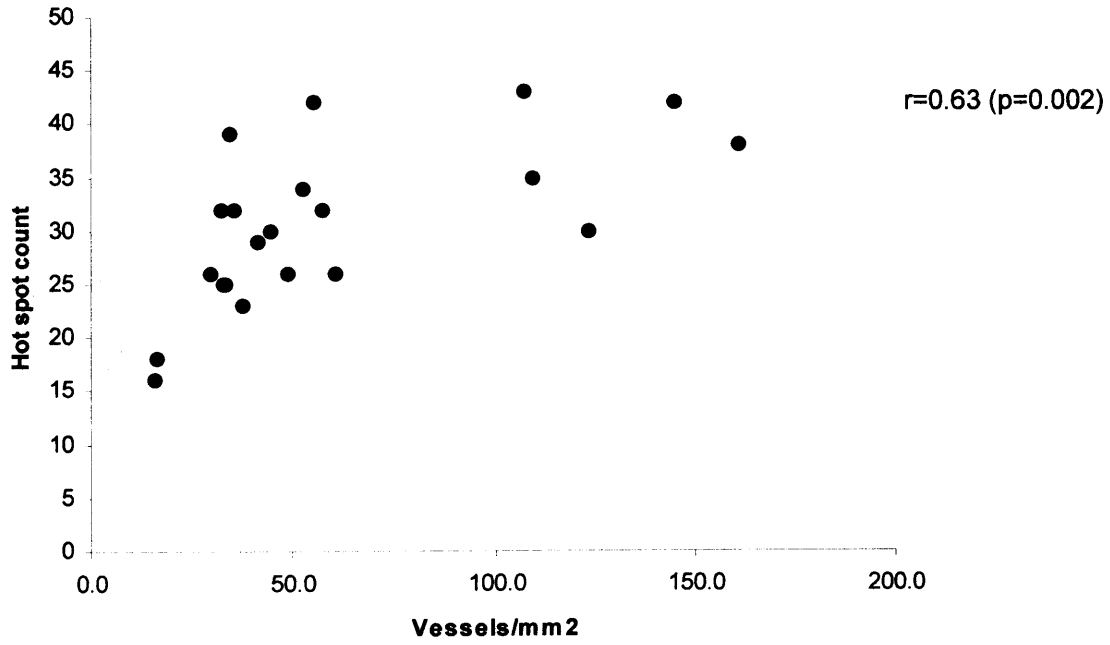

Figure 56 Plot of overall hot spot count vs overall vascular density for each tumour

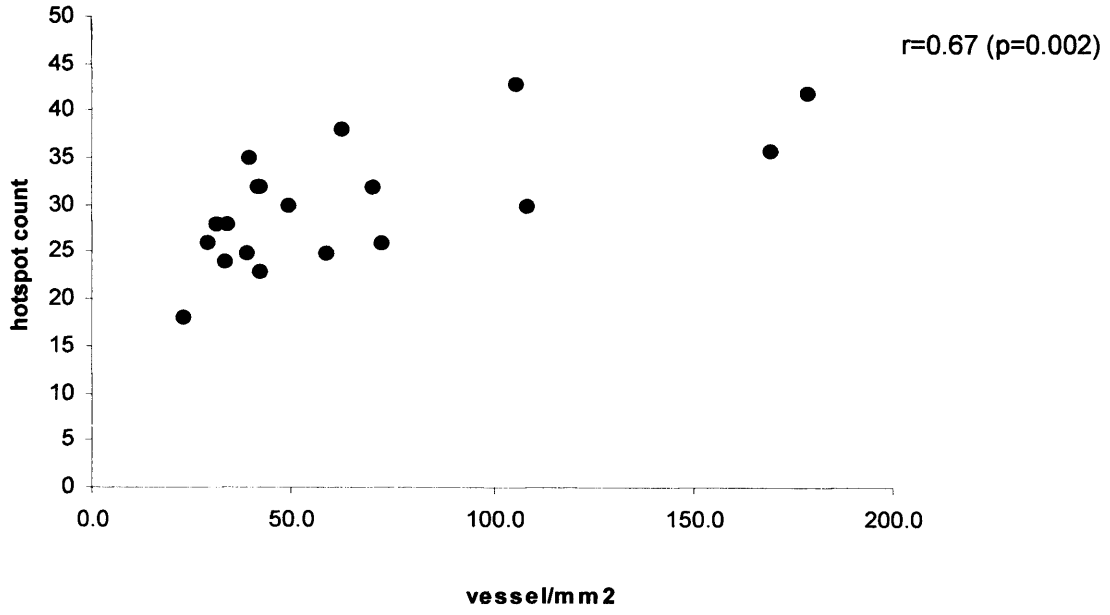

Figure 57 Plot of hot spot count vs vascular density for each tumour – hypoxic regions

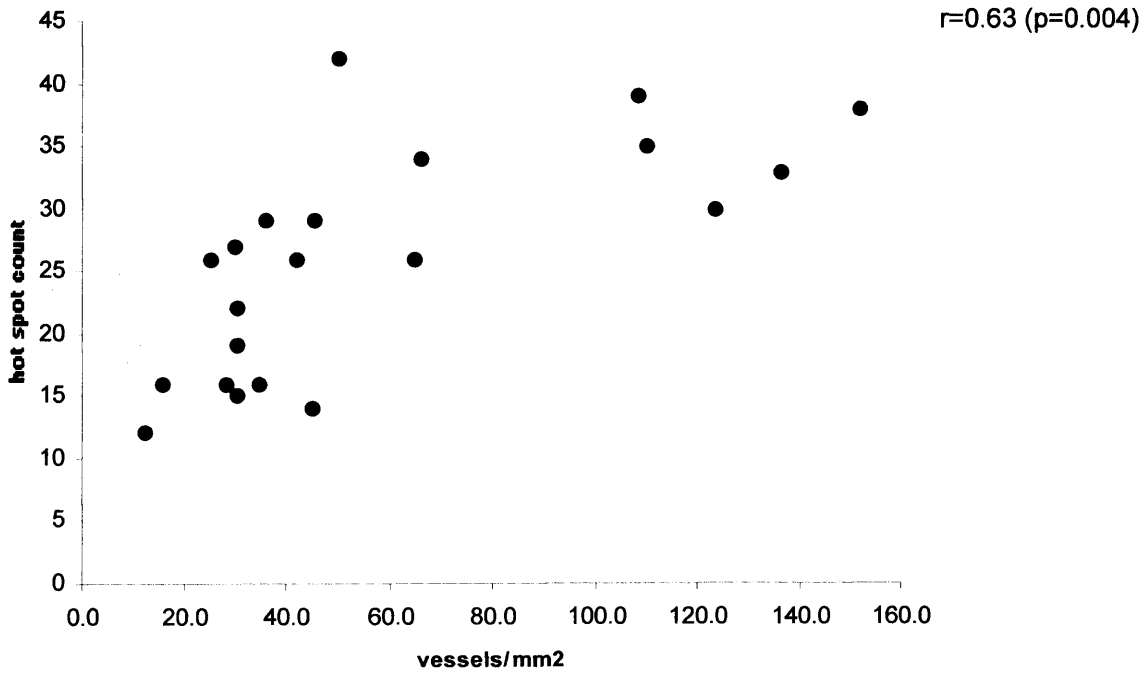

Figure 58 Plot of hot spot count vs vascular density for each tumour –oxic regions

Relationship between pimonidazole stained fraction and vascularity

There was no relationship between the degree of pimonidazole staining and overall vascularity, measured by either vessel count or hot spot count (figures 59 and 60). There was no statistically significant relationship between the degree of pimonidazole staining and the coefficient of variation of overall vascularity (r=0.31, p=0.16) (figure 61).

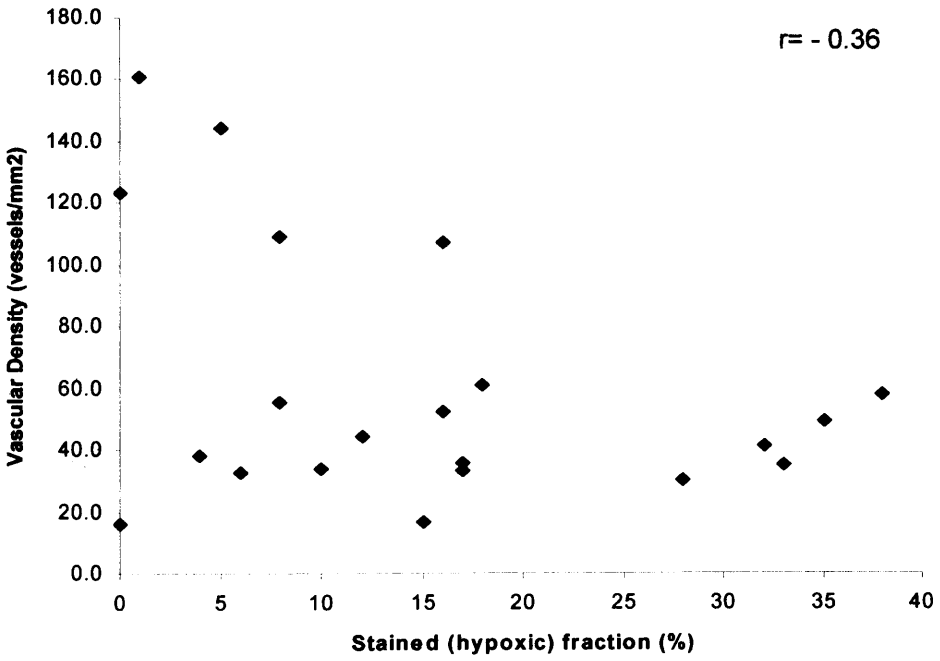

Figure 59 Scatter plot of vascular density vs hypoxic fraction assessed by pimonidazole

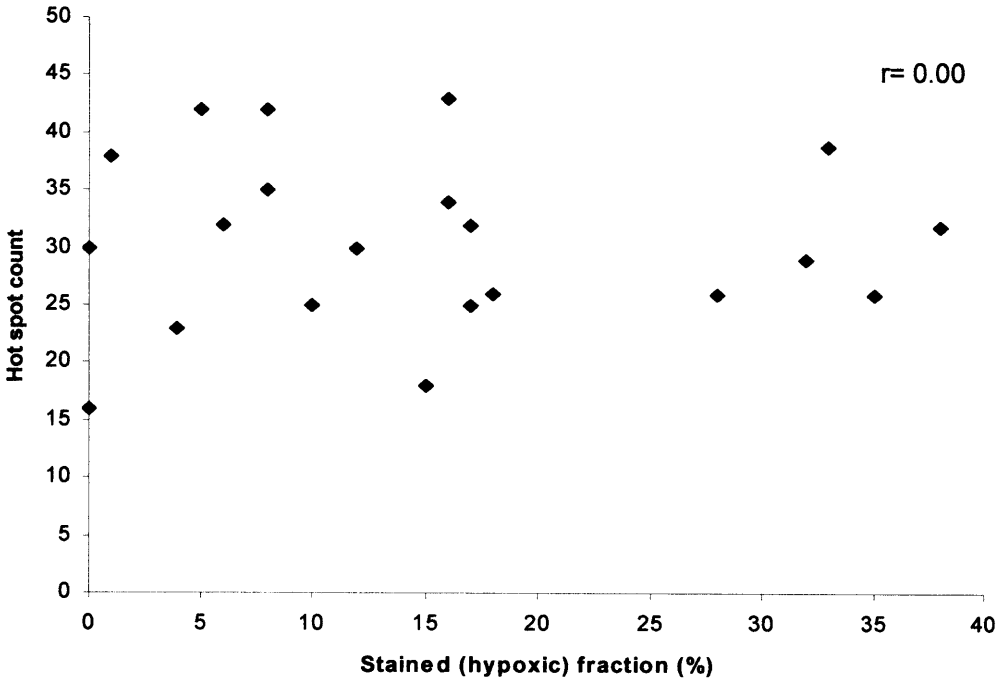

Figure 60 Hot spot count vs hypoxic fraction assessed by pimonidazole

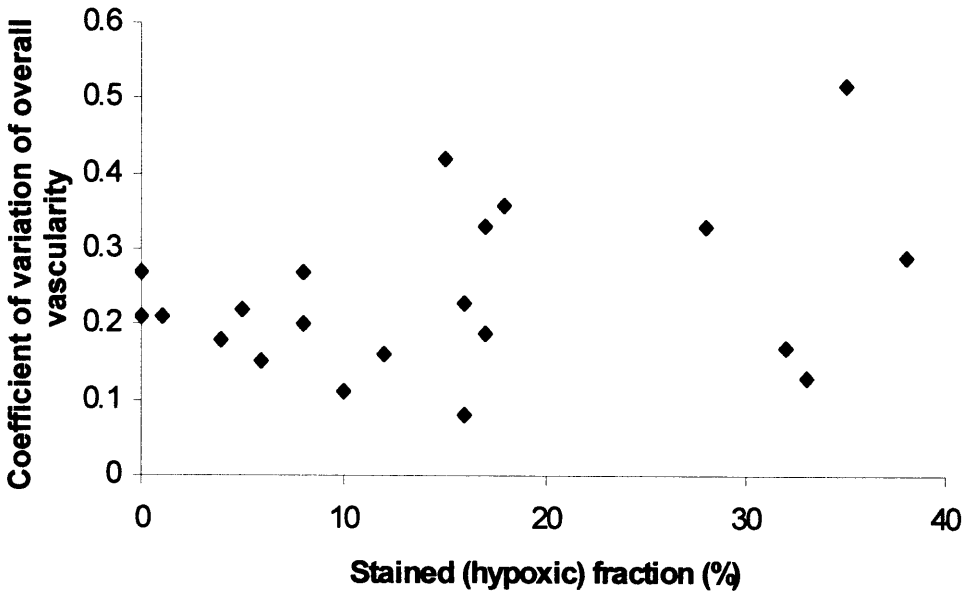

Figure 61 Scatter plot of the coefficiant of variation of vascular density vs hypoxic fraction assessed by pimonidazole

Vessel to hypoxia distance

The median distance from regions of hypoxia (edge of light pimonidazole staining) to the nearest vessel was 100 (range 8 to 231) microns for all measurements across all tumours (figure 62). The median vessel to hypoxia distance, range of distances and the coefficient of variation for each patient are shown in table 14. No relationship between the median vessel to hypoxia distance or the coefficient of variation and hypoxic fraction was evident (figures 63 and 64).

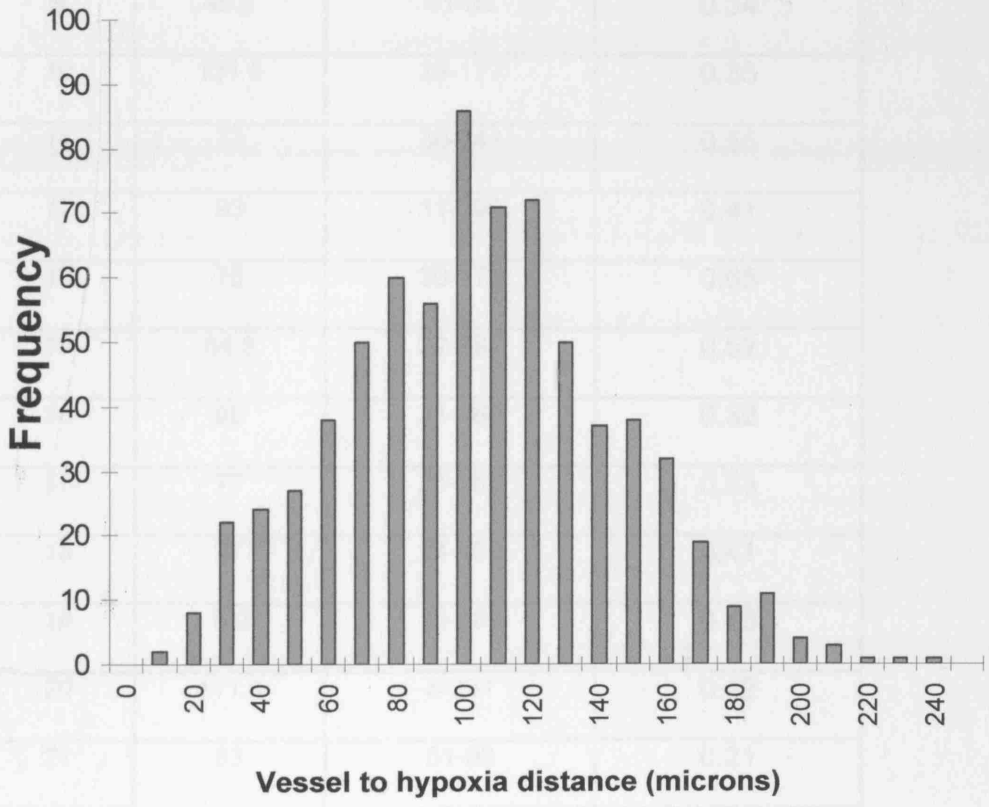

Figure 62 Histogram of distances from vessels to hypoxia, pooled from all tumours

Patient	Median (microns)	Range (microns)	Coefficient of Variation
1	108.5	62-182	0.27
2	105	26-181	0.37
4	94.5	31-188	0.41
5	76	53-83	0.21
6	103	30-185	0.31
7	101.5	38-174	0.35
8	105	53-157	0.31
9	49.5	41-83	0.34
10	131.5	25-177	0.35
11	73	30-141	0.55
12	93	11-190	0.41
13	76	20-175	0.65
15	84.5	22-181	0.52
16	98	31-160	0.32
17	77	25-165	0.53
18	97	24-169	0.41
19	102	18-181	0.43
20	111.5	8-231	0.42
21	83	51-98	0.21

Table 14 Median and range of vessel to hypoxia distance for each tumour

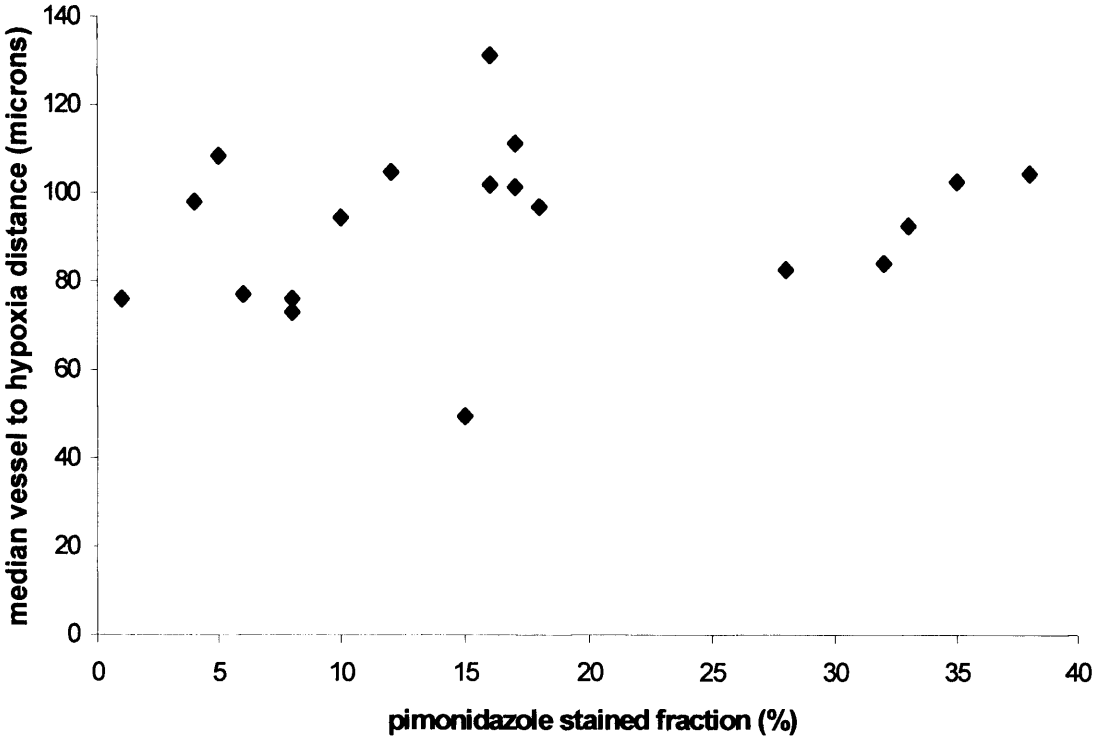

Figure 63 Scatterplot of median vessel to hypoxia distance vs the pimonidazole stained fraction

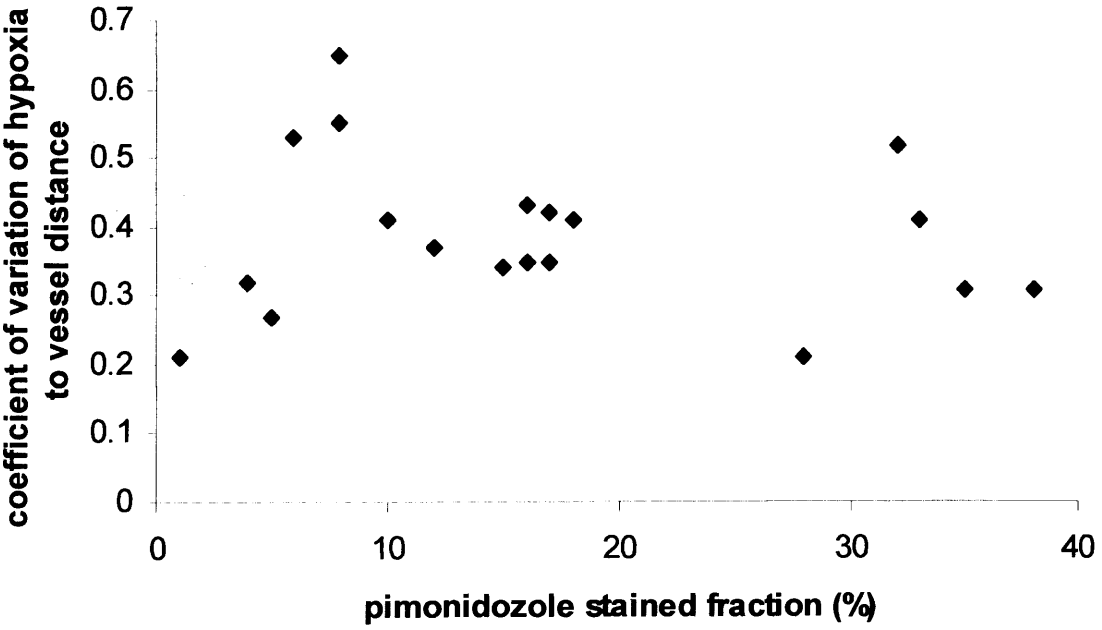

Figure 64 Scatterplot of median vessel to hypoxia distance coefficient of variation vs the pimonidazole stained fraction

Discussion

Methods of measuring vascularity

The results have shown a positive relationship between two methods of measuring vascularity. The physiological consequences of variations in vascularity are a feature of both the structural arrangement of blood vessels and function in terms of oxygen and nutrient delivery which is dependent upon blood flow and composition. The technique of measuring vascularity may reflect either of these components to different degrees. The hotspot technique is thought to reflect the degree of angiogenesis. A number of studies have shown the hot spot count correlates with expression of angiogenic factors, vascular endothelial growth factor and platelet derived growth factor (147, 294-296). The hot spot method is well established and widely used since originally described by Weidner in 1991 in a study of breast carcinoma (293). The disadvantages of this analysis include the subjective nature of localising the hotspot and the intrinsic variability of the staining process (minimised here by performing all stains in a single batch). The magnification used here of 200x (20-x objective and 10-x eyepiece) matches the method described by Weidner, however the sensitivity of the technique may be enhanced by using a higher magnification. Vermeulen showed a doubling of the microvessel density when the magnification used was 400 times in a series of breast carcinomas (297). Despite this, the prognostic power of microvessel density would not have altered because the ranking order would remain the same.

Measuring intervessel distance should reflect the efficiency of oxygen and nutrient delivery, which in turn should correlate with the degree of hypoxia. The plain count per unit area performed here was employed which, although time consuming, left less room for observer bias from the subjective nature of localising hotspots. In

addition, the plain vessel count would arguably reflect angiogenesis as well as vessel number.

The influence of the method used to measure vascularity was shown in a study of cervix tumours (298). Poorly vascularised tumours, when defined as having a long mean intercapillary distance, were more hypoxic (measured by the Eppendorf probe) and exhibited inferior local control. However, poorly vascularised tumours, when defined by a low vascular density, had superior local control and were not necessarily hypoxic. This might have been because tumours with fewer vessels may have had more effective vascular function leading to less hypoxia and therefore a better response to treatment.

The vessel to hypoxia distances

The median distance from vessel to pimonidazole staining was 100 microns. There was great variability with a few measurements as low as 8 and some over 200 microns. The figures need to be interpreted with some caution because the process of cutting and staining the tissue sections causes an element of shrinkage, which may artificially shorten the measurements. However, this shrinkage would affect each sample consistently. Considering the median distance only and the equation devised by Tomlinson and Gray (21) where the oxygen diffusion distance in microns could be described by:

$$\sqrt{\frac{4 \, x \text{ oxygen diffusion coefficient } x \text{ } pO_2 \text{ (mmHg)}}{\text{oxygen consumed /ml/ sec}}}$$

the threshold tissue pO_2 for staining is about 1% (10mmHg). This is subject to assumptions of oxygen diffusion and consumption, and serves as an approximation only. The range of measurements taken illustrates this huge variability.

The short, medium and long-range distances may represent different aspects of oxygen delivery to tumour tissue. The long distances are most likely to be regions in which vessels out of the plane of the tissue section contribute to the oxygenation of the cells between the vessel and pimonidazole stain in question. This may be from an entirely separate vessel or a different part of the same vessel being measured (figure 65 and 66).

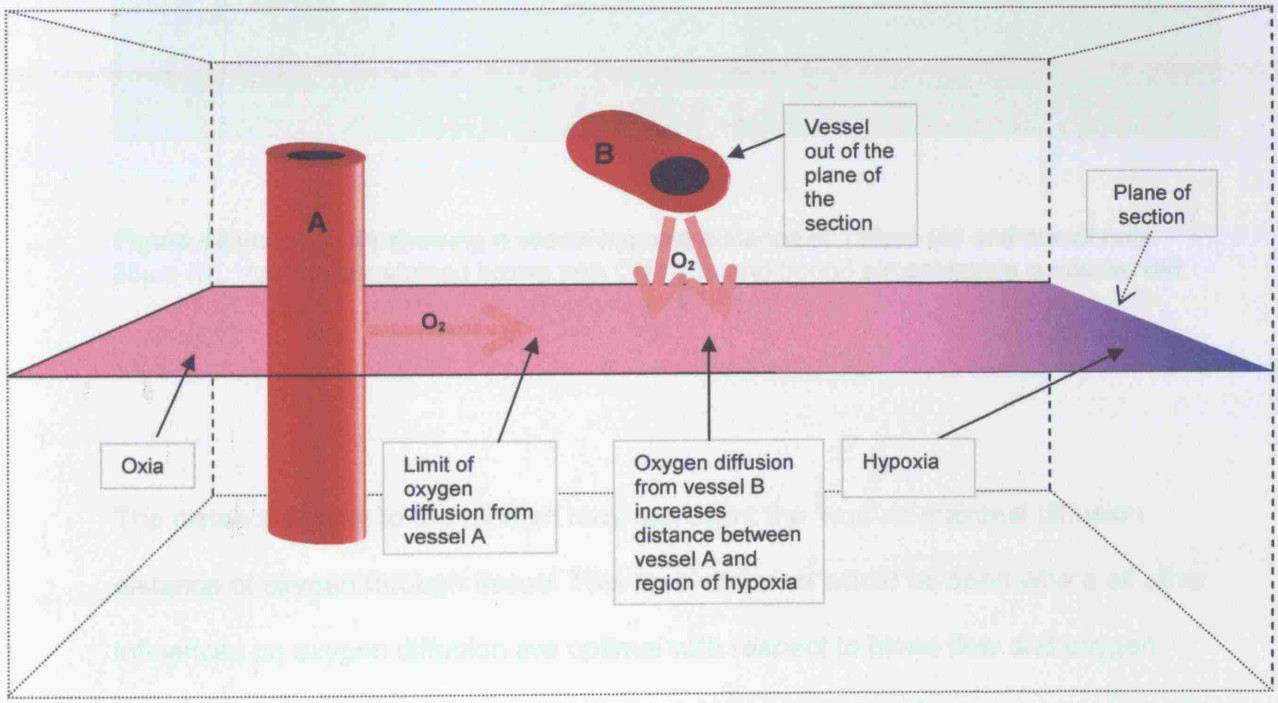

Figure 65 Schematic diagram explaining the finding of long vessel to hypoxia distances using the methods described.

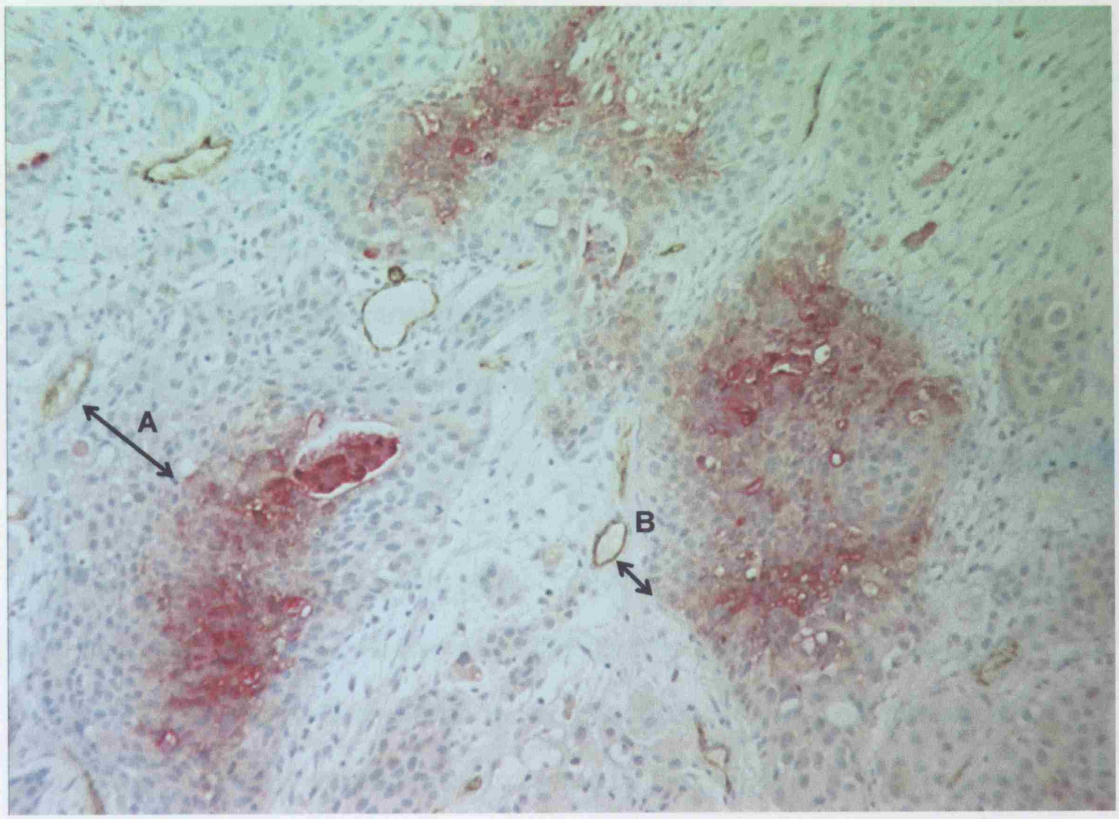

Figure 66 Image (x10) showing a vessel-hypoxia distance of 135μm (A) and one of only 35μm (B), Vessels are stained brown with CD31/34 and bound pimonidazole is stained red.

The distances close to the median may represent the 'true' or maximal diffusion distance of oxygen through tissue. This 'true' distance would be seen where all other influences on oxygen diffusion are optimal with respect to blood flow and oxygen concentration in the vessel in question. Variability in these mid range measurements may mirror the variability in these components of oxygen delivery. For example, the oxygen concentration along the length of a capillary would be greater at its arteriolar end than at its venous end; the oxygen diffusion distance would therefore vary according to where along the capillary the section cuts through. Dewhirst et al have

shown that such 'longitudinal' gradients, as opposed to 'perpendicular' gradients, exist in R3230AC mammary tumours (299). This may give rise to the majority of hypoxia seen in tumours.

There may also be variability in the oxygen consumption of the cells between the vessel and hypoxia stain. The proliferation marker sections examined showed that there was remarkably little variability in the proliferative index as a function of distance from the vessel, and the proliferation fell sharply only where hypoxia occurred.

Geometrical considerations would also account for some of the variability in these mid range measurements. According to the Tomlinson-Gray model of oxygen diffusion (21) tumour cells are arranged in cylindrical cords of oxygenated cells, centred on a perfused vessel and surrounded by hypoxic cells as the oxygen concentration falls further away from the vessel. If the section does not cut across the oxygenated cord perpendicularly, the measured distance from the vessel to hypoxia would be artifactually high (figure 67). Examples of how the section cuts through oxygenated tumour cord in different ways is shown in figure 68.

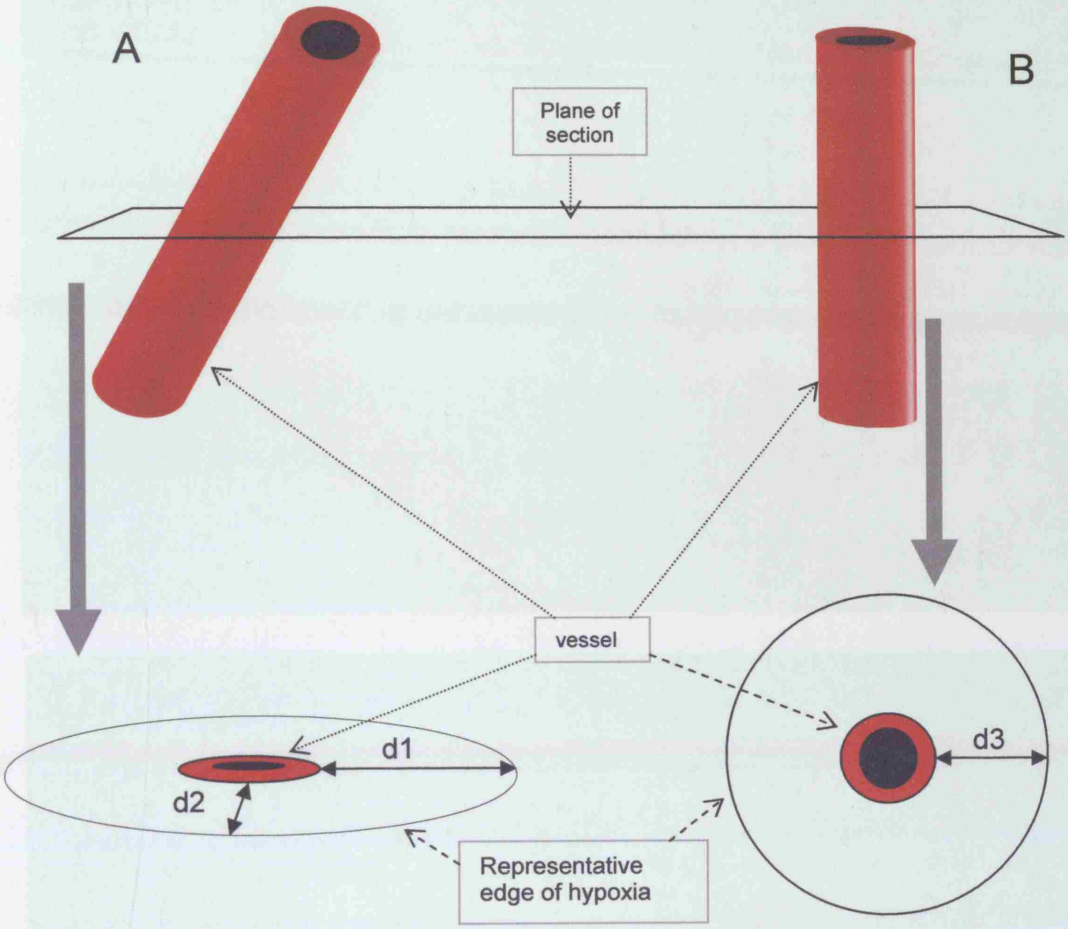

Figure 67 Figure illustrating variability in vessel to hypoxia distances due to the geometrical section through a vessel. Vessel A is not sectioned perpendicularly, leading to the measured distances being either longer (d1) or shorter (d2) than the 'true' vessel to hypoxia distance if the vessel is sectioned at the perfect perpendicular (vessel B, distance d3).

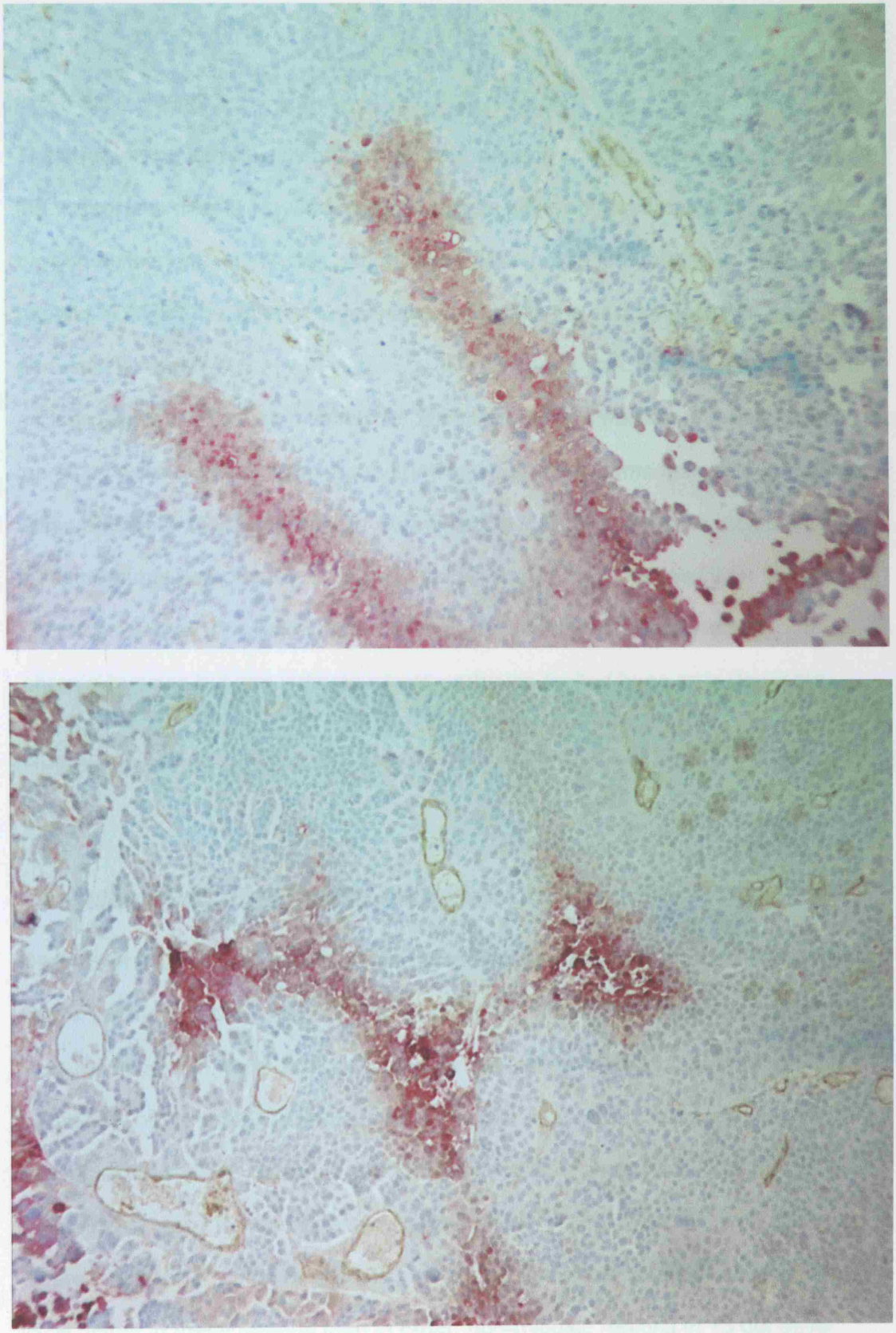

Figure 68 Upper image (x10) shows hypoxic distribution (red) and vessel pattern (brown) consistant with the section having been cut approximately along the axis of the vessel direction. The lower image (x10) shows hypoxic distribution and vessel pattern consistant with the section having been cut approximately across the axis of the vessel direction

The short-range diffusion distances indicate regions where the oxygen content of the vessel was clearly very low. These vessels were not functioning in terms of oxygen delivery, at least when pimonidazole was present in the tissue. These regions highlight the difference between the definitions of acute hypoxia and perfusion limited hypoxia, which are sometimes used interchangeably. All of these regions represent perfusion-limited hypoxia, but there is no way of telling for how long they were hypoxic. It has been shown in animal systems that oxygen tensions within and close to vessels can be chronically low (300), where microelectrode measurements demonstrated 25% of vessels had pO_2 values less than 1mmHg. Therefore, vessel to hypoxia distance cannot distinguish between 'acute' and 'chronic' hypoxia but can indicate where perfusion-limited hypoxia is dominant.

Vascular density related to hypoxia

Regions of hypoxia represent a failure of the vessel development and distribution or vessel function within a tissue's vascular system. It was hypothesised that the vascular density in these regions would be low, reflecting the presumed poor vascularity of the area. No vessels were seen in any section *within* any region of pimonidazole staining, consistent with this hypothesis although some vessels were present very close to hypoxia. However, when the vascular density was measured in an area *close* to a region of hypoxia counterintuitively, the vascular density tended to be higher in these regions than in other, non-hypoxic regions in 13 out of 19 tumours. The mixed results obtained are another reflection of the heterogeneity of the tumour microenvironment. In retrospect, this measure of vascular density was not in hypoxic regions per se, but possibly in regions under the influence of the

hypoxic cells nearby. The inter tumour variability may reflect the different stages or degrees of angiogenesis evolution in response to local hypoxia. Those hypoxic regions with a relatively low local vascular density may be early in their development, whereas those regions with a high local vascular density may have been hypoxic long enough for response to the angiogenic stimulus to be expressed. Alternatively, the oxic regions of the tumour may have been previously hypoxic, increased raised their vascularity and reduced the local hypoxia, therefore being comparable with the higher vascularity in hypoxic areas. A third possibility is that high vascular density, measured with the techniques employed here, may represent more tortuous, more 'chaotic' vasculature, which may be less efficient (or rather more inefficient) and thus give rise to local hypoxia (301). The most likely explanation is that all three processes occur to differing degrees. The nature of the technique has demonstrated just a snapshot of an evolving adaptive process.

Four other studies have explored the relationship between hypoxia and vascularity. The study by West et al (298), mentioned above, showed varying results according to the method of assessing vascularity, using the Eppendorf probe. Koukourides et al showed in a series of head and neck carcinomas that a high level of CA9 expression was associated with a low overall microvessel density. The hot spot method was used and the whole tumour section was assessed without separating hypoxic and oxic regions (302). The authors suggest that this indicated poor vascularity relates to tumour hypoxia. Beasley et al, however, found that a high CA9 expression was associated with a higher overall microvessel density, also in a series of head and neck carcinomas suggesting the hypoxic upregulation of angiogenic cytokines was demonstrated (217). Another study of non-small cell lung cancer biopsies looked at vascular density using the hot spot method in fields adjacent to hypoxia marked by CA9 compared to oxic fields (303). Here, there was a higher microvessel density in hypoxic regions, similar to results in the present study. The

data for individual tumours was not given. There was also no correlation between overall vascularity and CA9 expression. This emphasises the microregional nature of the influence of hypoxic cells and their upregulated cytokines, as seen in this study. The varying results across these studies show that there may be a number of processes continuing in parallel with additional non-hypoxic influences also affecting vascularity. However, there appears to be a definite influence of hypoxia on its local microenvironment. This may go some way to explain the worse prognosis of hypoxic tumours, with local vascular upregulation giving hypoxic cells a route to metastasise.

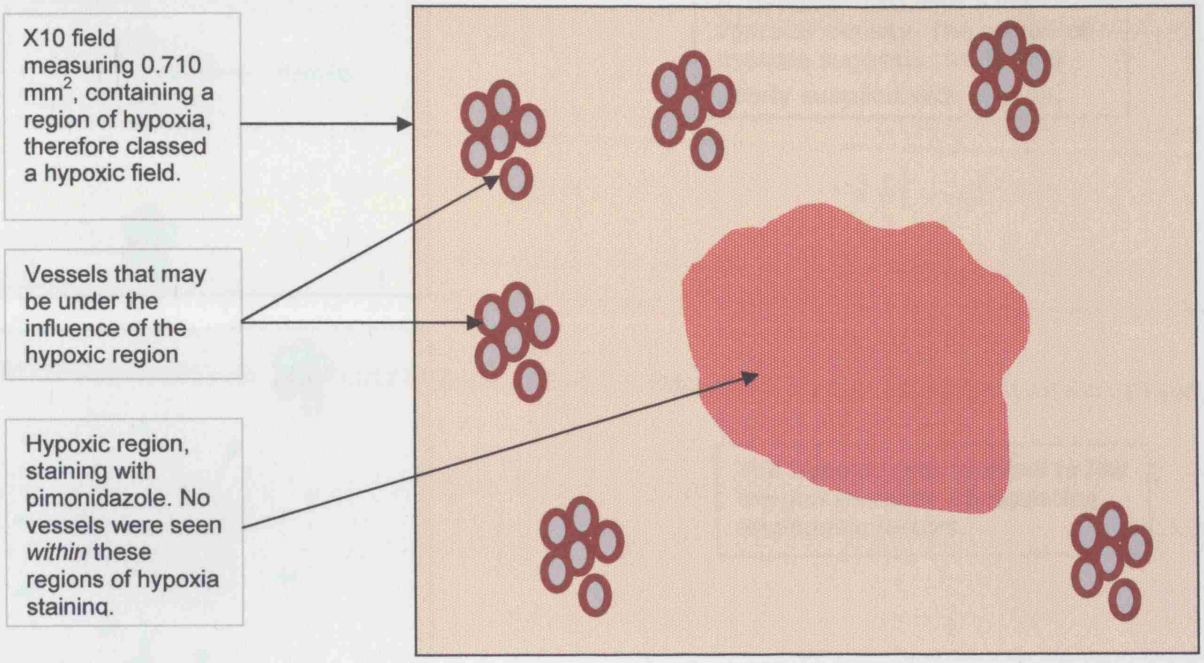

Figure 69 Schema of how fields were classified as hypoxic, and explanation of the spatial relationship between hypoxia and vessels.

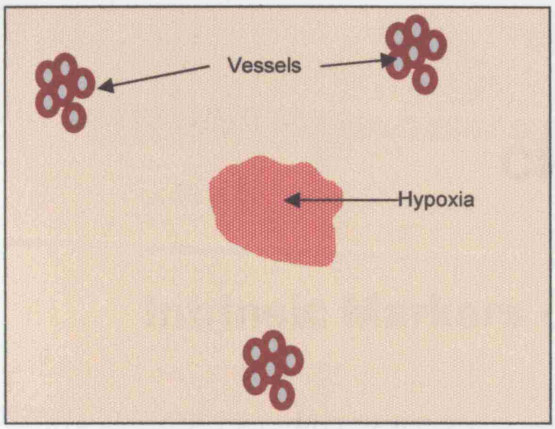

A 'hypoxic' field with a low vascular density. The region of hypoxia suggests this field is poorly supplied with oxygen.

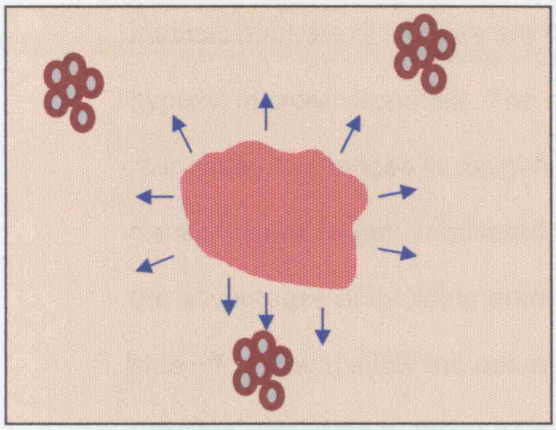

The hypoxic cells respond to low oxygen levels by upregulating angiogenic factors.

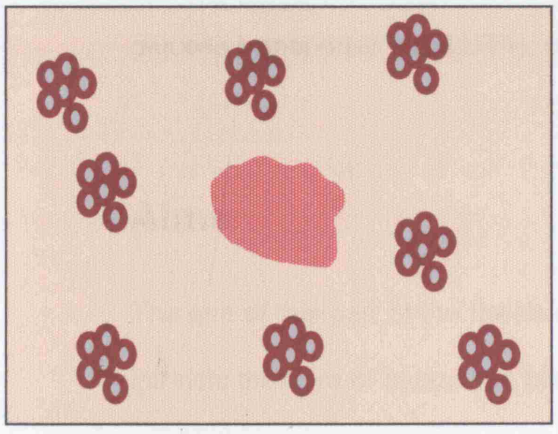

Angiogenesis occurs but although immature vessels are numerous, hypoxia still exists due to their poor functioning, giving rise to a region with high vascular density and hypoxia.

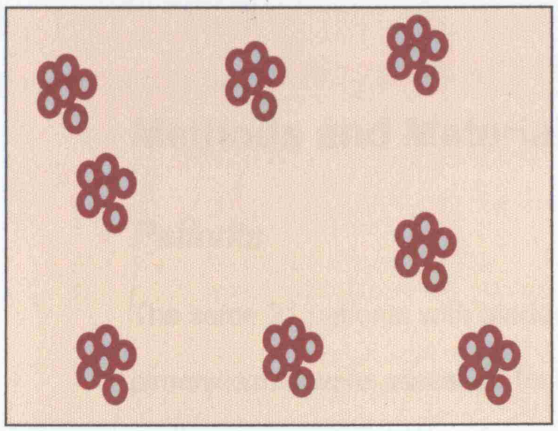

Vessels mature and improve in function, leaving a region with a high vascular density and no hypoxia.

Figure 70 Schematic diagram of the various stages of evolution of angiogenesis in response to hypoxia that may have been 'caught in the act' by the technique used in this study.

CHAPTER FIVE

Intrinsic Markers of Hypoxia in Bladder Cancer

Intrinsic markers of hypoxia are factors upregulated by cells in response to a hypoxic microenvironment. The recent increase in understanding of cellular responses to changes in oxygen levels and the identification of HIF with its transcriptional targets motivated the search for such intrinsic markers. They have the advantages of avoiding administration of an extrinsic marker, the associated side effects, and allow the assessment of hypoxia on archived material. Two possible candidate proteins have emerged - carbonic anhydrase 9 (CA9) and glucose transporter 1 (GLUT1), (see Chapter 1).

Aims

The aim of this part of the thesis was to assess the presence and extent of the intrinsic markers of hypoxia in bladder cancer and to perform a quantitative and qualitative comparison with the extrinsic marker of hypoxia, pimonidazole.

Methods and Materials

Patients

The same 21 patients with bladder carcinoma who had been injected with pimonidazole were assessed for GLUT1 and CA9. Serial sections were studied such that an indirect comparision could be made within the same patient.

Procedure

The tumour samples, representing a range of pimonidazole staining, were selected and serial sections were stained for GLUT1 and double stained for CA9 with CD31/34.

Immunohistochemical procedures

Staining for GLUT1

- Slides were de waxed in xylene for 5 minutes and rehydrated through graded alcohols (100,90, 70%) to water.
- Slides were transferred to 10mM citric acid pH6 and microwaved on high power for a total of 12 minutes. They were then left to stand for 10 minutes before being washed in running tap water
- The section was then encircled with resin using a resin pen to well in the solutions used in the rest of the staining process.
- Endogenous peroxidase activity was blocked with Dako peroxidase block (Envision kit) for five minutes at room temperature, then washed well in water and rinsed in tris buffer saline.
- Protein block (Dako X0909) was added and left for five minutes. The excess was tipped off.
- Anti GLUT1 antibody mixture was added left on the slide for one hour at room temperature, and washed off with tris buffered saline three times for a total of three minutes.
- Envision Horseradish peroxidase mouse polymer (Dako K4006) was added for 30 minutes and washed off with tris buffered saline three times for a total of three minutes.
- Diaminobenzine substrate was then added (Vector SK4100) for five minutes.

- The section was rinsed in tris buffer saline, then washed well in running tap water.
- To stain nuclei blue, the sections were placed in Gills Haematoxylin for between 10 to 60 seconds and then washed well in tap water.
- Finally the sections were dehydrated through graded alcohols, cleared by xylene and sections mounted in DPX (Merck 360294H) mounting media.

The resulting section shows nuclei as blue, and GLUT1 as brown (figure 71).

Double staining for CA9 and CD31/34

- Slides were de waxed in xylene for 5 minutes and rehydrated through graded alcohol (100, 90, 70%) to water.
- The section was then encircled with resin using a resin pen to well in the solutions used in the rest of the staining process.
- Endogenous peroxidase was blocked with Dako peroxidase block (Envision Kit) at room temperature for 5 minutes, then washed well in water.
- Protein block (Dako X0909) was added and left for five minutes. The excess was tipped off.
- Anti CA9 antibody mixture was added left on the slide for one hour at room temperature.
- The slide was then washed with tris buffered saline three times for a total of three minutes.
- Envision Horseradish peroxidase mouse polymer (Dako K4006) was applied for 30 minutes and washed off with tris buffered saline three times for a total of three minutes.
- Diaminobenzine substrate was then added (Vector SK4100) for five minutes.
- The section was rinsed in tris buffer saline, then washed in water

- Anti-CD31/CD34 antibody cocktail (Dako M0823/M7080) was applied diluted 1/50 and 1/60 respectively by tris buffer saline for 30 to 60 minutes, and then washed three times in tris buffer saline.
- Envision Alkaline Phosphatase mouse polymer (Dako K4017) was applied for 30 minutes and then washed three times in Tris buffer saline.
- Vector Alkaline Phosphatase red substrate (Vector SK5100) was applied for 5 to 10 minutes then rinsed in buffer and then washed well in running tap water.
- Sections were transferred to 10mM citric acid pH6 and microwaved on high for 12 minutes. Slides were left to stand for ten minutes, then washed well in running tap water and rinsed in tris buffer saline.
- To stain nuclei blue, the sections were placed in Gills Haematoxylin for between 10 to 60 seconds and then washed well in tap water.
- Finally the sections were dehydrated through graded alcohols, cleared by xylene and sections mounted in DPX (Merck 360294H) mounting media.

The resulting section shows nuclei as blue, CA9 bound cells as brown and blood vessels as red (figure 71).

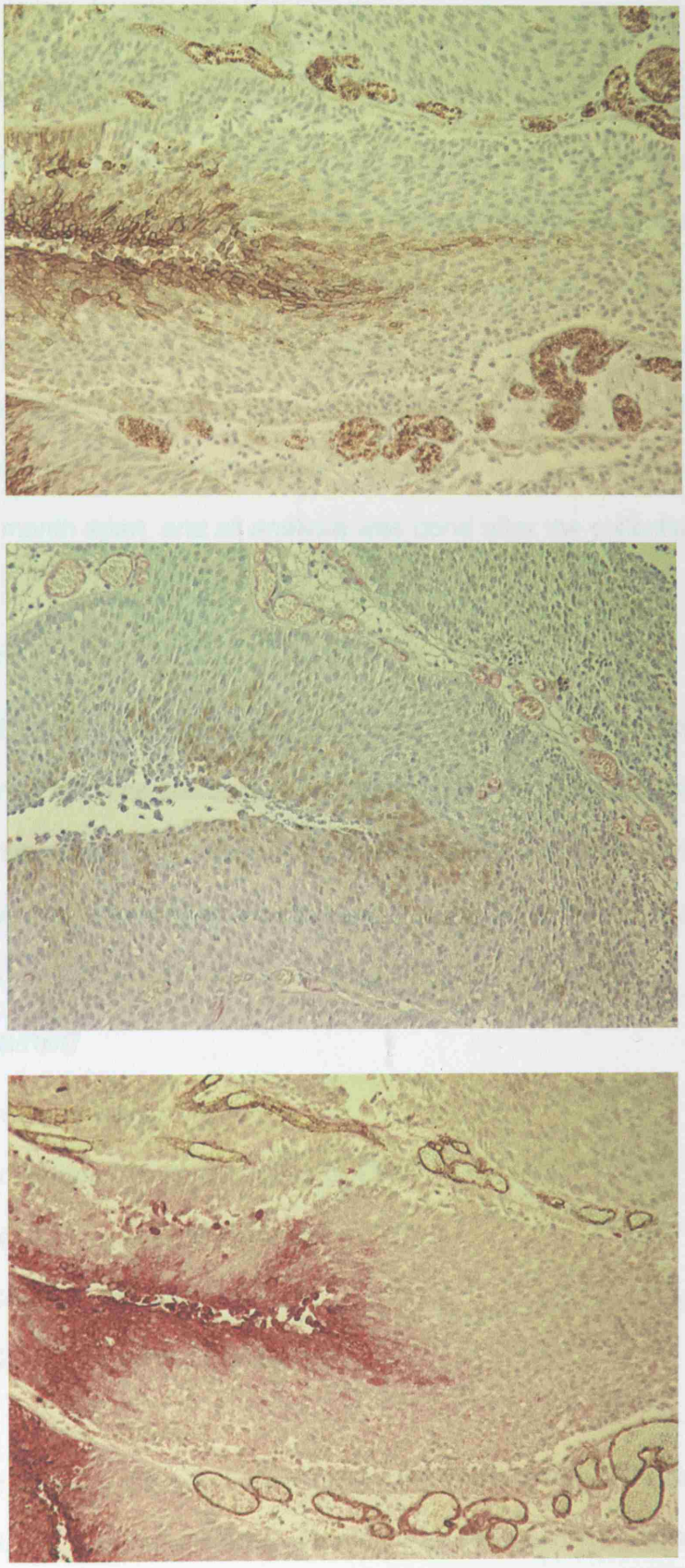

Figure 71 Three images showing images of the same region of bladder tumour stained for GLUT1 (top panel),CA9 with CD31/34 (middle panel) and pimonidazole with CD31/34 (lower panel), at x10 magnification

Image analysis

The set up and the procedure for the image analysis was the same as for the image analysis for pimonidazole stained sections (chapter 2). The area of the tumour section staining for GLUT1 was assessed for all the tumour samples and then repeated for CA9 to avoid bias. The distance from a vessel to CA9 and vessel to GLUT1 was measured using the same method as that for the vessel to pimonidazole stain distance described in chapter 3. Each series of sections was reviewed a month apart, and all analysis was done after the collection of raw data to avoid bias.

Statistics

The stained fractions of GLUT1 and CA9 were compared with that of pimonidazole by calculating Pearsons correlation coefficient, where $p<0.05$ was considered statistically significant. The vessel to CA9 and GLUT1 distance was compared with that of the vessel to pimonidazole stain using a 2 sided, unpaired Students t-test, and $p<0.05$ was considered statistically significant.

Data obtained

The following data were obtained:

Proportion of tumour section staining for CA9

Proportion of tumour section staining for GLUT1

Vessel to CA9 staining distance

Vessel to GLUT1 staining distance

The degree of co-localisation between the CA9 and pimonidazole staining and between GLUT1 and pimonidazole staining was assessed subjectively. For example in figure 71 the co-localisation was judged to be high because matching regions stained to some degree with all three stains.

Results

Comparison of stained fractions of GLUT1 and CA9

The median stained fraction of tumour stained for GLUT1 was 15%, range 0 to 45%. The median stained fraction of tumour stained for CA9 was 12%, range 0 to 35% (figures 72 and 73). This compares to a median stained fraction for pimonidazole in the same sections of 9%, range 0 to 38%.

The correlation coefficients comparing the stained fraction for each of the stains are shown in figure 74 and 75. Both markers were significantly correlated with pimonidazole.

The difference between staining proportions for each marker in each tumour section is shown in figures 76 to 78.

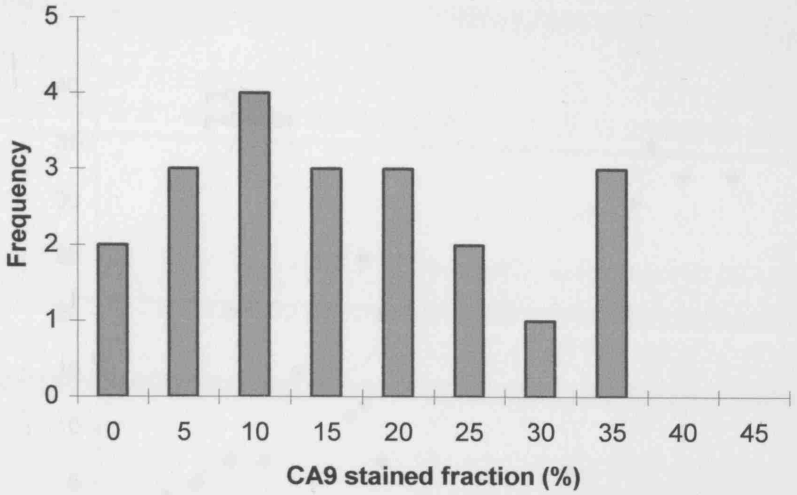

Figure 72 Histogram of CA9 stained fractions

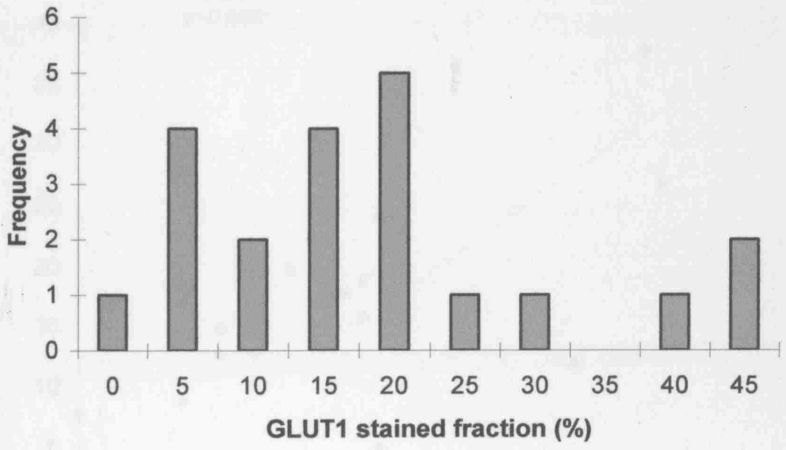

Figure 73 Histogram of GLUT1 stained fractions

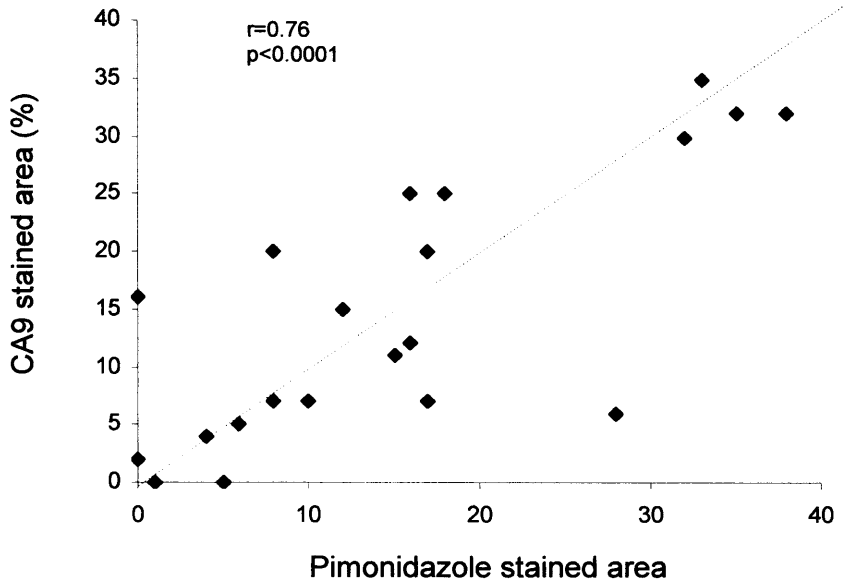

Figure 74 Plot of Carbonic Anhydrase 9 stained area against pimonidazole stained area for each tumour. The dotted line indicates the line of equity, showing most tumours have more pimonidazole staining than CA9 staining.

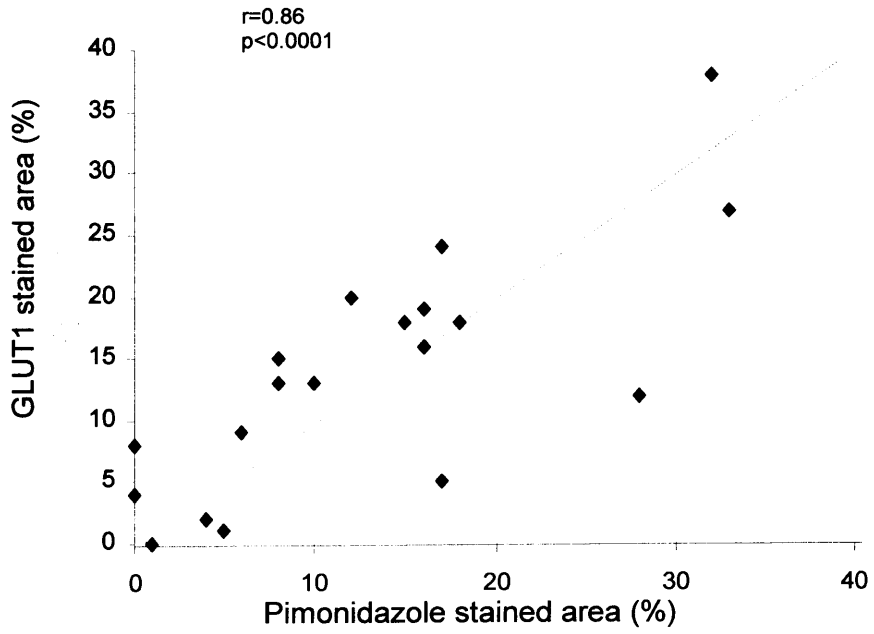

Figure 75 Plot of GLUT1 stained area against pimonidazole stained area for each tumour. The dotted line indicates the line of equity, showing most tumours with more GLUT1 staining than pimonidazole staining.

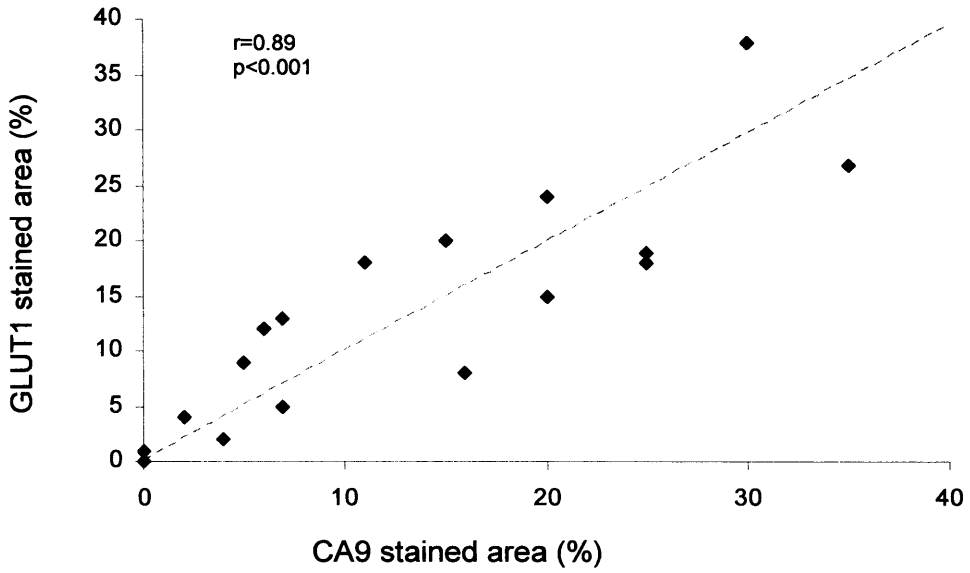

Figure 76 Plot of GLUT1 stained area against CA9 stained area for each tumour. The dotted line indicates the line of equity.

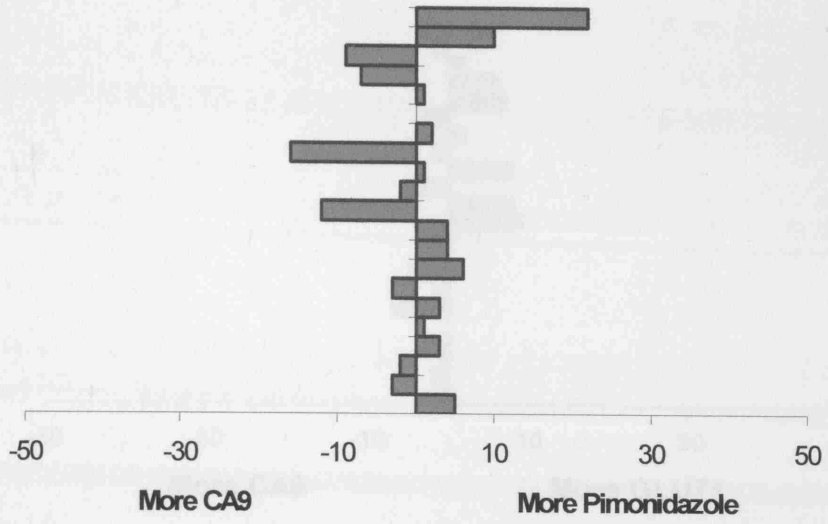

Figure 76 The absolute percentage difference between the area of pimonidazole staining and CA9 staining for each tumour, 1 to 21.

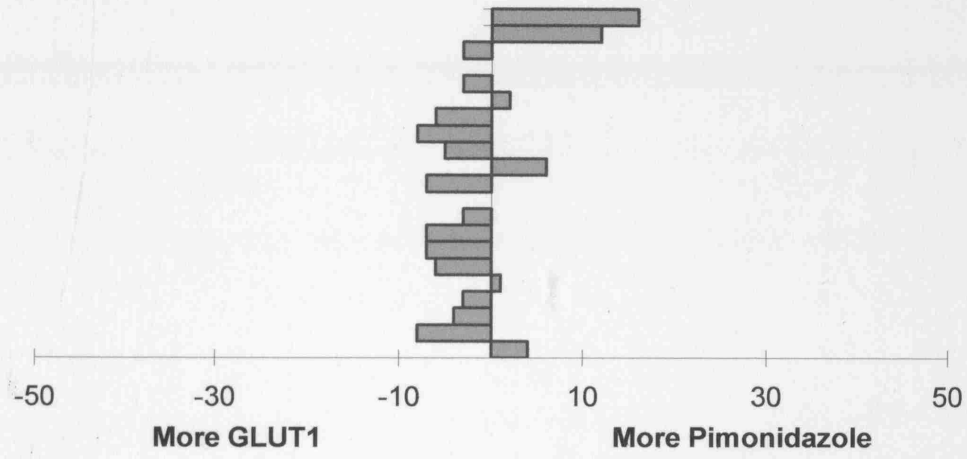

Figure 77 The absolute percentage difference between the area of pimonidazole staining and GLUT1 staining for each tumour, 1 to 21

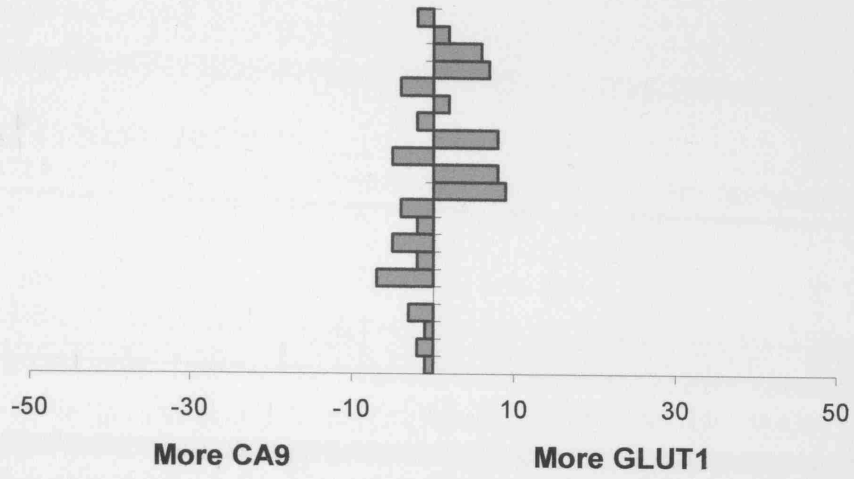

Figure 78 The absolute percentage difference between the area of CA9 staining and GLUT1 staining for each tumour 1 to 21.

Vessel to stain distance

Table 15 and figure 79 show the median and range of the vessel to stain distances for each individual tumour. The coefficient of variation for the vessel to stain distances is shown in table 16. This varied between 1.78 to 4.50 for pimonidazole, 2.95 to 11.24 for CA9 and 3.03 to 9.23 for GLUT1. The median vessel to CA9 distances were significantly different to that of the vessel to pimonidazole distances in 5 of 19 tumours and for GLUT1 in 8 of 19 tumours (table17). Histograms of the pooled distances are shown in figures 81 and 82.

When data are pooled, the mean distances for CA9 and GLUT1 are 110μm and 84μm respectively. The differences between these and that of the vessel to pimonidazole distances (100μm) are statistically significant ($p < 0.0001$ and $p < 0.0001$ respectively, figures 83 and 84).

Patient	Stained Fraction (%)			Number of measurements			Median distance (range) in μm		
	PIMO	*CA9*	*GLUT1*	*PIMO*	*CA9*	*GLUT1*	*PIMO*	*CA9*	*GLUT1*
1	5	0	1	14	0	6	108.5 (62 - 182)	-	98.5 (68- 109)
2	12	15	20	33	29	33	105 (26 - 181)	109 (61 - 178)	95 (41 - 179)
3	0	2	4	0	7	12	-	99 (89 -114)	91 (68 - 110)
4	10	7	13	34	22	25	94.5 (31- 188)	92 (52 - 156)	68 (49 - 129)
5	1	0	0	3	0	0	76 (53 - 83)	-	-
6	35	32	41	88	94	80	103 (30 - 185)	113 (29 - 193)	90.5 (18 - 161)
7	17	20	24	58	72	66	101 (38 - 174)	112 (58 - 198)	84 (18 -166)
8	38	32	45	19	24	28	105 (53 - 157)	124.5 (59 - 159)	85 (33 - 126)
9	15	11	18	12	12	12	49.5 (41 - 83)	100 (80- 128)	82 (59 - 107)
10	5	0	1	26	0	5	131.5 (25 - 177)	-	95 (75 - 100)
11	8	20	15	11	23	33	73 (30 - 141)	112 (80- 180)	71 (25 - 99)
12	33	35	27	88	50	45	93 (11 - 190)	111.5 (32 - 181)	73 (19 - 99)
13	8	7	13	16	17	19	76 (20 - 175)	106 (79 - 170)	75 (66 - 99)
14	0	16	8	0	32	20	-	106 (62 - 130)	75 (32 - 107)
15	32	30	38	34	38	42	84.5 (22 - 181)	102 (61 -188)	88 (55 - 124)
16	4	4	2	29	28	19	98 (31 -161)	106.5 (65 - 153)	84.5 (48 - 127)
17	6	5	9	25	7	13	77 (25 - 165)	99 (95 - 154)	79 (65 - 138)
18	18	25	18	31	28	28	97 (24 -169)	106.5 (57 - 196)	80 (33 - 104)
19	16	25	19	25	33	40	102 (69 - 181)	113 (83 - 188)	100 (50 - 161)
20	17	7	5	88	38	25	111.5 (14 - 231)	114(85 - 144)	88 (20 - 117)
21	28	6	12	11	9	7	83 (51 - 98)	103 (92 - 118)	69.5 (59 - 88)

Table 15 The stained fractions, the number of distance measurements taken and the median and range of vessel to stain distances. Blank cells are where no hypoxic stain was present.

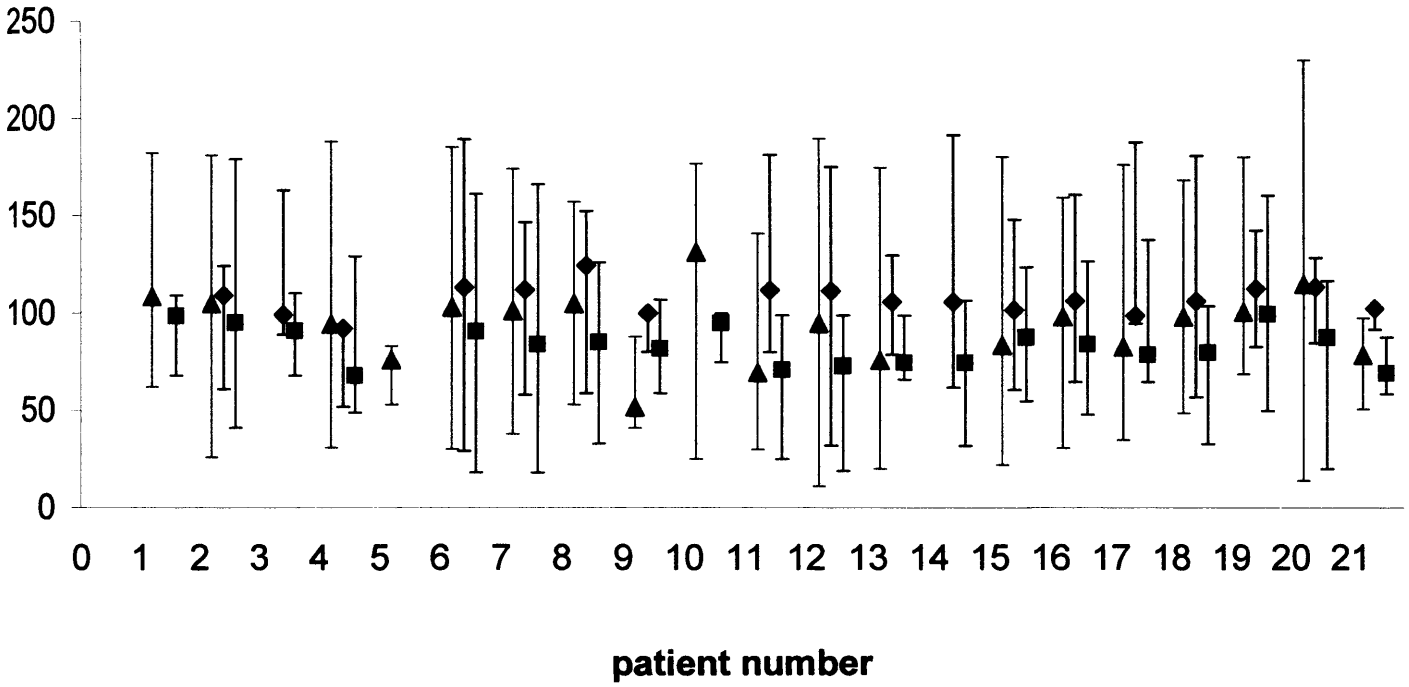

Figure 79 Plot of the median vessel to stain distances in μm (x-axis) for pimonidazole (green triangles), CA9 (blue diamonds) and GLUT1 (pink squares). The error bars indicate the range of distances for each tumour.

	PIMONIDAZOLE			CA9			GLUT1		
Patient	*Standard Deviation*	*Mean distance*	*Coefficient of variantion*	*Standard Deviation*	*Mean distance*	*Coefficient of variantion*	*Standard Deviation*	*Mean distance*	*Coefficient of variantion*
1	72	110	3.76	-	-	-	51	93	5.78
2	70	105	2.68	66	114	4.63	65	97	3.19
3	-	-	-	9	101	11.24	14	89	6.55
4	70	96	2.50	60	100	2.95	46	77	3.36
5	38	71	4.50	-	-	-	-	-	-
6	65	107	3.34	67	116	3.56	55	95	3.26
7	63	101	2.85	64	116	4.35	60	86	3.03
8	57	107	3.31	59	118	4.33	42	84	3.59
9	31	58	3.65	53	102	6.79	41	83	4.58
10	45	117	2.58	0	-	-	10	91	9.23
11	52	86	2.15	67	118	4.96	35	71	4.00
12	69	95	2.46	64	113	3.17	33	72	3.99
13	66	88	1.78	67	110	4.22	37	77	8.55
14	-	-	-	48	100	4.88	41	73	3.47
15	63	86	1.98	65	112	3.46	36	89	5.29
16	60	101	3.47	60	107	5.75	51	87	4.18
17	64	101	2.33	65	110	5.19	53	89	3.55
18	60	104	3.11	71	113	3.54	37	79	5.15
19	65	111	3.64	66	121	4.16	57	104	4.16
20	85	119	2.51	56	113	9.23	49	86	3.11
21	35	77	4.41	54	105	10.89	36	74	6.97

Table 16 The mean, standard deviation, and coefficient of variation for the vessel to stain distances in each tumour. Blank cells are where no hypoxic stain was present.

	Pimonidazole			CA9				GLUT1			
Patient	Mean	95%confidence intervals		Mean	95%confidence intervals		p-value (cf pimo)	Mean	95%confidence intervals		p-value (cf pimo)
1	110	125	95	-	-	-	-	93	115	70	0.1839
2	105	116	92	114	126	101	0.2662	97	109	84	0.3592
3	-	-	-	101	110	93		89	98	93	-
4	96	107	85	100	114	83	0.6890	77	91	64	0.0424
5	71	114	27	-	-	-	-	-	-	-	-
6	107	114	100	116	122	109	0.0719	95	101	88	0.0070
7	101	109	92	116	123	109	0.0054	86	93	78	0.0090
8	107	120	92	118	130	106	0.2080	84	94	74	0.0092
9	58	67	49	102	111	93	0.0000	83	94	73	0.0015
10	117	134	100	-	-	-	-	91	129	52	0.2100
11	86	101	70	118	131	105	0.0889	71	80	62	0.0942
12	95	103	87	113	123	102	0.0092	72	77	66	0.0002
13	88	105	70	110	129	90	0.1120	77	92	61	0.3572
14	-	-	-	100	117	83	-	73	91	55	-
15	86	97	75	112	124	99	0.0061	89	99	80	0.6628
16	101	110	91	107	116	97	0.3500	87	99	75	0.0811
17	101	117	84	110	141	80	0.5741	89	110	67	0.3761
18	104	115	92	113	125	100	0.2700	79	88	68	0.0005
19	111	122	99	121	131	110	0.2006	104	112	95	0.3027
20	119	127	108	113	110	117	0.4686	86	103	68	0.0013
21	77	87	67	105	115	95	0.0005	74	86	61	0.6284

Table 17 Table showing the mean vessel to stain distances for each tumour, with 95% confidence intervals, and p values from homoscedastic unpaired students t-test comparing CA9 and GLUT1 each with pimonidazole. Blank cells are where no hypoxic stain was present.

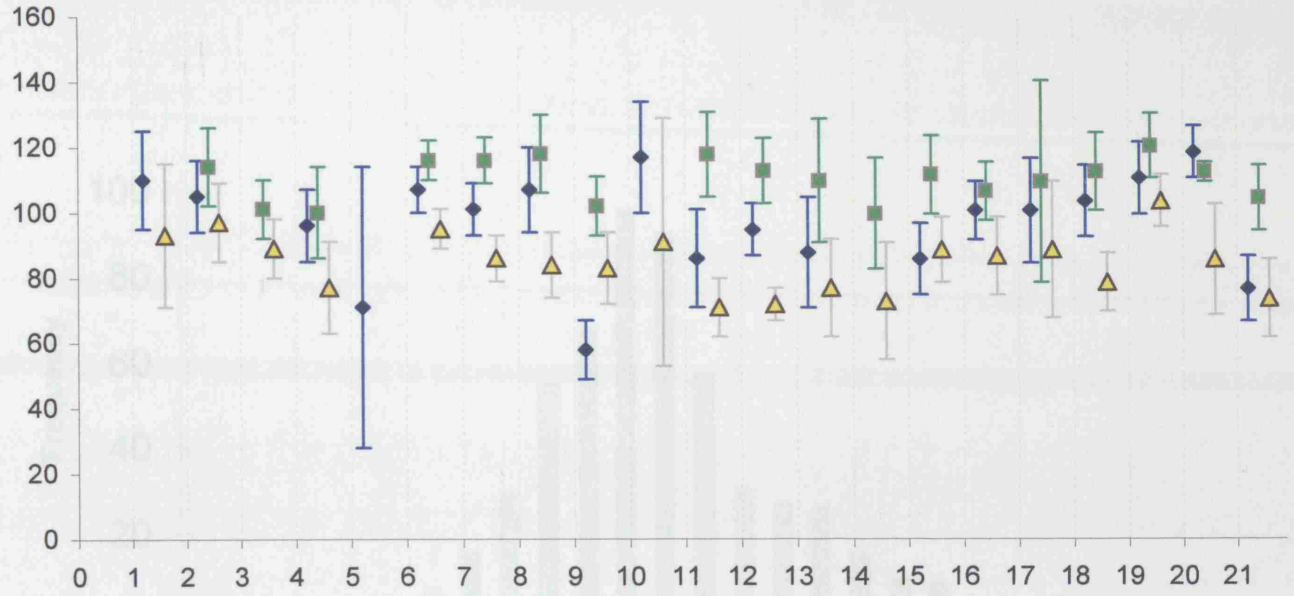

Figure 80 Plot of the mean vessel to stain distances in μm (x-axis) for pimonidazole (blue diamonds), CA9 (green squares) and GLUT1 (yellow triangles). The error bars indicate the 95% confidence intervals.

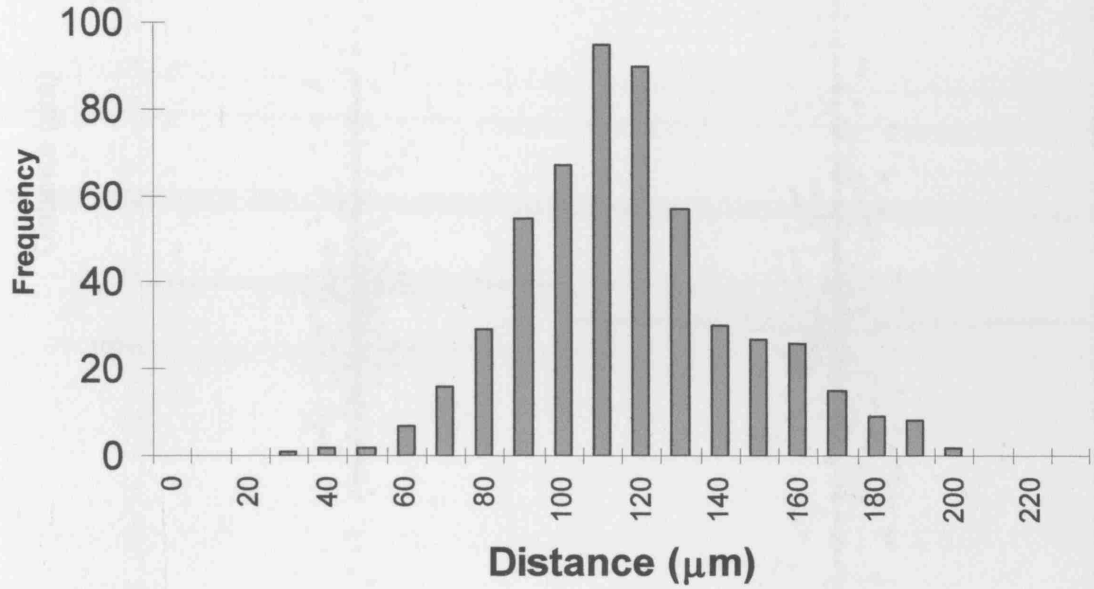

Figure 81 Histogram of vessel to CA9 stain distances

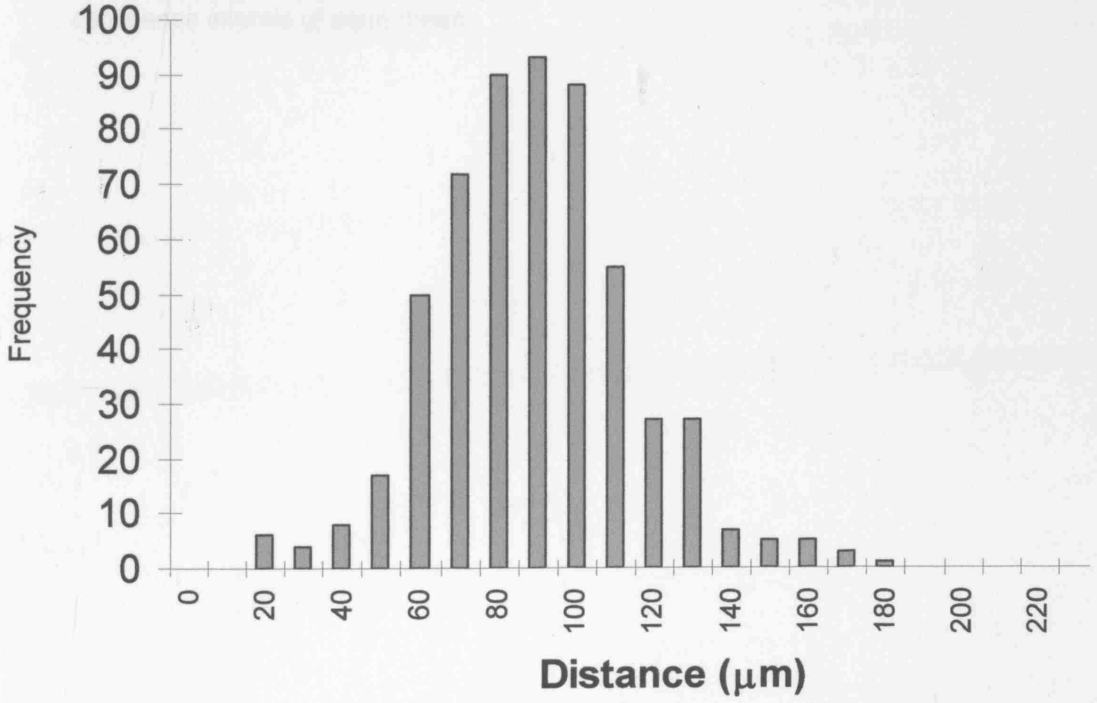

Figure 82 Histogram of vessel to GLUT1 stain distances

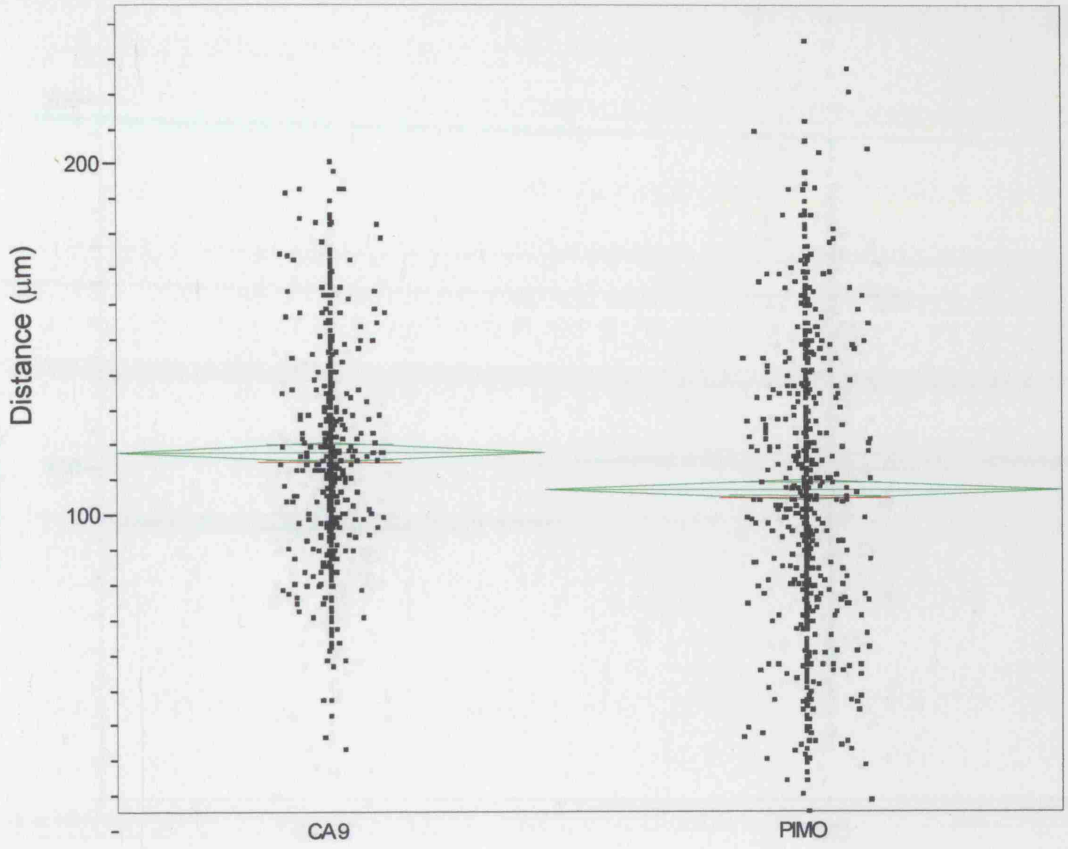

Figure 83 Comparison of vessel to pimonidazole and vessel to CA9 distances pooled for all tumours: red lines indicate the median. Green diamonds indicate the means and the 95% confidence interals of each mean.

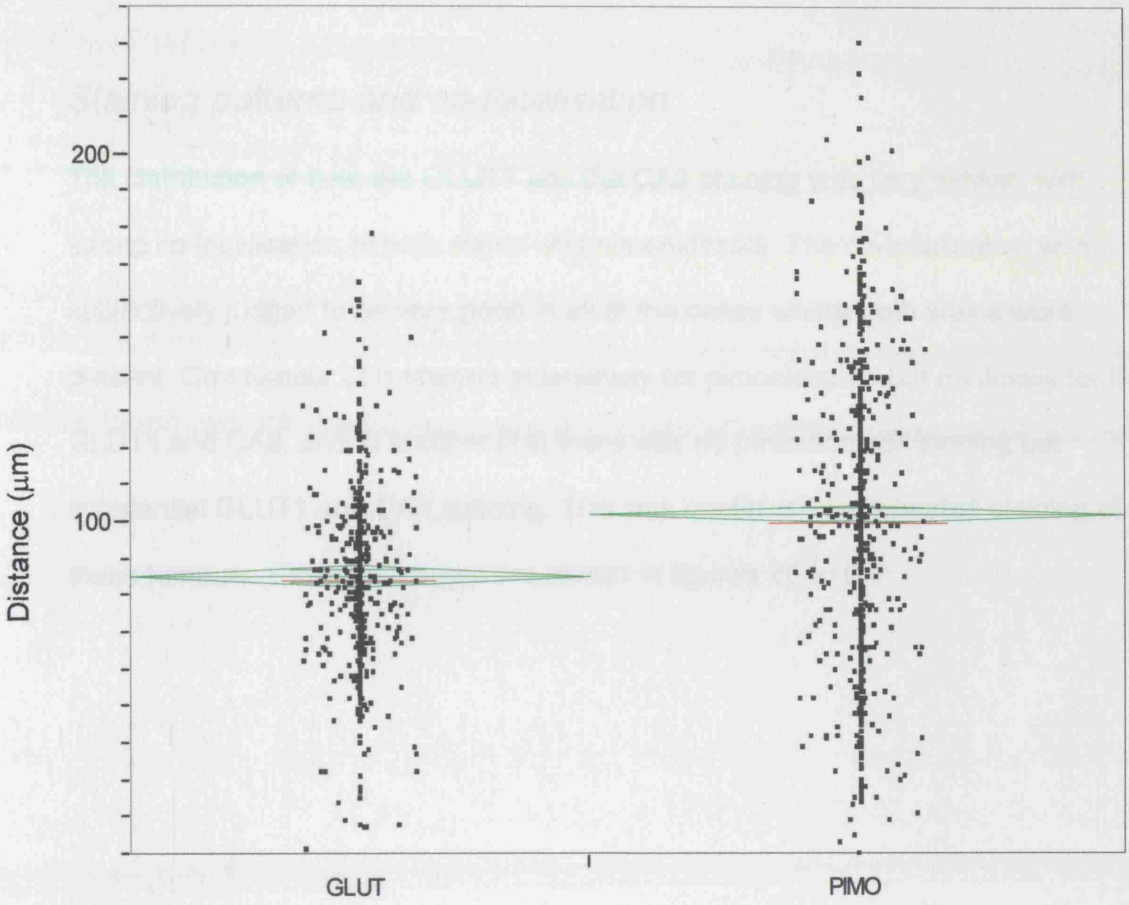

Figure 84 Comparison of vessel to pimonidazole and vessel to GLUT1 distances pooled for all tumours: red lines show the median. Green diamonds indicate the means and the 95% confidence interals of each mean.

Staining patterns and co-localisation.

The distribution of both the GLUT1 and the CA9 staining was very similar, with strong co-localisation of both stains with pimonidazole. The co-localisation was subjectively judged to be very good in all of the cases where both stains were present. One tumour (21) stained extensively for pimonidazole but minimally for both GLUT1 and CA9, and in another (14) there was no pimonidazole binding but substantial GLUT1 and CA9 staining. This was confirmed on repeated staining of these tumours. Example images are shown in figures 85 to 90.

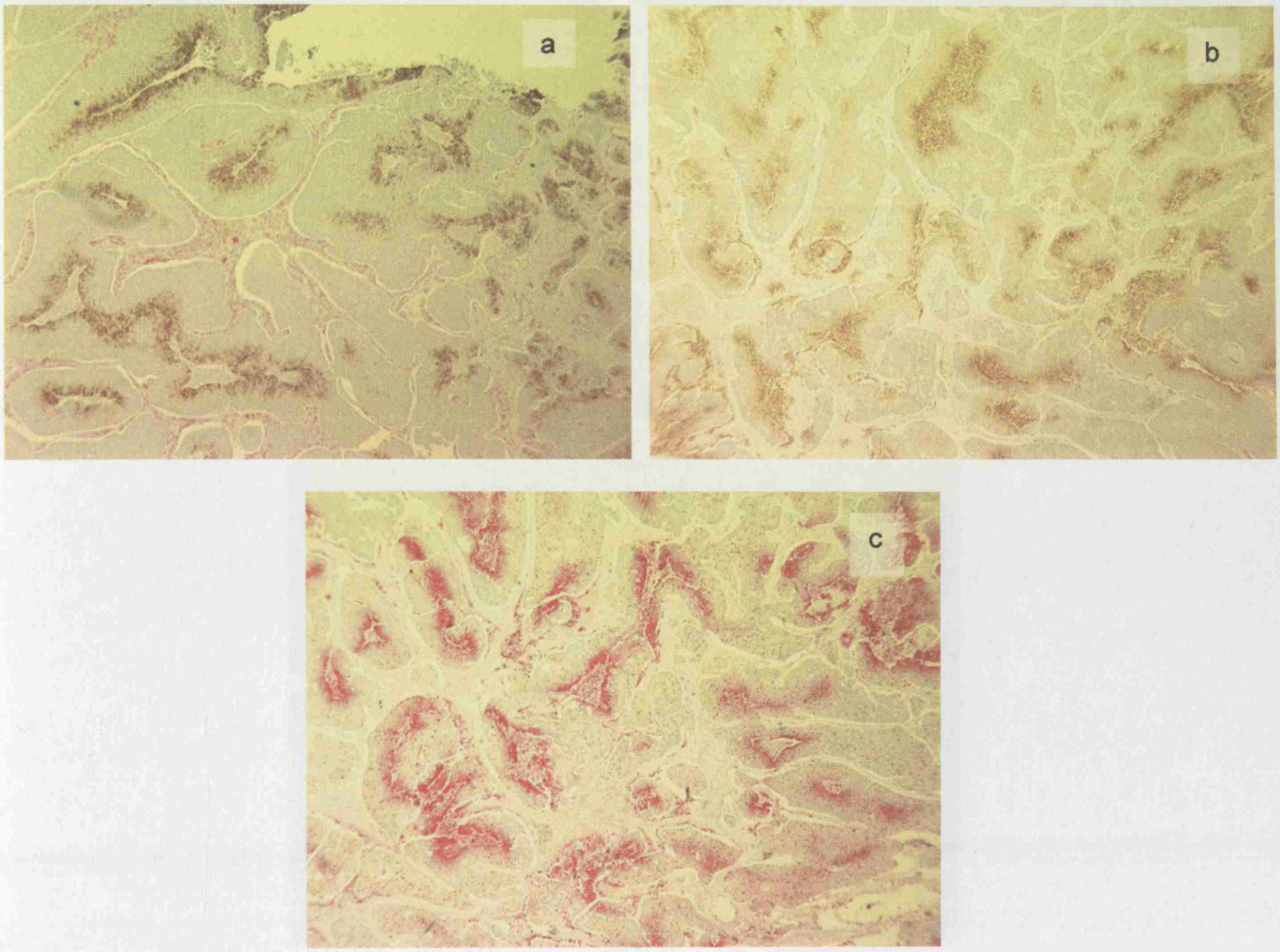

Figure 85 Example of a field at low magnification with good overall co-localisation of each stain for hypoxia (Panel a is of CA9 , panel b is of GLUT1 and panel c is pimonidazole)

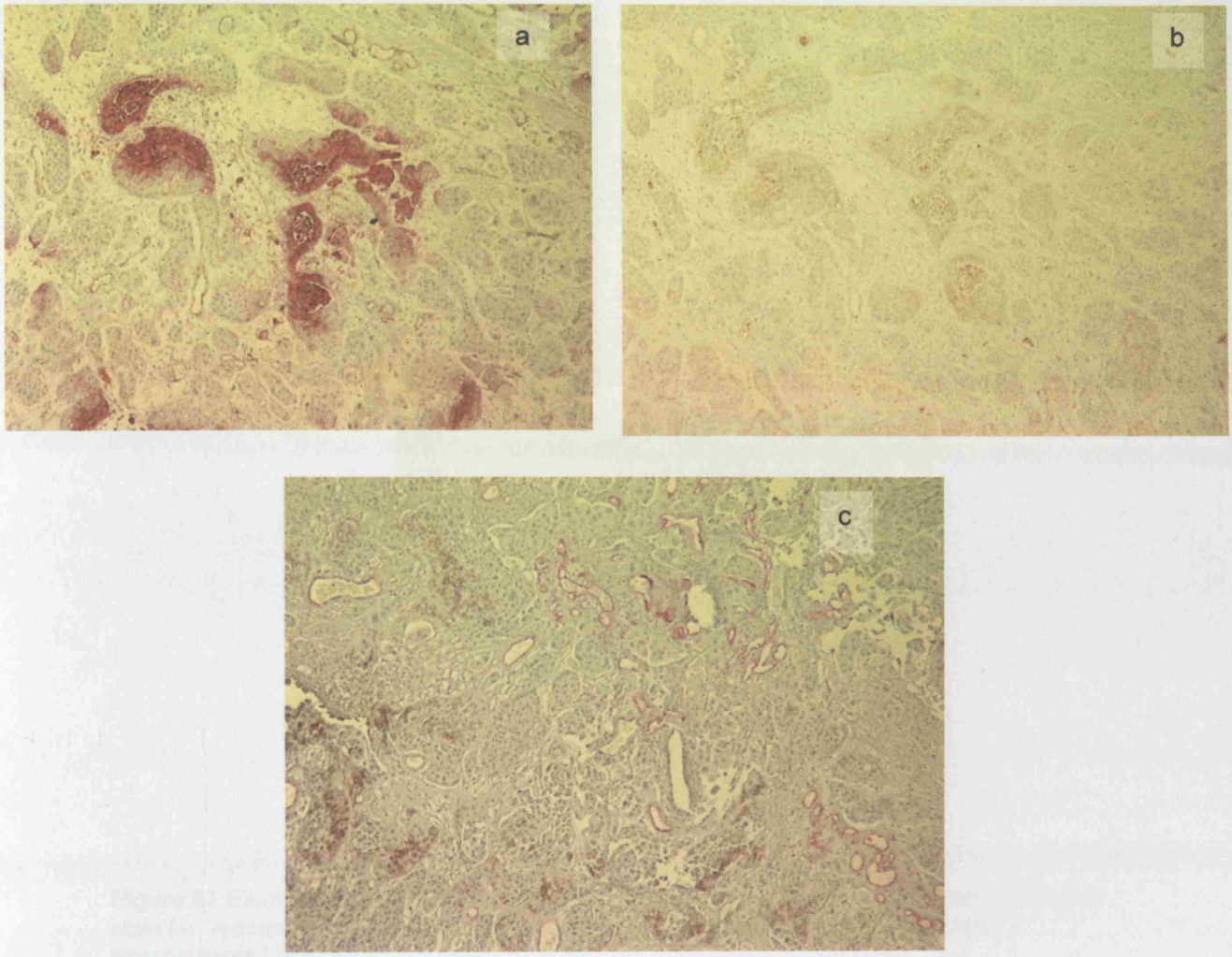

Figure 86 Example of more extensive staining for pimonidazole (a) and relatively little staining for GLUT1 (b) and CA9 (c)

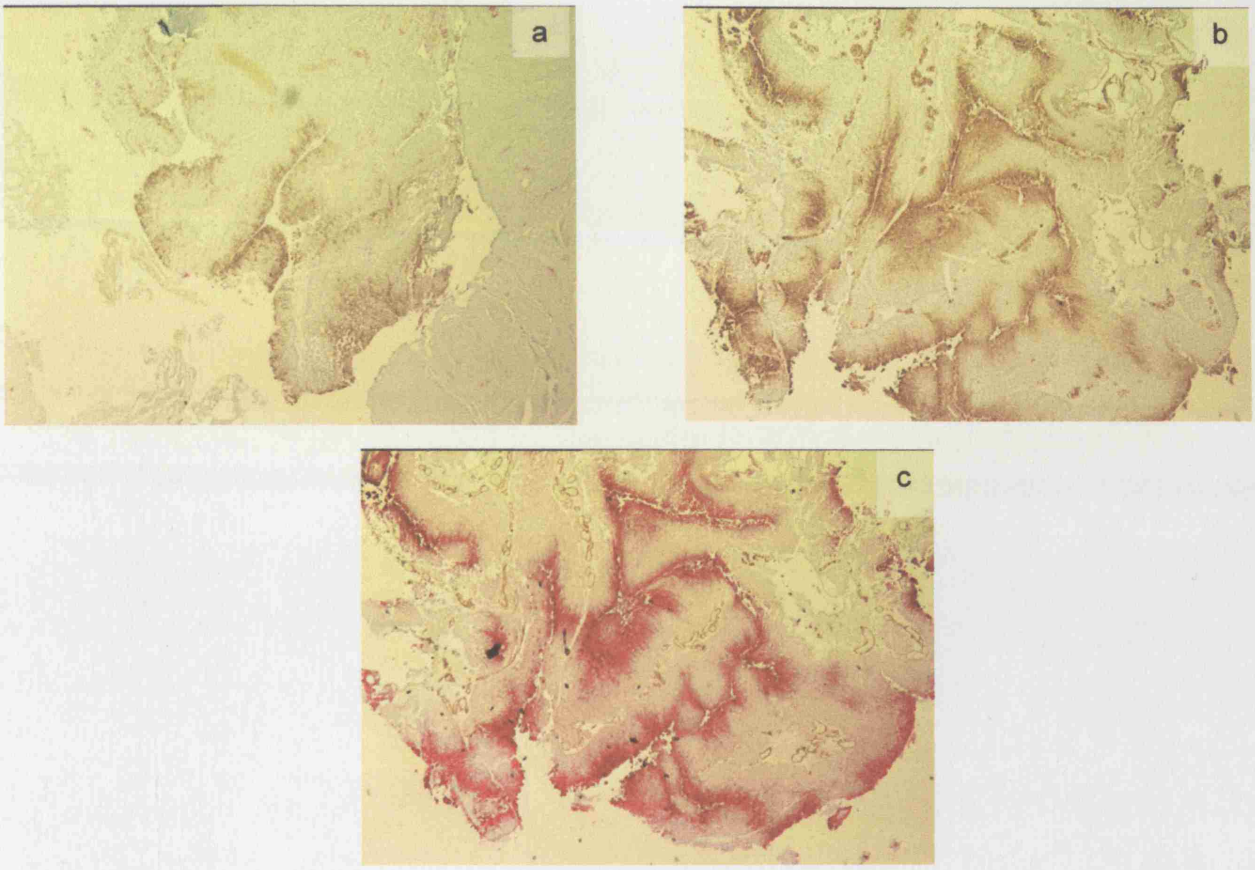

Figure 87 Example of a field at low magnification with good overall co-localisation of each stain for hypoxia but less extensive CA9 (a) stain compared with GLUT1 (b) and pimonidazole (c).

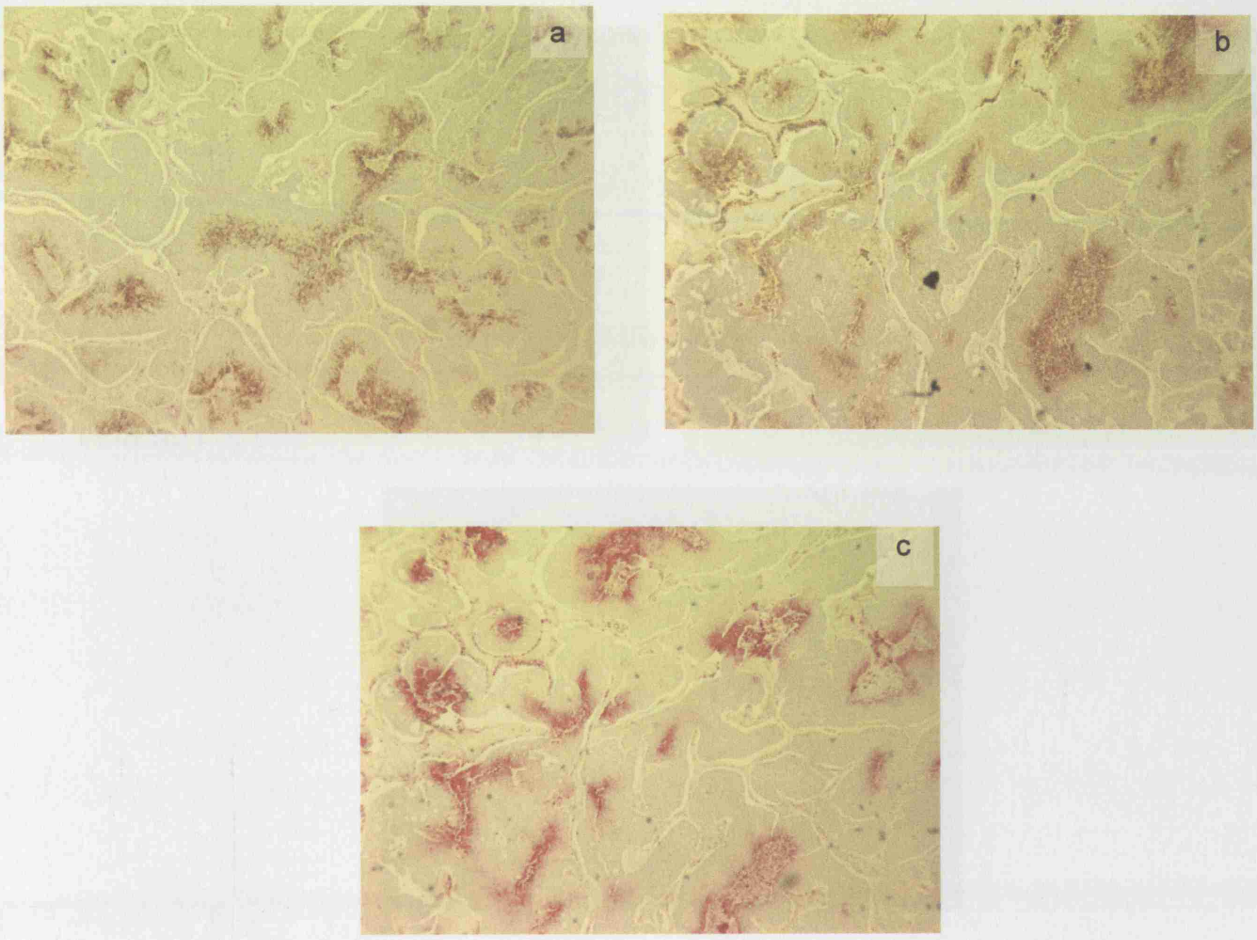

Figure 88 Example of a field at low magnification with moderate overall co-localisation of each stain for hypoxia, but with similar stained fraction for each marker. Panel a is of CA9 , panel b is of GLUT1 and panel c is pimonidazole.

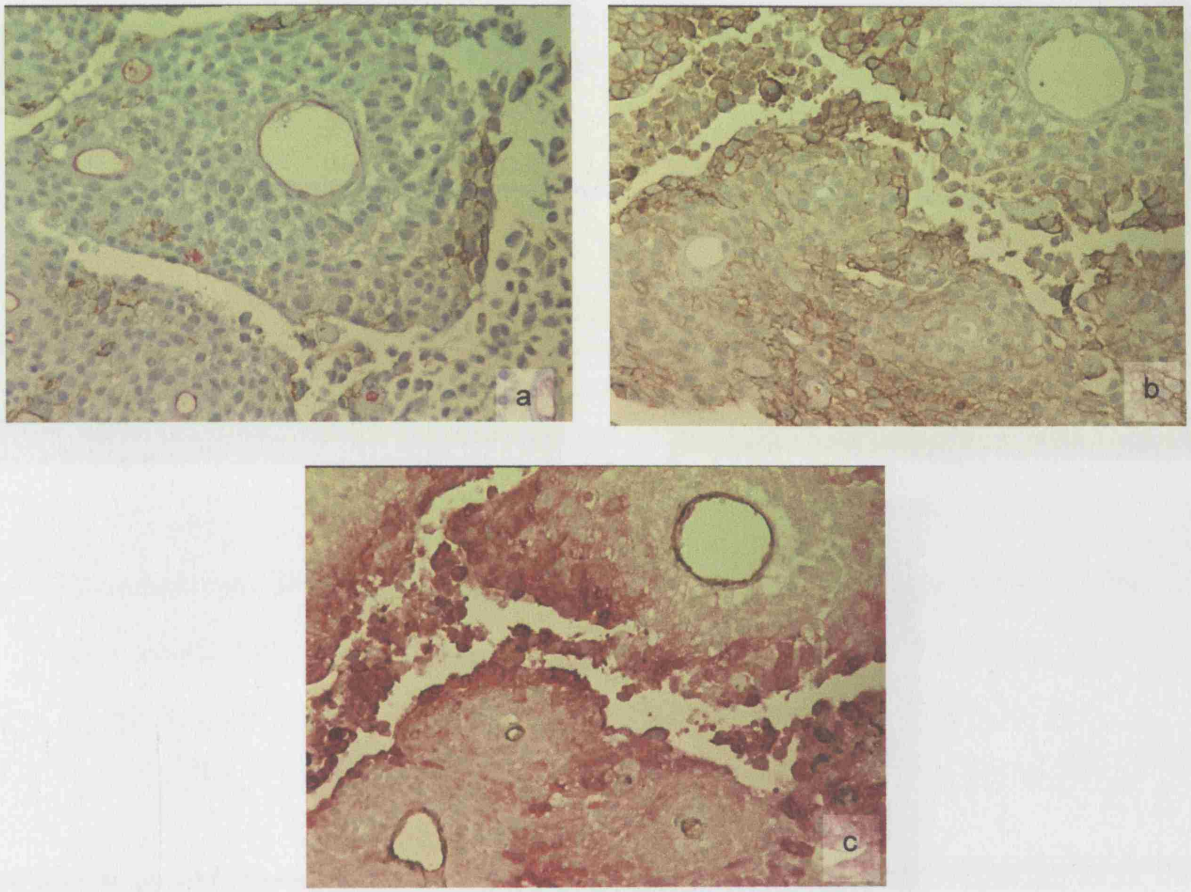

Figure 89 An example of a field at high magnification (x20) with good co-localisation of each stain for hypoxia, with a lesser degree of CA9 staining (a) compared with that of GLUT1 (b) and pimonidazole (c). The difference in the vessel to stain distances are also evident.

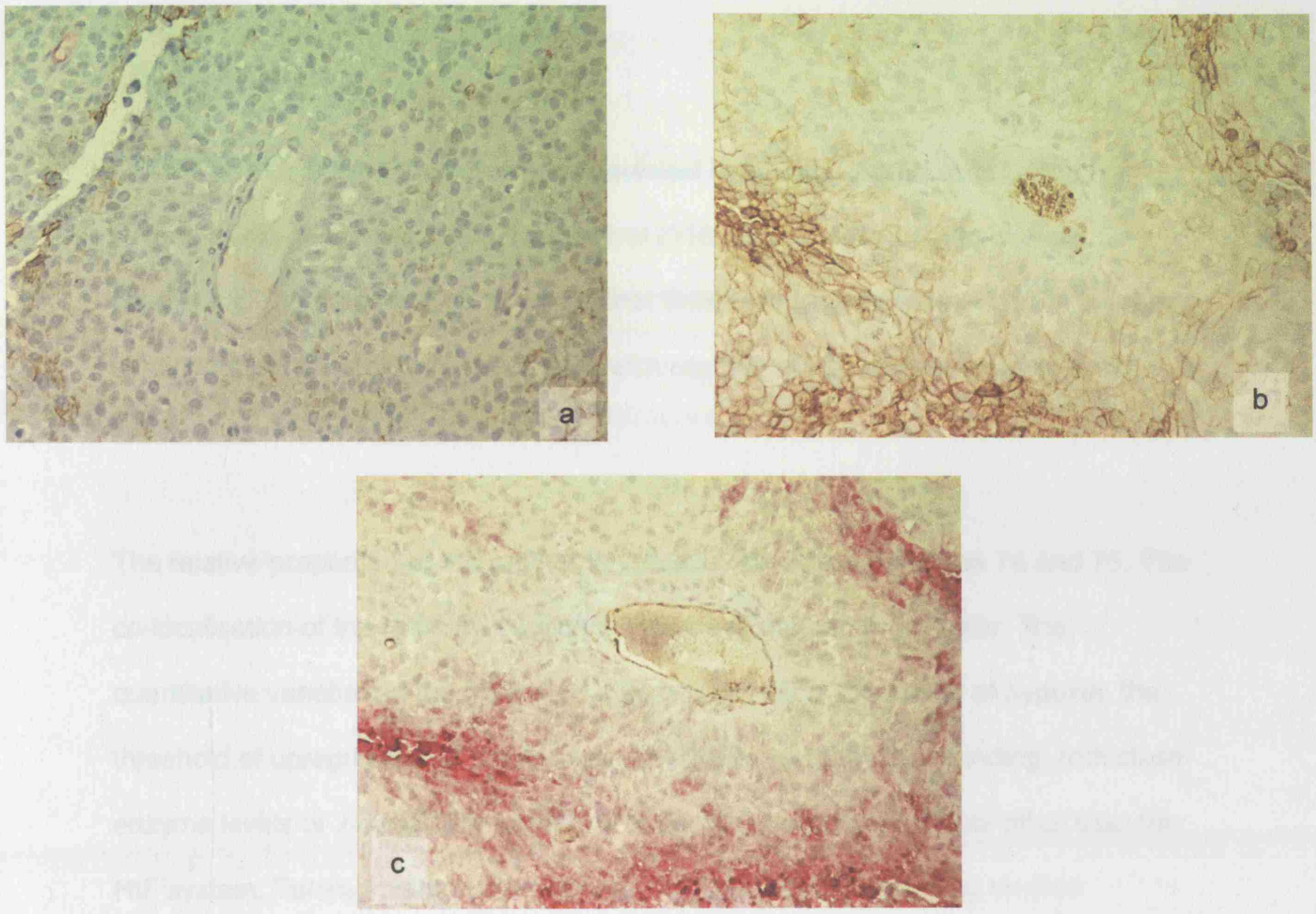

Figure 90 An example of a field at high magnification (x20) with good co-localisation of each stain for hypoxia, with a lesser degree of CA9 staining (a) compared with that of GLUT1 (b) and pimonidazole (c). The differences in the vessel to stain distances are also evident

Discussion

GLUT1 and CA9 are known to be upregulated in human tumour cells by the HIF system of oxygen dependent gene control (118, 232) in response to hypoxic conditions. The data here demonstate that these markers are expressed in bladder carcinoma, and are closely associated with regions of pimonidazole binding, an extrinsic marker of hypoxia.

The relative proportion of the marker is variable, as shown in figures 74 and 75. The co-localisation of the markers suggests hypoxia is the common factor. The quantitative variation of the intrinsic markers may reflect the timing of hypoxia, the threshold of upregulation of the markers relative to pimonidozole binding, reductase enzyme levels or indicate the existence of some regulatory elements other than the HIF system. Tumour cells would express GLUT1 or CA9 depending on their metabolic requirement to import glucose or adjust cellular pH.

There are two other published studies that compare CA9 and pimonidazole staining in human tumours. A series of eighteen cervix carcinomas were examined showing tight colocalization of the two markers (304). In contrast to the data presented here, the CA9 stained area represented double the number of cells that stained for pimonidazole. A second study, as part of an in depth survey of novel hypoxia induced genes, also found an almost identical pattern of expression between pimonidazole and CA9 in two oropharyngeal squamous carcinomas (135). The CA9 and pimonidazole staining here was performed and compared on 16 of the bladder cancer specimens by another group (118). There was some variation in the staining proportions (different sections and therefore different parts of the tumour were examined) but there was a tendency to a larger area of pimonidazole staining over CA9 staining. Why there should be difference between two tumour types is not

clear. It may reflect different enzyme levels or thresholds of upregulation that vary from cell type to cell type; transitional cells of the bladder may be adapted to a generally alkaline urinary pH.

The mean vessel to GLUT1 distance measured across all tumours was significantly lower than that of the pimonidazole stain, and the vessel to CA9 stain was in turn significantly higher. There was a wide range of measurements for each stain, shown by the varied coefficient of variation between tumours. The number of tumours here are too small to draw any firm conclusions on the significance of this variation, but does reflect the recurring heterogeneity seen in many studies of tumour biology. The method used was chosen to avoid any bias in measurement with each series of sections being reviewed a month apart, and all analysis being done after the collection of raw data. The results may suggest that GLUT1 is upregulated at a higher O_2 concentration than that at which pimonidozole binding occurs and CA9 at lower concentrations. Alongside this, the data may also reflect that markers are upregulated in different timeframes. There were more regions of GLUT1 close to vessels than CA9, which may suggest that GLUT1 is upregulated more rapidly. Rapid changes in expression of GLUT1 have been described within minutes of a change on pO_2, probably by activation of pre-existing GLUT1 on the cell surface (227) or rapid transport of GLUT1 stored intracellular vesicles (228). However the upregulation of CA9 occurs over a relatively long time frame, in vitro studies showing initial upregulation after 4 hours of hypoxia to a maximum after 16 hours (118). GLUT1 may therefore mark for more 'acute' hypoxia than CA9.

Other potential intrinsic markers of hypoxia have been studied all of which are linked by their HIF dependent upregulation. VEGF immunostaining was compared with pimonidazole staining (305) in an experimental biliary cirrhosis model, showing concordant staining in adjacent sections during the angiogenic phase of the fibrotic

development. However, a separate study that stained for VEGF and pimonidazole in a series of human cervix carcinomas found a poor correlation between the two (152). This was explained by diffusion of VEGF to cells other than their site of production, or the influence of other stimuli such as bFGF, TGFα and epidermal growth factor. As a result, study of VEGF mRNA is thought to be more useful. HIF1α and HIF2α have been examined in a series of breast adenocarcinomas and strong expression at the tumour necrosis margin was observed. However, protein was also demonstrable in other areas including the tumour/stromal margin (270).

The intrinsic markers of hypoxia may have clinical applications in two respects. It has been suggested that they may be suitable candidates for targeted anticancer treatment, using gene therapy. The disadvantage with this concept is that both of the markers considered here are expressed in normal tissue: CA9 is abundantly expressed in normal gut tissue as well as normal ovarian, endometrium and cervical cells whereas GLUT1 is expressed in erythrocytes. However, identification of hypoxic cells would allow identification of tumours in which selective 'Gene-Directed Enzyme Therapy' (G-DEPT) targeted to hypoxia may be effective (306). HIF 1 has been investigated as a suitable candidate (307, 308).

The other potential use for these markers is as possible pre-treatment identifiers of prognosis and selection for hypoxia sensitisation. The well established prognostic value of low tumour oxygen levels measured by the Eppendorf probe may be reflected by the hypoxic fraction as measured by either CA9 or GLUT1, and weak correlations have been identified in carcinoma of the cervix (309-311). Identification of substantial areas of hypoxia may lead to specific therapeutic interventions to reverse it, such as with carbogen and nicotinamide. The influence of the these

intrinsic markers on the outcome in a series of bladder carcinoma patients will be shown in chapter 6.

Conclusion

The expression of GLUT1 and Carbonic anhydrase 9 matches that of pimonidazole binding, supporting their role as hypoxia regulated proteins. The match, however, is not perfect and in some tumours non-existent, implying other components of the tumour microenvironment may influence these proteins or that metabolic disturbances to which GLUT1 and CA9 can occur in isolation of hypoxia. Each of these markers may also be upregulated in different time frames or at different levels of hypoxia, indicated by their differing median distance from vessels.

CHAPTER SIX

The influence of hypoxia, proliferation and vascularity on outcome in a cohort of patients with muscle invasive bladder cancer treated by accelerated radiotherapy, carbogen and nicotinamide: intrinsic markers of hypoxia in practice

Aims

The aim of this study was to determine the relationship between hypoxia, vascularity and proliferation and outcome in a cohort of bladder cancer patients treated with accelerated radiotherapy, carbogen and nicotinamide (ARCON). The putative intrinsic markers of hypoxia, GLUT1 and CA9 were used to determine the degree of hypoxia.

Methods and Materials

Ethical Approval

Ethical approval for the study was gained from the Local Ethics Committees.

Patients

Patients were recruited within a phase I/II study of ARCON in the treatment for invasive bladder carcinoma (312). A total of 64 patients were studied from an available treated population of 93. Analysis was dependant on availability of archival paraffin-embedded tumour specimens from the pre-treatment TURBT and

permission from the patient to use the material for this study. All patients had invasive transitional cell carcinoma confirmed by one of two pathologists at Mount Vernon Hospital. Initial staging was defined at cystoscopy under anaesthetic. All patients received treatment at Mount Vernon Hospital according to the ARCON protocol as described below as sole treatment.

Patient and tumour characteristics for the study population and the whole treated cohort are shown in table 18.

Patient, treatment and tumour characteristics	Analysed Group		Whole treated group
Sex (male:female)	56:8		81:11
Age median (range)	72.9 years (38.3 – 87.4)		71 years (37.2 – 87.4)
Dose of radiotherapy	55Gy		55Gy
Number receiving full course of nicotinamide (%)	33/64 (52%)		45/92 (49%)
Number receiving >50% of course of nicotinamide (%)	48/64 (76%)		63/92 (70%)
Number receiving carbogen (%)	59/64 (92%)		82/92 (89.1%)
Number receiving planned RT dose	64/64 (100%)		91/92 (99%)
T stage – number of patients (%)	T1	6 (9.3%)	7 (7.6%)
	T2	19 (29.7%)	29 (31.5%)
	T3	38 (59.4%)	56 (60.8 %)
	T4	1 (1.6%)	1 (1.1%)
Grade - number of patients (%)	G1	2 (3.1%)	6 (6.5%)
	G2	17 (26.6%)	27 (29.3%)
	G3	45 (70.3%)	59 (64.1%)

Table 18 Characteristics of study population and available patients

Treatment details

The ARCON protocol consists of patients receiving oral nicotinamide, breathing carbogen gas (5%), and undergoing an 'accelerated' schedule of external beam radiotherapy.

Nicotinamide

Oral nicotinamide was taken at least 1 hour after food and 1.5 hours before each fraction of radiotherapy. The time interval corresponds to the attainment of peak plasma concentrations of the drug. The dose was 80mg/kg. Thirty-one patients did not receive the full course of nicotinamide either due to co-existing vascular disease or patient refusal.

Carbogen breathing

5% carbogen gas (ie 95%O_2/5%CO_2) was administered at a rate of 15 litres per minute via a closed loop system and sealed breathing mask during radiotherapy. The breathing was started 5 minutes before irradiation and continued through treatment. It was tolerated by all but 1 patient for the whole course of 20 fractions.

Radiotherapy details

The radiotherapy was planned using CT scans, with patients positioned supine and the bladder empty. The planning target volume included the whole bladder with a margin of 2 centimetres. Treatment was delivered via two lateral wedged fields and an anterior field on a linear accelerator. All fields were irradiated each treatment day. Ten patients received 50 Gy and 54 patients received 55Gy, all in 20 fractions, treating 5 days a week. Doses were prescribed to the intersection point.

Follow up

Patients were assessed for local recurrence by 6 monthly cystoscopy. Metastatic disease recurrence was assessed by regular interview and clinical examination. One

patient was lost to follow up and censored at the time of last review. The median follow up time was 24 months (range 4 to 86 months).

Procedure

Serial sections of archived specimens were double stained for the following

GLUT1 and CD31

GLUT1 and Ki67

CA9 and CD31

CA9 and Ki67

The immunohistochemical procedure was as described in chapter 5

Image Analysis

The image analysis was performed as described in chapter 2 for stained CA9 and GLUT1 fractions. The double staining process meant the fraction of each of these markers was assessed on three sections. Overall vascularity and hot spot counting was performed, as in chapter 4 on two sections and overall Ki67 index was as described in chapter 3 on two sections for each patient.

Data obtained

The following data were obtained from image analysis:

Fraction of tumour stained for GLUT1

Fraction of tumour stained for CA9

Vascular density

Hot spot count

Ki67 proliferative index

Statistics

Relationships between biological parameters (as continuous variables), T stage and grade were tested using one-way analysis of variance and the Chi squared test. The biological parameters were compared by either the Pearson correlation coefficient for continuous variables or by calculation of the kappa value and chi squared statistic. Survival intervals were calculated using the Kaplan Meier product limit method. In the calculation of local recurrence free survival and metastasis free survival, non-failures were censored at last follow up or at death. For cause specific survival, patients who died as a result of bladder cancer were classed as failures and non-failures were censored at death from other causes or at last follow up. For overall survival patients who died of any cause were classed as failures and non-failures were censored at last follow-up. All time intervals were calculated from the date of first radiotherapy treatment. Individual factors were tested using the log rank test, where $p<0.05$ was considered significant. Patients were dichotomised about the median values for GLUT1 stained area, CA9 stained area, KI67 index, vascular density and vessel hotspot count.

The Cox proportional hazard model was used for multiple regression analysis, to assess the effects of patient and tumour variables on clinical outcome. A range of possible prognostic factors was examined: Age (continuous variable), T-stage (ordinal variable), grade (ordinal variable) and Ki67 index (continuous variable). The GLUT1 staining area (above or below median) and CA9 staining area (above or below median) were each added to the models individually.

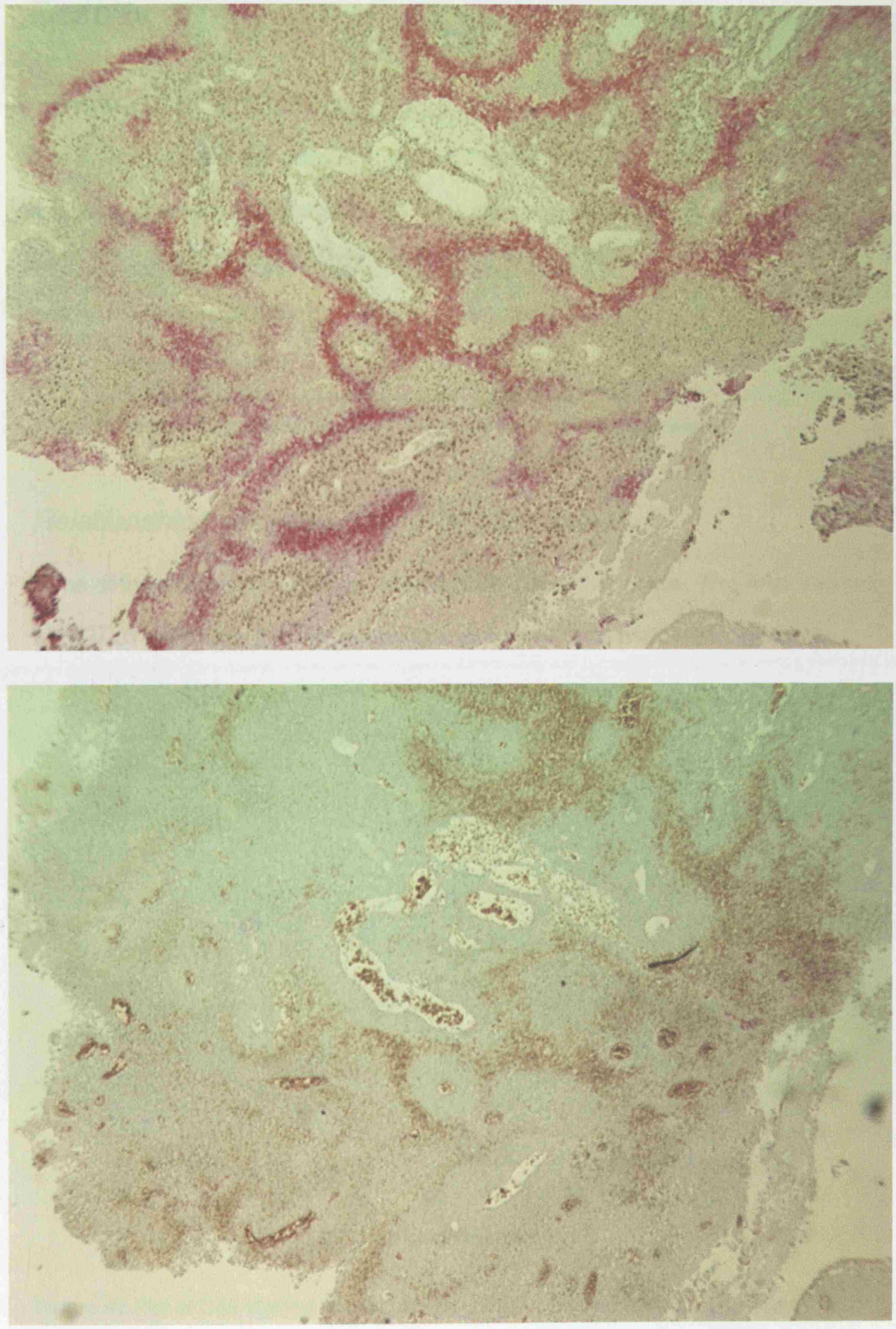

Figure 91 Low power (x5) images of CA9 + Ki67(upper panel) and GLUT1 + CD31/34 (lower panel) stains of archived sections of bladder carcinoma

Results

Biological parameters

The median values with ranges of the Ki67 index, vascular density, hot spot count and stained areas of CA9 and GLUT1 are shown in table 19.

Parameter	Median	Range
Ki67 index (%)	35.7	2.6 to 61.7
Vascular density (vessels/mm^2)	55.8	21.1 to 179.7
Hotspot count	30	12 to 55
GLUT1 stained fraction (%)	6.5	0 to 67
CA9 stained fraction (%)	3.5	0 to 62

Table 19 Median values and ranges of biological parameters assessed

Relationships between biological parameters

None of the parameters were associated with T stage or grade. The area stained with GLUT1 correlated strongly with that of CA9 ($r=0.96$ $p<0.0001$, figure 92)

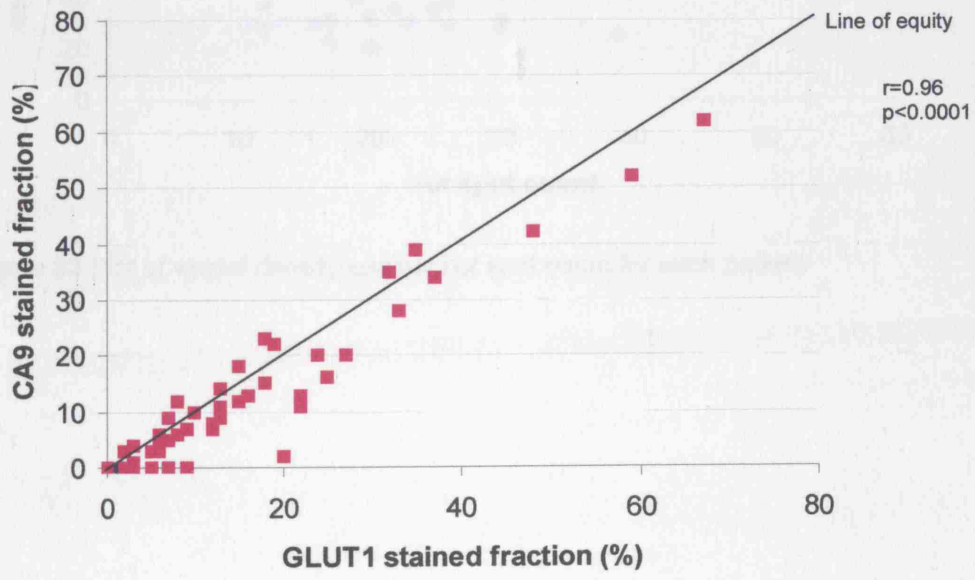

Figure 92 Plot of CA9 stained fraction against GLUT1 stained fraction, with line of equity

There was strong agreement between the groups divided about the median of the CA9 fraction and the GLUT1 fraction (kappa = 0.81, Chi square 48.9, $p<0.0001$). Neither the GLUT1 nor the CA9 stained fractions were associated with the vascular density or hot spot count. There was a tendency towards a higher GLUT1 fraction in those with a Ki67 index above the median (analysis of variance $p <0.06$; the corresponding p value for the CA9 comparison was $p<0.07$).

The vascular density and the hotspot count were correlated ($r = 0.65$ $p<0.0001$) (figure 93).

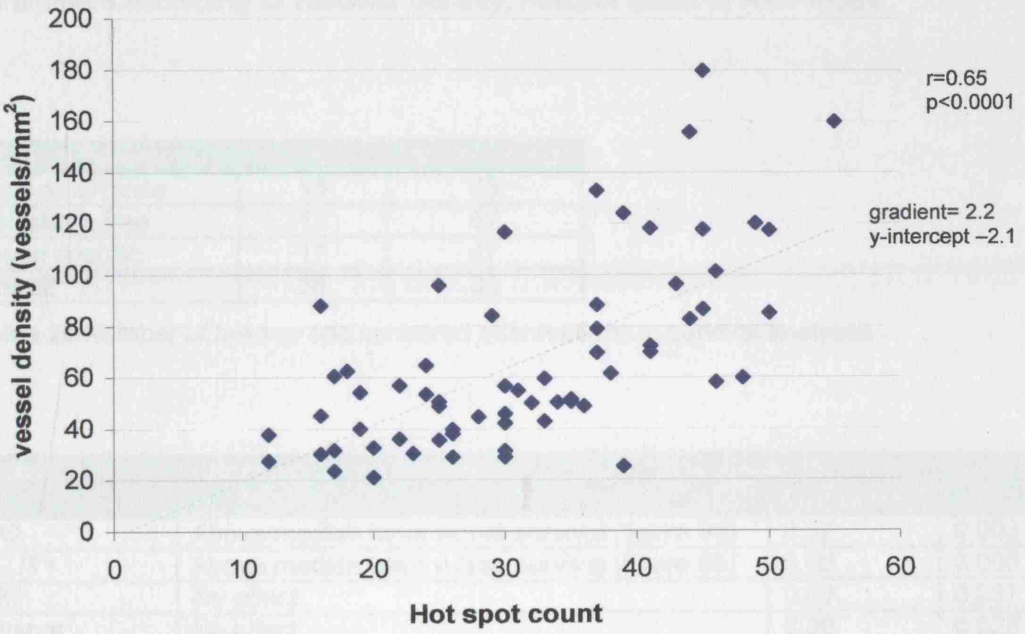

Figure 93 Plot of vessel density against hot spot count for each patient

Relationship of biological parameters with outcome

Univariate analyses

The Kaplan Meier plots of local relapse free survival, metastasis free survival, cause specific survival and overall survival are shown in figure 94 to 97. The results of the univariate analyses are shown in tables 20 to 24. Those tumours with intrinsic hypoxia marker staining above the median value had a statistically significantly worse cause specific and overall survival. There was no difference in the survival parameters according to vascular density, hotspot count or Ki67 index.

Survival Parameter	N Failed	N Censored
Local recurrence	16	48
Metastasis free	12	52
Cause specific	17	47
Overall	26	38

Table 20 Number of failures and censored observations in survival analyses

Factor	Effect on Overall survival	Chi squared	p-value
CA9	Above median have worse survival (figure 94)	8.57	0.003
GLUT1	Above median have worse survival (figure 95)	8.06	0.005
Ki67	No effect	0.00	0.937
Hotspot	No effect	0.39	0.528
Vessel Density	No effect	0.00	0.960

Table 21 Results of univariate analysis of overall survival (all cause)

Factor	Effect on cause specific survival	Chi squared	p-value
CA9	Above median have worse survival (figure 96)	8.57	0.003
GLUT1	Above median have worse survival (figure 97)	8.06	0.005
Ki67	No effect	0.63	0.427
Hotspot	No effect	0.40	0.523
Vessel Density	No effect	0.00	0.965

Table 22 Results of univariate analysis of cause specific survival

Factor	Effect on local recurrence free survival	Chi squared	p-value
CA9	No effect	0.81	0.365
GLUT1	No effect	1.56	0.212
Ki67	No effect	2.23	0.136
Hotspot	No effect	0.00	0.939
Vessel Density	No effect	0.06	0.794

Table 23 Results of univariate analysis of local recurrence free survival

Factor	Effect on metastasis free survival	Chi squared	p-value
CA9	No effect	0.28	0.591
GLUT1	No effect	0.22	0.633
Ki67	No effect	1.39	0.240
Hotspot	No effect	0.60	0.433
Vessel Density	No effect	0.01	0.914

Table 24 Results of univariate analysis of metastasis free survival

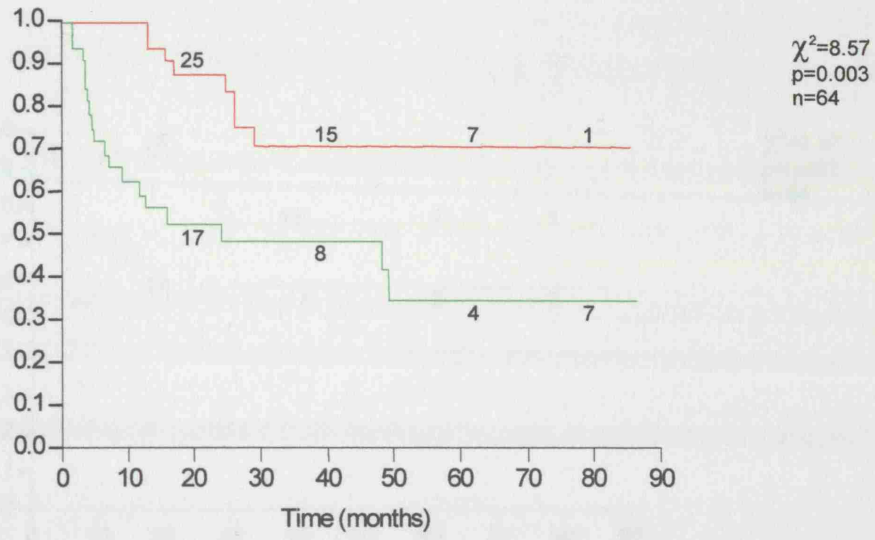

Figure 94 Overall survival plot comparing above (green) and below (red) median CA9 fraction (y-axis = surviving fraction).

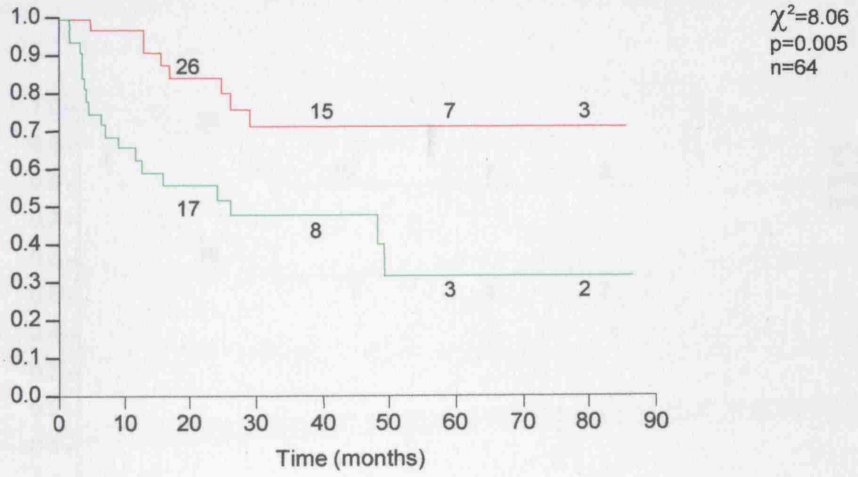

Figure 95 Overall survival plot comparing above (green) and below (red) median GLUT1 fraction (y-axis = surviving fraction).

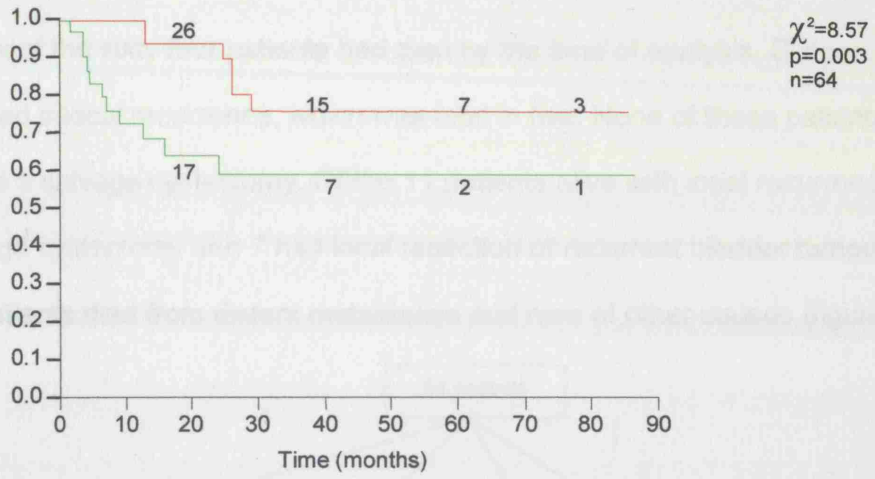

Figure 96 Cause specific survival plot comparing above (green) and below (red) median CA9 fraction (y-axis = surviving fraction).

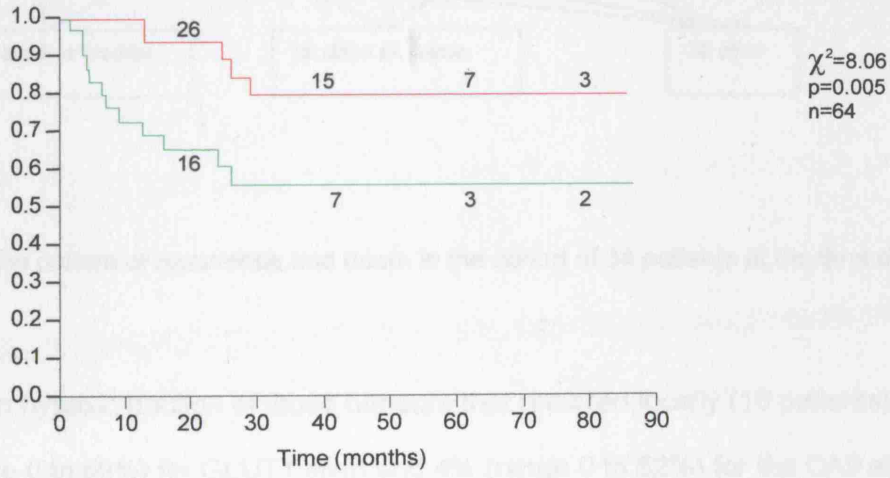

Figure 97 Cause specific survival plot comparing above (green) and below (red) median GLUT1 fraction (y-axis = surviving fraction).

Hypoxic fraction and the pattern of treatment failure

Twenty-six of the sixty four patients had died by the time of analysis. Sixteen patients had a local recurrence, which was fatal in five. None of these patients underwent a salvage cystectomy. Of the 11 patients alive with local recurrence 4 had salvage cystectomy and 7 had local resection of recurrent bladder tumour. Twelve patients died from distant metastases and nine of other causes (figure 98) .

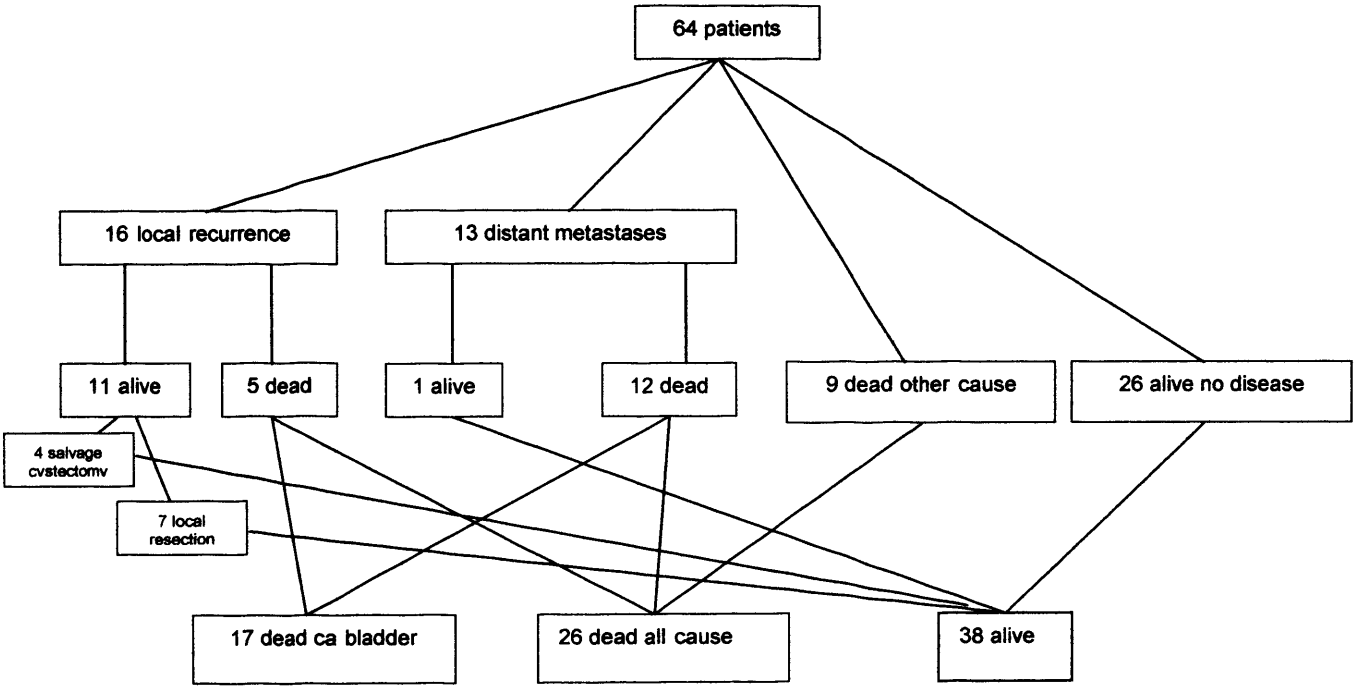

Figure 98 The pattern of recurrence and death in the cohort of 64 patients at the time of analysis

The median hypoxic fraction of those tumours that recurred locally (16 patients) was 9.5% (range 0 to 59%) for GLUT1 stain and 4% (range 0 to 52%) for the CA9 stain. In the five patients who died from local disease, the original tumours had a median hypoxic fraction of 20% (range 15 to 59%) for GLUT1 and 18% (range 2 to 52%) for the CA9 stain.

In the 13 patients that developed metastases, the median hypoxic fraction of the original tumours was 10% (range 0 to 67%) for GLUT1 stain and 9% (range 0 to 62%) for CA9. In the 12 patients who died from metastatic disease, the original tumours had a median hypoxic fraction of 11.5% (range 0 to 67%) for GLUT1 and 9.5% (range 0 to 62%) for CA9. The patient who died from another cause had no hypoxia in the original tumour measured by either stain.

There were a total of 29 failures. The cause specific survival curve comparing tumours above with those below the median hypoxic fraction in the tumours that recurred is shown in figure 99 and 100. In this group the cause specific survival was statistically significantly worse in the more hypoxic group, suggesting that tumours were more like to be fatal if they were originally hypoxic.

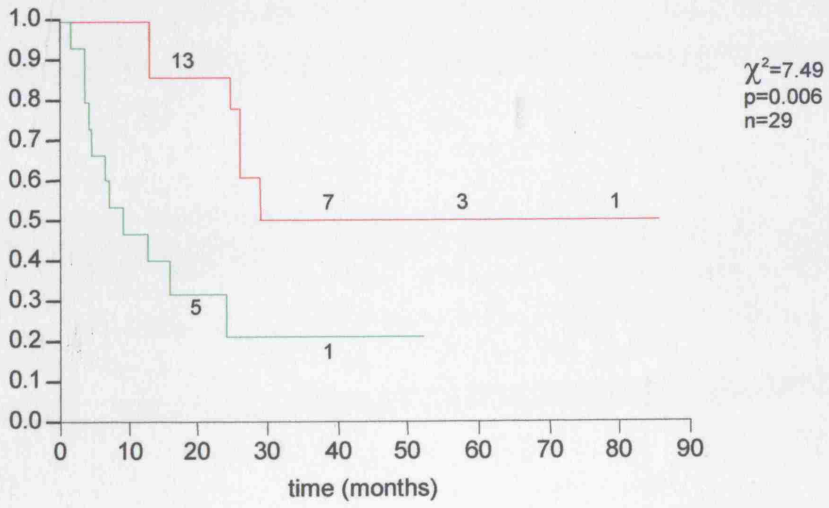

Figure 99 Cause specific survival plot comparing above (green) and below (red) median CA9 fraction in those patients developing recurrent disease (local and distant). The hypoxic fraction is that of the original tumour at diagnosis (y-axis = surviving fraction).

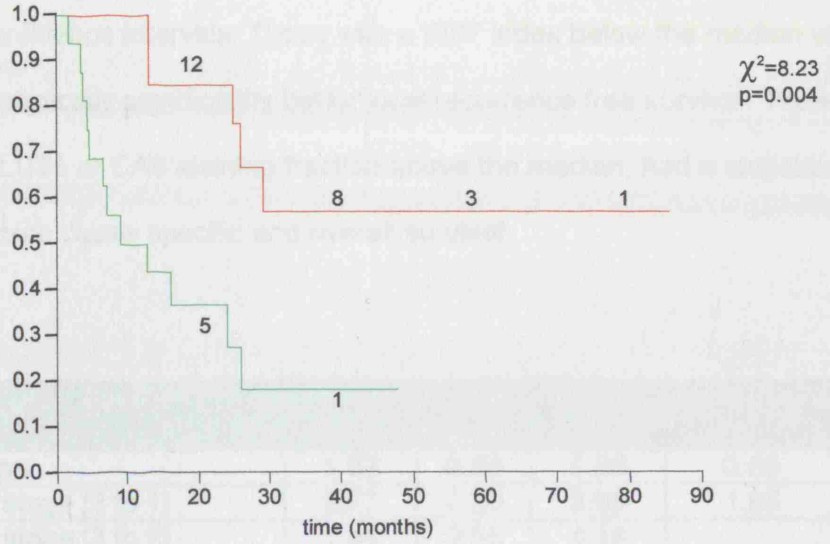

Figure 100 Cause specific survival plot comparing above (green) and below (red) median GLUT1 fraction in those patients developing recurrent disease (local and distant). The hypoxic fraction is that of the original tumour at diagnosis.

Multivariate analyses

The details of the multivariate analysis are given in tables 25 to 32. The risk ratios for each parameter for the various survival measures are shown with 95% confidence intervals. Those with a Ki67 index below the median value had a statistically significantly better local recurrence free survival. Those with either GLUT1 or CA9 staining fraction above the median, had a statistically significant worse cause specific and overall survival.

Factor	Risk Ratio	Lower CL	Upper CL	chi-square	p value
Age	1.02	0.98	1.06	0.53	0.47
T stage [2 to 1]	0.77	0.20	3.68	1.85	0.60
T stage [3 to 2]	1.44	0.55	4.18		
T stage [4 to 3]	0.00	.	3.08		
grade [2 to 1]	0.21	.	.	2.35	0.31
grade [3 to 2]	1.14	.	.		
ki67 median [below]	0.93	.	.	0.10	0.75
vessel median [below]	0.97	.	.	0.03	0.87
CA9 median [below]	0.52	.	.	9.98	**0.002**

Table 25 Risk Ratios for each prognostic parameter for overall survival including CA9

Factor	Risk Ratio	Lower CL	Upper CL	chi-square	p value
Age	1.01	0.97	1.05	0.22	0.64
T stage [2 to 1]	0.83	0.21	4.02	1.27	0.74
T stage [3 to 2]	1.18	0.44	3.49		
T stage [4 to 3]	0.00	.	4.22		
grade [2 to 1]	0.33	.	.	1.15	0.56
grade [3 to 2]	1.29	.	.		
ki67 median [below]	0.96	.	.	0.03	0.86
vessel median [below]	0.96	.	.	0.04	0.84
GLUT median [below]	0.57	.	.	7.00	**0.008**

Table 26 Risk Ratios for each prognostic parameter for overall survival including GLUT1

Factor	Risk Ratio	Lower CL	Upper CL	chi-square	p value
Age	1.01	0.96	1.06	0.10	0.75
T stage [2 to 1]	2.06	0.30	41.20	1.643	0.65
T stage [3 to 2]	1.25	0.41	4.41		
T stage [4 to 3]	0.00	.	8.10		
grade [2 to 1]	0.16	.	.	1.98	0.37
grade [3 to 2]	2.27	.	.		
ki67 median [below]	0.83	.	.	0.51	0.48
vessel median [below]	1.08	.	.	0.09	0.76
CA9 median [below]	0.58	.	.	4.56	**0.03**

Table 27 Risk Ratios for each prognostic parameter for cause specific survival including CA9

Factor	Risk Ratio	Lower CL	Upper CL	chi-square	p value
Age	1.00	0.95	1.06	0.02	0.89
T stage [2 to 1]	2.10	0.29	42.47	1.38	0.71
T stage [3 to 2]	1.10	0.34	4.05		
T stage [4 to 3]	0.00	.	9.33		
grade [2 to 1]	0.28	.	.	1.557	0.46
grade [3 to 2]	2.43	.	.		
ki67 median [below]	0.85	.	.	0.35	0.55
vessel median [below]	1.08	.	.	0.09	0.76
GLUT median [below]	0.56	.	.	5.08	**0.02**

Table 28 Risk Ratios for each prognostic parameter for cause specific survival including GLUT1

Factor	Risk Ratio	Lower CL	Upper CL	chi-square	p value
Age	1.01	0.96	1.07	0.14	0.70
T stage [2 to 1]	1.38	.	.	5.83	0.12
T stage [3 to 2]	1.14	0.36	3.75		
T stage [4 to 3]	0.00	.	2.20		
grade [2 to 1]	0.19	.	.	3.74	0.15
grade [3 to 2]	0.45	.	.		
ki67 median [below]	0.55	.	.	4.45	**0.03**
vessel median [below]	0.89	.	.	0.20	0.65
CA9 median [below]	0.63	.	.	2.61	0.10

Table 29 Risk Ratios for each prognostic parameter for local recurrence free survival including CA9

Factor	Risk Ratio	Lower CL	Upper CL	chi-square	p value
Age	1.01	0.96	1.06	0.04	0.83
T stage [2 to 1]	1.40	.	.	5.52	0.14
T stage [3 to 2]	1.06	0.331	3.52		
T stage [4 to 3]	0.00	.	2.534		
grade [2 to 1]	0.36	.	.	2.72	0.26
grade [3 to 2]	0.48	.	.		
ki67 median [below]	0.57	.	.	3.91	**0.048**
vessel median [below]	0.90	.	.	0.14	0.71
GLUT median [below]	0.66	.	.	2.14	0.14

Table 30 Risk Ratios for each prognostic parameter for local recurrence free survival including GLUT1

Factor	Risk Ratio	Lower CL	Upper CL	chi-square	pvalue
Age	0.99	0.94	1.07	0.01	0.91
T stage [2 to 1]	0.78	0.07	18.38	2.75	0.43
T stage [3 to 2]	3.00	0.71	20.79		
T stage [4 to 3]	0.00	.	26.82		
grade [2 to 1]	2.41	.	.	2.28	0.32
grade [3 to 2]	3.40	.	.		
ki67 median [below]	0.73	.	.	1.03	0.31
vessel median [below]	1.15	.	.	0.22	0.64
CA9 median [below]	0.88	.	.	0.20	0.66

Table 31 Risk Ratios for each prognostic parameter for metastasis free survival including CA9

Factor	Risk Ratio	Lower CL	Upper CL	chi-square	p value
Age	0.99	0.94	1.07	0.019	0.89
T stage [2 to 1]	0.81	0.07	18.59	2.67	0.44
T stage [3 to 2]	2.97	0.69	20.52		
T stage [4 to 3]	0.00	.	29.01		
grade [2 to 1]	2.47	.	.	2.467	0.29
grade [3 to 2]	3.50	0.60	66.32		
ki67 median [below]	0.73	0.37	1.33	1.05	0.31
vessel median [below]	1.15	0.62	2.12	0.21	0.6
GLUT median [below]	0.92	0.50	1.71	0.07	0.79

Table 32 Risk Ratios for each prognostic parameter for metastasis free survival including GLUT1

Discussion

This study has assessed the relationship of intrinsic markers of hypoxia, vascularity and proliferation with outcome in a cohort of bladder carcinomas treated with a hypoxia-modifying regimen. The group is representative of that treated with radiotherapy in the wider clinical setting (263). It has shown that CA9 and GLUT1 are each unrelated to local or distant failure, but are related to overall and cause specific survival as independent predictive factors in this cohort. Those tumours with a higher proliferation index had a worse local control rate when other factors were adjusted for in the multivariate analysis. Vascularity was not significantly related to outcome.

There have not been any other studies relating CA9 to outcome in bladder carcinoma. There are studies that do so in head and neck carcinoma, non-small cell lung carcinoma and in breast carcinoma. Koukourakis et al (302) found strong CA9 expression in 20 of 75 head and neck tumours and that these had significantly lower hotspot counts. The median CA9 stained fraction for the whole cohort was 7.7%. The tumours that expressed CA9 had a significantly worse complete response rate to chemoradiotherapy compared to CA9 negative tumours. The study confirmed the clinical importance of CA9 staining in head and neck cancer and it was argued that it might serve as a means of identifying those patients who may benefit from hypoxia reducing treatment. A study of non-small cell lung carcinoma, by Giatromanolaki et al (303), stained 107 non-small cell lung carcinoma biopsy specimens for CA9 from patients treated with surgery alone. Those with strong staining (39 of 107) had a significantly poorer overall survival. Data on local and distant relapse were not given. The third study examined CA9 staining in conventionally treated invasive breast carcinoma and found strong expression in 49 of 103 cases. This was

associated with a higher relapse rate and a poorer overall survival. Data on the site of relapse were not given (313).

There have been two studies relating GLUT1 expression to outcome in bladder cancer. Chang et al (314) showed GLUT1 was specific to bladder carcinoma and not expressed in normal bladder. There was greater expression of GLUT1 in invasive transitional cell carcinoma than in superficial disease. They found no correlation between recurrence and GLUT1 in superficial bladder tumours. Invasive disease was not studied. Another study by a group from Texas (315) stained specimens from forty patients with invasive TCC of the bladder for GLUT1. All patients were treated with cystectomy and did not receive any adjuvant radiotherapy. In a univariate analysis, those patients with more than 10% of tumour stained had a significantly worse overall survival than those with less staining. A multivariate analysis was not performed. The adverse prognostic influence of GLUT1 expression has also been shown in human gastric and ovarian carcinoma (224, 226).

The present study confirms the presence of these markers, and thus hypoxia in invasive bladder carcinoma (see chapter 5). The results are consistent with the study by Younes, but add to the data in demonstrating no difference in local control between those tumours with more or less hypoxia when treated with ARCON. This may imply that ARCON is successful in overcoming the adverse impact of hypoxia on local radiotherapy.

The mechanism by which hypoxia worsens treatment outcome may relate to the function of CA9 which catalyses the reversible interchange of carbon dioxide and water to carbonic acid. This brings about a low extracellular pH, which has been shown to protect mitochondria from hypoxic stress in liver cells (316). The protective

effect of acidosis against cell death was associated with the inhibition of NAD(P)H oxidation and delayed loss of the mitochondrial membrane potential that was maximal at pH 6.4.

A low pH has also been shown to inhibit the anti-tumour immune response within solid tumours. Fischer et al showed the secretion of tumour necrosis factor-α (TNFα) and Fas/FasL mediated apoptosis by killer T-lymphocytes was reduced in a low pH environment. At a pH of 5.8 a substantial reduction of cytotoxic effector cell functions occurred. Mitochondrial activity and regulation of intracellular pH fell with declining extracellular pH. Acidic conditions also suppress TNF mediated apoptosis killer T-cell function. Cellular immunity is suppressed in acidic conditions, with inhibition at a pH of 5.8 in vitro (317). These mechanisms may enable cell survival and be another way in which hypoxia engenders more aggressive tumour behaviour in addition to imparting radioresistance.

High expression of CA9 or GLUT1 did not adversely affect local control or the development of metastases in this cohort. This may reflect the treatment used, as carbogen and nicotinamide may have reversed the adverse effect of hypoxia in some tumours. The staining was performed on diagnostic specimens, taken many days before the start of treatment. It is not known how stable the hypoxic fraction is and thus what the hypoxic status of these tumours was at the time of treatment. The fraction of chronic hypoxia may become lower through necrosis or angiogenesis, or higher through formation of poorly vascularised regions from tumour growth. The fraction of acute hypoxia is, by definition, changing frequently. This issue would be difficult to resolve with the methods used in this study because the very act of taking the biopsy changes the nature of the tumour and thus the hypoxic fraction. Non-

invasive imaging methods, such as serial imaging, may be more suited to evaluating changes in tumour oxygenation over time.

The poorer survival of patients with higher tumour levels of hypoxic marker contrasts with the local and distant control figures. This may be a result of ARCON overcoming the effect of hypoxia on local control. Analysis of the patients who suffered a local or distant recurrence revealed the cause specific survival was statistically significantly worse in the more hypoxic group. This suggests that tumours were more like to be fatal if they were originally hypoxic, a reflection of their more aggressive biology. Such a finding is consistent with the in vitro evidence that hypoxia may select for a more aggressive tumour cell phenotype (90). None of the patients who died of local recurrence underwent a salvage cystectomy, whereas 4 of those who remain alive with local recurrence did. This difference may account for some of the survival differences but still suggests that more aggressive disease and the degree of tumour hypoxia are connected.

In this study, tumours with higher proliferation indices had a poorer local control rate. This is consistent with other studies that also used Ki67 as a marker in transitional cell bladder cancer. Popov et al (318) found significantly lower progression free and disease specific survival rates in patients with higher Ki67 indices, using the median value (28%) as the cut off. Similar prognostic value was seen in studies by Rodel et al, who found a median Ki67 index of 8.8% (319) and Moonen et al who used a median value of 14%. The median value in the present series was 35%, higher because the majority of tumours were invasive, T2 or T3 and of grades 2 and 3, each associated with greater degrees of proliferation (320). Lara et al, however, found that the median Ki67 of 33.1% was not related to local control in fifty-five patients treated with radical radiotherapy. However, the lower tercile (less than 27%) had significantly better local control than the upper two terciles. The authors state

that an accelerated radiotherapy regime should increase tumour cure rates by restricting the time available for tumour cell repopulation and in slowly proliferating tumours, repopulation is not a major concern (321). Although there are studies in bladder carcinoma exploring the benefit of altered fractionation (322-324), the present study does not support this hypothesis. However, the measures taken here and the studies cited above were of baseline proliferation rates, and it is not known how this relates to the capacity for bladder tumours to trigger accelerated repopulation. In addition, the marginal benefit of accelerated radiotherapy in tumours with a higher degree of proliferation is not known, as there is no comparator group who received conventional radiotherapy. Studies examining this question have not assessed proliferation using Ki67 but have been based on the potential doubling time (Tpot) in animal tumours and thymidine labelling index in head and neck tumours. Begg et al found the initial Tpot give a much better indication of the proliferation rate of surviving cells after fractionated radiotherapy than the labelling index in three cell lines (325). Awaad et al (326) showed that the thymidine labelling index predicted for a better outcome in head and neck carcinomas treated with adjuvant (post operative) accelerated radiotherapy

Vascularity, whether measured by overall vessel density or with the hotspot technique, did not relate to outcome. This contrasts with other studies. Dickinson et al (327) examined 45 tumours using the Chalkley point method and found high counts were of poor prognostic significance in a multivariate analysis of overall survival. Three patients were treated with cystectomy, 31 with conventionally fractionated radical radiotherapy (60Gy in 32 fractions over 42 days) and 16 with palliative radiotherapy. One patient was treated with intravesical BCG. No details on survival by treatment type were given in this study. Hawke et al used the hotspot method to assess the vascular density in 42 bladder tumours from cystectomy specimens and 29 tumours from biopsy material. They found a weak correlation

between vascular density and survival by univariate analysis that was absent on multivariate analysis (328). Bochner also used the hot spot method and found it to be associated with disease progression in multivariate analysis in 164 patients treated with by cystectomy (329). The absence of vascularity as a prognostic factor in the present study may be due to a lack of statistical power, or may indicate ARCON counteracts the adverse effect in some way. This could be related to the accelerated fractionation, where vascularity is linked in some way to the capacity for accelerated repopulation or to the responsiveness of tumours to carbogen and nicotinamide. The marginal benefit for highly angiogenic tumours may be greater than for those displaying less angiogenicity. Alternatively, nicotinamide may be effective in improving flow in redundant capillary beds in otherwise poorly vascularised tumours.

This study has shown that CA9 and GLUT1 staining may be useful in predicting prognosis in bladder cancer and needs to be tested in a randomised controlled trial. It may also predict whether individual patients would benefit from a hypoxia modifying treatment. However, the practical use of such measures has to be considered in the light of what the therapeutic ratio of the treatment is. If there were a clinically useful marginal benefit for all patients, then stratification would not be helpful. If the treatment was very toxic, then stratification would be helpful to avoid unnecessary morbidity. ARCON does not have any significant life threatening toxicity. Nicotinamide causes troublesome nausea that may be reduced by dose reduction or concurrent antiemetics. Carbogen breathing is well tolerated by most patients. In addition, the dynamic nature of tumour circulation and tumour growth mean that even a small amount of hypoxia in a tumour may be enough to worsen the prognosis. The median stained fraction in this cohort for GLUT1 was 6.5% and for CA9 was only 3.5%. On balance then, it may be appropriate to treat all patients with ARCON, irrespective of the hypoxic fraction assessed at diagnosis. These

questions along with those of the role of proliferation and vascularity should be answered in the Phase III trial of ARCON in bladder cancer currently under way, testing the following hypotheses:

- The marginal benefit of ARCON is greater in tumours with hypoxia detectable by the intrinsic markers compared to treatment without carbogen and nicotinamide.
- The marginal benefit of ARCON is greater in tumours with a high proliferative index measured by Ki67 compared to a more protracted radiotherapy regimen
- The marginal benefit of ARCON is greater in more angiogenic tumours compared to conventional radiotherapy.

Conclusion

This study has demonstrated CA9 and GLUT1 staining are of prognostic influence with respect to survival but not local control or the development of metastasis. These discrepancies may arise from the treatment used. The study has generated hypotheses on the use of these markers, as well as those of vascularity and proliferation in the context of a treatment designed to address the problems of hypoxia and accelerated proliferation.

Overall Conclusions

The basic hypothesis of this thesis, that hypoxia exists in bladder carcinoma, has been confirmed. The clinical applicability of pimonidazole as a marker of hypoxia has been demonstrated in a tumour site unsuitable for the established methods of measuring tumour oxygenation. The use of pimonidazole has allowed the relationship between hypoxia and both proliferation and vascularity to be explored. A second method of measuring hypoxia using intrinsic markers has been compared with pimonidazole staining, and this has been taken forward to a retrospective study of hypoxia in a cohort of bladder tumours treated with a hypoxia reducing regimen.

In a cohort of 26 transitional cell bladder tumours, the hypoxic fraction assessed with pimonidazole staining ranged between 0 and 38% with a median value of 9%. Less proliferation, assessed by Ki67 staining, was seen in hypoxic regions. However some hypoxic regions close to vessels had proliferation indices similar to non-hypoxic regions, suggesting the hypoxic had not been present for long enough to supress proliferation. A similar pattern of proliferation was seen when assessed using CyclinA, although the proliferative indices assesses by CyclinA staining were less than with Ki67. This reflected the fact that cyclinA is upregulated in a limited part of the cell cycle whereas Ki67 is expressed thoughought the cell cycle. In the study of vascularity and hypoxia in these tumours, tumour that was close to a region of hypoxia tended to greater vascularity, perhaps demonstrating an angiogenic stimulus from hypoxic regions. The hypoxic fractions in this cohort of bladder tumours assessed by the intrinsic markers of hypoxia, CA9 and GLUT1, correlated well with that of pimonidazole. In the retrospective study of bladder tumours that had

been treated with ARCON, those with a hypoxic fraction greater than the median value had a poorer cause specific and overall survival. However, no difference was found in the local recurrence free survival between these groups implying that local control may be achieved in hypoxic tumours when ARCON is used but if the reccur, they are more likely to be fatal if they were originally more hypoxic.

Hypoxia is a heterogenous phenomenon and the data here, alongside other literature, suggest both a temporal and spatial dynamism resulting from the 'chaotic' tumour vascular network. As a result, all methods of measuring hypoxia are limited because they are only snapshots of the state of the tumour at the time of measurement. These methods cannot take into account the phenomenon of reoxygenation during treatment. To do so would require a method that assesses tumour oxygenation rapidly and non-invasively allowing repeated evaluation during and though treatment. Furthermore, because the hypoxic cells that are able to maintain their clonagenic potential are those responsible for treatment failure, straightforward measures of hypoxia alone may not be adequate for selecting those tumours that would benefit from hypoxia modification using, for example, ARCON. Also, there is no clear evidence that such stratification would be necessary. If it only requires a microregions of hypoxic cells to be treatment resistant the argument for hypoxia reduction in all tumours holds. The answer to this questions will only be found in randomised controlled trials evaluating the role of hypoxia modification.

References

1. West JB. Respiratory Physiology - the essentials. 6th ed. London (UK): Williams & Wilkins; 1999.

2. Hockel M, Vaupel P. Tumor Hypoxia: Definitions and Current Clinical, Biologic, and Molecular Aspects. J Natl Cancer Inst 2001;93(4):266-276.

3. Hockel M, Vaupel P. Tumor hypoxia: definitions and current clinical, biologic, and molecular aspects. J Natl Cancer Inst 2001;93(4):266-76.

4. Honing CR. Modern Cardiovascular Physiology. Boston (MA): Little and Brown; 1988.

5. Vaupel P, Fortmeyer HP, Runkel S, Kallinowski F. Blood flow, oxygen consumption, and tissue oxygenation of human breast cancer xenografts in nude rats. Cancer Res 1987;47(13):3496-503.

6. Kallinowski F, Schlenger KH, Runkel S, Kloes M, Stohrer M, Okunieff P, et al. Blood flow, metabolism, cellular microenvironment, and growth rate of human tumor xenografts. Cancer Res 1989;49(14):3759-64.

7. Vaupel P, Schaefer C, Okunieff P. Intracellular acidosis in murine fibrosarcomas coincides with ATP depletion, hypoxia, and high levels of lactate and total Pi. NMR Biomed 1994;7(3):128-36.

8. Marshall RS, Koch CJ, Rauth AM. Measurement of low levels of oxygen and their effect on respiration in cell suspensions maintained in an open system. Radiat Res 1986;108(1):91-101.

9. Starlinger H, Lubbers DW. Methodical studies on the polarographic measurement of respiration and "critical oxygen pressure" in mitochondria and isolated cells with menbrane covered platinum electrodes. Pflugers Arch 1972;337:19-28.

10. Robiolo M, Rumsey WL, Wilson DF. Oxygen diffusion and mitochondrial respiration in neuroblastoma cells. Am J Physiol 1988;256:C1207-13.

11. Schwartz G. Ueber Desensibilisierung gegen Rontgen- und Radiumstrahlen. Munchener Medizinische Wochenschrift 1909;24:1-2.

12. Mottram JC. Brit J Rad 1935;viii:32.

13. Lacassagne A. Compt Rend Acad Sci 1942;215:231.

14. Evans TC, Goodrich JP, Slaughter JC. Radiology 1942;xxxvii:201.

15. Hollcraft JW, Lorenz E, Matthews M. JNCI 1952;xii:751.

16. Read J. Brit Journal Rad 1952;xxv:89.

17. Giles NH, Beatty AV. Science 1950;cxii:643.

18. Hollaender A, Baker WK, Anderson E. Cold Harbour Symposium 1951;xvi:315.

19. Glass B, Plaine HL. Proc Nat Acad Sci 1952;1942(xxxviii):697.

20. Gray LH, Conger AD, Ebert M, Hornsey S, Scott OCA. The concentration of oxygen dissolved in tissues at the time of irradiation as a factor in radiotherapy. Brit Journ Rad 1953;xxvi:638-648.

21. Tomlinson RH, Gray LH. The histological structure of some human lung cancers and the possible implications for radiotherapy. Brit J Cancer 1955;IX(4):539-549.

22. Powers WE, Tolmach LJ. Demonstration of an anoxic component in a mouse tumour cell population by an in vivo assay of survival following irradiation. Radiology 1964;83:328-336.

23. Rockwell S, Moulder JE. Hypoxic fractions of human tumors xenografted into mice: a review. Int J Radiat Oncol Biol Phys 1990;19(1):197-202.

24. Churchill-Davidson I, Sanger C, Thomlinson RH. High pressure oxygen and radiotherapy. Lancet 1955:1091-1095.

25. Henk JM, Kunkler PB, Smith CW. Radiotherapy and hyperbaric oxygen in head and neck cancer. Final report of first controlled clinical trial. Lancet 1977;2(8029):101-3.

26. Ward AJ, Dixon B. Carcinoma of the cervix: results of a hyperbaric oxygen trial associated with the use of the cathetron. Clin Radiol 1979;30(4):383-7.

27. Fletcher GH, Lindberg RD, Caderao JB, Wharton JT. Hyperbaric oxygen as a radiotherapeutic adjuvant in advanced cancer of the uterine cervix: preliminary results of a randomized trial. Cancer 1977;39(2):617-23.

28. Watson ER, Halnan KE, Dische S, Saunders MI, Cade IS, McEwen JB, et al. Hyperbaric oxygen and radiotherapy: a Medical Research Council trial in carcinoma of the cervix. Br J Radiol 1978;51(611):879-87.

29. Cade IS, McEwen JB, Dische S, Saunders MI, Watson ER, Halnan KE, et al. Hyperbaric oxygen and radiotherapy: a Medical Research Council trial in carcinoma of the bladder. Br J Radiol 1978;51(611):876-8.

30. Plenk HP. Hyperbaric radiation therapy. Preliminary results of a randomized study of cancer of the urinary bladder and review of the "oxygen experience". Am J Roentgenol Radium Ther Nucl Med 1972;114(1):152-7.

31. Van den Brenk HA. Hyperbaric oxygen in radiation therapy. An investigation of dose-effect relationships in tumor response and tissue damage. Am J Roentgenol Radium Ther Nucl Med 1968;102(1):8-26.

32. Cade IS, McEwen JB. Clinical trials of radiotherapy in hyperbaric oxygen at Portsmouth, 1964--1976. Clin Radiol 1978;29(3):333-8.

33. Overgaard J. Modification of hypoxia - from Gottwald Schwarz to nicotinamide. Have we learned the lesson? Proceedings 5th International Meeting on Progress in Radio-Oncology,Salzburg, . 1995:pp469.

34. Dische S. Hyperbaric oxygen. Br J Radiol 1979;52(618):508.

35. Adams GEAG, Clarke ED, Gray P, Jacobs RS, Stratford IJ, Wardman P, Watts ME, Parrick J, Wallace RG, Smithen CE. Structure-activity relationships in the

development of hypoxic cell radiosensitizers. Int J Radiat Biol Relat Stud Phys Chem Med 1979;35(2):133- 160.

36. Foster JL, Willson RL. Radiosensitization of anoxic cells by metronidazole. Br J Radiol 1973;46(543):234-5.

37. Gutin PH, Wara WM, Phillips TL, Wilson CB. Hypoxic cell radiosensitizers in the treatment of malignant brain tumors. Neurosurgery 1980;6(5):567-76.

38. Overgaard J, Hansen HS, Andersen AP, Hjelm-Hansen M, Jorgensen K, Sandberg E, et al. Misonidazole combined with split-course radiotherapy in the treatment of invasive carcinoma of larynx and pharynx: report from the DAHANCA 2 study. Int J Radiat Oncol Biol Phys 1989;16(4):1065-8.

39. Sealy R, Cridland S, Barry L, Norris R. Irradiation with misonidazole and hyperbaric oxygen: final report on a randomized trial in advanced head and neck cancer. Int J Radiat Oncol Biol Phys 1986;12(8):1343-6.

40. Eschwege F, Sancho-Garnier H, Chassagne D, Brisgand D, Guerra M, Malaise EP, et al. Results of a European randomized trial of Etanidazole combined with radiotherapy in head and neck carcinomas. Int J Radiat Oncol Biol Phys 1997;39(2):275-81.

41. Lee DJ, Cosmatos D, Marcial VA, Fu KK, Rotman M, Cooper JS, et al. Results of an RTOG phase III trial (RTOG 85-27) comparing radiotherapy plus etanidazole with radiotherapy alone for locally advanced head and neck carcinomas. Int J Radiat Oncol Biol Phys 1995;32(3):567-76.

42. A trial of Ro 03-8799 (pimonidazole) in carcinoma of the uterine cervix: an interim report from the Medical Research Council Working Party on advanced carcinoma of the cervix. Radiother Oncol 1993;26(2):93-103.

43. Chaplin DJ, Horsman MR. Tumor blood flow changes induced by chemical modifiers of radiation response. Int J Radiat Oncol Biol Phys 1992;22(3):459-62.

44. Timothy AR, Overgaard J, Overgaard M. A phase I clinical study of Nimorazole as a hypoxic radiosensitizer. Int J Radiat Oncol Biol Phys 1984;10(9):1765-8.

45. Overgaard J, Hansen HS, Overgaard M, Bastholt L, Berthelsen A, Specht L, et al. A randomized double-blind phase III study of nimorazole as a hypoxic radiosensitizer of primary radiotherapy in supraglottic larynx and pharynx carcinoma. Results of the Danish Head and Neck Cancer Study (DAHANCA) Protocol 5-85. Radiother Oncol 1998;46(2):135-46.

46. Cottrill CP, Bishop K, Walton MI, Henk JM. Pilot study of nimorazole as a hypoxic-cell sensitizer with the "chart" regimen in head and neck cancer. Int J Radiat Oncol Biol Phys 1998;42(4):807-10.

47. Du Sault LA. The effect of oxygen on the response of spontaneous tumours in mice to radiotherapy. Brit J Radiol 1963;36:749-754.

48. Inch WR, McCredie JA, Kruuv J. Effect of breathing 5 per cent carbon dioxide and 95 per cent oxygen at atmospheric pressure on tumour radiocurability. Acta Radiol Ther Phys Biol 1966;4(1):17-25.

49. Bergsjo P, Evans JC. Tissue oxygen tension of cervix cancer. Comparison of effects of breathing a carbon dioxide mixture and pure oxygen. Acta Radiol Ther Phys Biol 1968;7(1):1-11.

50. Siemann DW, Hill RP, Bush RS. The importance of the pre-irradiation breathing times of oxygen and carbogen (5% CO2: 95% O2) on the in vivo radiation response of a murine sarcoma. Int J Radiat Oncol Biol Phys 1977;2(9-10):903-11.

51. Reinhold HS, Blachiewicz B, Berg-Blok A. Reoxygenation of tumours in "sandwich" chambers. Eur J Cancer 1979;15(4):481-9.

52. Yamaura H, Matsuzawa T. Tumor regrowth after irradiation; an experimental approach. Int J Radiat Biol Relat Stud Phys Chem Med 1979;35(3):201-19.

53. Brown JM. Evidence for acutely hypoxic cells in mouse tumours, and a possible mechanism of reoxygenation. Br J Radiol 1979;52(620):650-6.

54. Franko AJ, Raleigh JA, Sutherland RG, Soderlind KJ. Metabolic binding of misonidazole to mouse tissues. Comparison between labels on the ring and side chain, and the production of tritiated water. Biochem Pharmacol 1989;38(4):665-70.

55. Chaplin DJ, Durand RE, Olive PL. Acute hypoxia in tumors: implications for modifiers of radiation effects. Int J Radiat Oncol Biol Phys 1986;12(8):1279-82.

56. Trotter MJ, Chaplin DJ, Durand RE, Olive PL. The use of fluorescent probes to identify regions of transient perfusion in murine tumors. Int J Radiat Oncol Biol Phys 1989;16(4):931-4.

57. Chaplin DJ, Peters CE, Horsman MR, Trotter MJ. Drug induced perturbations in tumor blood flow: therapeutic potential and possible limitations. Radiother Oncol 1991;20 Suppl 1(7):93-101.

58. Chaplin DJ, Hill SA. Temporal heterogeneity in microregional erythrocyte flux in experimental solid tumours. Br J Cancer 1995;71(6):1210-3.

59. Pigott KH, Hill SA, Chaplin DJ, Saunders MI. Microregional fluctuations in perfusion within human tumours detected using laser Doppler flowmetry. Radiother Oncol 1996;40(1):45-50.

60. Ben-Hur E, Elkind MM. Poly(ADP-ribose) metabolism in X-irradiated Chinese hamster cells: its relation to repair of potentially lethal damage. Int J Radiat Biol Relat Stud Phys Chem Med 1984;45(5):515-23.

61. Ben-Hur E, Utsumi H, Elkind MM. Inhibitors of poly(ADP-ribose) synthesis enhance X-ray killing of log-phase Chinese hamster cells. Radiat Res 1984;97(3):546-55.

62. Ben-Hur E, Utsumi H, Elkind MM. Inhibitors of poly (ADP-ribose) synthesis enhance radiation response by differentially affecting repair of potentially lethal versus sublethal damage. Br J Cancer Suppl 1984;6:39-42.

63. Brown DM, Evans JW, Brown JM. The influence of inhibitors of poly (ADP-ribose) polymerase on X-ray-induced potentially lethal damage repair. Br J Cancer Suppl 1984;6:27-31.

64. Hayaishi O, Ueda K. Poly- and mono(ADP-ribosyl)ation reactions: their significance in molecular biology. In: Hayaishi O, Ueda K, editors. ADP- ribosylation reactions. Biology and medicine. New York: Academic Press; 1982. p. 3-16.

65. Horsman MR, Chaplin DJ, Brown JM. Radiosensitization by nicotinamide in vivo: a greater enhancement of tumor damage compared to that of normal tissues. Radiat Res 1987;109(3):479-89.

66. Horsman MR, Brown JM, Hirst VK, Lemmon MJ, Wood PJ, Dunphy EP, et al. Mechanism of action of the selective tumor radiosensitizer nicotinamide. Int J Radiat Oncol Biol Phys 1988;15(3):685-90.

67. Horsman MR, Wood PJ, Chaplin DJ, Brown JM, Overgaard J. The potentiation of radiation damage by nicotinamide in the SCCVII tumour in vivo. Radiother Oncol 1990;18(1):49-57.

68. Chaplin DJ, Olive PL, Durand RE. Intermittent blood flow in a murine tumor: radiobiological effects. Cancer Res 1987;47(2):597-601.

69. Chaplin DJ, Horsman MR, Aoki DS. Nicotinamide, Fluosol DA and Carbogen: a strategy to reoxygenate acutely and chronically hypoxic cells in vivo. Br J Cancer 1991;63(1):109-13.

70. Kjellen E, Joiner MC, Collier JM, Johns H, Rojas A. A therapeutic benefit from combining normobaric carbogen or oxygen with nicotinamide in fractionated X-ray treatments. Radiother Oncol 1991;22(2):81-91.

71. Kaanders JH, Pop LA, Marres HA, van der Maazen RW, van der Kogel AJ, van Daal WA. Radiotherapy with carbogen breathing and nicotinamide in head and neck cancer: feasibility and toxicity. Radiother Oncol 1995;37(3):190-8.

72. Bernier J, Denekamp J, Rojas A, Minatel E, Horiot J, Hamers H, et al. ARCON: accelerated radiotherapy with carbogen and nicotinamide in head and neck squamous cell carcinomas. The experience of the Co-operative group of radiotherapy of the european organization for research and treatment of cancer (EORTC). Radiother Oncol 2000;55(2):111-9.

73. Hoskin PJ, Saunders MI, Phillips H, Cladd H, Powell ME, Goodchild K, et al. Carbogen and nicotinamide in the treatment of bladder cancer with radical radiotherapy. Br J Cancer 1997;76(2):260-3.

74. Denny WA. The role of hypoxia-activated prodrugs in cancer therapy. Lancet Oncol 2000;1(1):25-9.

75. Denny WA, Wilson WR, Hay MP. Recent developments in the design of bioreductive drugs. Br J Cancer Suppl 1996;27:S32-8.

76. Breider MA, Pilcher GD, Graziano MJ, Gough AW. Retinal degeneration in rats induced by CI-1010, a 2-nitroimidazole radiosensitizer. Toxicol Pathol 1998;26(2):234-9.

77. Knox RJ, Friedlos F, Boland MP. The bioactivation of CB 1954 and its use as a prodrug in antibody-directed enzyme prodrug therapy (ADEPT). Cancer Metastasis Rev 1993;12(2):195-212.

78. Belcourt MF, Hodnick WF, Rockwell S, Sartorelli AC. Exploring the mechanistic aspects of mitomycin antibiotic bioactivation in Chinese hamster ovary cells overexpressing NADPH:cytochrome C (P-450) reductase and DT-diaphorase. Adv Enzyme Regul 1998;38(7):111-33.

79. Tomasz M, Palom Y. The mitomycin bioreductive antitumor agents: cross-linking and alkylation of DNA as the molecular basis of their activity. Pharmacol Ther 1997;76(1-3):73-87.

80. Aamdal S, Lund B, Koier I, Houten M, Wanders J, Verweij J. Phase I trial with weekly EO9, a novel bioreductive alkylating indoloquinone, by the EORTC Early Clinical Study Group (ECSG). Cancer Chemother Pharmacol 2000;45(1):85-8.

81. Hwang JT, Greenberg MM, Fuchs T, Gates KS. Reaction of the hypoxia-selective antitumor agent tirapazamine with a C1'-radical in single-stranded and double-stranded DNA: the drug and its metabolites can serve as surrogates for molecular oxygen in radical-mediated DNA damage reactions. Biochemistry 1999;38(43):14248-55.

82. von Pawel J, von Roemeling R, Gatzemeier U, Boyer M, Elisson LO, Clark P, et al. Tirapazamine plus cisplatin versus cisplatin in advanced non-small-cell lung cancer: A report of the international CATAPULT I study group. Cisplatin and Tirapazamine in Subjects with Advanced Previously Untreated Non-Small-Cell Lung Tumors. J Clin Oncol 2000;18(6):1351-9.

83. Lee DJ, Trotti A, Spencer S, Rostock R, Fisher C, von Roemeling R, et al. Concurrent tirapazamine and radiotherapy for advanced head and neck carcinomas: a Phase II study. Int J Radiat Oncol Biol Phys 1998;42(4):811-5.

84. Gatzemeier U, Rodriguez G, Treat J, Miller V, von Roemeling R, Viallet J, et al. Tirapazamine-cisplatin: the synergy. Br J Cancer 1998;77 Suppl 4:15-7.

85. Raleigh SM, Wanogho E, Burke MD, McKeown SR, Patterson LH. Involvement of human cytochromes P450 (CYP) in the reductive metabolism of AQ4N, a hypoxia activated anthraquinone di-N-oxide prodrug. Int J Radiat Oncol Biol Phys 1998;42(4):763-7.

86. McKeown SR, Hejmadi MV, McIntyre IA, McAleer JJ, Patterson LH. AQ4N: an alkylaminoanthraquinone N-oxide showing bioreductive potential and positive interaction with radiation in vivo. Br J Cancer 1995;72(1):76-81.

87. Wilson WR, Moselen JW, Cliffe S, Denny WA, Ware DC. Exploiting tumor hypoxia through bioreductive release of diffusible cytotoxins: the cobalt(III)-nitrogen mustard complex SN 24771. Int J Radiat Oncol Biol Phys 1994;29(2):323-7.

88. Giaccia AJ. Hypoxic Stress Proteins: Survival of the Fittest. Semin Radiat Oncol 1996;6(1):46-58.

89. Webster L, Hodgkiss RJ, Wilson GD. Cell cycle distribution of hypoxia and progression of hypoxic tumour cells in vivo. Br J Cancer 1998;77(2):227-34.

90. Graeber TG, Osmanian C, Jacks T, Housman DE, Koch CJ, Lowe SW, et al. Hypoxia-mediated selection of cells with diminished apoptotic potential in solid tumours. Nature 1996;379(6560):88-91.

91. Soengas MS, Alarcon RM, Yoshida H, Giaccia AJ, Hakem R, Mak TW, et al. Apaf-1 and caspase-9 in p53-dependent apoptosis and tumor inhibition. Science 1999;284(5411):156-9.

92. Wang GL, Jiang BH, Rue EA, Semenza GL. Hypoxia-inducible factor 1 is a basic-helix-loop-helix-PAS heterodimer regulated by cellular O2 tension. Proc Natl Acad Sci U S A 1995;92(12):5510-4.

93. Antoch MP, Song EJ, Chang AM, Vitaterna MH, Zhao Y, Wilsbacher LD, et al. Functional identification of the mouse circadian Clock gene by transgenic BAC rescue. Cell 1997;89(4):655-67.

94. Sun ZS, Albrecht U, Zhuchenko O, Bailey J, Eichele G, Lee CC. RIGUI, a putative mammalian ortholog of the Drosophila period gene. Cell 1997;90(6):1003-11.

95. Tei H, Okamura H, Shigeyoshi Y, Fukuhara C, Ozawa R, Hirose M, et al. Circadian oscillation of a mammalian homologue of the Drosophila period gene. Nature 1997;389(6650):512-6.

96. Crosthwaite SK, Dunlap JC, Loros JJ. Neurospora wc-1 and wc-2: transcription, photoresponses, and the origins of circadian rhythmicity. Science 1997;276(5313):763-9.

97. Wang X, Thomsen JS, Santostefano M, Rosengren R, Safe S, Perdew GH. Comparative properties of the nuclear aryl hydrocarbon (Ah) receptor complex from several human cell lines. Eur J Pharmacol 1995;293(3):191-205.

98. Zelzer E, Wappner P, Shilo BZ. The PAS domain confers target gene specificity of Drosophila bHLH/PAS proteins. Genes Dev 1997;11(16):2079-89.

99. Crews ST. Control of cell lineage-specific development and transcription by bHLH-PAS proteins. Genes Dev 1998;12(5):607-20.

100. Jiang BH, Semenza GL, Bauer C, Marti HH. Hypoxia-inducible factor 1 levels vary exponentially over a physiologically relevant range of O2 tension. Am J Physiol 1996;271(4 Pt 1):C1172-80.

101. Zhong H, De Marzo AM, Laughner E, Lim M, Hilton DA, Zagzag D, et al. Overexpression of hypoxia-inducible factor 1alpha in common human cancers and their metastases. Cancer Res 1999;59(22):5830-5.

102. Zhong H, Agani F, Baccala AA, Laughner E, Rioseco-Camacho N, Isaacs WB, et al. Increased expression of hypoxia inducible factor-1alpha in rat and human prostate cancer. Cancer Res 1998;58(23):5280-4.

103. Gradin K, McGuire J, Wenger RH, Kvietikova I, fhitelaw ML, Toftgard R, et al. Functional interference between hypoxia and dioxin signal transduction pathways: competition for recruitment of the Arnt transcription factor. Mol Cell Biol 1996;16(10):5221-31.

104. Huang LE, Arany Z, Livingston DM, Bunn HF. Activation of hypoxia-inducible transcription factor depends primarily upon redox-sensitive stabilization of its alpha subunit. J Biol Chem 1996;271(50):32253-9.

105. Huang LE, Gu J, Schau M, Bunn HF. Regulation of hypoxia-inducible factor 1alpha is mediated by an O2-dependent degradation domain via the ubiquitin-proteasome pathway. Proc Natl Acad Sci U S A 1998;95(14):7987-92.

106. Kallio PJ, Pongratz I, Gradin K, McGuire J, Poellinger L. Activation of hypoxia-inducible factor 1alpha: posttranscriptional regulation and conformational change by recruitment of the Arnt transcription factor. Proc Natl Acad Sci U S A 1997;94(11):5667-72.

107. Ivan M, Kondo K, Yang H, Kim W, Valiando J, Ohh M, et al. HIFalpha targeted for VHL-mediated destruction by proline hydroxylation: implications for O2 sensing. Science 2001;292(5516):464-8.

108. Zhu H, Bunn HF. Oxygen sensing and signaling: impact on the regulation of physiologically important genes. Respir Physiol 1999;115(2):239-47.

109. Stebbins CE, Kaelin WG, Pavletich NP. Structure of the VHL-ElonginC-ElonginB complex: implications for VHL tumor suppressor function. Science 1999;284(5413):455-61.

110. Ohh M, Takagi Y, Aso T, Stebbins CE, Pavletich NP, Zbar B, et al. Synthetic peptides define critical contacts between elongin C, elongin B, and the von Hippel-Lindau protein. J Clin Invest 1999;104(11):1583-91.

111. Maxwell PH, Wiesener MS, Chang GW, Clifford SC, Vaux EC, Cockman ME, et al. The tumour suppressor protein VHL targets hypoxia-inducible factors for oxygen-dependent proteolysis. Nature 1999;399(6733):271-5.

112. Chilov D, Camenisch G, Kvietikova I, Ziegler U, Gassmann M, Wenger RH. Induction and nuclear translocation of hypoxia-inducible factor-1 (HIF-1): heterodimerization with ARNT is not necessary for nuclear accumulation of HIF-1alpha. J Cell Sci 1999;112(Pt 8)(2):1203-12.

113. Kallio PJ, Okamoto K, O'Brien S, Carrero P, Makino Y, Tanaka H, et al. Signal transduction in hypoxic cells: inducible nuclear translocation and recruitment of the CBP/p300 coactivator by the hypoxia-inducible factor-1alpha. Embo J 1998;17(22):6573-86.

114. Yin H, Blanchard KL. DNA methylation represses the expression of the human erythropoietin gene by two different mechanisms. Blood 2000;95(1):111-9.

115. Wood SM, Wiesener MS, Yeates KM, Okada N, Pugh CW, Maxwell PH, et al. Selection and analysis of a mutant cell line defective in the hypoxia-inducible factor-1 alpha-subunit (HIF-1alpha). Characterization of hif-1alpha-dependent and -independent hypoxia-inducible gene expression. J Biol Chem 1998;273(14):8360-8.

116. Eckhart AD, Yang N, Xin X, Faber JE. Characterization of the alpha1B-adrenergic receptor gene promoter region and hypoxia regulatory elements in vascular smooth muscle. Proc Natl Acad Sci U S A 1997;94(17):9487-92.

117. Cormier-Regard S, Nguyen SV, Claycomb WC. Adrenomedullin gene expression is developmentally regulated and induced by hypoxia in rat ventricular cardiac myocytes. J Biol Chem 1998;273(28):17787-92.

118. Wykoff CC, Beasley NJ, Watson PH, Turner KJ, Pastorek J, Sibtain A, et al. Hypoxia-inducible expression of tumor-associated carbonic anhydrases. Cancer Res 2000;60(24):7075-83.

119. Yamashita K, Discher DJ, Hu J, Bishopric NH, Webster KA. Molecular regulation of the endothelin-1 gene by hypoxia. Contributions of hypoxia-inducible factor-1, activator protein-1, GATA-2, AND p300/CBP. J Biol Chem 2001;276(16):12645-53.

120. Hu J, Discher DJ, Bishopric NH, Webster KA. Hypoxia regulates expression of the endothelin-1 gene through a proximal hypoxia-inducible factor-1 binding site on the antisense strand. Biochem Biophys Res Commun 1998;245(3):894-9.

121. Iyer NV, Leung SW, Semenza GL. The human hypoxia-inducible factor 1alpha gene: HIF1A structure and evolutionary conservation. Genomics 1998;52(2):159-65.

122. Jiang BH, Rue E, Wang GL, Roe R, Semenza GL. Dimerization, DNA binding, and transactivation properties of hypoxia-inducible factor 1. J Biol Chem 1996;271(30):17771-8.

123. Behrooz A, Ismail-Beigi F. Stimulation of Glucose Transport by Hypoxia: Signals and Mechanisms. News Physiol Sci 1999;14:105-110.

124. Zhang JZ, Behrooz A, Ismail-Beigi F. Regulation of glucose transport by hypoxia. Am J Kidney Dis 1999;34(1):189-202.

125. Lee PJ, Jiang BH, Chin BY, Iyer NV, Alam J, Semenza GL, et al. Hypoxia-inducible factor-1 mediates transcriptional activation of the heme oxygenase-1 gene in response to hypoxia. J Biol Chem 1997;272(9):5375-81.

126. Feldser D, Agani F, Iyer NV, Pak B, Ferreira G, Semenza GL. Reciprocal positive regulation of hypoxia-inducible factor 1alpha and insulin-like growth factor 2. Cancer Res 1999;59(16):3915-8.

127. Tazuke SI, Mazure NM, Sugawara J, Carland G, Faessen GH, Suen LF, et al. Hypoxia stimulates insulin-like growth factor binding protein 1 (IGFBP-1) gene

expression in HepG2 cells: a possible model for IGFBP-1 expression in fetal hypoxia. Proc Natl Acad Sci U S A 1998;95(17):10188-93.

128. Melillo G, Musso T, Sica A, Taylor LS, Cox GW, Varesio L. A hypoxia-responsive element mediates a novel pathway of activation of the inducible nitric oxide synthase promoter. J Exp Med 1995;182(6):1683-93.

129. Carmeliet P, Dor Y, Herbert JM, Fukumura D, Brusselmans K, Dewerchin M, et al. Role of HIF-1alpha in hypoxia-mediated apoptosis, cell proliferation and tumour angiogenesis. Nature 1998;394(6692):485-90.

130. Pugh CW, O'Rourke JF, Nagao M, Gleadle JM, Ratcliffe PJ. Activation of hypoxia-inducible factor-1; definition of regulatory domains within the alpha subunit. J Biol Chem 1997;272(17):11205-14.

131. Tacchini L, Bianchi L, Bernelli-Zazzera A, Cairo G. Transferrin receptor induction by hypoxia. HIF-1-mediated transcriptional activation and cell-specific post-transcriptional regulation. J Biol Chem 1999;274(34):24142-6.

132. Gerber HP, Condorelli F, Park J, Ferrara N. Differential transcriptional regulation of the two vascular endothelial growth factor receptor genes. Flt-1, but not Flk-1/KDR, is up-regulated by hypoxia. J Biol Chem 1997;272(38):23659-67.

133. Sowter HM, Ratcliffe PJ, Watson P, Greenberg AH, Harris AL. HIF-1-dependent regulation of hypoxic induction of the cell death factors BNIP3 and NIX in human tumors. Cancer Res 2001;61(18):6669-73.

134. Marme D. Tumor angiogenesis: the pivotal role of vascular endothelial growth factor. World J Urol 1996;14(3):166-74.

135. Lal A, Peters H, St Croix B, Haroon ZA, Dewhirst MW, Strausberg RL, et al. Transcriptional response to hypoxia in human tumors. J Natl Cancer Inst 2001;93(17):1337-43.

136. Pal S, Datta K, Mukhopadhyay D. Central role of p53 on regulation of vascular permeability factor/vascular endothelial growth factor (VPF/VEGF) expression in mammary carcinoma. Cancer Res 2001;61(18):6952-7.

137. Salven P, Manpaa H, Orpana A, Alitalo K, Joensuu H. Serum vascular endothelial growth factor is often elevated in disseminated cancer. Clin Cancer Res 1997;3(5):647-51.

138. Ocharoenrat P, Rhys-Evans P, Eccles SA. Expression of vascular endothelial growth factor family members in head and neck squamous cell carcinoma correlates with lymph node metastasis. Cancer 2001;92(3):556-68.

139. Salven P, Heikkila P, Anttonen A, Kajanti M, Joensuu H. Vascular endothelial growth factor in squamous cell head and neck carcinoma: expression and prognostic significance. Mod Pathol 1997;10(11):1128-33.

140. Ahn MJ, Jang SJ, Park YW, Choi JH, Oh HS, Lee CB, et al. Clinical prognostic values of vascular endothelial growth factor, microvessel density,and p53 expression in esophageal carcinomas. J Korean Med Sci 2002;17(2):201-7.

141. Lennard CM, Patel A, Wilson J, Reinhardt B, Tuman C, Fenton C, et al. Intensity of vascular endothelial growth factor expression is associated with increased risk of recurrence and decreased disease-free survival in papillary thyroid cancer. Surgery 2001;129(5):552-8.

142. Baillie R, Carlile J, Pendleton N, Schor AM. Prognostic value of vascularity and vascular endothelial growth factor expression in non-small cell lung cancer. J Clin Pathol 2001;54(2):116-20.

143. White JD, Hewett PW, Kosuge D, McCulloch T, Enholm BC, Carmichael J, et al. Vascular endothelial growth factor-D expression is an independent prognostic marker for survival in colorectal carcinoma. Cancer Res 2002;62(6):1669-75.

144. Abdulrauf SI, Edvardsen K, Ho KL, Yang XY, Rock JP, Rosenblum ML. Vascular endothelial growth factor expression and vascular density as prognostic markers of survival in patients with low-grade astrocytoma. J Neurosurg 1998;88(3):513-20.

145. Blancher C, Moore JW, Talks KL, Houlbrook S, Harris AL. Relationship of hypoxia-inducible factor (HIF)-1alpha and HIF-2alpha expression to vascular

endothelial growth factor induction and hypoxia survival in human breast cancer cell lines. Cancer Res 2000;60(24):7106-13.

146. De Paola F, Granato AM, Scarpi E, Monti F, Medri L, Bianchi S, et al. Vascular endothelial growth factor and prognosis in patients with node-negative breast cancer. Int J Cancer 2002;98(2):228-33.

147. Toi M, Inada K, Suzuki H, Tominaga T. Tumor angiogenesis in breast cancer: its importance as a prognostic indicator and the association with vascular endothelial growth factor expression. Breast Cancer Res Treat 1995;36(2):193-204.

148. Plate KH, Breier G, Weich HA, Risau W. Vascular endothelial growth factor is a potential tumour angiogenesis factor in human gliomas in vivo. Nature 1992;359(6398):845-8.

149. Grugel S, Finkenzeller G, Weindel K, Barleon B, Marme D. Both v-Ha-Ras and v-Raf stimulate expression of the vascular endothelial growth factor in NIH 3T3 cells. J Biol Chem 1995;270(43):25915-9.

150. Kieser A, Weich HA, Brandner G, Marme D, Kolch W. Mutant p53 potentiates protein kinase C induction of vascular endothelial growth factor expression. Oncogene 1994;9(3):963-9.

151. Parliament MB, Allalunis-Turner MJ, Franko AJ, Olive PL, Mandyam R, Santos C, et al. Vascular endothelial growth factor expression is independent of hypoxia in human malignant glioma spheroids and tumours. Br J Cancer 2000;82(3):635-41.

152. Raleigh JA, Calkins-Adams DP, Rinker LH, Ballenger CA, Weissler MC, Fowler WC, et al. Hypoxia and vascular endothelial growth factor expression in human squamous cell carcinomas using pimonidazole as a hypoxia marker. Cancer Res 1998;58(17):3765-8.

153. Minchenko A, Bauer T, Salceda S, Caro J. Hypoxic stimulation of vascular endothelial growth factor expression in vitro and in vivo. Lab Invest 1994;71(3):374-9.

154. Levy NS, Chung S, Furneaux H, Levy AP. Hypoxic stabilization of vascular endothelial growth factor mRNA by the RNA-binding protein HuR. J Biol Chem 1998;273(11):6417-23.

155. Akiri G, Nahari D, Finkelstein Y, Le SY, Elroy-Stein O, Levi BZ. Regulation of vascular endothelial growth factor (VEGF) expression is mediated by internal initiation of translation and alternative initiation of transcription. Oncogene 1998;17(2):227-36.

156. Griffiths L, Dachs GU, Bicknell R, Harris AL, Stratford IJ. The influence of oxygen tension and pH on the expression of platelet-derived endothelial cell growth factor/thymidine phosphorylase in human breast tumor cells grown in vitro and in vivo. Cancer Res 1997;57(4):570-2.

157. Kimura H, Weisz A, Kurashima Y, Hashimoto K, Ogura T, D'Acquisto F, et al. Hypoxia response element of the human vascular endothelial growth factor gene mediates transcriptional regulation by nitric oxide: control of hypoxia-inducible factor-1 activity by nitric oxide. Blood 2000;95(1):189-97.

158. Ivanov SV, Kuzmin I, Wei MH, Pack S, Geil L, Johnson BE, et al. Down-regulation of transmembrane carbonic anhydrases in renal cell carcinoma cell lines by wild-type von Hippel-Lindau transgenes. Proc Natl Acad Sci U S A 1998;95(21):12596-601.

159. Airley RE, Loncaster J, Raleigh JA, Harris AL, Davidson SE, Hunter RD, et al. GLUT-1 and CAIX as intrinsic markers of hypoxia in carcinoma of the cervix: relationship to pimonidazole binding. Int J Cancer 2003;104(1):85-91.

160. Blagosklonny MV, An WG, Romanova LY, Trepel J, Fojo T, Neckers L. p53 inhibits hypoxia-inducible factor-stimulated transcription. J Biol Chem 1998;273(20):11995-8.

161. Wenger RH, Camenisch G, Desbaillets I, Chilov D, Gassmann M. Up-regulation of hypoxia-inducible factor-1alpha is not sufficient for hypoxic/anoxic p53 induction. Cancer Res 1998;58(24):5678-80.

162. Ravi R, Mookerjee B, Bhujwalla ZM, Sutter CH, Artemov D, Zeng Q, et al. Regulation of tumor angiogenesis by p53-induced degradation of hypoxia-inducible factor 1alpha. Genes Dev 2000;14(1):34-44.

163. Brown JM, Giaccia AJ. Tumour hypoxia: the picture has changed in the 1990s. Int J Radiat Biol 1994;65(1):95-102.

164. Koong AC, Chen EY, Giaccia AJ. Hypoxia causes the activation of nuclear factor kappa B through the phosphorylation of I kappa B alpha on tyrosine residues. Cancer Res 1994;54(6):1425-30.

165. Kolstad P. Intercapillary distance, oxygen tension and local recurrence in cervix cancer. Scand J Clin Lab Invest Suppl 1968;106:145-57.

166. Vaupel P, Kallinowski F, Okunieff P. Blood flow, oxygen and nutrient supply, and metabolic microenvironment of human tumors: a review. Cancer Res 1989;49(23):6449-65.

167. Vaupel P, Schlenger K, Knoop C, Hockel M. Oxygenation of human tumors: evaluation of tissue oxygen distribution in breast cancers by computerized O2 tension measurements. Cancer Res 1991;51(12):3316-22.

168. Grischke EM, von Fournier D, Sohn C, Wallwiener D, Bastert G. [Diagnostic value of Doppler ultrasound in evaluation of breast tumors]. Zentralbl Gynakol 1996;118(10):553-9.

169. Hohenberger P, Felgner C, Haensch W, Schlag PM. Tumor oxygenation correlates with molecular growth determinants in breast cancer. Breast Cancer Res Treat 1998;48(2):97-106.

170. Fuller J, Feldmann HJ, Molls M, Sack H. [Studies on oxygen partial pressure in tumor tissue under radiotherapy and thermoradiotherapy]. Strahlenther Onkol 1994;170(8):453-60.

171. Gatenby RA, Kessler HB, Rosenblum JS, Coia LR, Moldofsky PJ, Hartz WH, et al. Oxygen distribution in squamous cell carcinoma metastases and its

relationship to outcome of radiation therapy. Int J Radiat Oncol Biol Phys 1988;14(5):831-8.

172. Nordsmark M, Overgaard M, Overgaard J. Pretreatment oxygenation predicts radiation response in advanced squamous cell carcinoma of the head and neck. Radiother Oncol 1996;41(1):31-9.

173. Brizel DM, Sibley GS, Prosnitz LR, Scher RL, Dewhirst MW. Tumor hypoxia adversely affects the prognosis of carcinoma of the head and neck. Int J Radiat Oncol Biol Phys 1997;38(2):285-9.

174. Stadler P, Becker A, Feldmann HJ, Hansgen G, Dunst J, Wurschmidt F, et al. Influence of the hypoxic subvolume on the survival of patients with head and neck cancer. Int J Radiat Oncol Biol Phys 1999;44(4):749-54.

175. Hockel M, Vorndran B, Schlenger K, Baussmann E, Knapstein PG. Tumor oxygenation: a new predictive parameter in locally advanced cancer of the uterine cervix. Gynecol Oncol 1993;51(2):141-9.

176. Hockel M, Schlenger K, Hockel S, Aral B, Schaffer U, Vaupel P. Tumor hypoxia in pelvic recurrences of cervical cancer. Int J Cancer 1998;79(4):365-9.

177. Fyles AW, Milosevic M, Wong R, Kavanagh MC, Pintilie M, Sun A, et al. Oxygenation predicts radiation response and survival in patients with cervix cancer. Radiother Oncol 1998;48(2):149-56.

178. Knocke TH, Weitmann HD, Feldmann HJ, Selzer E, Potter R. Intratumoral pO2-measurements as predictive assay in the treatment of carcinoma of the uterine cervix. Radiother Oncol 1999;53(2):99-104.

179. Brizel DM, Scully SP, Harrelson JM, Layfield LJ, Bean JM, Prosnitz LR, et al. Tumor oxygenation predicts for the likelihood of distant metastases in human soft tissue sarcoma. Cancer Res 1996;56(5):941-3.

180. Nordsmark M, Alsner J, Keller J, Nielsen OS, Jensen OM, Horsman MR, et al. Hypoxia in human soft tissue sarcomas: adverse impact on survival and no association with p53 mutations. Br J Cancer 2001;84(8):1070-5.

181. Collingridge DR, Young WK, Vojnovic B, Wardman P, Lynch EM, Hill SA, et al. Measurement of tumor oxygenation: a comparison between polarographic needle electrodes and a time-resolved luminescence-based optical sensor. Radiat Res 1997;147(3):329-34.

182. Chapman JD, Reuvers AP, Borsa J, Henderson JS, Migliore RD. Nitroheterocyclic drugs as selective radiosensitizers of hypoxic mammalian cells. Cancer Chemother Rep 1974;58(4):559-70.

183. Raleigh JA, Chapman JD, Reuvers AP, Biaglow JE, Durand RE, Rauth AM. Nitropyrrole radiosensitizers: structure function relationships. Br J Cancer Suppl 1978;37(3):6-10.

184. Varghese AJ, Gulyas S, Mohindra JK. Hypoxia-dependent reduction of 1-(2-nitro-1-imidazolyl)-3-methoxy-2-propanol by Chinese hamster ovary cells and KHT tumor cells in vitro and in vivo. Cancer Res 1976;36(10):3761-5.

185. Hodgkiss RJ. Use of 2-nitroimidazoles as bioreductive markers for tumour hypoxia. Anticancer Drug Des 1998;13(6):687-702.

186. Mason RP, Holtzman JL. The mechanism of microsomal and mitochondrial nitroreductase. Electron spin resonance evidence for nitroaromatic free radical intermediates. Biochemistry 1975;14(8):1626-32.

187. Wardman P. Hypoxic cell radiosensitizers--chemical aspects and in vitro models. Strahlentherapie [Sonderb] 1978;75(1):20-6.

188. Heimbrook DC, Sartorelli AC. Biochemistry of misonidazole reduction by NADPH-cytochrome c (P-450) reductase. Mol Pharmacol 1986;29(2):168-72.

189. Raleigh JA, Franko AJ, Koch CJ, Born JL. Binding of misonidazole to hypoxic cells in monolayer and spheroid culture: evidence that a side-chain label is bound as efficiently as a ring label. Br J Cancer 1985;51(2):229-35.

190. Chapman JD, Lee J, Meeker BE. Keynote address: cellular reduction of nitroimidazole drugs: potential for selective chemotherapy and diagnosis of hypoxic cells. Int J Radiat Oncol Biol Phys 1989;16(4):911-7.

191. Chapman JD. Measurement of tumor hypoxia by invasive and non-invasive procedures: a review of recent clinical studies. Radiother Oncol 1991;20 Suppl 1(4):13-9.

192. Chapman JD, Baer K, Lee J. Characteristics of the metabolism-induced binding of misonidazole to hypoxic mammalian cells. Cancer Res 1983;43(4):1523-8.

193. Koch CJ, Stobbe CC, Baer KA. Metabolism induced binding of 14C-misonidazole to hypoxic cells: kinetic dependence on oxygen concentration and misonidazole concentration. Int J Radiat Oncol Biol Phys 1984;10(8):1327-31.

194. Hodgkiss RJ, Middleton RW, Parrick J, Rami HK, Wardman P, Wilson GD. Bioreductive fluorescent markers for hypoxic cells: a study of 2-nitroimidazoles with 1-substituents containing fluorescent, bridgehead-nitrogen, bicyclic systems. J Med Chem 1992;35(10):1920-6.

195. Begg AC, Sheldon PW, Foster JL. Demonstration of radiosensitization of hypoxic cells in solid tumours by metronidazole. Br J Radiol 1974;47(559):399-404.

196. Chapman JD, Franko AJ, Sharplin J. A marker for hypoxic cells in tumours with potential clinical applicability. Br J Cancer 1981;43(4):546-50.

197. Franko AJ, Koch CJ. Binding of misonidazole to V79 spheroids and fragments of Dunning rat prostatic and human colon carcinomas in vitro: diffusion of oxygen and reactive metabolites. Int J Radiat Oncol Biol Phys 1984;10(8):1333-6.

198. Urtasun RC, Chapman JD, Raleigh JA, Franko AJ, Koch CJ. Binding of 3H-misonidazole to solid human tumors as a measure of tumor hypoxia. Int J Radiat Oncol Biol Phys 1986;12(7):1263-7.

199. Raleigh JA, Miller GG, Franko AJ, Koch CJ, Fuciarelli AF, Kelly DA. Fluorescence immunohistochemical detection of hypoxic cells in spheroids and tumours. Br J Cancer 1987;56(4):395-400.

200. Cline JM, Thrall DE, Page RL, Franko AJ, Raleigh JA. Immunohistochemical detection of a hypoxia marker in spontaneous canine tumours. Br J Cancer 1990;62(6):925-31.

201. Cline JM, Thrall DE, Rosner GL, Raleigh JA. Distribution of the hypoxia marker CCI-103F in canine tumors. Int J Radiat Oncol Biol Phys 1994;28(4):921-33.

202. Raleigh JA, Zeman EM, Rathman M, LaDine JK, Cline JM, Thrall DE. Development of an ELISA for the detection of 2-nitroimidazole hypoxia markers bound to tumor tissue. Int J Radiat Oncol Biol Phys 1992;22(3):403-5.

203. Zeman EM, Calkins DP, Cline JM, Thrall DE, Raleigh JA. The relationship between proliferative and oxygenation status in spontaneous canine tumors. Int J Radiat Oncol Biol Phys 1993;27(4):891-8.

204. Azuma C, Raleigh JA, Thrall DE. Longevity of pimonidazole adducts in spontaneous canine tumors as an estimate of hypoxic cell lifetime. Radiat Res 1997;148(1):35-42.

205. Arteel GE, Thurman RG, Yates JM, Raleigh JA. Evidence that hypoxia markers detect oxygen gradients in liver: pimonidazole and retrograde perfusion of rat liver. Br J Cancer 1995;72(4):889-95.

206. Kennedy AS, Raleigh JA, Perez GM, Calkins DP, Thrall DE, Novotny DB, et al. Proliferation and hypoxia in human squamous cell carcinoma of the cervix: first report of combined immunohistochemical assays. Int J Radiat Oncol Biol Phys 1997;37(4):897-905.

207. Evans SM, Hahn S, Pook DR, Jenkins WT, Chalian AA, Zhang P, et al. Detection of hypoxia in human squamous cell carcinoma by EF5 binding. Cancer Res 2000;60(7):2018-24.

208. Hodgkiss RJ, Begg AC, Middleton RW, Parrick J, Stratford MR, Wardman P, et al. Fluorescent markers for hypoxic cells. A study of novel heterocyclic compounds that undergo bio-reductive binding. Biochem Pharmacol 1991;41(4):533-41.

209. Zavada J, Zavadova Z, Pastorekova S, Ciampor F, Pastorek J, Zelnik V. Expression of MaTu-MN protein in human tumor cultures and in clinical specimens. Int J Cancer 1993;54(2):268-74.

210. Pastorekova S, Parkkila S, Parkkila AK, Opavsky R, Zelnik V, Saarnio J, et al. Carbonic anhydrase IX, MN/CA IX: analysis of stomach complementary DNA sequence and expression in human and rat alimentary tracts. Gastroenterology 1997;112(2):398-408.

211. Saarnio J, Parkkila S, Parkkila AK, Haukipuro K, Pastorekova S, Pastorek J, et al. Immunohistochemical study of colorectal tumors for expression of a novel transmembrane carbonic anhydrase, MN/CA IX, with potential value as a marker of cell proliferation. Am J Pathol 1998;153(1):279-85.

212. Karhumaa P, Kaunisto K, Parkkila S, Waheed A, Pastorekova S, Pastorek J, et al. Expression of the transmembrane carbonic anhydrases, CA IX and CA XII, in the human male excurrent ducts. Mol Hum Reprod 2001;7(7):611-6.

213. Liao SY, Aurelio ON, Jan K, Zavada J, Stanbridge EJ. Identification of the MN/CA9 protein as a reliable diagnostic biomarker of clear cell carcinoma of the kidney. Cancer Res 1997;57(14):2827-31.

214. Turner JR, Odze RD, Crum CP, Resnick MB. MN antigen expression in normal, preneoplastic, and neoplastic esophagus: a clinicopathological study of a new cancer-associated biomarker. Hum Pathol 1997;28(6):740-4.

215. Vermylen P, Roufosse C, Burny A, Verhest A, Bosschaerts T, Pastorekova S, et al. Carbonic anhydrase IX antigen differentiates between preneoplastic malignant lesions in non-small cell lung carcinoma. Eur Respir J 1999;14(4):806-11.

216. Kivela AJ, Saarnio J, Karttunen TJ, Kivela J, Parkkila AK, Pastorekova S, et al. Differential expression of cytoplasmic carbonic anhydrases, CA I and II, and membrane-associated isozymes, CA IX and XII, in normal mucosa of large intestine and in colorectal tumors. Dig Dis Sci 2001;46(10):2179-86.

217. Beasley NJ, Wykoff CC, Watson PH, Leek R, Turley H, Gatter K, et al. Carbonic Anhydrase IX, an Endogenous Hypoxia Marker, Expression in Head and Neck Squamous Cell Carcinoma and its Relationship to Hypoxia, Necrosis, and Microvessel Density. Cancer Res 2001;61(13):5262-7.

218. Ivanov S, Liao SY, Ivanova A, Danilkovitch-Miagkova A, Tarasova N, Weirich G, et al. Expression of hypoxia-inducible cell-surface transmembrane carbonic anhydrases in human cancer. Am J Pathol 2001;158(3):905-19.

219. Mueckler M. Facilitative glucose transporters. Eur J Biochem 1994;219(3):713-25.

220. Nagase Y, Takata K, Moriyama N, Aso Y, Murakami T, Hirano H. Immunohistochemical localization of glucose transporters in human renal cell carcinoma. J Urol 1995;153(3 Pt 1):798-801.

221. Mellanen P, Minn H, Grenman R, Harkonen P. Expression of glucose transporters in head-and-neck tumors. Int J Cancer 1994;56(5):622-9.

222. Cornford EM, Hyman S, Black KL, Cornford ME, Vinters HV, Pardridge WM. High expression of the Glut1 glucose transporter in human brain hemangioblastoma endothelium. J Neuropathol Exp Neurol 1995;54(6):842-51.

223. Brown RS, Wahl RL. Overexpression of Glut-1 glucose transporter in human breast cancer. An immunohistochemical study. Cancer 1993;72(10):2979-85.

224. Cantuaria G, Magalhaes A, Penalver M, Angioli R, Braunschweiger P, Gomez-Marin O, et al. Expression of GLUT-1 glucose transporter in borderline and malignant epithelial tumors of the ovary. Gynecol Oncol 2000;79(1):33-7.

225. Cantuaria G, Fagotti A, Ferrandina G, Magalhaes A, Nadji M, Angioli R, et al. GLUT-1 expression in ovarian carcinoma: association with survival and response to chemotherapy. Cancer 2001;92(5):1144-50.

226. Kawamura T, Kusakabe T, Sugino T, Watanabe K, Fukuda T, Nashimoto A, et al. Expression of glucose transporter-1 in human gastric carcinoma: association

with tumor aggressiveness, metastasis, and patient survival. Cancer 2001;92(3):634-41.

227. Shi Y, Liu H, Vanderburg G, Samuel SJ, Ismail-Beigi F, Jung CY. Modulation of GLUT1 intrinsic activity in clone 9 cells by inhibition of oxidative phosphorylation. J Biol Chem 1995;270(37):21772-8.

228. Diamond DL, Carruthers A. Metabolic control of sugar transport by derepression of cell surface glucose transporters. An insulin-independent recruitment-independent mechanism of regulation. J Biol Chem 1993;268(9):6437-44.

229. Ismail-Beigi F, Vanderburg G. Effect of GLUT1 glucose transporter overexpression on the stimulation of glucose transport in response to inhibition of oxidative phosphorylation. Arch Biochem Biophys 1996;331(2):201-7.

230. Behrooz A, Ismail-Beigi F. Dual control of glut1 glucose transporter gene expression by hypoxia and by inhibition of oxidative phosphorylation. J Biol Chem 1997;272(9):5555-62.

231. Ebert BL, Firth JD, Ratcliffe PJ. Hypoxia and mitochondrial inhibitors regulate expression of glucose transporter-1 via distinct Cis-acting sequences. J Biol Chem 1995;270(49):29083-9.

232. Chen C, Pore N, Behrooz A, Ismail-Beigi F, Maity A. Regulation of glut1 mRNA by hypoxia-inducible factor-1. Interaction between H-ras and hypoxia. J Biol Chem 2001;276(12):9519-25.

233. Rasey JS, Grunbaum Z, Krohn K, Nelson N, Chin L. Comparison of binding of [3H]misonidazole and [14C]misonidazole in multicell spheroids. Radiat Res 1985;101(3):473-9.

234. Rasey JS, Koh WJ, Grierson JR, Grunbaum Z, Krohn KA. Radiolabelled fluoromisonidazole as an imaging agent for tumor hypoxia. Int J Radiat Oncol Biol Phys 1989;17(5):985-91.

235. Rasey JS, Grunbaum Z, Magee S, Nelson NJ, Olive PL, Durand RE, et al. Characterization of radiolabeled fluoromisonidazole as a probe for hypoxic cells. Radiat Res 1987;111(2):292-304.

236. Biskupiak JE, Grierson JR, Rasey JS, Martin GV, Krohn KA. Synthesis of an (iodovinyl)misonidazole derivative for hypoxia imaging. J Med Chem 1991;34(7):2165-8.

237. Mannan RH, Mercer JR, Wiebe LI, Somayaji VV, Chapman JD. Radioiodinated 1-(2-fluoro-4-iodo-2,4-dideoxy-beta-L-xylopyranosyl)-2-nitroimidazole: a novel probe for the noninvasive assessment of tumor hypoxia. Radiat Res 1992;132(3):368-74.

238. Mannan RH, Somayaji VV, Lee J, Mercer JR, Chapman JD, Wiebe LI. Radioiodinated 1-(5-iodo-5-deoxy-beta-D-arabinofuranosyl)-2-nitroimidazole (iodoazomycin arabinoside: IAZA): a novel marker of tissue hypoxia. J Nucl Med 1991;32(9):1764-70.

239. Cherif A, Wallace S, Yang DJ, Newman RA, Harrod VL, Nornoo A, et al. Development of new markers for hypoxic cells: [131I]Iodomisonidazole and [131I]Iodoerythronitroimidazole. J Drug Target 1996;4(1):31-9.

240. Linder KE, Chan YW, Cyr JE, Malley MF, Nowotnik DP, Nunn AD. TcO(PnA.O-1-(2-nitroimidazole)) [BMS-181321], a new technetium-containing nitroimidazole complex for imaging hypoxia: synthesis, characterization, and xanthine oxidase-catalyzed reduction. J Med Chem 1994;37(1):9-17.

241. Wiebe LI, Stypinski D. Pharmacokinetics of SPECT radiopharmaceuticals for imaging hypoxic tissues. Q J Nucl Med 1996;40(3):270-84.

242. Parliament MB, Chapman JD, Urtasun RC, McEwan AJ, Golberg L, Mercer JR, et al. Non-invasive assessment of human tumour hypoxia with 123I-iodoazomycin arabinoside: preliminary report of a clinical study. Br J Cancer 1992;65(1):90-5.

243. Urtasun RC, Parliament MB, McEwan AJ, Mercer JR, Mannan RH, Wiebe LI, et al. Measurement of hypoxia in human tumours by non-invasive spect imaging of iodoazomycin arabinoside. Br J Cancer Suppl 1996;27(5):S209-12.

244. Vaupel P, Schlenger K, Hoeckel M. Blood flow and tissue oxygenation of human tumors: an update. Adv Exp Med Biol 1992;317:139-51.

245. Groshar D, McEwan AJ, Parliament MB, Urtasun RC, Golberg LE, Hoskinson M, et al. Imaging tumor hypoxia and tumor perfusion. J Nucl Med 1993;34(6):885-8.

246. Rasey JS, Koh WJ, Evans ML, Peterson LM, Lewellen TK, Graham MM, et al. Quantifying regional hypoxia in human tumors with positron emission tomography of [18F]fluoromisonidazole: a pretherapy study of 37 patients. Int J Radiat Oncol Biol Phys 1996;36(2):417-28.

247. Chapman JD, Engelhardt EL, Stobbe CC, Schneider RF, Hanks GE. Measuring hypoxia and predicting tumor radioresistance with nuclear medicine assays. Radiother Oncol 1998;46(3):229-37.

248. Cook GJ, Houston S, Barrington SF, Fogelman I. Technetium-99m-labeled HL91 to identify tumor hypoxia: correlation with fluorine-18-FDG. J Nucl Med 1998;39(1):99-103.

249. Honess DJ, Hill SA, Collingridge DR, Edwards B, Brauers G, Powell NA, et al. Preclinical evaluation of the novel hypoxic marker 99mTc-HL91 (Prognox) in murine and xenograft systems in vivo. Int J Radiat Oncol Biol Phys 1998;42(4):731-5.

250. Kinuya S, Yokoyama K, Konishi S, Li XF, Watanabe N, Shuke N, et al. Increased uptake of 99mTc-HL91 in tumor cells exposed to X-ray radiation. Ann Nucl Med 2000;14(2):139-41.

251. Okada RD, Johnson G, Nguyen KN, Edwards B, Archer CM, Kelly JD. 99mTc-HL91. Effects of low flow and hypoxia on a new ischemia-avid myocardial imaging agent. Circulation 1997;95(7):1892-9.

252. Raleigh JA, Franko AJ, Treiber EO, Lunt JA, Allen PS. Covalent binding of a fluorinated 2-nitroimidazole to EMT-6 tumors in Balb/C mice: detection by F-19 nuclear magnetic resonance at 2.35 T. Int J Radiat Oncol Biol Phys 1986;12(7):1243-5.

253. Li SJ, Jin GY, Moulder JE. Prediction of tumor radiosensitivity by hexafluoromisonidazole retention monitored by [1H]/[19F] magnetic resonance spectroscopy. Cancer Commun 1991;3(5):133-9.

254. Kwock L, Gill M, McMurry HL, Beckman W, Raleigh JA, Joseph AP. Evaluation of a fluorinated 2-nitroimidazole binding to hypoxic cells in tumor-bearing rats by 19F magnetic resonance spectroscopy and immunohistochemistry. Radiat Res 1992;129(1):71-8.

255. Raleigh JA, Franko AJ, Kelly DA, Trimble LA, Allen PS. Development of an in vivo 19F magnetic resonance method for measuring oxygen deficiency in tumors. Magn Reson Med 1991;22(2):451-66.

256. Maxwell RJ, Workman P, Griffiths JR. Demonstration of tumor-selective retention of fluorinated nitroimidazole probes by 19F magnetic resonance spectroscopy in vivo. Int J Radiat Oncol Biol Phys 1989;16(4):925-9.

257. Aboagye EO, Kelson AB, Tracy M, Workman P. Preclinical development and current status of the fluorinated 2-nitroimidazole hypoxia probe N-(2-hydroxy-3,3,3-trifluoropropyl)-2-(2-nitro-1-imidazolyl) acetamide (SR 4554, CRC 94/17): a non-invasive diagnostic probe for the measurement of tumor hypoxia by magnetic resonance spectroscopy and imaging, and by positron emission tomography. Anticancer Drug Des 1998;13(6):703-30.

258. Parker SL, Tong T, Bolden S, Wingo PA. Cancer Statistics. CA Cancer J Clin 1997;47:5-27.

259. Morrison AS, Buring JE, Verhoek WG, other AN. An international study of smoking and bladder cancer. J Urol 1984;131:650-4.

260. Patton SE, Hall MC, Ozen H. Bladder Cancer. Current Opinion in Oncology 2002;14:265–272.

261. Yasuma T, Koikawa Y, Uozumi J. Clinical study of asymptomatic microscopic haematuria. Int J Urol Nephrol 1994;26:1-6.

262. Stein JP, Lieskovsky G, Cote R, Groshen S, Feng AC, Boyd S, et al. Radical cystectomy in the treatment of invasive bladder cancer: long-term results in 1,054 patients. J Clin Oncol 2001;19(3):666-75.

263. Petrovich Z, Jozsef G, Brady LW. Radiotherapy for carcinoma of the bladder: a review. Am J Clin Oncol 2001;24(1):1-9.

264. Zenser TV, Mattammal MB, Palmier MO, Davis BB. Microsomal nitroreductase activity of rabbit kidney and bladder: implications in 5-nitrofuran-induced toxicity. J Pharmacol Exp Ther 1981;219(3):735-40.

265. Raleigh JA, Chou SC, Arteel GE, Horsman MR. Comparisons among pimonidazole binding, oxygen electrode measurements, and radiation response in C3H mouse tumors. Radiat Res 1999;151(5):580-9.

266. Raleigh JA, Chou S, Bono EL, Thrall DE, Varia MA. Semiquantitative immunohistochemical analysis for hypoxia in human tumors. Int J Radiat Oncol Biol Phys 2001;49(2):569-574.

267. Durand RE, Raleigh JA. Identification of nonproliferating but viable hypoxic tumor cells in vivo. Cancer Res 1998;58(16):3547-50.

268. Bussink J, Kaanders JH, Rijken PF, Martindale CA, van der Kogel AJ. Multiparameter analysis of vasculature, perfusion and proliferation in human tumour xenografts. Br J Cancer 1998;77(1):57-64.

269. Evans SM, Hahn SM, Magarelli DP, Koch CJ. Hypoxic heterogeneity in human tumors: EF5 binding, vasculature, necrosis, and proliferation. Am J Clin Oncol 2001;24(5):467-72.

270. Talks KL, Turley H, Gatter KC, Maxwell PH, Pugh CW, Ratcliffe PJ, et al. The expression and distribution of the hypoxia-inducible factors HIF-1alpha and HIF-

2alpha in normal human tissues, cancers, and tumor-associated macrophages. Am J Pathol 2000;157(2):411-21.

271. Tsang RW, Fyles AW, Milosevic M, Syed A, Pintilie M, Levin W, et al. Interrelationship of proliferation and hypoxia in carcinoma of the cervix. Int J Radiat Oncol Biol Phys 2000;46(1):95-9.

272. Raleigh JA, Zeman EM, Calkins DP, McEntee MC, Thrall DE. Distribution of hypoxia and proliferation associated markers in spontaneous canine tumors. Acta Oncol 1995;34(3):345-9.

273. Nordsmark M, Hoyer M, Keller J, Nielsen OS, Jensen OM, Overgaard J. The relationship between tumor oxygenation and cell proliferation in human soft tissue sarcomas. Int J Radiat Oncol Biol Phys 1996;35(4):701-8.

274. Bedford JS, Mitchell JB. The effect of hypoxia on the growth and radiation response of mammalian cells in culture. Br J Radiol 1974;47(562):687-96.

275. Koch CJ, Kruuv J, Frey HE, Snyder RA. Plateau phase in growth induced by hypoxia. Int J Radiat Biol Relat Stud Phys Chem Med 1973;23(1):67-74.

276. Pettersen EO, Lindmo T. Low concentrations of misonidazole counteract effects of extreme hypoxia on cells in S. Br J Cancer 1981;43(3):355-66.

277. Amellem O, Pettersen EO. Cell inactivation and cell cycle inhibition as induced by extreme hypoxia: the possible role of cell cycle arrest as a protection against hypoxia-induced lethal damage. Cell Prolif 1991;24(2):127-41.

278. Amellem O, Stokke T, Sandvik JA, Pettersen EO. The retinoblastoma gene product is reversibly dephosphorylated and bound in the nucleus in S and G2 phases during hypoxic stress. Exp Cell Res 1996;227(1):106-15.

279. Amellem O, Sandvik JA, Stokke T, Pettersen EO. The retinoblastoma protein-associated cell cycle arrest in S-phase under moderate hypoxia is disrupted in cells expressing HPV18 E7 oncoprotein. Br J Cancer 1998;77(6):862-72.

280. Koritzinsky M, Wouters BG, Amellem O, Pettersen EO. Cell cycle progression and radiation survival following prolonged hypoxia and re-oxygenation. Int J Radiat Biol 2001;77(3):319-28.

281. Spiro IJ, Rice GC, Durand RE, Stickler R, Ling CC. Cell killing, radiosensitization and cell cycle redistribution induced by chronic hypoxia. Int J Radiat Oncol Biol Phys 1984;10(8):1275-80.

282. Duchrow M, Schluter C, Wohlenberg C, Flad HD, Gerdes J. Molecular characterization of the gene locus of the human cell proliferation-associated nuclear protein defined by monoclonal antibody Ki-67. Cell Prolif 1996;29(1):1-12.

283. Gerdes J, Schwab U, Lemke H, Stein H. Production of a mouse monoclonal antibody reactive with a human nuclear antigen associated with cell proliferation. Int J Cancer 1983;31(1):13-20.

284. Srivastava M, Pollard HB. Molecular dissection of nucleolin's role in growth and cell proliferation: new insights. Faseb J 1999;13(14):1911-22.

285. Munakata S, Hendricks JB. A multilabeling technique for simultaneous demonstration and quantitation of Ki-67 and nucleolar organizer regions (AgNORs) in paraffin-embedded tissue. J Histochem Cytochem 1994;42(6):789-3.

286. Endl E, Gerdes J. The Ki-67 protein: fascinating forms and an unknown function. Exp Cell Res 2000;257(2):231-7.

287. Sandal T. Molecular aspects of the mammalian cell cycle and cancer. Oncologist 2002;7(1):73-81.

288. Raleigh JA, Chou SC, Calkins-Adams DP, Ballenger CA, Novotny DB, Varia MA. A clinical study of hypoxia and metallothionein protein expression in squamous cell carcinomas. Clin Cancer Res 2000;6(3):855-62.

289. Denekamp J, Michael BD, Harris SR. Hypoxic cell radiosensitizers: comparative tests of some electron affinic compounds using epidermal cell survival in vivo. Radiat Res 1974;60(1):119-32.

290. Adams GE, Bremner JC, Stratford IJ, Wood PJ. Can 31P magnetic resonance spectroscopy measurements of changes in experimental tumour metabolism be related to modification of oxygenation status? BJR Suppl 1992;24(1):137-41.

291. Nagle WA, Moss AJ, Roberts HG, Baker ML. Effects of 5-thio-D-glucose on cellular adenosine triphosphate levels and deoxyribonucleic acid rejoining hy hypoxic and aerobic Chinese hamster cells. Radiology 1980;137(1 Pt 1):203-11.

292. Gerweck LE, Seneviratne T, Gerweck KK. Energy status and radiobiological hypoxia at specified oxygen concentrations. Radiat Res 1993;135(1):69-74.

293. Weidner N, Semple JP, Welch WR, Folkman J. Tumor angiogenesis and metastasis--correlation in invasive breast carcinoma. N Engl J Med 1991;324(1):1-8.

294. Toi M, Hoshina S, Takayanagi T, Tominaga T. Association of vascular endothelial growth factor expression with tumor angiogenesis and with early relapse in primary breast cancer. Jpn J Cancer Res 1994;85(10):1045-9.

295. Toi M, Inada K, Hoshina S, Suzuki H, Kondo S, Tominaga T. Vascular endothelial growth factor and platelet-derived endothelial cell growth factor are frequently coexpressed in highly vascularized human breast cancer. Clin Cancer Res 1995;1(9):961-4.

296. Takano S, Yoshii Y, Kondo S, Suzuki H, Maruno T, Shirai S, et al. Concentration of vascular endothelial growth factor in the serum and tumor tissue of brain tumor patients. Cancer Res 1996;56(9):2185-90.

297. Vermeulen PB, Gasparini G, Fox SB, Toi M, Martin L, McCulloch P, et al. Quantification of angiogenesis in solid human tumours: an international consensus on the methodology and criteria of evaluation. Eur J Cancer 1996;32A(14):2474-84.

298. West CM, Cooper RA, Loncaster JA, Wilks DP, Bromley M. Tumor vascularity: a histological measure of angiogenesis and hypoxia. Cancer Res 2001;61(7):2907-10.

299. Dewhirst MW, Ong ET, Braun RD, Smith B, Klitzman B, Evans SM, et al. Quantification of longitudinal tissue pO2 gradients in window chamber tumours: impact on tumour hypoxia. Br J Cancer 1999;79(11-12):1717-22.

300. Dewhirst MW, Ong ET, Klitzman B, Secomb TW, Vinuya RZ, Dodge R, et al. Perivascular oxygen tensions in a transplantable mammary tumor growing in a dorsal flap window chamber. Radiat Res 1992;130(2):171-82.

301. Konerding MA, Malkusch W, Klapthor B, van Ackern C, Fait E, Hill SA, et al. Evidence for characteristic vascular patterns in solid tumours: quantitative studies using corrosion casts. Br J Cancer 1999;80(5-6):724-32.

302. Koukourakis MI, Giatromanolaki A, Sivridis E, Simopoulos K, Pastorek J, Wykoff CC, et al. Hypoxia-regulated carbonic anhydrase-9 (CA9) relates to poor vascularization and resistance of squamous cell head and neck cancer to chemoradiotherapy. Clin Cancer Res 2001;7(11):3399-403.

303. Giatromanolaki A, Koukourakis MI, Sivridis E, Pastorek J, Wykoff CC, Gatter KC, et al. Expression of hypoxia-inducible carbonic anhydrase-9 relates to angiogenic pathways and independently to poor outcome in non-small cell lung cancer. Cancer Res 2001;61(21):7992-8.

304. Olive PL, Aquino-Parsons C, MacPhail SH, Liao SY, Raleigh JA, Lerman MI, et al. Carbonic anhydrase 9 as an endogenous marker for hypoxic cells in cervical cancer. Cancer Res 2001;61(24):8924-9.

305. Rosmorduc O, Wendum D, Corpechot C, Galy B, Sebbagh N, Raleigh J, et al. Hepatocellular hypoxia-induced vascular endothelial growth factor expression and angiogenesis in experimental biliary cirrhosis. Am J Pathol 1999;155(4):1065-73.

306. Greco O, Dachs GU. Gene directed enzyme/prodrug therapy of cancer: historical appraisal and future prospectives. J Cell Physiol 2001;187(1):22-36.

307. Jaffar M, Williams KJ, Stratford IJ. Bioreductive and gene therapy approaches to hypoxic diseases. Adv Drug Deliv Rev 2001;53(2):217-28.

308. Hofer T, Desbaillets I, Hopfl G, Gassmann M, Wenger RH. Dissecting hypoxia-dependent and hypoxia-independent steps in the HIF-1alpha activation cascade: implications for HIF-1alpha gene therapy. Faseb J 2001;15(14):2715-7.

309. Nordsmark M, Loncaster J, Chou SC, Havsteen H, Lindegaard JC, Davidson SE, et al. Invasive oxygen measurements and pimonidazole labeling in human cervix carcinoma. Int J Radiat Oncol Biol Phys 2001;49(2):581-6.

310. Loncaster JA, Harris AL, Davidson SE, Logue JP, Hunter RD, Wycoff CC, et al. Carbonic anhydrase (CA IX) expression, a potential new intrinsic marker of hypoxia: correlations with tumor oxygen measurements and prognosis in locally advanced carcinoma of the cervix. Cancer Res 2001;61(17):6394-9.

311. Airley R, Loncaster J, Davidson S, Bromley M, Roberts S, Patterson A, et al. Glucose transporter glut-1 expression correlates with tumor hypoxia and predicts metastasis-free survival in advanced carcinoma of the cervix. Clin Cancer Res 2001;7(4):928-34.

312. Hoskin PJ, Saunders MI, Dische S. Hypoxic radiosensitizers in radical radiotherapy for patients with bladder carcinoma: hyperbaric oxygen, misonidazole, and accelerated radiotherapy, carbogen, and nicotinamide. Cancer 1999;86(7):1322-8.

313. Chia SK, Wykoff CC, Watson PH, Han C, Leek RD, Pastorek J, et al. Prognostic significance of a novel hypoxia-regulated marker, carbonic anhydrase IX, in invasive breast carcinoma. J Clin Oncol 2001;19(16):3660-8.

314. Chang S, Lee S, Lee C, Kim JI, Kim Y. Expression of the human erythrocyte glucose transporter in transitional cell carcinoma of the bladder. Urology 2000;55(3):448-52.

315. Younes M, Juarez D, Lechago LV, Lerner SP. Glut 1 expression in transitional cell carcinoma of the urinary bladder is associated with poor patient survival. Anticancer Res 2001;21(1B):575-8.

316. Bronk SF, Gores GJ. Acidosis protects against lethal oxidative injury of liver sinusoidal endothelial cells. Hepatology 1991;14(1):150-7.

317. Fischer B, Muller B, Fischer KG, Baur N, Kreutz W. Acidic pH inhibits non-MHC-restricted killer cell functions. Clin Immunol 2000;96(3):252-63.

318. Popov Z, Hoznek A, Colombel M, Bastuji-Garin S, Lefrere-Belda MA, Bellot J, et al. The prognostic value of p53 nuclear overexpression and MIB-1 as a proliferative marker in transitional cell carcinoma of the bladder. Cancer 1997;80(8):1472-81.

319. Rodel C, Grabenbauer GG, Rodel F, Birkenhake S, Kuhn R, Martus P, et al. Apoptosis, p53, bcl-2, and Ki-67 in invasive bladder carcinoma: possible predictors for response to radiochemotherapy and successful bladder preservation. Int J Radiat Oncol Biol Phys 2000;46(5):1213-21.

320. Moonen L, Ong F, Gallee M, Verheij M, Horenblas S, Hart AA, et al. Apoptosis, proliferation and p53, cyclin D1, and retinoblastoma gene expression in relation to radiation response in transitional cell carcinoma of the bladder. Int J Radiat Oncol Biol Phys 2001;49(5):1305-10.

321. Lara PC, Rey A, Santana C, Afonso JL, Diaz JM, Gonzalez GJ, et al. The role of Ki67 proliferation assessment in predicting local control in bladder cancer patients treated by radical radiation therapy. Radiother Oncol 1998;49(2):163-7.

322. Moonen L, van der Voet H, Horenblas S, Bartelink H. A feasibility study of accelerated fractionation in radiotherapy of carcinoma of the urinary bladder. Int J Radiat Oncol Biol Phys 1997;37(3):537-42.

323. Plataniotis G, Michalopoulos E, Kouvaris J, Vlahos L, Papavasiliou C. A feasibility study of partially accelerated radiotherapy for invasive bladder cancer. Radiother Oncol 1994;33(1):84-7.

324. Vikram B, Malamud S, Silverman P, Hecht H, Grabstald H. A pilot study of chemotherapy alternating with twice-a-day accelerated radiation therapy as an

alternative to cystectomy in muscle infiltrating (stages T2 and T3) cancer of the bladder: preliminary results. J Urol 1994;151(3):602-4.

325. Begg AC, Hofland I, Kummermehr J. Tumour cell repopulation during fractionated radiotherapy: correlation between flow cytometric and radiobiological data in three murine tumours. Eur J Cancer 1991;27(5):537-43.

326. Awwad HK, Khafagy Y, Barsoum M, Ezzat S, el-Attar I, Farag H, et al. Accelerated versus conventional fractionation in the postoperative irradiation of locally advanced head and neck cancer: influence of tumour proliferation. Radiother Oncol 1992;25(4):261-6.

327. Dickinson AJ, Fox SB, Persad RA, Hollyer J, Sibley GN, Harris AL. Quantification of angiogenesis as an independent predictor of prognosis in invasive bladder carcinomas. Br J Urol 1994;74(6):762-6.

328. Hawke CK, Delahunt B, Davidson PJ. Microvessel density as a prognostic marker for transitional cell carcinoma of the bladder. Br J Urol 1998;81(4):585-90.

329. Bochner BH, Cote RJ, Weidner N, Groshen S, Chen SC, Skinner DG, et al. Angiogenesis in bladder cancer: relationship between microvessel density and tumor prognosis. J Natl Cancer Inst 1995;87(21):1603-12.